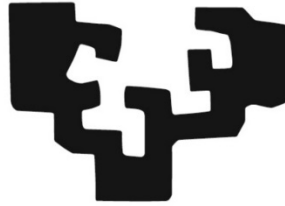eman ta zabal zazu

Universidad del País Vasco

Euskal Herriko Unibertsitatea

CHARACTERIZATION OF BUSPIRONE EFFECT ON OUTPUT BASAL GANGLIA NUCLEI IN 6-HYDROXYDOPAMINE LESIONED RATS WITH AND WITHOUT LONG-TERM LEVODOPA TREATMENT

Doctoral thesis presented by Sergio Vegas Suárez

Leioa, 2020

Agradecimientos

El presente trabajo no hubiera sido posible sin la ayuda y complicidad de muchas personas a las que quiero dar las gracias en estas hojas de agradecimientos.

En primer lugar, quiero agradecer a Luisa Ugedo y a Cristina Miguélez por darme la oportunidad de entrar en su laboratorio y dirigirme esta tesis. Gracias Luisa y Cris, por vuestra dedicación durante toda la tesis y los consejos, pero sobretodo por hacerme pensar, enseñarme a investigar y no me olvido las intensas correcciones de estas últimas semanas. Siempre seréis las "air-one" del laboratorio.

Muchas gracias también a mi "compi" de aventuras desde el primer día, y que tanto me ha ayudado durante estos cuatro años, y que, por suerte para mí, pasará antes por el tribunal, muchas gracias (casi) Dra. Elena Paredes-Rodriguez. Tampoco me puedo olvidar del segundo cómplice de "fechorías", muchas gracias Mario, nuestro hacker personal. Muchísimas gracias a mis "electro teachers", Ainhoa Sagarduy, Cris Bruzos y Nerea Llamosas. Gracias a Teresa Morera por tus aportaciones, anédoctas e involucrarme el maravilloso mundo de la trifásica. José Ángel, ¿necesitas otra revancha en la casa de escape, o ya te rindes? Jejeje. A don Asier Aristieta, *que no me he olvidado de ti*, que tú también eres mi "postdoc" favorito aunque yo no lo diga tan abiertamente… Tampoco me olvido de la artista del grupo, Lorena (que ya te tocará a ti pronto escribir los agradecimientos), y de nuestra última incorporación, Lise. A los alumnos de TFG, Maialen y Alberto, que si no es por ellos seguiría analizando densidades ópticas, ¡muchas gracias!

Thanks to Michelle Morari for accepting me in his lab with "open arms" and introducing me into the microdialysis world. Thanks also to all the people from Morari´s lab (Daniela, Salvatore, Clarissa, Andrea, Federica and the other students). All of you made my stay in Ferrara (and in Italy) very pleasant. *Grazie a tutti voi.*

No pueden faltar tampoco, Laura Escobar del Achucarro y su maravilloso escáner automático, y de Ricardo Andrade del SGiker y su confocal de última generación, que si no es por ellos todavía seguiría haciendo fotos… ¡Eskerrik asko! A los trabajadores del

animalario por su buen trato y todo el soporte que nos han facilitado. A José Vicente, Harkaitz, Cata y demás miembros del departamento de Neurociencias… Gracias por ayudarme a introducirme en el "maravilloso" mundo de las inmunos… A Tere, por hacernos las tardes mucho más amenas y por ser nuestra segunda amatxu en la uni, gracias de todo corazón. También quiero agradecer al resto de profesores del departamento y a los becarios "precarios" ¡¡¡Mila esker!!! Iria y Muneta, ¡tampoco me he olvidado de citaros a vosotras! A Ainho e Unai alías "caba", que han conseguido que el máster y mi tesis haya sido "pura fantasía" siempre seré vuestro "Thor". No me olvido de todas/os mis "andereños" y profes, de los que tanto he aprendido y tanto admiro, ¡Muchas gracias! A mis amigos del cole, la uni y de Medina, aunque no puedo citaros a todos, en especial quiero agradecer a Teresa, Verounica Lancaster-Gate Empire State-building, Jorge (y no me olvido de María), Iñaki, y a mis enfermeras favoritas, Ezti (ya está aquí), Leire. Muchas gracias a toda/os vosotras/os.

A la familia que se escoge, que los pobres son los que más me aguantan, mis mejores compañeros de viajes, y los que siempre saben qué regalarme (turrón de Suchard). Y, sobretodo, me han acompañado en toda esta aventura. Osane, eres capaz de conseguir muchas más cosas de las que crees, y sé que por mi cogerías cualquier avión sin importar el destino. *Por estar siempre*, aunque la distancia nos separe. Estoy deseando organizar nuestro viaje de los treinta. David, gracias por tus consejos científicos y "*no tan científicos*", por ayudarme siempre, y por demonstrarme que puedes reinventarte tras una tesis y que el mundo es un lugar lleno de sitios, personas y momentos maravillosos pero que, si no te aventuras a viajar, a vivirlos, nunca podrás conocerlos. Como bien canta Sabina, "*yo no quiero París con aguacero, ni Venecia sin ti*". Así que me imagino que voy haciendo ya la maleta para Vietnam, Camboya o Nueva York... Lo prometo. No pueden faltar tampoco, Marta y Ugaitz, gracias por participar en el diseño de la portada tan chula y porque sin vosotros *no sabemos* salir de una casa de escape.

Y finalmente, gracias a los verdaderos artífices de que haya llegado hasta el día de hoy. Papá, gracias por creer siempre en mí, aunque tengo mis limites, ¡eh! Siempre recordaré lo triste que te quedaste en el aeropuerto cuando me iba a Italia porque pocas veces te he visto triste. Cuánto dolemos los hijos… Ay, mamá, gracias por luchar siempre por tus hijos, por trabajar en el hospital, y luego más en casa, por pasar tus tardes libres con nosotros haciendo los deberes, por alimentar siempre nuestra curiosidad y por intentar

hacer de nosotros tus "hombrecitos" de provecho. Miranos, los dos científicos. Dicen que "detrás de un gran hombre, hay una gran mujer", y yo siempre he sabido que se refería a vosotras, las madres. Sé que no te lo digo mucho, pero gracias mamá. Jorge, no imagino una vida sin ti y desde bien pequeño he sabido que vas a hacer cosas extraordinarias porque eres más grande de lo que piensas, hermano. Estoy muy orgulloso de ti. A los pequeñajos de la casa, Gala y Brian que me llenan de alegría, "energía" y me arreglan muchos de mis días... A mis primas y primos, a mis tías y tíos, pero en especial a mis tías Coro y Satur, porque junto a mi madre, las tres, habéis hecho lo imposible por cuidar de la abuela y os estaré siempre agradecido. Y a mi tía Eva, por enseñarme que hay que luchar hasta el final. Gracias también a mi tía abuela Dora, por tus historias salmantinas, tus anécdotas, y por guardarme recortes de la Gaceta que me recuerdan a mi abuelo, tu hermano. Gracias, Dora. Pero, en especial, quiero dedicar estos agradecimientos a mis cuatro abuelos, Antonio, Carmen, Nino y Feli, que tuvieron que dejar pronto la escuela, vivieron su infancia durante la posguerra, emigraron a Bilbao (e incluso Luxemburgo) trabajando muy duro, aprovechando vuestro esfuerzo, abuelos, yo he podido estudiar un poco más. Gracias a Feli y Nino por los veranos en el pueblo y por estar siempre disponibles cuando mis padres tenían que trabajar. Pero, sí, estas últimas líneas son para mi abuela Feli, porque se graduó en el colegio, se "licenció" y se va a doctorar conmigo. Abuela, recuerdo el día que me ofrecieron realizar esta tesis doctoral y lo malita que estuviste la noche anterior, pero desde entonces, y como ha sido así siempre, hemos ido saliendo adelante poco a poco… Y, ¡Lo hemos conseguido una vez más! Siempre dicen que el *mejor regalo* para un abuelo es "tener un nieto" pero yo como nieto digo que el mejor regalo, sin duda, es haber tenido unos abuelos como vosotros.

Y finalmente, y no por ello menos importante, quiero agradecer a todas las pobres ratas cuyo destino fue cruzarse conmigo. Todas ellas, a su manera, han sido claves en esta tesis. No os olvidaré.

¡¡¡ Gracias!!!

A mis abuelos Nino y Feli

Esto que yo hago, ¿a quién importa aquí? ¿A quién contaré el gozo producido por mi pequeño descubrimiento que no se ría desdeñosamente o no se mueva a compasión irritante? Si acierto, ¿quién aplaudirá?, y si me equivoco, ¿quién me corregirá y me alentará para proseguir?

Santiago Ramón y Cajal. *Reglas y Consejos Sobre Investigación Biológica.*

INDEX

4. RESULTS   83

ABBREVIATION LIST

5-HT	Serotonin or 5-hydroxytryptamine
5-HT$_{1A}$	5-hydroxytryptamine-1A receptor or serotonin-1A receptor
6-OHDA	6-hydroxydopamine
8-OH-DPAT	8-hydroxy-2-dipropylamino tetralin
α-syn	Alpha-synuclein or α-synuclein
Acc	Accumbens
AIMs	Abnormal Involuntary Movements
ALO	Axial, limb and orolingual
AMPA	Ionotropic glutamatergic α-amino-3-hydroxy-5-methyl-4-isoxazolepropionate receptors
ANOVA	Analysis of the variance
AUC	Area Under the Curve
BG	Basal Ganglia
ChR2	Channelrhodopsin-2
COX	Cytochrome c oxidase
CL	Contralateral
COMT	catechol-O-methyltransferase inhibitors
CV	Coefficient of variation
DA	Dopamine
DAB	3,3′-diaminobenzidine
DAT	Dopamine transporter
DBS	Deep Brain Stimulation
D$_1$-D$_5$	Dopaminergic D$_1$-D$_5$ receptor.
DRN	Dorsal raphe nucleus
DRD	Dorsal region of the dorsal raphe nucleus
DRL	Lateral region of the dorsal raphe nucleus
DRV	Ventral region of the dorsal raphe nucleus
ECoG	Electrocorticogram

EP	Entopeduncular
FUS	Focused ultrasound
GABA	Gamma-aminobutyric acid
Glu	Glutamate
GPe	External (segment of the) Globus Pallidus
GPi	Internal (segment of the) Globus Pallidus
IL	Ipsilateral
IOD	Integrated optical density
i.p.	Intraperitoneal
i.v.	Intravenous
KPBS	Potassium-phosphate buffer
L-DOPA	Levodopa or 3,4-Dihydroxy-L-phenylalanine methyl ester
LID	L-DOPA-induced dyskinesia
LFP	Local Field Potential
M_1	Motor cortex
MAO-B	Monoamine oxidase type B inhibitors
MPTP	1-methyl-4-phenyl-1,2,3,6-tetrahydropyridine
NMDA	Ionotropic glutamatergic N-methyl-D-aspartate (NMDA) receptor
PB	Phosphate buffer
PBS	Phosphate saline buffer
PD	Parkinson´s Disease
SERT	Serotonin transporter
SN	Substantia nigra
SNc	Substantia nigra pars compacta
SNr	Substantia nigra pars reticulata
SPNs/MSNs	Spiny projection neurons or medium spiny neurons
SSRI	Serotonin selective reuptake inhibitor
STN	Subthalamic nucleus
TH	Tyrosine hydroxylase
TS	Trizma base saline

1. INTRODUCTION

1. INTRODUCTION

1.1. PARKINSON'S DISEASE

Parkinson's disease (PD) is the second most common neurodegenerative disorder, after Alzheimer's disease. The global prevalence is estimated to be 2% of the world population older than 60 years and 3% of those over the age of 80 (Tysnes & Storstein, 2017). Due to increasing life expectancy, the prevalence and incidence of PD are growing, and are expected to double by 2030 (Lee & Gilbert, 2016). Nevertheless, the prevalence and incidence of PD vary depending on geographical location, race, ethnicity, genetic interactions, and exposure to different environmental factors or economic resources (Goetz et al., 2016; Tysnes & Storstein, 2017). In general, PD prevalence is higher in Europe and the United States and lower in Asia, Latin America, and, especially, on the African continent (Benito-Leon, 2018).

The annual cost caused by PD in the United States is estimated to be over $50 billion by 2040 (Huse et al., 2005). There are at least 300,000 patients diagnosed with PD in Spain, and each year there is one new case per 10,000 habitants. PD has a considerable impact on the quality of life of these patients, and the mean cost per patient may exceed 17,000 € per year (García-Ramos et al., 2016).

1.1.1. Principal hallmarks of Parkinson's disease

The milestones in our understanding of PD is shown in **Figure 1.1**. In 1817, James Parkinson described PD as a neurological condition in his publication "An essay on the shaking palsy" (Parkinson, 1817). He outlined some key motor symptoms, resting tremor, postural instability, and gait festination that he had observed in six patients. Five decades later, the neurologist Jean-Martin Charcot who was particularly interested in Parkinson's work, renamed the disorder "Parkinson's disease", established the clinical definition, and made some important contributions, such as describing bradykinesia and rigidity (Charcot, 1875).

1. Introduction

In 1912, Frederick Lewy reported the presence of intracellular inclusion bodies in the brain of patients with PD, now named "Lewy bodies". In 1919, Konstantin Tretiakoff discovered that the substantia nigra pars compacta (SNc) is the main structure affected in PD. Between the 1950s and 1960s, the role of dopamine (DA) as a cerebral neurotransmitter and its relevance in the striatum were discovered by Montagu and Carlsson (Carlsson et al., 1958; Montagu, 1957). Later, a DA deficit in both the striatum and the SNc was observed in patients with PD (Ehringer and Hornykiewicz, 1960), and DA signalling was shown to play a crucial role in motor control. After these discoveries, small oral doses of 3,4-dihydroxyphenylalanine or levodopa (L-DOPA) were demonstrated to improve motor symptoms of PD (Cotzias, 1968), and L-DOPA became the gold-standard treatment for PD. Since then, significant progress has been made in the development of new pharmacological and surgical tools to treat PD motor symptoms, and other cell types and molecular mechanisms have been implicated in the development of PD.

During the late 1980s, deep brain stimulation (DBS) emerged as a possible treatment for PD, but it was not approved for clinical use by the US Food and Drug Administration (FDA) until 1997 (Coffey, 2009). In the late 1990s, due to improvements in molecular and genetic techniques, the first PD-associated mutation was identified, the human alpha-synuclein (α-syn) protein (SNCA) (Polymeropoulos et al., 1997). In 1998, Spillantini and collaborators reported that the α-syn protein was the main component of the protein aggregates in Lewy bodies which are found in the soma and neurites of the few surviving dopaminergic neurons of the SNc (Spillantini et al., 1998). Since then, it has been revealed that apart from the SNc, other brain areas are also affected in the early and late stages of the disease. Braak and collaborators (2003) postulated a six-stage theory for the development of Lewy pathology in sporadic PD. This theory considers that Lewy bodies sequentially advance via neuroanatomical interconnected pathways until they reach the SNc. The areas affected in the first stages (stage 1 and 2) are non-dopaminergic regions including the olfactory bulb, the dorsal nucleus of the vagal nerve, the *locus coeruleus,* and the caudal raphe nuclei. The Lewy body lesions then extend to the amygdala, the pedunculopontine tegmental nucleus, and the SNc (stages 3 and 4). Finally, in stages 5 and 6, a large part of the brain is affected, including the cortical areas, mesocortex, temporal lobe, and hippocampus (Braak et al., 2003). Overall, although it is clear that abnormal α-syn deposition occurs early in PD, the pathway that drives the

misfolding of α-syn aggregates still remains unclear, and many hypotheses have been proposed.
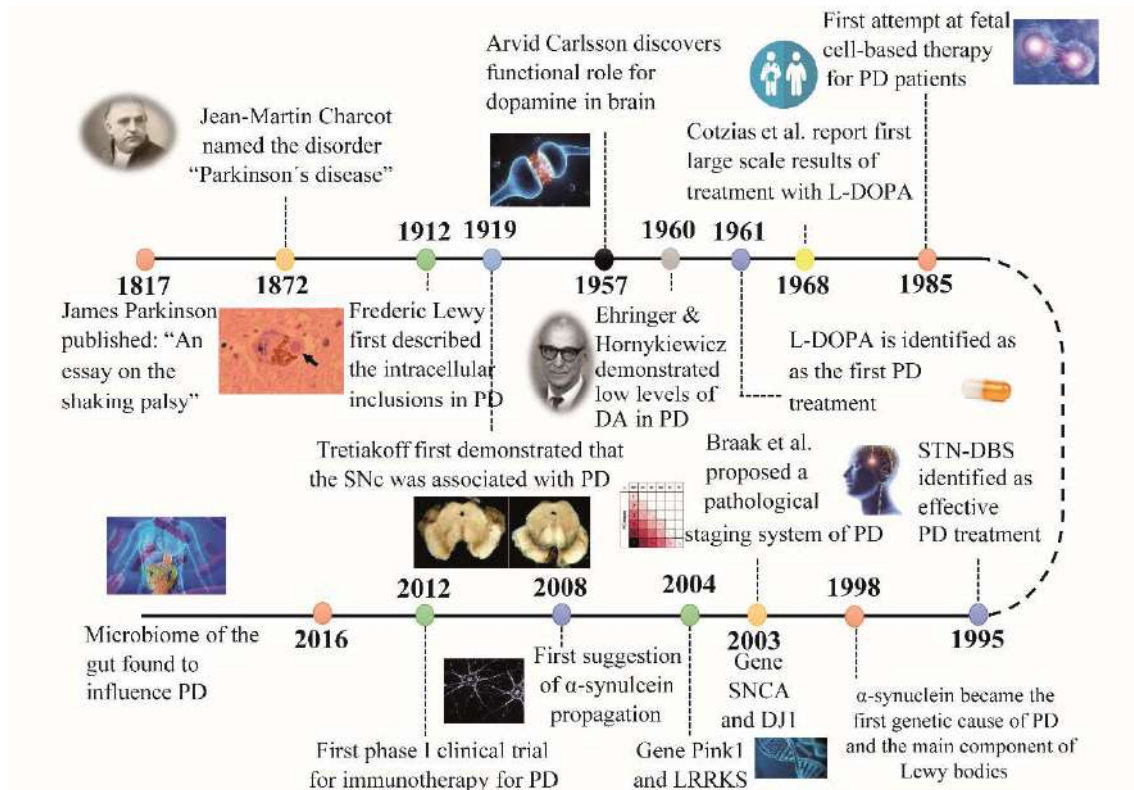
Figure 1.1. The hallmarks of Parkinson's disease over time. DA: dopamine; L-DOPA: levodopa; PD: Parkinson´s disease; STN-DBS: subthalamic deep brain stimulation; SNCA: human alpha-synuclein protein; SNc: substantia nigra pars compacta.

1.1.2. Aetiology and pathogenesis of Parkinson's disease

PD is a progressive and chronic disorder characterized by the gradual degeneration of dopaminergic neurons in the SNc of the midbrain causing a massive loss of DA in the striatum (Kish et al., 1988) and the presence of Lewy bodies in many brain regions. Lewy bodies are cytoplasmic aggregations formed by more than 25 compounds, but principally α-syn and ubiquitin, with a diameter of 8–30 μm (Samii et al., 2004). PD is likely a result of multiple factors: aging, genetic predispositions, and environmental risk factors. Advanced age is considered the main risk factor for PD. However, environmental risk factors, such as exposure to various toxins like 1-methyl-4-phenyl-1,2,3,6-tetrahydropyridine (MPTP) or pesticides like rotenone or paraquat (Betarbet et al., 2000; Langston et al., 1983; Thiruchelvam et al., 2000) and lifestyle are key elements underlying the pathogenesis of idiopathic PD (Tanner, 1989, 2010; Tysnes & Storstein,

2017). While the majority of diagnosed cases represent idiopathic or sporadic PD (Gasser, 2003) whose causes are still largely unknown, gene mutations are responsible for some familiar forms: these forms are less frequent (15% of total cases), generally have an early onset (before 45 years of age), and a strong genetic component (autosomal dominant, recessive, or X-linked). The literature shows that at least 23 loci and 19 causative genes are linked to PD, such as SNCA/PARK1/4, parkin/PARK2, UCHL1/PARK5, PINK1, DJ1/PARK7, and LRRK2/PARK8 which encodes dardarin (For a review see Del Rey et al., 2018). Besides genetics, epigenetic alterations seem to be involved in the pathogenesis of PD. Thus, abnormal changes in epigenetic mechanisms regulating gene expression such as DNA methylation (Coupland et al., 2014; Fernández-Santiago et al., 2015; Masliah et al., 2013), histone modifications (Park et al., 2016), or microRNAs (miRNAs) (Kim et al., 2007) have been reported and linked to PD.

These days, PD is considered a multifactorial disorder and, in addition to the loss of dopaminergic neurons in the SNc and the presence of Lewy bodies, other cellular and molecular mechanisms have been involved in its pathogenesis. In the following paragraphs, we briefly explain the main mechanisms.

Mitochondrial dysfunction. The mitochondria play a key role in energetic metabolism, thermogenesis, calcium maintenance, and redox signalling (Zhang et al., 2018). Mitochondrial dysfunction in PD is caused by bioenergetics defects, mitochondria-associated gene mutations (SNCA, LRRK2, Parkin, PINK1, and others), and morphological and functional alterations (Surmeier, 2018; Zhang et al., 2018). Impairments of mitochondrial electron chain complex I and also complex IV or cytochrome c oxidase (COX) (Itoh et al., 1996; Schapira et al., 1990), as well as a close relationship between α-syn aggregation and mitochondrial impairments in SNc neurons, have been observed in patients with PD (Poewe et al., 2017). Several changes in mitochondrial protein expression have been described, such as molecular chaperones in the SNc and prefrontal cortex of patients with PD (Ferrer et al., 2007), aberrant increases in the activity of serine protease, HTRA2, in patients with PD and animal models (Vande Walle et al., 2008), and changes in mitochondrial haemoglobin (a and b) expression in the nigral cells in patients with PD and animal models (Freed & Chakrabarti, 2016).

Oxidative stress. Reactive oxygen species and other reactive species are needed for the maintenance of cellular homeostasis. These components are strictly regulated by the action of anti-oxidant proteins and systems (Puspita et al., 2017). Under pathological conditions, a failure in their regulation may increase oxidative stress that can lead to metabolic dysfunction and, as consequence, final cell death (Puspita et al., 2017). A large amount of evidence has shown an elevation in oxidative stress markers in nigral cells of patients with genetic and idiophatic PD (Surmeier et al., 2017a; Zhou et al., 2008), parkinsonism induced by neurotoxins like the 6-hydroxydopamine (6-OHDA) or MPTP, causing an excess of free radicals and leads to apoptosis (Jenner et al., 2003; Olanow, 1990).

Excitotoxicity. The increased glutamatergic neuron activity in PD results in an excessive glutamate (GLU) release, evoking the excessive stimulation of receptors which enhance intracellular calcium levels. This high calcium concentration can activate lipases, proteases and endonucleases, inducing nigral cell apoptosis (Giguère et al., 2018; Surmeier et al., 2017a).

Calcium homeostasis. The regulation of calcium levels is crucial for maintaining neuronal function. Some mutations have been correlated with the dysregulation of intracellular homeostasis and may be responsible for mitochondrial impairments, which may increase oxidative stress and apoptosis (Surmeier et al., 2017b; Verma et al., 2018).

Apoptosis. Programmed cell death has been considered as a pathogenic mechanism in PD since this process has first been observed in the SNc (Burke & Kholodilov, 1998; Tatton & Olanow, 1999; Tatton et al., 2003). However, it is not known if this mechanism is a sign of neuronal vulnerability to internal or external toxins (Jellinger, 2001). Supporting the role of apoptosis in PD, a gene mutation related to a familiar form of PD that leads to a reduction in antiapoptotic cell capacity has been described (Xu et al., 2005).

Protein homeostasis. The two main mechanisms underlying protein homeostasis are the ubiquitin-proteasome system, for the degradation of small proteins, and the autophagy-lysosome pathway for the elimination of bigger proteins and even damaged organelles. Abnormal protein homeostasis has been reported in PD (Zhang et al., 2018). Several findings, such as elevated ubiquitinated proteins in the striatum, underexpression

of some subunits of the proteasome in the SNc, and mutations of ubiquitin ligase and deubiquitinase activity, have been linked to PD (Seirafi et al., 2015; Toulorge et al., 2016). On the other hand, autophagy impairments mediated by chaperones (Cuervo & Wong, 2014) and increased levels of lysosomal macroautophagy markers such as LC3II (Dehay et al., 2010) and Beclin-1 (Miki et al., 2018) have been found in the SNc of patients with PD. Finally, lysosomal autophagy-related genes are altered in sporadic and genetic forms of PD (Koga & Cuervo, 2011; Miki et al., 2018; Toulorge et al., 2016).

Parkinson's disease as a prion-like disorder. This hypothesis proposes the key involvement of misfolded α-syn propagation from cell to cell, from one brain region to another, and also to the peripheral nerves of the autonomic nervous system, in the progression of PD (Braak et al., 2003; Braak & Del Tredici, 2017; Brundin & Melki, 2017). The propagation of α-syn can occur via anterograde or retrograde transport (Brahic et al., 2016), and failures of the lysosomal or proteasome system increase the secretion of α-syn (Bandyopadhyay et al., 2007). Therefore, α-syn inclusions pathogenic forms can be taken up by neighbouring neurons as well as by microglia and astrocytes and trigger (as a "seed") the aggregation of native α-syn (Reyes et al., 2015) as well as by microglia or astrocytes (Lim et al., 2018b).

Neuroinflammation. Neuroinflammation is a key feature in PD, but its exact role has not been identified yet (Deczkowska et al., 2018). Dopaminergic neurons in the SNc have been shown to be prone to neuroinflammation due to the small proportion of astrocytes regulating the microglia (Mena & García De Yébenes, 2008; Whitton, 2007). While some studies support the notion that the inflammatory response appears as a consequence of nigral cell death, others suggest that neuroinflammation precedes neurodegeneration (Halliday & Stevens, 2011; Harms et al., 2017). High levels of different inflammatory markers including interleukins, TNFα, and IFN-γ have been identified in patients with PD or animal models (Barcia et al., 2005, 2011; Plaza-Zabala et al., 2017; Toulorge et al., 2016). Several studies point out that inflammatory responses during PD cause uncontrolled glial cell activation and collateral damage to healthy tissue and neurons, thus initiating a neurodegenerative process (Deczkowska et al., 2018; Dzamko et al., 2015; Halliday & Stevens, 2011).

1.1.3.   Clinical features of Parkinson's disease

1.1.3.1. Motor symptoms

The diagnosis of PD is generally made at the onset of the first motor symptoms. When the clinical signs of PD become evident, about 80% of striatal and 50–60% of nigral dopaminergic neurons are already lost (Brooks, 1998; Fearnley & Lees, 1991; Rice, 1984). The classic motor features of PD include resting tremor, rigidity, and bradykinesia, but other motor symptoms such as walking problems or difficulties with balance and coordination (postural instability) may also occur. Tremor and rigidity are denominated "positive" phenomena, while bradykinesia, together with postural reflex abolition and freezing, is considered a "negative" phenomenon and the most disabling problem for patients with PD.

Tremor, defined as an involuntary rhythmic oscillatory movement of a body part that affects the coordination and execution of targeted movements, is the most common and most easily recognized symptom of PD. The localization of tremor is variable: most patients show hand tremors, unilateral or even bilateral, but also occur in the legs or the head (at a frequency of 4–6 Hz) (Louis, 2016). Rigidity is defined as an increase in passive muscle tone in flexor and extensor muscle groups that reduces the range of movement. Bradykinesia, also a characteristic clinical feature of PD, refers to reductions in movement velocity and difficulty in initiating movement. Postural instability refers to the gradual development of poor balance, increasing the risk of falls, and is usually absent in the early stages of the disease. In the advanced stages of PD, additional motor features such as impairments in gait and balance develop (Bloem et al., 2004). In addition to these features, changes in the patient's voice are commonly experienced in advanced PD; their speech becomes soft and monotone and sometimes difficult to understand, and swallowing deficits can cause choking episodes, coughing, and drooling.

1.1.3.2. Non-motor symptoms

Non-motor symptoms are also common and can appear before the onset of motor symptoms. Non-motor symptoms can be as disabling as motor symptoms (Sullivan et al., 2007) and often represent the major complication to treat. These symptoms include psychiatric symptoms, severe cognitive decline, and autonomic dysfunction, but also involve pain and sleep disturbances (**Figure 1.2**). Psychosis is highly prevalent in PD. Up to 60% of patients with PD experience psychosis over the course of the disease, manifesting in hallucinations, illusions, a false sense of presence or passage, or delusions (Fénelon & Alves, 2010; Forsaa et al., 2010; Ravina et al., 2007). Anxiety or depression often emerge several years before the onset of typical motor symptoms. Depression affects approximately 40%–50% of patients with PD (Reijnders et al., 2008) and may occur at any stage of the disease, while anxiety is present in approximately 40% of patients (Pontone et al., 2009).

PD is also characterized by sleep disturbances, including insomnia and alterations in sleep and wake cycles, as well as by excessive daytime sleepiness or fatigue. The sleep disorders often appear before the onset of motor symptoms (Galbiati et al., 2019; Postuma et al., 2009). In PD, and other synucleinopathies, there is a loss of rapid eye movement sleep paralysis, leading to patients "acting out" their dreams (St Louis et al., 2017). Cognitive decline is one of the most disabling features of PD, evident from the time of diagnosis, with severe and progressive impairments manifesting several years later (Aarsland et al., 2009; Hely et al., 2008; Williams-Gray et al., 2007). Patients with PD also experience olfactory dysfunctions or anosmia and, earlier, dysfunctions of the autonomic nervous system. Some symptoms, like constipation, may occur earlier than the onset of motor symptoms, while others, like sweating and abnormal orthostatic hypotension, sexual dysfunction, urinary symptoms, and incontinence, only become clinically relevant at later stages of the disease. Visual disturbances are also present and can range from dry eyes and blurry vision to difficulty controlling eye movements. Finally, a moderate weight loss is common (for a review, see McGregor & Nelson, 2019).
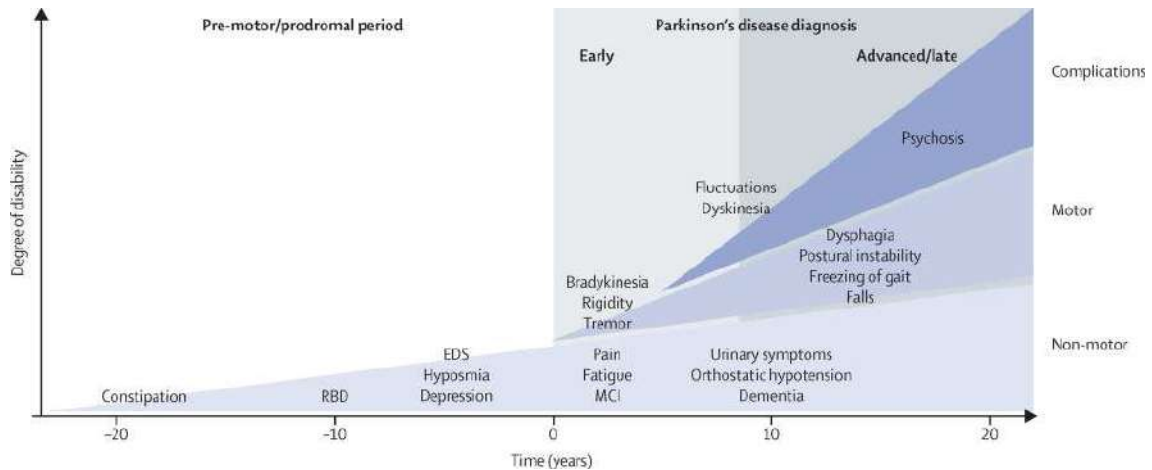
Figure 1.2. Clinical symptoms and time course of Parkinson's disease progression. Although the diagnosis of PD is made at the onset of the first motor symptoms (0 years), it can be preceded by non-motor symptoms by more than 20 years (premotor or prodromal phase). The manifestation of both motor and non-motor features tends to occur in advanced disease stages, together with long-term complications of dopamine replacement therapies, including fluctuations, dyskinesia, and psychosis. EDS: excessive daytime sleepiness; MCI: mild cognitive impairment; RBD: rapid eyes movement sleep behaviour disorder (taken from Kalia & Lang, 2015).

1.1.4. Treatment of Parkinson's disease

Currently, pharmacological treatment with DA replacement drugs is the first choice for the treatment of PD. Generally, the surgery is reserved for patients who do not tolerate the medication, develop strong side effects, or show small therapeutic benefits. All treatments available right now target symptomatic motor and non-motor manifestations, and are not able to stop the progression of the disease, let alone prevent it. However, the sooner the treatment is applied, the better the prognosis seems to be (Lang & Espay, 2018; Olanow, 2008).

1.1.4.1. Pharmacological treatment

For motor symptoms, L-DOPA is considered the gold-standard treatment. L-DOPA is the precursor of DA, and in contrast to DA it can cross the blood-brain barrier (Kageyama et al., 2000). Its administration exogenously replaces the DA deficit present in PD. Normally, L-DOPA is administered together with a DA decarboxylase inhibitor, such as carbidopa or benserazide that does not cross the blood-brain barrier, in order to avoid the peripheral transformation of L-DOPA in DA. L-DOPA improves striatal dopaminergic transmission, producing a rapid improvement of the signs and symptoms of the PD. L-DOPA can be used in all patients and at any stage of the disease.

Unfortunately, L-DOPA does not stop the development of the disease, and its efficacy decreases over time. Moreover, the prolonged treatment with L-DOPA produces new motor complications, such as dystonia or L-DOPA-induced dyskinesia (LID). Other pharmacological treatments for PD are therefore also used. These include DA agonists, monoamine oxidase type B inhibitors (MAO-B), catechol-O-methyltransferase inhibitors (COMT), and some non-dopaminergic drugs such as anticholinergic drugs and amantadine.

DA agonists act on dopaminergic receptors and mimic the DA effect. DA agonists are used especially in young patients during the early stages of PD, to delay the beginning of L-DOPA therapy and avoid the L-DOPA-induced motor complications. These drugs include apomorphine, bromocriptine, ropinirole, pramipexole, and rotigotine and can be taken alone or in combination with other PD medications including L-DOPA. In patients with advanced PD, apomorphine is the only approved drug for the acute rescue of "off-periods" when the medication wears off and, as a result, symptoms return before a new dose can be taken.

The MAO-B inhibitors rasagiline and selegiline can be taken in combination with L-DOPA. In addition to being effective drugs for the treatment of motor symptoms in PD, MAO-B inhibitors have shown neuroprotective effects in preclinical models of PD, but no conclusive results have been reported in clinical trials (Kong et al., 2015). New results might suggest that MAO-B inhibitor exposure could slow PD progression (Hauser et al., 2017). Finally, other PD medications, such as COMT inhibitors, entacapone, opicapone and tolcapone, are used in combination with L-DOPA. These three therapeutic strategies lead to an increase in DA levels and a reduction of motor symptoms.

Atropine, a muscarinic anticholinergic drug was widely used until the arrival of L-DOPA. Currently, however, the use of anticholinergic drug has drastically declined due to the occurrence of cognitive side effects. Anticholinergics drugs such as benzatropine and trihexyphenidyl can be used as initial treatment in young patients with resistant tremors. These drugs modulate the activity of acetylcholine to restore the balance between acetylcholine and DA, which is important in the regulation of movement, and can be used alone or in combination with other PD treatments. Amantadine is an N-methyl-D aspartate (NMDA) glutamatergic receptor antagonist approved to treat PD symptoms

such as slowness, stiffness and tremor, and dyskinesia. In August 2019, the FDA approved istradefylline, an adenosine receptor A_{2A} antagonist, as an add-on treatment to L-DOPA plus carbidopa to treat "off episodes".

Non-motor symptoms are also affected by PD therapy. DA replacement therapies with L-DOPA or DA agonists can alleviate some psychiatric symptoms, such as apathy (observed in 30–40% of patients) or anhedonia, but may also create new psychiatric symptoms in susceptible individuals, such as impulsive control disorders and the dopaminergic dysregulation syndrome. Impulsive control disorders include pathological gambling, hypersexuality, compulsive shopping, and eating disorders (McGregor & Nelson, 2019), while patients with PD and dopaminergic dysregulation syndrome develop an addiction to their dopaminergic therapy and become dependent on it.

Cognitive impairments can be classified into DA-dependent (alleviated or exacerbated by DA replacement therapy) and DA-independent (Sethi, 2008). DA-dependent cognitive decline tends to emerge earlier and includes deficits in attention, processing speed, set-switching, and verbal fluency (Robbins & Cools, 2014), while DA-independent symptoms tend to emerge later and include deficits in episodic memory and visuospatial function. In later stages of the disease, visual illusions and hallucinations are frequently developed and worsened by DA replacement therapy (Sethi, 2008). Pimavanserin, a serotonin inverse agonist, has been prescribed for the treatment of psychosis associated with PD. The antipsychotic drugs clozapine and quetiapine are less commonly used, because they can worsen motor symptoms due to their effect on the dopaminergic system. Cognitive decline is commonly treated with rivastigmine, an acetylcholinesterase inhibitor (Pagano et al., 2015). Finally, droxidopa, a prodrug of noradrenaline, is used in the management of neurogenic orthostatic hypotension in PD.

1.1.4.2. Other treatments

Surgical treatment and deep brain stimulation

Neurostimulation or DBS and ablation or lesion are alternative treatments for PD, especially when the pharmacological treatment is not improving L-DOPA side effects. DBS consists of the implantation of one or more electrodes in specific brain areas, the subthalamic nucleus (STN), the internal globus pallidus (GPi), or the pedunculopontine tegmental nucleus, and the application of electrical stimulation at frequencies between 100 and 200 Hz (Benabid, 2003; Starr et al., 1998). DBS is the current surgical procedure of choice, due to its reversibility, its low morbid-mortality rate, the possibility to remove the electrodes in case of problems or the availability of better treatment, and the possibility to customize the parameters for each patient in case of side effects. It has however some limitations, such as the fragility of the electrode system, elevated economic costs, and problems caused by battery replacement (Doshi, 2011; Oh et al., 2002).

Focused ultrasound

In July 2016, the FDA approved the use of focused ultrasound (FUS) for the treatment of tremor-dominated PD that does not benefit from medication. For some patients, FUS may be an alternative to DBS. Magnetic resonance-guided FUS is a non-invasive technique based on the application of focused acoustic energy (ultrasound) on selected brain areas (thalamus, GPi, STN) whose circuits are involved in tremor, akinesia, and LID (Martínez-Fernández et al., 2018). FUS may be performed in one or both brain hemispheres and minimizes damage to non-targeted healthy brain regions. One limitation of this method is that FUS causes permanent and irreversible changes in the brain.

Drug delivery systems

Therapeutic strategies these days are focused on developing new formulations and new drug-delivery systems that improve the absorption, bioavailability, and maintenance of constant plasma concentrations of antiparkinsonian drugs. Sublingual apomorphine formulations for the off-periods are also being developed. Some of the latest developments are subcutaneous pumps, sublingual formulations, and intraduodenal

administration systems. The subcutaneous delivery of apomorphine allows acute and continuous administration of the drug, while L-DOPA-carbidopa intestinal infusion (duodopa) provides a steady concentration of L-DOPA (Antonini & Nitu, 2018). Apomorphine and duodopa are last-term treatments used when the patient does not show a good response to previous treatments.

Neuroprotection

The target of neuroprotection is the reduction or stop of the progression of PD. The utilization of neurotrophic factors or growth factors like the glial cell line-derived neurotrophic factor which increases DA levels in the SNc (Hudson et al., 1995), and, in combination, the vascular endothelial growth factor which is a potent angiogenic factor, have demonstrated nigral neuron recovery in 6-OHDA-lesioned rats (Herrán et al., 2013, 2014).

Physical exercise

Regular and moderate-intensity physical exercise shows neuroprotective effects, because of its anti-inflammatory properties. Physical exercise may improve the patient's overall motor condition, increasing muscle strength and aerobic capacity and reducing balance and gait dysfunction (Gil-Martínez et al., 2018; Lang & Espay, 2018). Thus, regular exercise improves the quality of life of patients with PD.

Other experimental therapies

Currently, three different experimental strategies are under development with the aim of achieving clinical translation: gene therapy, cell transplantation, and immunotherapy.

Since the first cell therapy assays were published in the 1980s, several attempts with foetal cell transplants did not lead to improvements of PD and LID symptoms, despite inducing the reinnervation of the striatum (Freed et al., 2001; Olanow et al., 2003). However, the discovery of stem cells with the ability to multiply and differentiate into several cell types, including dopaminergic cells, represents a promising treatment option

for PD. Recent studies have shown that human embryonic and induced stem cells can survive grafting in animals and supply functional recovery (Barker et al., 2015). In spite of the commercial and scientific interest in stem cell therapies for PD, such therapies are far from being commercially available.

Gene therapy allows to introduce specific genes into the cells of a patient, by reprogramming, in order to restore expression deficits. At the moment, two gene therapy approaches, based on the use of viral vectors, are being tested: (1) viral expression vectors of growth factors, glial cell line-derived neurotrophic factor and neurturin, both preventing the death of dopaminergic neurons in animal models (Bartus & Johnson, 2017a, 2017b; Poewe et al., 2017) and (2) viral expression of key DA metabolism enzymes, such as TH and other cofactors, and GLU decarboxylase (Björklund et al., 2009; Carlsson et al., 2005; LeWitt et al., 2011). There is in fact a second open-label trial (VY-AADC01) that evaluates the gene delivery infusion of enzyme aromatic L-amino acid decarboxylase into the striatum. The safety and tolerability of this method have been reported in non-human primates before (Hadaczek et al., 2010; San Sebastian et al., 2013). However, there are not enough randomized clinical trials that confirm the efficacy of this therapeutic approach.

Finally, both active and passive immunological strategies are under clinical development. The first is the active immunization with a vaccine (AFFITOPE, AFFiRiS) generated from short peptides homologous to α-syn, which induce the formation of antibodies. This vaccine has completed the phase I/II safety trial in patients with PD and has provided evidence for antibody formation as well as immunological efficacy up to 3 years after treatment (Fields et al., 2019). A placebo-controlled phase II trial of a second vaccine (AFF03) is currently ongoing. The second is passive immunization with monoclonal antibodies against α-syn (Bergström et al., 2016). Different compounds are currently studied (NI-202, PRX002, MEDI1341), with one compound, PRX002 (Schenk et al., 2017), now entering a phase II randomized and double-blind clinical trial that should be completed by June 2021.

1.1.5. Levodopa-induced dyskinesia

Soon after the clinical confirmation of L-DOPA treatment efficacy in alleviating motor symptoms of PD, the appearance of LID was also reported (Cotzias et al., 1969). LID is typically characterized by choreic or dystonic movements involving the limbs, the orofacial musculature, and the trunk. LID can present in three clinical forms, "peak-dose dyskinesia", the most common form that often consists of stereotypic, choreic, or ballistic movements involving the head, trunk, and limbs and sometimes respiratory muscles and occurs at the peak of L-DOPA plasma concentrations, "diphasic dyskinesia", occurring at the beginning and the end of L-DOPA treatment, and "off-period dystonia", where the concentration of L-DOPA in the brain is low, manifesting in abnormal dystonic postures affecting mainly the lower limbs (Guridi et al., 2012). Approximately 40% of patients develop LID after 4–6 years of L-DOPA treatment and 90% of patients after 10 years (Ahlskog & Muenter, 2001). LID can disable patients over time, impairing their quality of life, affecting their daily activities and routines, and increasing the caregiver burden and stress (Ahlskog & Muenter, 2001; Khlebtovsky et al., 2012; Perez-Lloret & Rascol, 2018). The current treatment strategy consists in improving the pharmacokinetics and bioavailability of L-DOPA, changing the frequency and amount of the dose, switching to an extended-release formulation, or adding DA agonist or MAO-B or COMT inhibitors. Initially, amantadine (symmetrel) was approved by the FDA with the indication as an antiviral agent and antiparkisonian drug and later as antidyskinetc drug. In 2017, an extended release formulation of amantadine (Gocovri) was approved by the FDA to treat dyskinesia in patients with PD. At the moment, amantadine is the only effective and available medication for the treatment of LID. Another effective treatment appears to be DBS. While STN-DBS can reduce the required dose of DA therapy and ameliorate LID, GPi-DBS provides greater antidyskinetic effects but does not allow to reduce medication (Ramirez-Zamora & Ostrem, 2018).

The development of LID has been associated with several factors, such as earlier age at the onset of L-DOPA treatment, total L-DOPA exposure, female sex, and possible genetic factors (Zappia et al., 2005). Nevertheless, the pathophysiological changes involved in LID are not fully understood. Nigrostriatal degeneration and exposure to L-DOPA are considered the two main factors for the development of LID (Guridi et al.,

2012; Papathanou et al., 2011). However, in the last decades, many studies have shown roles of different neurotransmitter systems in LID.

Nigrostriatal degeneration and L-DOPA therapy induce turnover and downstream signaling of striatal dopaminergic D_1 receptors and very probably also D_3 receptors (Aubert et al., 2005; Bézard et al., 2003). LID is associated with several molecular changes, such as increased FosB and prodynorphin expression at the striatal level, which are likely mediated by D_1 receptor overactivity. The increased sensitivity of the D_1 receptor enhances the activation of cAMP-dependent protein kinase A, which phosphorylates several proteins including DARPP-32. Phosphorylated DARPP-32, together with two mitogen-activated protein kinases, the extracellular signal-regulated kinases 1 and 2, has been implicated in the development of LID in PD rodents (Picconi et al., 2003; Santini et al., 2007, 2009). The striatal expression of FosB-related proteins and prodynorphin is also altered and involved in the severity of LID in PD rodents (Cenci et al., 1998; Doucet et al., 1996). The expression of other proteins such as proenkephalin or the glutamic acid decarboxylase GAD67 is also associated with the development of LID (Andersson et al., 1999; Cenci et al., 1998; Henry et al., 1999).

Apart from dysregulated DA neurotransmission, other neurotransmitters systems have been involved in the pathogenesis of LID, including the glutamatergic, noradrenergic, serotonergic, cannabinoid, cholinergic, and opioidergic systems (Espay et al., 2018; Vijayakumar & Jankovic, 2016a, 2016b). Experimental and clinical findings have provided compelling evidence for the prominent role of the serotonergic system in the pathophysiology of PD and LID (Carta et al., 2007; Navailles et al., 2011). The mechanisms underlying LID are poorly understood, but there is a consensus that the serotonergic system plays a relevant role, since L-DOPA is transformed into DA and stored and released by the serotonergic terminals (Miller & Abercrombie, 1999). These and other findings that will be discussed later suggest that the serotonergic system plays a relevant role in LID.

1.2. BASAL GANGLIA

The basal ganglia (BG) are a group of highly interconnected subcortical structures which are involved in the control and initiation of motor movement, emotion, and cognition (Lanciego et al., 2012). The BG are composed by the striatum (caudate and putamen), the external globus pallidus (GPe) and internal globus pallidus (GPi) or the entopeduncular nucleus (EP) in rodents, the subthalamic nucleus (STN), and the SNc and substantia nigra pars reticulata (SNr). The BG nuclei are shown in **Figure 1.3**.
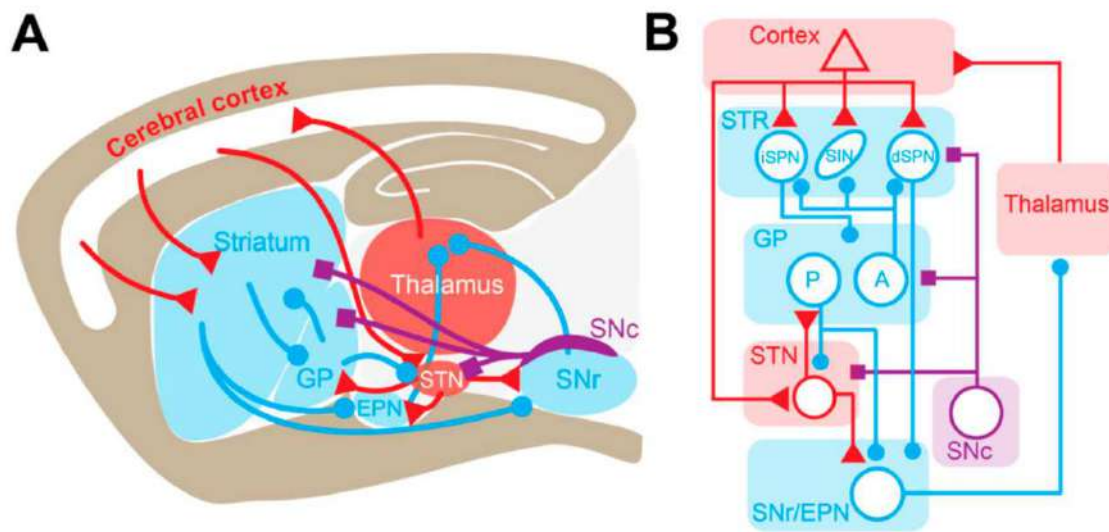
Figure 1.3. The basal ganglia nuclei and their main connections. Scheme representing the main connections of the BG network in a sagittal section of the rodent brain (A). Anatomical-functional diagram adapted from the classic model of BG circuits (B). Dopaminergic, GABAergic, and glutamatergic projections and nuclei are depicted in blue, purple, and red, respectively. Some additional connections between BG nuclei are omitted for simplicity; see the text for details. A: arkypallidal neuron; dSPN: direct-pathway spiny projection neuron; EPN: entopeduncular nucleus; GP: globus pallidus; iSPN: indirect-pathway spiny projection neuron; P: prototypic neuron; SNc: substantia nigra pars compacta; SNr: substantia nigra pars reticulata; SIN: striatal interneurons; STN: subthalamic nucleus (taken from Mallet et al., 2019).

1.2.1. Striatum

The primary afferent structure and the largest subcortical brain structure of the BG is the striatum, which is formed by the caudate (medial dorsal striatum) and the putamen (lateral dorsal striatum) nuclei divided by the fibres of the internal capsule. The nucleus accumbens (Acc) is the main component of the ventral striatum. In rats, the striatum consists of 2.8 million neurons. The striatum is mainly composed of gamma-aminobutyric acid (GABA) spiny projection neurons or medium spiny projection neurons (SPN or MSNs) that receive cortical innervation and represent 90–95% of all neurons, depending on the species, and are divided into several types of interneurons in two interlaced compartments known as "patches" (also called striosomes) and the "matrix" (Crittenden & Graybiel, 2011). The MSNs are divided into two equal proportional groups based on projections patterns: dMSNs express dynorphin (or substantia P) and dopaminergic D_1 receptor, while iMSNs express enkephalin and dopaminergic receptor D_2. Striatal dMSNs project to the GPi/SNr, while iMSNs connect to the GPe; dMSNs do however also send collaterals to the GPe (Gerfen & Surmeier, 2011). Other neurons, called interneurons, are found in the striatum: cholinergic interneurons (1–2% of all neurons) which do not present spines, the big aspiny somatostatin interneurons, and small aspiny GABAergic interneurons (Tepper et al., 2018; Tepper & Bolam, 2004). The striatum receives glutamatergic projections from the cerebral cortex and the thalamus as well as the STN, and GABAergic projections from the GPe; it is the principal recipient of dopaminergic inputs from the SNc (Hazrati et al., 1990). In addition, the striatum receives serotonergic projections from the dorsal raphe nucleus (DRN) (Huang et al., 2019; Steinbusch et al., 1981) and also discrete noradrenergic input from the *locus coeruleus* (Fitoussi et al., 2013; Mason & Fibiger, 1979).

1.2.2. Globus pallidus

The globus pallidus is located medially to the putamen and can be divided into the external (GPe, or simply named GP in rodents) and the internal (GPi/EP) nucleus. In rats, the GPe consists of approximately 45,000 big ovoid GABAergic projection neurons (Oertel and Mugnaini, 1984) that can be divided in two subtypes, the so-called prototypic and arkypallidal neurons (Abdi et al., 2015; Mallet et al., 2012). Prototypic neurons are the convectional neurons and represent approximately two-thirds of all GPe neurons, they

often express parvalbumin and innervate downstream nuclei (the STN, the SNr, and the EP) but also the striatum (Abdi et al., 2015; Saunders et al., 2016). Arkypallidal neurons (one-fourth of all neurons) often express preproenkephalin and innervate the striatum exclusively, which certainly constitutes the main GABAergic projection of the striatum (Abdi et al., 2015; Mallet et al., 2012). The GPe receives afferents from striatal iMSNs, while the GPi/EP receives afferents from the striatal dMSNs as well as glutamatergic inputs from the STN (Reiner & Anderson, 1990). Both the GPe and GPi also receive serotonergic projections from the DRN (Perkins and Stone, 1983). Finally, the GPe also receives dopaminergic inputs from the SNc; the dopaminergic innervation is however much weaker than that from the striatum (Rommelfanger & Wichmann, 2010).

1.2.3.   Subthalamic nucleus

The STN is located ventral to the thalamus and is the only glutamatergic nucleus of the BG. A total of 23,000 neurons has been determined in rats (Hardman et al., 2002). The STN neurons mainly express AMPA and NMDA glutamatergic receptors, but other neurotransmitter receptors are located there as well (Mallet et al., 2019). Apart from these glutamatergic neurons, GABAergic interneurons have been detected, but only in the human STN (Hamani et al., 2004; Lévesque & André, 2005; Parent & Hazrati, 1995).

The intrinsic organization and the afferent and efferent connections of the STN divide the nucleus into the following functional domains (Temel et al., 2005). The medial part of the STN projects to the ventral GPe and is connected to the associative and limbic functions. In contrast, the lateral part of the STN projects to the dorsal parts of the GPe, the GPi/EP and the SNr, and is connected to sensorimotor cortical functions. Specifically, the STN innervates mainly the SNr, but the STN-SNc connection is nevertheless considered one of the principal mechanisms underlying the control of DA release in the SNc (Benarroch, 2009; Parent & Hazrati, 1995). Apart from that, the STN also innervates the striatum, the ventral tegmental area, and the pedunculopontine tegmental nucleus (Kita & Kitai, 1987; Parent & Hazrati, 1995).

The STN, on the other hand, receives information from the sensorimotor cortex and the striatum (Parent and Hazrati, 1995), but also serotonergic input, mainly from the DRN, that clearly modulates its neuronal activity (Di Matteo, 2008). Additionally, the

STN receives glutamatergic projections from the thalamus, dopaminergic inputs from the SNc, and cholinergic innervation from the pedunculopontine tegmental nucleus (for a detailed review see Hamani et al., 2004).

1.2.4.   Substantia nigra

The substantia nigra (SN) is located in the ventral midbrain and is composed by two distinct functional regions. The most dorsal region is called "compacta" (SNc) and contains mainly dopaminergic neurons, while the ventral region is called "reticulata" (SNr) and contains mainly GABAergic neurons. The SNc is a densely packed nuclear region with a high neuromelanin pigment content, which is produced in the DA biosynthesis pathway. The SNc is formed by dopaminergic neurons and is one of the most important dopaminergic nuclei in the central nervous system. It also contains a population of GABAergic interneurons.

The SNc sends dopaminergic projections to the putamen, and the caudate nuclei (or the striatum), through the medial forebrain bundle (Giménez-Amaya & Graybiel, 1990). These projections inhibit iMSNs and stimulate dMSNs. Over 70% of SNc inputs are GABAergic afferent projections from the SNr, striatum, and GP (Tepper et al., 1995). Moreover, the SNc receives glutamatergic innervation from the STN, the pedunculopontine tegmental nucleus, and the medial prefrontal cortex (Naito & Kita, 1994). The SNc also receives serotonergic projections from the medial raphe and DRN (Corvaja et al., 1993; Moukhles et al., 1997), and noradrenergic innervation from the *locus coeruleus* (Baldo et al., 2003; Mejías-Apuonte et al., 2009).

1.2.5. The basal ganglia output nuclei

The main BG output nuclei are the EP/GPi and the SNr. The classical BG model of motor control (Alexander et al., 1986; DeLong, 1990) described the EP and SNr as performing the same function. In the last years, a number of studies have demonstrated that each BG output nucleus performs different functions with differential effects on both limbic and sensorimotor subcircuits. The sensorimotor regions of the EP and SNr appear to be more similar in function. Both target motor thalamic regions and primarily consist of GABAergic projection neurons. While the EP projects to lateral portions of the ventrolateral thalamus, the SNr seems to project mostly to the medial ventrolateral and ventromedial thalamus and the superior colliculus (Oh et al., 2014; Root et al., 2018; Wallace et al., 2017) (see **Figure 1.4**). This anatomical difference suggests that each BG output nucleus represents a different function in the BG-thalamo-cortical loops. Since this thesis focuses on the BG output nuclei, these nuclei will be described in detail.
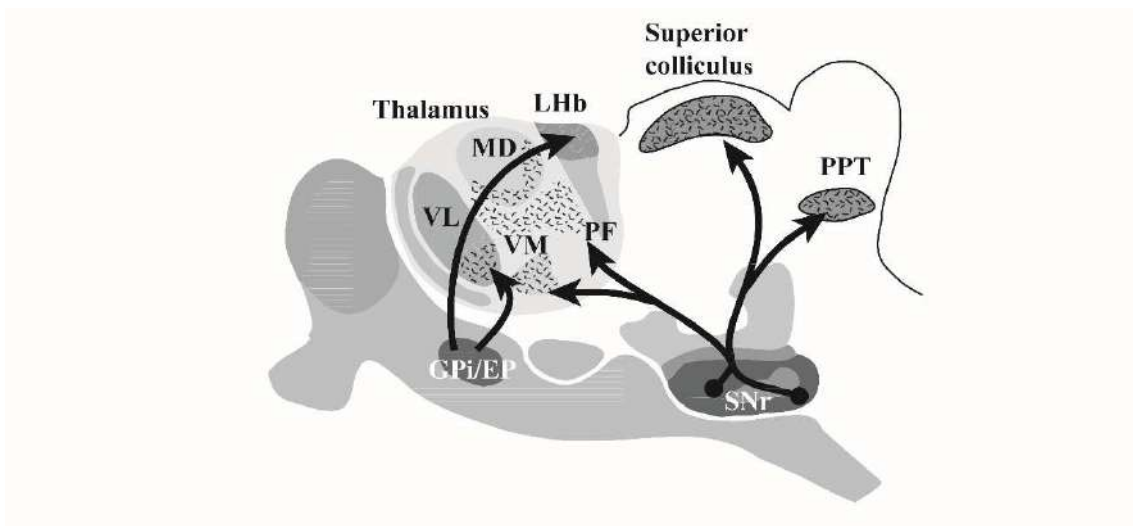
Figure 1.4. Basal ganglia output pathways arise from GABAergic neurons in the internal globus pallidus and the substantia nigra pars reticulata. The GPi/EP output is directed to the VL thalamus and to the LHb. The SNr output is directed to the MD, and PF, and VM thalamic nuclei, to the intermediate layers of the superior colliculus, and to the PPT. GPi/EP: internal globus pallidus; LHb: lateral habenula; MD: mediodorsal thalamus; PF: parafascicular thalamus; PPT: pedunculopontine tegmental nucleus; SNr: substantia nigra pars reticulata; VL: ventrolateral thalamus; VM: metromedial thalamus. Adapted from Dudman & Gerfen, 2015.

1.2.5.1. Entopeduncular nucleus

The GPi, or EP in rodents, is a major BG output nucleus and the smallest nucleus of the circuit with a population of 3,000 neurons (Oorschot, 1996). Anatomical studies have revealed the existence of cellular heterogeneity within the rodent EP and GPi of humans and primates (Miyamoto and Fukuda, 2015; Parent et al., 2001; Takada et al., 1994). It is now known that the EP is not only a GABA-releasing nucleus but the main brain structure containing dual glutamatergic-GABAergic neurons (Root et al., 2018). Additional molecular profiling has shown the existence of three neuronal subtypes and has specified their molecular identity. The proportions of these three populations have been estimated as one fourth of parvalbumin neurons, two fourths of somatostatin neurons, and one fourth of non-parvalbumin neurons (Wallace et al., 2017).

The different classes of neurons are distributed along the EP, with the rostral or anterior region expressing somatostatin while neurons in the caudal or posterior region express parvalbumin. Most parvalbumin EP neurons are purely GABAergic neurons (Penney & Young, 1981), and somatostatin EP neurons are capable of co-releasing both GABA and glutamate. However, a small subpopulation of parvalbumin EP neurons are exclusively glutamatergic and are mostly found at the borders of the EP and at the interface between the parvalbumin and somatostatin zones. Interestingly, these two classes of neurons and the differential expression of somatostatin and parvalbumin are preserved across mammals (Grillner & Robertson, 2016).

Types of receptors in the entopeduncular nucleus

The rat EP neurons express different types of receptors. One recent immunohistochemical study revealed that the dopaminergic system can modulate EP activity directly via DA transporter (DAT) and dopaminergic receptors (D_{1-5}) (Lavian et al., 2018). The glutamatergic AMPA receptor (GluR1, GluR2/3, GluR4) and glutamatergic NMDA (NR1) receptors are localized in the EP (Clarke & Bolam, 1998). $GABA_A$ receptors mainly contain subunits α1, β2, and γ2, but α2, α3, β1, β3, and γ1 are also expressed. The $GABA_B$ subunits R1 and R2 are strongly expressed (Boyes & Bolam, 2007). Serotonin (5-HT) receptors are also localized in the GPi/EP. The 5-HT_{1B} subtype is highly expressed, but 5-HT_{1A}, 5-HT_{1D}, 5-HT_{2A}, and 5-HT_{2C} are also present (Di Matteo

et al., 2008). Although cholinergic receptors within the BG nuclei have not been well characterized, it is known that nicotinic and muscarinic M_2 type receptors are localized in the EP (Luo & Kiss, 2016). Finally, the μ, κ, and δ opioid and CB_1 endocannabinoid receptors are also present in the EP (Mansour et al., 1993; Schroeder & Schneider, 2002; Sharif & Hughes, 1989; Svíženská et al., 2008).

Afferents and efferents of the entopeduncular nucleus

The EP receives glutamatergic projections from the STN (Alexander, 1990), but also from the prefrontal cortex including the insular, orbitofrontal, and anterior cingulate cortex (Naito & Kita, 1994). It also receives GABAergic projections from the GPe (Hazrati et al., 1990) and from striatal iMSNs (Gerfen et al., 1990). Like the GPe, the EP exhibits moderately dense innervation from the DRN (Moore et al., 1978; Perkins & Stone, 1983) and, to a lesser extent, dopaminergic projections from the SNc (Lindvall & Björklund, 1979).

The GPi/EP principally sends projections to the ventral anterior and ventral lateral regions of the thalamus that are also connected to the cortex. However, the GPi/EP also projects to the centromedian thalamic nucleus, the lateral habenula, and the pedunculopontine tegmental nucleus (Parent and Hazrati, 1995) (**Figure 1.4**). Apart from these projections, in rats, the EP sends fibres to the parafascicular thalamic nucleus (Carter & Fibiger, 1978) and to the deeper layers of the superior colliculus (Takada et al., 1994). Somatostatin EP neurons are known to project to the lateral habenula, while parvalbumin EP neurons innervate the motor thalamus (Stephenson-Jones et al., 2016; Wallace et al., 2017). Therefore, EP-thalamic neurons are innervated by parvalbumin GPe neurons and matrix iMSNs, while EP-lateral habenula neurons receive inputs from non-parvalbumin GPe neurons and striosome dMSNs, suggesting that each population takes part in the distinct functional networks. It has been proposed that EP-thalamic projection neurons process motor control tasks, such as movement initiation and organization as well as action selection, while lateral habenula-EP projection neurons participate in the evaluation of the motor outcome, that is, localization and direction of a targeted movement (Stephenson-Jones et al., 2016; Wallace et al., 2017).

1.2.5.2. Substantia nigra pars reticulata

The SNr is the other main BG output nucleus. While the SNr has classically been considered a homogeneous nucleus, it is known now that this nucleus is mainly formed by GABAergic neurons, discrete clusters of dopaminergic neurons are however also found in the caudomedial region (González-Hernández & Rodríguez, 2000). Thus, the SNr is composed of approximately 30,000 GABAergic neurons and 7,000 dopaminergic neurons per hemisphere in the rat (Oorschot, 1996). The majority of SNr GABAergic neurons express parvalbumin and are localized in the lateral two-thirds of the entire rostrocaudal extent, the sensorimotor region of the SNr (Rajakumar et al., 1994; Reiner & Anderson, 1993). A small population of SNr GABAergic neurons express calretinin (Liang et al., 1996), nitric oxide synthase, or acetylcholine transferase (González-Hernández et al., 2000). In the rostrolateral region of the SNr, GABAergic neurons are large and contain parvalbumin and nitric oxide synthase. In the caudomedial region, most SNr neurons are small and express only parvalbumin, while in the rostromedial region, they are predominantly small and contain either calretinin, nitric oxide synthase, or parvalbumin (González-Hernández et al., 2000).

Types of receptors in the substantia nigra pars reticulata

Several dopaminergic receptors (D_1, D_4 and D_5) are expressed in SNr GABAergic neurons and astrocytes (Nagatomo et al., 2017; Rivera et al., 2003). Several subtypes of glutamatergic i.e. AMPA ($GluR_{2/3}$), NMDA (NR_1, NR_2 and $NR2_{A/B}$) and kainate receptors are also localized in the SNr (Albin et al., 1992; Chatha et al., 2000). The vast majority of parvalbumin SNr neurons display $GABA_A$ receptors mainly containing subunits α_{1-5}, $\beta_{2, 3}$, and γ_2 (Ng et al., 2000; Ng & Yung, 2001). On the other hand, SNr GABAergic neurons express several 5-HT receptors, with 5-HT_{2C} and 5-HT_{1B} highly expressed but 5-HT_{1A} and 5-HT_{1D} also present (Di Matteo, 2008). The SNr also expresses multiple cholinergic receptors, mainly muscarinic M_4 and nicotinic α_7 (Poisik et al., 2008; Turski et al., 1984; Xiang et al., 2012). The different subtypes of opioid receptors, μ, κ, δ, and NOP (nociceptin/orphanin FQ opioid peptide) receptors, are also found in the rat SNr (Mabrouk et al., 2008; Mansour et al., 1993; Tempel & Zukin, 1987). While CB_1 and CB_2 endocannabinoid receptors are also found in SNr neurons and glial cells (Herkenham et al., 1991; Gong et al., 2006), some SNr neurons express the purinergic receptor P2

(Amadio et al., 2007) and histamine receptors H_2 and H_3 (Vizuete et al., 1997; Zhou et al., 2006).

Afferents and efferents of the substantia nigra pars reticulata

The SNr receives GABAergic projections principally from the striatum and the GPe. Thus, dMSNs project to the SNr via the "direct pathway". In contrast, iMSNs project to the SNr via the GPe and STN via the "indirect pathway" (Gerfen et al., 1990; Alexander, 1990). The Acc also sends GABAergic innervation to the SNr (Deniau et al., 1994) and the STN emits glutamatergic projections to the SNr (Hammond et al., 1978; Kitai and Kita, 1987). In addition, the SNr receives dense serotonergic innervation from the DRN (Corvaja et al., 1993; Moukhles et al., 1997), cholinergic input from the pedunculopontine tegmental nucleus, and modulatory dopaminergic input from the SNc (Lee & Tepper, 2009).

As previously mentioned, while there is some overlap in the projections from the SNr and the EP, they predominantly target distinct structures in the thalamus (Gerfen, 1984; Steinbusch et al., 1981). The main target of the SNr is the motor thalamus (Kha et al., 2001) and four populations of SNr neurons have been described based on their axonal projections. Type I neurons project specifically to the motor thalamus, type II neurons target the thalamus, superior colliculus, and pedunculopontine tegmental nucleus, type III cells project to the periaqueductal grey matter and thalamus, and type IV neurons send projections to the deep mesencephalic nucleus and the superior colliculus (Brown et al., 2014; Cebrián et al., 2005; Deniau et al., 2007; Higgs & Wilson, 2016). However, while the EP/GPi projects to the ventral lateral thalamic nuclei and the lateral habenula, the SNr projects to the ventral medial, zona incerta, and intralaminar thalamic nuclei (see **Figure 1.4**). Thus, the SNr is associated with the motor control of orienting movements, head movement generation, and saccadic eye movements, as well as with the regulation of nigrostriatal dopaminergic neurons (Brown et al., 2014; Rizzi & Tan, 2019).

1.2.6.   Basal ganglia motor circuit

The BG nuclei are a highly organized network that connects the cerebral cortex to the thalamus, creating the cortico-BG-thalamo-cortical loop. Since the late 1980s, several authors have proposed a "classical" or functional mechanism of the BG motor circuit (Alexander et al., 1986; Albin et al., 1989). The implicated nuclei and their connections are shown in the schemes in **Figure 1.5**. This circuit can be separated into three different pathways, (a) the hyperdirect or cortico-subthalamo-pallidal/nigral pathway, (b) the direct cortico-striato-pallidal/nigral pathway, and (c) the indirect cortico-striatal-pallidal-subthalamo-pallidal/nigral pathway (Maurice et al., 1999). For a better understanding of the BG circuit, the three pathways are described in detail below.

According to the classical BG model, the striatum is the main input station of the BG. The direct pathway originates in the striatal dMSNs, which project directly to the GPi/EP and the SNr. The indirect pathway, on the other hand, originates in the striatal iMSNs, which project to the prototypic neurons of the GPe; the signal later arrives at the STN and, from here, is transmitted to the parvalbumin GABAergic neurons of the GPi/EP and the SNr. However, the STN likely functions as another input station of the BG, besides the striatum, because it receives direct cortical projections, especially from the frontal lobe and subdivisions of the premotor cortex. In addition, the cortico/STN neurons and cortico/striatal neurons belong to distinct populations. Thus, the hyperdirect pathway conveys powerful excitatory effects from the motor-related cortical areas to the GPi/EP and SNr, bypassing the striatum, with a very short conduction time (Maurice et al., 1999; Miocinovic et al., 2018; Monakow et al., 1978; Nambu et al., 2002).

The direct striato-EP/SNr and indirect striato-GPe-STN-EP/SNr pathways play opposite roles in the control of movements. The classical BG model predicts that the activation of cortico-striatal projections leads to the inhibition of the GPi/EP and the SNr via the direct pathway. This causes a reduction in the GABAergic inhibitory input to the thalamus, which leads to an increase in excitatory activity over the motor cortex and results in the release of movements. In contrast, activation of cortico-striatal projections leads to a reduction in GPe activity, inducing a lower inhibitory effect on the STN, leading to an increase in excitatory glutamatergic activity over the BG output nuclei. The GPi/EP and SNr nuclei then increase their inhibitory effect on the thalamus, thereby inhibiting

the thalamocortical connections and resulting in the suppression of movements. This effect is mediated via the indirect pathway (**Figure 1.5A**) (Albin et al., 1989; DeLong 1990; Gerfen et al., 1990; Kravitz et al., 2010; Chiken et al., 2015).

1.2.7. Basal ganglia nuclei in Parkinson's disease and levodopa-induced dyskinesia

According to the classical BG model *(*Alexander et al., 1986; Albin et al., 1989; DeLong, 1990), the nigrostriatal degeneration during PD induces a reduction in the activity of dMSNs in the direct pathway and, in consequence, a reduction in the inhibition over the GPi/EP and the SNr. On the other hand, there is a hyperactivity of striatal iMSNs in the indirect pathway which leads to an inhibition of the GPe, causing a hyperactivity of STN neurons and, in consequence, the STN releases more GLU and hyperactivates the BG output nuclei. The hyperactivity of the output BG nuclei then leads to hypoactivity of the thalamic-cortical projections and results in hypokinetic movements (**Figure 1.5B**). It is generally assumed that after chronic L-DOPA therapy, iMSNs and dMSNs are overstimulated, which leads to overactivity of the direct pathway and inhibition of the indirect pathway. These changes then lead to an increase in glutamatergic thalamo-cortical projections and result in excess motor movements or LID (**Figure 1.5C**).

The classical BG model hypothesized that the origin of motor dysfunction is the loss of DA, and that this loss induces an abnormal neuronal firing rate within the BG nuclei, which may be relevant in the pathophysiology of PD. However, the model fails to explain other features of neuronal firing that are observed in PD, such as the increased burst firing activity and the increased synchronization and oscillatory activity, particularly in the beta frequency band, in the BG nuclei (Wichmann & Dostrovsky, 2011).
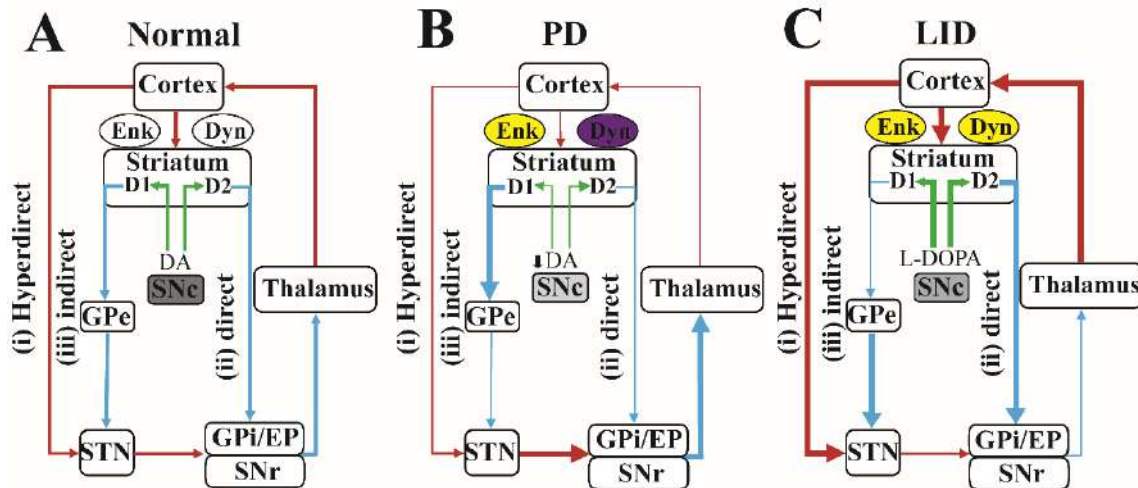
Figure 1.5. The classical basal ganglia model representing (A) normal, (B) Parkinson's disease, and (C) levodopa-induced dyskinesia conditions. Normally, DA input from the SNc facilitates motor movement through excitatory responses in the direct pathway via dopaminergic D_1 receptors and reduces motor movements through inhibitory responses in the indirect pathway via dopaminergic D_2 receptors. Loss of dopaminergic input from the SNc influences both the direct and the indirect pathway. There is underactivity of the direct pathway and overactivity of the indirect pathway, resulting in decreased glutamatergic output from the thalamus, thereby causing hypokinetic movements. Chronic L-DOPA therapy overstimulates both D_1 and D_2 receptors, with opposite influence on the direct and indirect pathways leading to increased thalamo-cortical glutamatergic output, thereby causing LID. Changes in the expression of Enk and Dyn are depicted in yellow (increased levels) and purple (decreased levels). The clear intensity of the grey colour of SNc represents the loss of dopaminergic neurons. Blue lines indicate GABAergic or inhibitory connections; red lines glutamatergic or excitatory connections, and green lines dopaminergic or modulatory connections. Changes in the rate of neural transmission are indicated with thick (increased activity) and thin (decreased activity) lines. DA: dopamine; Dyn: dynorphin; Enk: enkephalin; GPe: external globus pallidus; GPi: internal globus pallidus; L-DOPA: levodopa, STN: subthalamic nucleus; SNc: substantia nigra pars compacta; SNr: substantia nigra pars reticulata.

Oscillatory activity is a property of neurons and is defined as rhythmic neuronal fluctuations that occur periodically. This may be reflected in single-unit spikes, in the electroencephalogram (EEG), electrocorticogram (ECoG), or in local field potentials (LFPs). The ECoG provides rich information about synaptic currents from the deep layers of the cortex, while LFPs reflect net postsynaptic potential changes from synaptic input and do not necessarily correlate with spiking behaviour (Ellens and Leventhal, 2013). Neuronal oscillations are crucial for efficient communication within and across the brain circuits, and have been implicated in different processes such as cognition, locomotion, learning, and alert (Uhlhaas & Singer, 2006). Neuronal oscillations are organized in different frequency bands categorized into delta (< 4 Hz), theta (4–8 Hz), alpha (8–12 Hz), beta (12–30 Hz), gamma (30–90 Hz), and high-frequency (>90 Hz) oscillations, as well as into subdivisions within each band (Buzsáki & Chrobak, 1995; Assenza et al.,

2017). Under normal physiological conditions, low-frequency or delta oscillations are the most prominent EEG feature of human non-rapid eye movement sleep, also known as the "slow-wave" state (~1 Hz) (Steriade, 2006). These slow waves are also prominent in the cortex of anaesthetised rodents and reflect spontaneous neural activity from ECoGs, LFPs, and single-unit spikes. The examination of slow-wave oscillatory activity in anaesthetised rodents has become a useful tool to study the functional dynamics of activity in the BG networks. Interestingly, slow-wave oscillatory activity in the BG is enhanced by 6-OHDA lesions (Tseng et al., 2001). In addition, it is well documented that the pattern of burst activity after 6-OHDA lesions correlates with slow-wave frequency oscillations occurring in cortical networks (Magill et al., 2001; Tseng et al., 2001).

It has thus been proposed that a loss of DA alters the striatal processing of oscillatory cortical input that promotes the synchronization within the BG nuclei observed in anaesthetised rats. The increased phasic oscillatory activity in the GPe as a consequence of striatal output, in conjunction with convergent oscillatory input from the cortex, contributes to the oscillatory activity in the STN. In addition, increased oscillatory activity in the GPi/SNr is consistent with convergent inhibitory input from the GPe and excitatory oscillatory input from the STN (Mallet et al., 2006; Walters et al., 2007; Parr-Brownlie et al., 2007). **Figure 1.6** summarizes the passage of oscillatory signals within the BG nuclei. However, the other faster frequencies are also affected and contribute to the exaggerated oscillatory activity observed in patients with PD (Belluscio et al., 2007; Zold et al., 2012).

Abnormal oscillatory activity in the beta frequency band is the most prominent neuronal change detected in patients with PD and has been related to tremor and akinesia/bradykinesia syndromes in PD (Brown, 2006a, 2006b; Dostrovsky & Bergman, 2004), while abnormal oscillatory activity in the gamma frequency band is thought to be prokinetic and to underlie dyskinesia (Salvadè et al., 2016; Sharott et al., 2014). However, the abnormalities in beta and gamma oscillations cannot by themselves explain all the motor and non-motor symptoms underlying this pathophysiology and, together with pathological activity in other frequency bands, may result in different manifestations of PD.
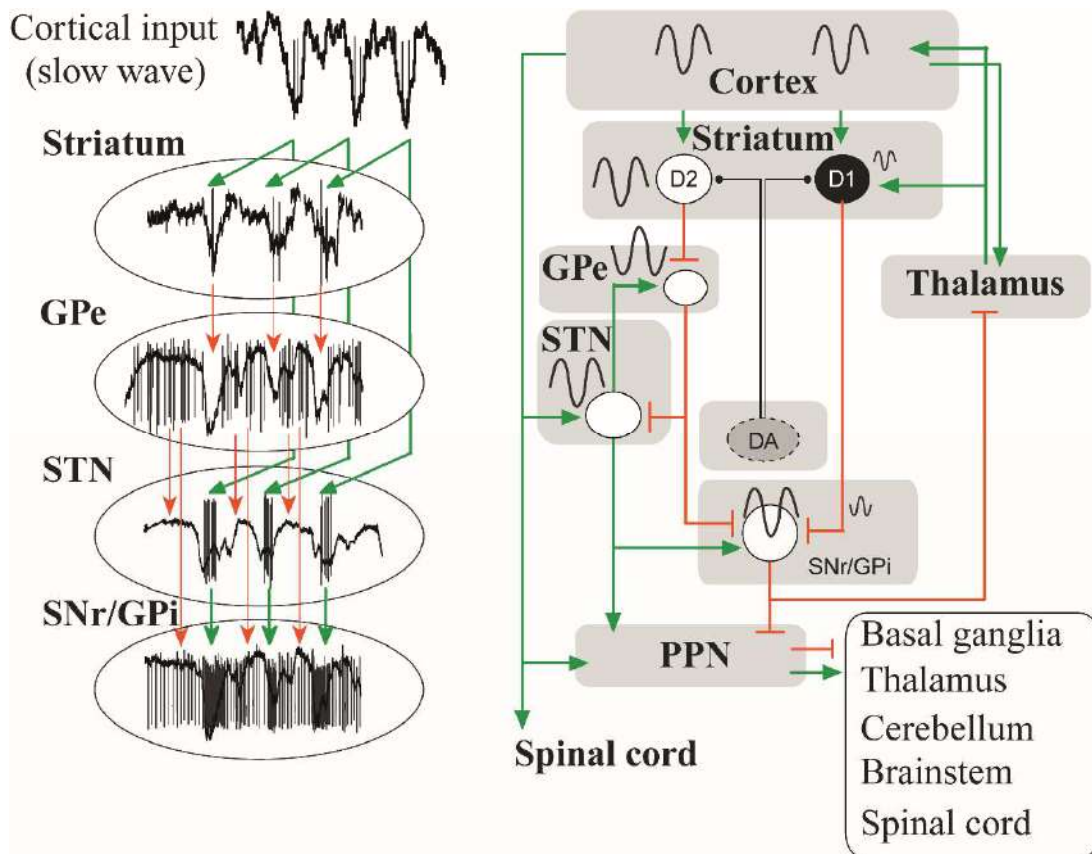
Figure 1.6. Illustration of the passage of oscillatory signals in the low frequency range (0.3–2.5 Hz (through the cortico-basal ganglia pathway after 6-hydroxydopamine lesion in anaesthetised rats. Left diagram: Examples of striatal, GPe, STN, and SNr/GPi spiking activity are shown with simultaneously recorded SNr/GPi LFPs. Right diagram: the loss of DA enhanced the transmission of oscillatory activity primarily through the indirect pathway, resulting in robust oscillatory activity in the BG output nuclei, SNr/GPi. The D2-iMSNs transmit patterned activity from the cortex to the GPe. The inhibitory GPe activity contributes to the timing of bursts in STN neuron activity, and pauses in inhibitory GPe output coincide with bursts in excitatory STN output, supporting enhanced oscillatory activity in SNr/GPi spike trains. Cortical oscillatory input to the striatum and STN is indicated. Green arrows indicate excitatory connections between nuclei, and red arrows or bars indicate inhibitory connections. DA: dopamine; Dopaminergic D_1 and D_2 receptors; GPi: internal globus pallidus; GPe: external globus pallidus; PPN: pedunculopontine nucleus; STN: subthalamic nucleus; SNc: substantia nigra pars compacta; SNr: substantia nigra pars reticulata (taken and adapted from Walters, 2016).

1.3. THE SEROTONERGIC SYSTEM IN PARKINSON'S DISEASE AND LEVODOPA-INDUCED DYSKINESIA

5-HT is synthesized from tryptophan by the enzyme tryptophan hydroxylase (Cooper & Melcer, 1961) and accumulates in secretory granules via a vesicular monoamine transporter before being released to the synaptic cleft. In the central nervous system, the action of 5-HT is terminated either via neuronal uptake by the 5-HT reuptake transporter (SERT) located in 5-HT axon terminals, or through enzymatic metabolism by monoamine oxidase to 5-hydroxyindoleacetaldehyde and the principal metabolite, 5-hydroxyindoleacetic acid (Dorszewska et al., 2014). 5-HT acts via 5-HT receptors, which are classified into seven families and at least 14 different subtypes, including the G-protein-coupled receptor subtypes (5-HT$_1$, 5-HT$_2$, 5-HT$_{4-7}$) and ligand-gated ion channels (5-HT$_3$) (Hoyer et al., 2002).

The main population of serotonergic neurons is located in the DRN (Peyron et al., 1998), which provides extensive innervation to almost the entire brain and controls multiple functions such as mood, cognition, emotion, motor behaviour, sleep, appetite, and regulation of the circadian rhythm (Benarroch, 2009). The serotonergic system is also involved in the aetiology of numerous neuropsychiatric disorders such as depression and anxiety. The serotonergic neurons from the DRN innervate almost all brain areas including the BG nuclei, the pedunculopontine nucleus, the ventral tegmental area, the thalamus, and the cortex (Huang et al., 2019; Muzerelle et al., 2016) (**Figure 1.7**). In addition, the BG nuclei contain 5-HT, SERT, and almost all 5-HT receptor subtypes that are differently distributed within the BG nuclei. However, the effects of 5-HT drugs on the BG nuclei are complex, since they are the result of the direct activation of 5-HT receptors in the different nuclei plus the activation of those located on serotonergic neurons that project to the BG (for a review, see Miguelez et al., 2014). Despite this complexity, it is well accepted that the serotonergic system modulates the activity of the BG (Benarroch, 2009; Di Matteo et al., 2008).
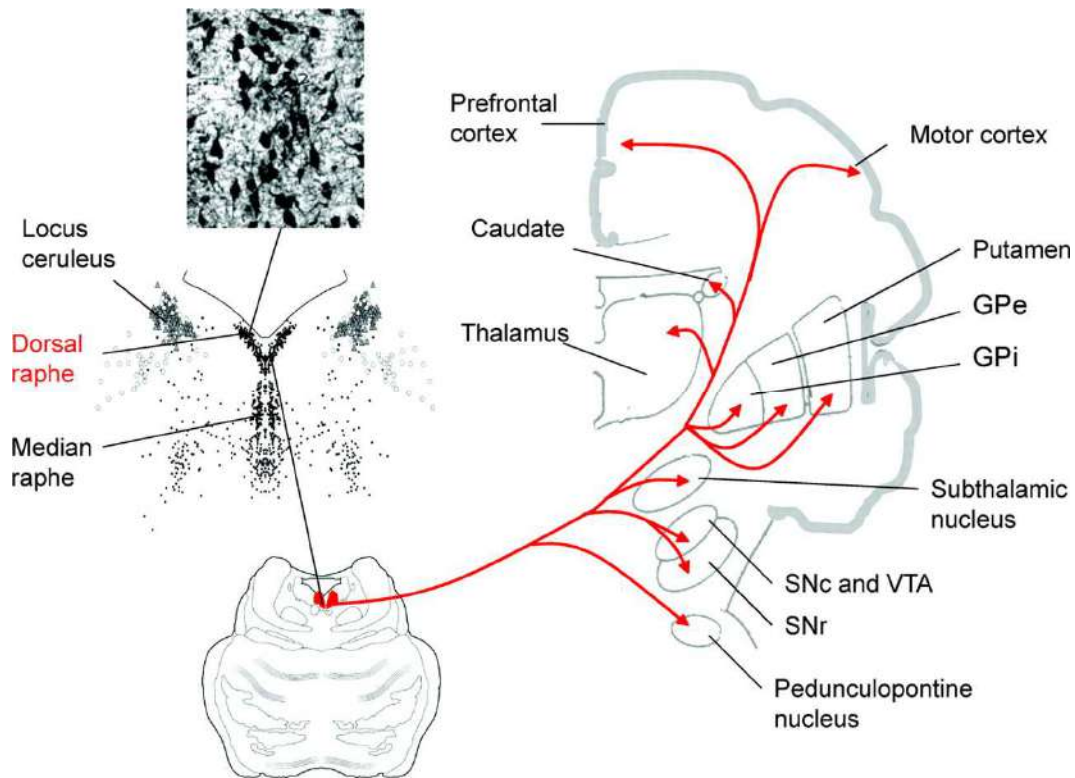
Figure 1.7. Serotonergic innervation of the basal ganglia nuclei. The dorsal raphe nucleus sends serotonergic projections to all components of the BG: the striatum, GPe, GPi, SNc, SNr, and subthalamic nucleus. Other nuclei such as the pedunculopontine nucleus and the ventral VTA also receive afferences from the dorsal raphe nucleus. GPi: internal globus pallidus; GPe: external globus pallidus; SNc: substantia nigra pars compacta; SNr: substantia nigra pars reticulata; PPN: pedunculopontine nucleus; VTA: ventral tegmental area. Taken from Benarroch (2009).

1.3.1. The serotonergic system in the progression of Parkinson's disease

According to the six-stage theory of Braak, the forebrain, including the *locus coeruleus*, reticular formation, raphe nuclei, and spinal cord, becomes affected in stage 2 of the disease, and specifically the raphe nuclei are entirely involved in stage 3 (Braak et al., 2003). Post-mortem studies from patients with PD who died during the early stages of Lewy pathology have shown intracellular accumulation of α-syn in the raphe nuclei (Braak et al., 2003), along with a loss of serotonergic neurons (Halliday et al., 1990) and dystrophic degeneration of serotonergic axons in the cortex, hippocampus, and SN (Azmitia & Nixon, 2008). Alterations of several components of 5-HT neurotransmission, such as a reduction in 5-HT and its metabolite 5-hydroxyindoleacetic acid, tryptophan hydroxylase, and SERT have been described in the striatum (Kish et al., 2007) and the hypothalamus (Shannak et al., 1994).

Studies in neurotoxic animal models of PD (6-OHDA, MPTP) have provided heterogeneous results regarding the serotonergic system, showing either no change or increased activity of 5-HT cells and diverse modifications of 5-HT receptor expression. In general, these animals show alterations involving the serotonergic system that depend on the loss of DA (for a review, see Gagnon et al., 2018; Miguelez et al., 2014). Interestingly, in transgenic mice expressing human mutant LRRK2 G2019S, a model of the most common genetic cause of PD, along with a progressive loss of dopaminergic fibers in the striatum, 5-HT levels declined, and $5-HT_{1A}$ receptor expression increased in the hippocampus (Lim et al., 2018a). Findings of stereological studies using MPTP parkinsonian monkeys revealed a sprouting of 5-HT axon varicosities in the striatum and GPe and GPi, while the density and morphology of serotonergic neurons in the DRN were unchanged (Gagnon et al., 2018). These results, according to the authors, suggest the rearrangement of the surviving serotonergic neurons (Gagnon et al., 2016; Gagnon et al., 2018).

1.3.2. The serotonergic system in levodopa-induced dyskinesia

The dopaminergic and serotonergic systems are functionally connected and 5-HT, via its numerous receptors, modulates dopaminergic transmission and DA levels in the striatum (Alex & Pehek, 2007; Lucas et al., 2000). Raphe-striatal serotonergic terminals contain the enzyme aromatic L-amino acid decarboxylase and are able to convert exogenous L-DOPA into DA, store it in vesicles, and release it. However, serotonergic neurons lack the proper autoregulatory mechanisms to control DA release and clearance, which can cause excessive DA levels in several brain regions (De Deurwaerdère et al., 2017; Miller & Abercrombie, 1999). It has been suggested that serotonergic neurons are mainly responsible for the increase in DA release in the striatum induced by chronic L-DOPA treatment (Carta et al., 2007, 2008). With the progression of PD, the dysregulated release of DA from serotonergic neurons acting as a "false neurotransmitter" plays a key role in LID development (Carta et al., 2007, 2008; Navailles et al., 2011; Nevalainen et al., 2011).

Long-term L-DOPA administration may damage the serotonergic system in PD. L-DOPA-derived DA displaces 5-HT in exocytotic vesicles, is trapped in the serotonergic terminal, and may be degraded by the enzyme MAO and auto-oxidation mechanisms,

resulting in the production of reactive oxygen species (Stansley & Yamamoto, 2014) and the subsequent detrimental effects (Navailles et al., 2011; Stansley & Yamamoto, 2015a). Thus, L-DOPA can promote oxidative stress, generate free radicals or toxic compounds (Stansley & Yamamoto, 2015b) and cause 5-HT cell death and the depletion of 5-HT content in a subregion of the DRN and the frontal cortex (Stansley & Yamamoto, 2014). **Figure 1.8** summarizes the factors associated with PD and chronic L-DOPA treatment that cause changes, damage, and dysfunction of the serotonergic system and that may be clinically relevant not only regarding motor and non-motor symptoms but also in terms of PD treatment.
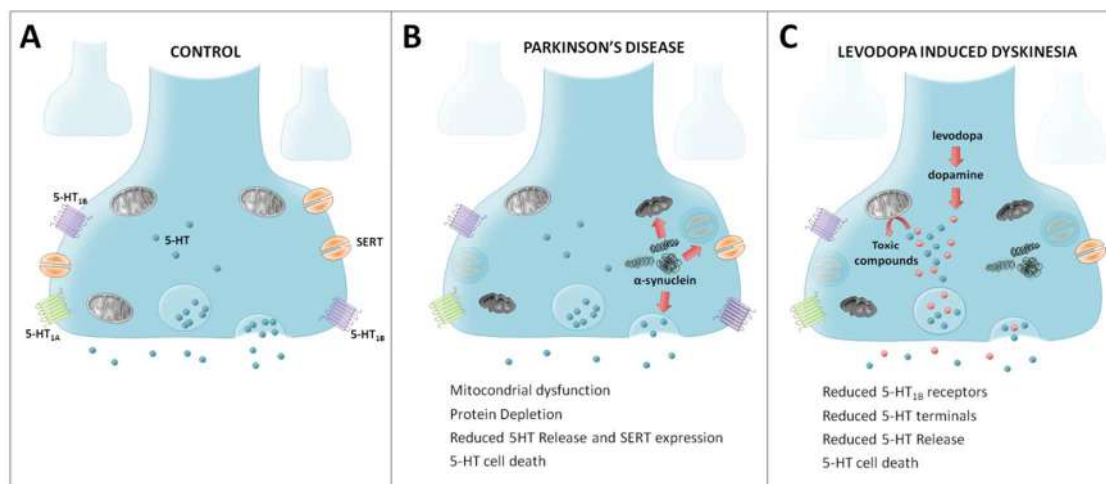
Figure 1.8. Serotonergic neuron modifications in Parkinson's disease and levodopa-induced dyskinesia. (A) Control situation. (B) In Parkinson's disease, α-syn accumulates in serotonergic neurons and leads to neuronal cell death by impacting mitochondrial function, protein depletion, serotonin (5-HT) release, and SERT expression. (C) During chronic treatment with levodopa, apart from the modifications produced by α-synuclein, L-DOPA-derived dopamine competes with 5-HT for entrance into exocytosis vesicles, and the accumulation of dopamine and 5-HT in the cytoplasm induces the synthesis of toxic compounds that are harmful for the cell. 5-HT: serotonin; SERT: serotonin transporter. Taken from Vegas-Suarez et al. (2019).

1.3.3. Serotonin-based therapies for the treatment of levodopa-induced dyskinesia

Despite the complexity of the serotonergic system, only three 5-HT-related targets have been studied with the aim to alleviate LID, 5-HT_{1A}, and 5-HT_{2A} receptors as well as SERT. Among these, the 5-HT_{1A} receptor agonists are the most studied when it comes to LID symptom management (Lanza & Bishop, 2018). A partial agonist of the 5-HT_{1A} receptor, buspirone, has been shown to reduce the abnormal involuntary movements induced by chronic L-DOPA treatment in different animal models (Aristieta et al., 2012; Dekundy et al., 2007; Eskow et al., 2007; Gerlach et al., 2011; Sagarduy et al., 2016). Buspirone has also shown efficacy in open-label trials performed in humans (Bonifati et al., 1994; Kleedorfer et al., 1991; Politis et al., 2014), where LID reduction was found to be associated with the modulation of striatal DA levels quantified by imaging techniques (Politis et al., 2014). Between 2015 and 2018, the antidyskinetic properties of buspirone have been re-evaluated in a clinical phase III trial (NCT02617017). The results are however still unpublished. Currently, the efficacy of a co-therapy of buspirone and amantadine in reducing LID in participants with PD is being investigated in a clinical phase I trial (NCT02589340). This study should be completed by December 2019.

Similar to buspirone, eltoprazine, a $5\text{-HT}_{1A/B}$-receptor agonist, has shown antidyskinetic effects in 6-OHDA-lesioned rats chronically treated with L-DOPA (Lindgren et al., 2010; Paolone et al., 2015) as well as in macaques (Bezard et al., 2013). In a double-blind, randomized, placebo-controlled and dose-finding phase I/IIa study conducted in 22 patients, a single dose showed antidyskinetic effects (Svenningsson et al., 2015). However, despite these promising results, no new clinical data have been published since then. On the other hand, sarizotan, a full 5-HT_{1A} receptor agonist, improved dyskinesia in macaques (Grégoire et al., 2009) and in a rat model of LID (Gerlach et al., 2011). However, in a phase III clinical trial in patients with PD, sarizotan did not counteract LID better than placebo (Goetz et al., 2007). Tandospirone, another full agonist of the 5-HT_{1A} receptor with a chemical structure similar to that of buspirone, seems to improve LID in rats, to some degree (Iderberg et al., 2015). In contrast, clinical studies have suggested that tandospirone has no significant effect on LID and may interfere with L-DOPA efficacy (Kannari et al., 2002; Yoshida et al., 1998).

Finally, ± 8-hydroxy-2-dipropylamino tetralin (± 8-OH-DPAT), a full agonist of the 5-HT_{1A} receptor, reduces D_1 and D_2 agonist-induced dyskinesia and LID in 6-OHDA-lesioned rats (Bishop et al., 2009; Dupre et al., 2007, 2008). It has also been reported that both buspirone and 8-OH-DPAT reverse the catalepsy observed in 6-OHDA-lesioned rats (Nayebi et al., 2010), improve their motor performance (Dupre et al., 2007), and reverse L-DOPA-induced increases in c-Fos and preprodynorphin (Bishop et al., 2009) and phosphorylated extracellular signal-regulated kinases 1 and 2 (Crane et al., 2007; Lindenbach et al., 2013). However, a reduction in motor activity and worsening motor symptoms have also been observed in 6-OHDA rats (Carta et al., 2007; Dupre et al., 2007) and MPTP-treated monkeys (Iravani et al., 2006). 8-OH-DAT induces a pronounced side effect, the 5-HT syndrome, when compared to other 5-HT-based drugs (Lindenbach et al., 2015). In the last years, selectively "biased" agonists for auto- or heteroreceptors, such as NLX-112, F13714, and F15599, which were first developed for the treatment of affective disorders, have been found to alleviate LID expression without worsening motor symptoms or lowering L-DOPA efficacy (Fisher et al., 2020; Iderberg et al., 2015; McCreary et al., 2016; Meadows et al., 2017). However, these new compounds have not yet been investigated clinically regarding PD or LID symptom management.

Clozapine, an atypical antipsychotic that acts as a 5-HT_{1A} and $5\text{-HT}_{2A}/5\text{-HT}_{2C}$ antagonist, reduces LID in 6-OHDA-lesioned rats and LID and psychosis-like behaviours in MPTP-treated marmosets (Lundblad et al., 2002; Visanji et al., 2006). Two clinical trials demonstrated that clozapine effectively reduces DA-induced psychosis and LID, without interfering with L-DOPA efficacy (Durif et al., 2004; Morgante et al., 2004). Low doses of clozapine have also shown tremor improvement in patients with PD. However, the use of clozapine has been limited because of its potential adverse effects and its stringent monitoring criteria (see the review by Fox, 2013). The selective 5-HT_{2A} antagonist EMD-281,014 successfully reduced LID in parkinsonian marmosets without affecting the anti-parkinsonian action of L-DOPA (Hamadjida et al., 2018), but the same treatment failed to reduce LID in 6-OHDA-lesioned rats (Frouni et al., 2018).

In addition to 5-HT drugs, selective 5-HT reuptake inhibitors (SSRI) appear to be a potential treatment for PD and LID. Furthermore, SSRI displayed the lowest motor side effect (i.e. 5-HT syndrome) profile, compared to other 5-HT drugs, in one study performed in 6-OHDA rats (Lindenbach et al., 2015). Citalopram improved behavioural

impulsivity in advanced PD (Ye et al., 2014) and led to LID improvement without interfering with L-DOPA efficacy in 6-OHDA rats (Bishop et al., 2012; Conti et al., 2014; Lindenbach et al., 2015) but it compromised L-DOPA efficacy in MPTP-treated monkeys (Fidalgo et al., 2015). Additionally, results on the effects of citalopram in the clinic are inconclusive, because it has been reported that PD symptoms either worsened (Linazasoro, 2000; Van De Vijver et al., 2002) or improved (Rampello et al., 2002). A retrospective study of 111 patients demonstrated that SSRI exposure within the first decade after the diagnosis of PD may delay the onset of LID without interfering with L-DOPA therapy (Mazzucchi et al., 2015). Another SSRI, fluoxetine, attenuated LID but compromised L-DOPA efficacy in 6-OHDA rats (Bishop et al., 2012) and, in a small clinical trial, reduced apomorphine-induced dyskinesia without exacerbating PD symptoms (Durif et al., 1995). Recently, an open-label multi-centre randomized study showed that SSRI therapy can improve depression and gait instability in patients with PD (Takahashi et al., 2018).

In summary, even though the aetiopathogenic basis of PD and LID has not been fully determined, growing evidence indicates that there is a reduction in the activity of the serotonergic system, and that this neurotransmitter system plays a role in motor and non-motor clinical manifestations. 5-HT-based therapies could be a good strategy for the treatment of PD and LID. However, the main problem is that despite showing promising results in preclinical studies, none of the so far investigated 5-HT drugs have achieved remarkable results in clinical trials and none has been approved for use in patients. More studies are therefore needed to elucidate the roles 5-HT-based drugs could play in the management of PD and LID symptoms.

2. HYPOTHESIS AND OBJECTIVES

2. HYPOTHESIS AND OBJECTIVES

A large body of evidences supported that PD is a multisystem disorder, involving several neurotransmitter and multiple brain regions. Apart from the dopaminergic system, experimental and clinical findings have suggested the prominent role of the serotonergic system and its degeneration in the manifestation of the motor and non-motor symptoms in PD. The BG nuclei contain 5-HT, SERT and almost all 5-HT receptors. Despite the complex effect of 5-HT, it is well accepted that 5-HT modulates BG activity. Several studies have documented the potential of 5-HT-based therapy to treat both motor and non-motor symptoms in PD. Buspirone, a partial 5-HT_{1A} receptor agonist, has shown promising results in patients with PD and animal models but the mechanism involved in this therapeutic effect are not fully understood. On the other hand, the involvement of the BG output nuclei, the SNr and GPi/EP, in PD and LID have been extensively documented both in patients with PD and animal models. Abnormal burst firing as well as abnormal oscillatory activity and synchronization within the cortical-BG-thalamus circuit have been reported during PD. However, few studies have tested the effect of 5-HT-based therapies on the BG output nuclei activity and on the oscillatory activity within the BG nuclei.

Taking these findings into account we hypothesize that the antiparkinsonian and antidyskinetic properties of buspirone might be a consequence of normalizing the aberrant neuron activity of the BG output nuclei via 5-HT_{1A} receptors.

The global aim of this study was to characterize the effect of buspirone on the BG the activity of the SNr and GPi/EP, in order to define whether these nuclei are good targets to investigate potential antiparkisonian and antidyskinetic 5-HT-based treatments.

The specific objectives of the present study were:

I. To characterize the electrophysiological and amino acid release changes in the SNr induced by buspirone in sham, 6-OHDA-lesioned, and long-term L-DOPA treated 6-OHDA-lesioned rats.

II. To characterize the electrophysiological changes induced by buspirone in the EP from sham, 6-OHDA-lesioned, and long-term L-DOPA treated 6-OHDA-lesioned rats.

III. To investigate the modulation of the STN and EP electrophysiological activity by optogenetic stimulation of the STN and how buspirone alters EP neuron response induced by optogenetic stimulation of the STN.

IV. To investigate the effect of buspirone in the cortical-nigral and cortical-EP information transmission through the BG circuits by electrical stimulation of motor cortex in sham and 6-OHDA-lesioned rats.

V. To evaluate SERT and 5-HT$_{1A}$ receptor immunoreactivity expression and COX activity within the BG nuclei and the DRN in sham, 6-OHDA-lesioned, and long-term L-DOPA treated 6-OHDA-lesioned rats.

3. MATERIAL AND METHODS

3. MATERIALS AND METHODS

3.1. MATERIALS

3.1.1. Animals

Male Sprague–Dawley rats (150 g at the beginning of the experiment, SGiker facilities, University of Basque Country, UPV/EHU) were housed in standard laboratory conditions (22 ± 1 °C, 55 ± 5% of relative humidity, and a 12:12 h light/dark cycle) with ad libitum access to food and water. Experimental procedures were approved by the Local Ethical Committee of the University of Basque Country (UPV/EHU, CEEA/M20/2016/176) following European (2010/63/UE) and Spanish (RD 53/2013) regulations for the care and use of laboratory animals. Microdialysis experiments were performed in male Sprague-Dawley rats (150 g; Charles River, Calco, Lecco, Italy) following protocols approved by the Ethical Committee of the University of Ferrara and the Italian Ministry of Health (license n. 714/2016-PR). Every effort was made to minimize animal suffering and to use the minimum number of animals per group and experiment.

3.1.2. Drugs

All drugs used in this study are specified in **Table 3.1**.

Table 3.1. Used drugs and their pharmacological activity.

Drug	Activity	Purchased from
Isofluorane	Anaesthetic	ESTEVE
Urethane ethyl carbamate	Anaesthetic	Sigma- Merck
Desipramine hydrochloride	Preferential Noradrenaline reuptake inhibitor	Sigma-Merck

Pargyline hydrochloride	Monoamine Oxidase B Inhibitor	Sigma-Merck
6-OHDA 6-hydroxydopamine hydrochloride	Catecholaminergic neurotoxin	Sigma-Merck
Buspirone hydrochloride	5-HT$_{1A}$ receptor partial agonist	Sigma -Merck
Levodopa, L-DOPA 3,4-dihydroxy-L-phenylalanine methyl ester hydrochloride	Precursor of DA	Sigma- Merck
Benserazide hydrochloride	Peripheral DOPA decarboxylase inhibitor	Sigma- Merck
WAY-100635 maleate N-[2-(4-[2-Methoxyphenyl]-1-piperazinyl)ethyl]-N-2-pyridinylcyclohexanecarboxamide Maleate Salt	5-HT$_{1A}$ receptor antagonist	Tocris Biogen
8-OH-DPAT ($\pm$)-8-Hydroxy-2-(dipropylamino)-tetralin hydrobromide	5-HT$_{1A}$ receptor full agonist	Tocris Biogen

Desipramine, pargyline, L-DOPA, benserazide, buspirone, 8-OH-DPAT, WAY-100635, were prepared in saline (NaCl 0.9%). 6-OHDA was dissolved in Milli-Q water containing 0.02% ascorbic acid. For local administration, buspirone was dissolved in Dulbecco's buffered saline solution containing (in mM): NaCl 136.9, KCl 2.7, NaH_2PO_4 8.1, KH_2PO_4 1.5, $MgCl_2$ 0.5, and $CaCl_2$ 0.9 (pH of 7.40). For microdialysis, buspirone was dissolved in Ringer´s solution (1.2 mM $CaCl_2$, 2.7 mM KCl, 148 mM NaCl, and 0.85 mM $MgCl_2$). With the exception of urethane, all drugs were prepared on the day of the experiment.

3.1.3. Antibodies

Antibodies used for immunohistochemical assays are summarized in **Table 3.2**.

Table 3.2. Characteristics of the primary and secondary antibodies.

Antigen	Host	Cat. No.	Manufacturer
Tyrosine Hydroxylase	Rabbit	AB152	Merck Millipore
5-HT$_{1A}$ receptor	Rabbit	GTX104703	Genetex
SERT	Rabbit	24330	Immunostar
Biotinylated anti-rabbit	Goat	BA-1000	Vector Laboratories
Biotinylated anti-rabbit	Donkey	711-005-152	Jackson Immunoresearch

3.1.4. Viral vectors

Adeno-associated viral vectors (AVV) were used for the expression of channelrhodopsin-2 (ChR2) in the STN. The viral vector AAV-hSyn-hChR2(H134R)-EYFP (Addgene plasmid no. 26973, Karl Deisseroth) was produced by UNC Vector Core (University North Carolina at Chapel Hill, USA) (**Figure 3.1**). This vector expresses channelrhodopsin 2 (ChR2) tagged with enhanced yellow fluorescent protein (eYFP) driven by hSynapsin promoter and it is used for optogenetic excitation. Viral concentration was 4.6×10^{12} viral particles/ml dissolved in 350 mM Nacl and 1.5% sorbitol in PBS). The viral vector was aliquoted right after arrival and stored t −80°C until use.
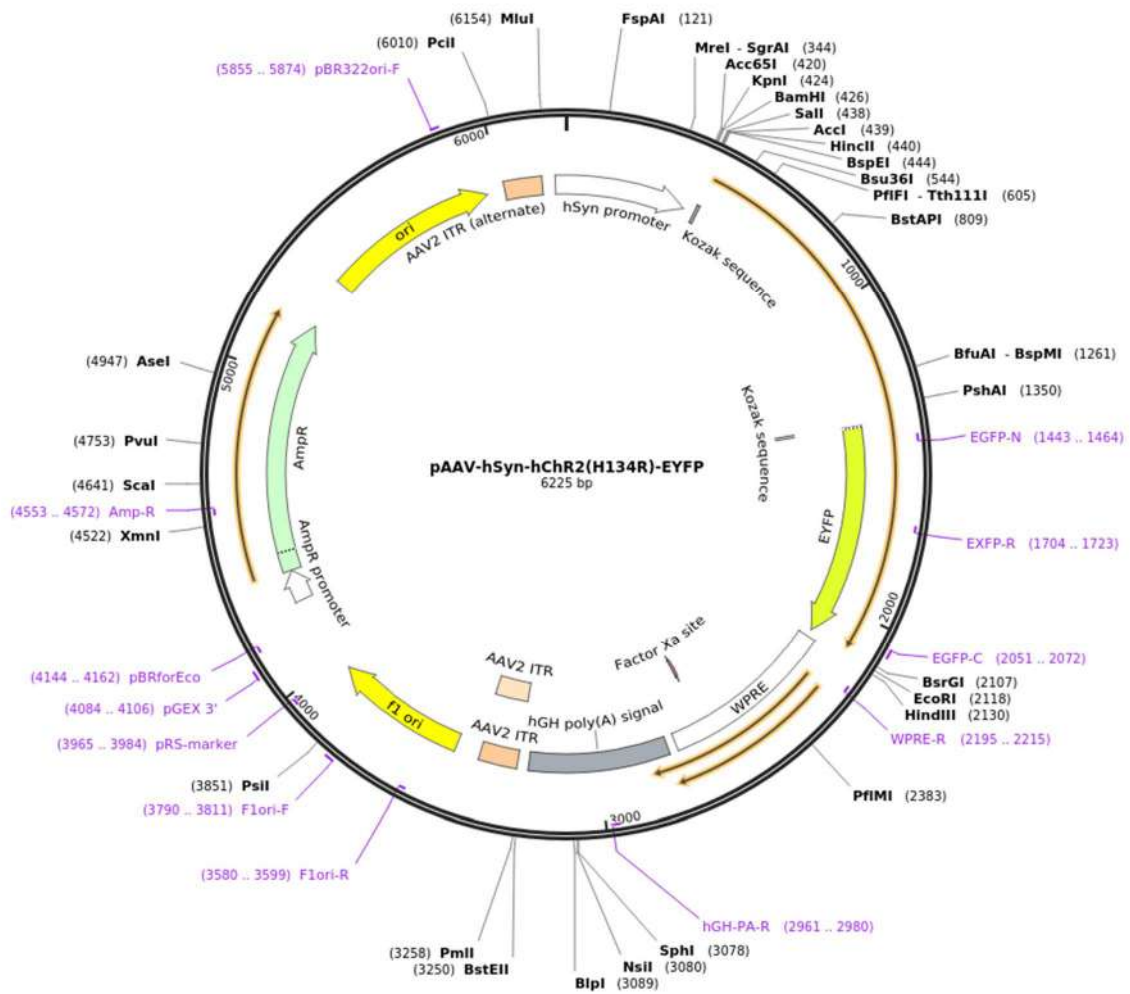
Figure 3.1. Maps of the of AAV-hSyn-hChR2(H134R)-EYFP plasmid. Produced by Karl Deisseroth´s laboratory.

3.1.5. Nomenclature of targets and ligands

Key protein targets and ligands in this document are hyperlinked to corresponding entries in http://www.guidetopharmacology.org, the common portal for data from the IUPHAR/BPS Guide to PHARMACOLOGY (Harding et al., 2018), and are permanently archived in the Concise Guide to PHARMACOLOGY 2017/18 (Alexander et al., 2017).

3.2. METHODS

3.2.1.   Stereotaxic surgery

3.2.1.1. Dopaminergic lesion with 6-hydroxydopamine

Thirty minutes before surgery, rats were pretreated with desipramine (25 mg/kg, intraperitoneal [i.p.]) and pargyline (50 mg/kg i.p.) in order to preserve the noradrenergic system and the degradation of the toxin, respectively. Then, rats were deeply anaesthetised with isoflurane, used at concentrations of 4% for induction and 1.5–2.0% for maintenance, and placed in the stereotaxic frame (David Kopf® Instruments). Sagittal incision was performed to expose the skull surface and drilled a burr hole above the coordinates of the MFB and meninges were carefully removed (**Figure 3.2**). The 6-OHDA (3.5 µg/µl, in 0.02% ascorbic acid in Milli-Q water) or vehicle was infused using a 10 µl-Hamilton syringe. A total of 7.5 µg and 6 µg, respectively was injected in two sites at the right MFB: 2.5 µl at anteroposterior (AP) − 4.4 mm, mediolateral (ML) + 1.2 mm and dorsoventral (DV) − 7.8 mm, relative to bregma and dura with the toothbar set at − 2.4, and 2 µl at AP − 4.0 mm, ML + 0.8 mm, and DV − 8 mm, with the toothbar at + 3.4 (Paxinos and Watson, 1997).

6-OHDA was infused at a rate of 1 µl/min by a single syringe infusion pump (KDS Scientific, Massachusetts, USA). The needle was left in the site for additional 2-3 mins to allow the toxin to diffuse, and then it was slowly retracted. 6-OHDA was prepared daily for each surgery session and changed every 2-3 hours. The solution was kept dark and on ice during surgery to avoid oxidation, which would be indicated by a color change (clear to brown-pink color). Rats were allowed to recover at least two weeks from the 6-OHDA lesion. After that period, DA degeneration was stabilized and inflammation was reduced.
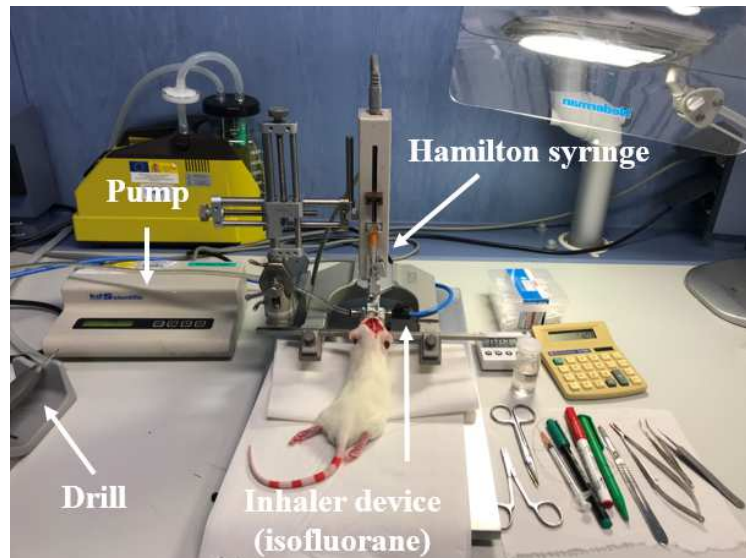
Figure 3.2. 6-hydroxydopamine lesion procedure. Animals were mounted on a stereotaxic frame and maintained under isofluorane anaesthesia. A hole was drill on the skull and 6-OHDA was injected by means of a Hamilton syringe connected to a pump.

3.2.1.2. Injection of viral vectors

Rats were deeply anaesthetised with isoflurane (4% for induction and 1.5–2.0% for maintenance) and placed in the stereotaxic frame. The head was oriented in the horizontal plane and a sagittal incision was performed to expose the skull surface. Meninges were carefully removed. The viral vector AAV5-hSyn-hChR2-(H134R)-EYFP was delivered unilaterally with a calibrated thick-walled micropipette (7087-07, BLAUBRAND®, intraMark, Germany) which was previously broken (tip diameter approximately 40 μm). Pulses (50–150 ms) were applied by means of Picospritzer™ II (General Valve Corporation, Fairfield, NJ, USA) at rate of 0.25 μl/min.

A total volume of 500 nl of viral vector was delivered into the STN in two injections at the following coordinates (relative to bregma and dura matter): 250 nl at AP: -3.6 mm, ML: -2.5 mm, DV: - 7.5 mm and 250 nl at AP: -3.9 mm, ML: -2.5 mm, DV: - 7.5 mm (Paxinos and Watson, 1997). After the injections, the micropipette was left in the site for additional 2–3 mins to allow the diffusion of the virus, and then it was slowly removed.

3.2.2. Behavioural studies

All behavioural studies were conducted between 8.00 and 17.00 hours. Motor activity in rats was evaluated by means of three non-drug-induced tests specific for different motor abilities. Work surface and objects were cleaned with ethanol 33% to remove odour traces before each trial. The cylinder, drag and bar tests were used for screening the DA depletion prior to electrophysiological, immunostaining or microdialysis experiments. These test were performed between 2 and 3 weeks after the 6-OHDA lesion when the animals were completely recovered from the surgery and the dopaminergic depletion was stabilized. The cylinder test was performed in one session. Bar test and drag test were repeated in two consecutive days, first the bar test and second drag test.

3.2.2.1. Cylinder test

The cylinder test evaluates the forelimb use asymmetry by determining the ability of the animal to support their body-weight against the wall of a glass cylinder during explorative behaviour (**Figure 3.3**). Rats were individually placed in transparent glass cylinders (Ø 20 cm) with two mirrors positioned at a 90-degree angle behind the cylinder to allow a complete view of the exploratory activity. Each animal was left in place until freely performing at least 20 weight-bearing touches with any of both forelimbs on the glass walls or 5 min. Rats were videotaped and scored at a later date. The percentage of contralateral or ipsilateral forelimb use with respect to the total touches was calculated.
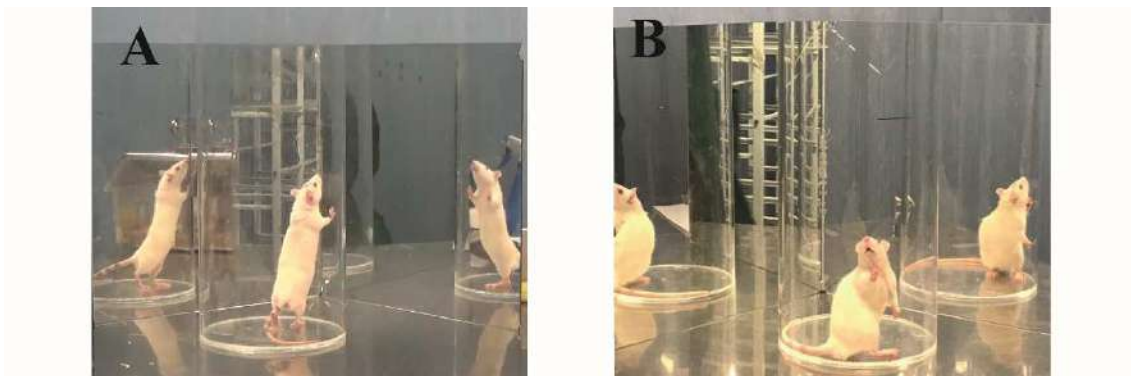
Figure 3.3. Cylinder test (spontaneous forelimb use). This test evaluated the ability to perform explorative behaviour. Sham animals (A) used right and left paws equally. 6-OHDA-lesioned animals (B) used predominatly the paw ipsilateral to the lesion.

3.2.2.2. Bar test

The bar test (Catalepsy test) was performed as previously described by Arcuri et al. (2018) to measure the ability of the animal to react to an externally imposed position. The ipsilateral and contralateral forelimbs were alternatively placed on three blocks of increasing heights (3, 6 and 9 cm) (**Figure 3.4**). The immobility time (in seconds) of each forelimbs on the blocks was recorded (cut-off time in each step of 20s).

Figure 3.4. Bar test (Catalepsy test). This test measured the ability of the animal to react to an externally imposed position. Naïve animals immediately retracted and equally used both paws. However, 6-OHDA-lesioned animals (in the figure) showed more immobility when the contralateral forelimb to the lesion was placed on the bar.

3.2.2.3. Drag test

The drag test (Akinesia/bradykinesia test) was performed as reported by Arcuri et al. (2018). This test measures the ability of the animal to balance its body posture using the forelimbs, in response to backward dragging. Briefly, each rat was lifted from the abdomen leaving the forelimb on the table and dragged backwards through a fixed distance of 1m at a constant speed of 20 cm/s (**Figure 3.5**). Two different observers counted the number of touches made by each forelimb.

Figure 3.5. Drag test (Akinesia/bradykinesia test). Example of the appropriate positioning of a rat during the drag test for forelimb akinesia. Control animals used symmetrically both left and right forelimb. However, 6-OHDA-lesioned animal tended to support its weight on only one forelimb.

3.2.2.4. Levodopa-induced dyskinesia score

Abnormal involuntary movements (AIMs) were induced in 6-OHDA-lesioned rats by long-term injections of L-DOPA (6 mg/kg, i.p.) in combination with the peripheral decarboxylase inhibitor benserazide (12 mg/kg, i.p.) over 3 weeks. The development of L-DOPA-induced AIMs were scored according to the scale described by Cenci & Lundblad (2007). On the testing days, rats were placed individually in transparent empty plastic cages for at least 10 minutes before drug administration. Each rat was observed for one full minute every 20th minute around 200 minutes. The severity of the three subtypes of dyskinetic movements (axial, limb and orolingual; ALO AIMs) was rated on two scales based on the frequency and amplitude of ALO AIMs. Locomotive AIMs were separately evaluated.

Frequency of AIMs was scored on a 0 to 4 scale, where 0 meant that the movement was not present; 1 that the movement was occasional and present less than 30 seconds; 2 that the movement become frequent and present more than 30 seconds; 3 that the movement was present constantly during the observation time but interrupted by repeated strong sensory stimuli; and 4 that the movement was continuous and not interrupted by repeated strong sensory stimuli. In addition to the frequency scale, the amplitude of the AIMs was also scored using 1-4 points. For limb AIMs, "1" referred to small movements of the paw around a fixed position; "2" referred to low amplitude movements resulting in visible displacement of the whole limb; "3" consisted of notable translocation of the whole limb and visible contraction of the shoulder muscles, and "4" referred to vigorous limb movements of maximum amplitude and speed with contraction of proximal and extensor muscles. The amplitude of the axial AIMs was also scored on a scale from 1 to 4. Thus, "1" referred to lateral flexion of the head and neck, at approximately 30º angle; "2" equaled sustained deviation of the head and neck at an angle ≤ 60º; "3" equaled sustained torsion of the upper trunk at an angle from 60 to 90º with the rat in a bipedal position; and "4" referred to sustained torsion of the upper trunk at an angle > 90º, causing the rat to lose the balance. Finally, the orolingual AIMs was also scored on a scale from 1 to 4. Thus, "1" referred to twitching of facial muscles accompanied by small masticatory movements without jaw opening; "2" twitching of facial muscles accompanied by noticeable masticatory movements and occasionally leading jaw opening; "3" movements with broad involvement of facial muscles and masticatory muscles. Jaw opening is

frequent, tongue protrusion occasional; and "4" all the above muscle categories are involved to the maximal possible degree.

Data were expressed as the AIM score/session for ALO, which is calculated by multiplying the frequency score by the amplitude scores during each monitoring period, with all of these products summed for each testing sessions (Lindgren et al., 2010). We will refer this score as "Global AIM score" Locomotive AIM is represented separately. All 6-OHDA-lesioned animals chronically treated with L-DOPA developed severe dyskinetic movements that reach the peak between 40 and 100 minutes after a single injection of L-DOPA and had a total score > 100 on ALO AIMs by the last testing session.

3.2.3. In vivo single-unit extracellular recordings of substantia nigra pars reticulata and entopeduncular neuron activity in anaesthetised rats

3.2.3.1. Animal preparation and surgery

Rats were anaesthetised with urethane (1.2 g/kg, i.p.) and the right jugular vein was cannulated for systemic drugs administration with a polyethylene cannula (Clay Adams, Becton Dickinson and Company Division, model PE-240). Next, rats were placed in a stereotaxic frame and the body temperature was maintained at ~37ºC for the entire experiment by heating pad connected to a rectal probe.

For all recordings, the head was oriented in the horizontal plane. A burr hole (1-2 mm diameter approximately) was drilled and an electrode was placed in the following coordinates (relative to bregma): AP: -5.3 mm, ML: -2.5 mm, DV: -7.5 to 8.5 mm for SNr recordings. In the same way, for EP recordings, a hole was drilled and an electrode was placed in the following coordinates (relative to bregma): AP: -2.3 to -3 mm, ML: -2.5 mm, DV: -7 to -8.5 mm (Paxinos & Watson, 1997).

3.2.3.2. Recording electrode preparation

For single-unit and LFP recording electrode preparation, a thin wall glass capillary with filament (TW150F-4, World Precision Instruments, UK) was stretched using an automatic vertical electrode stretcher (Narishige Scientific Instrument Lab, model PE-2, Japan). After that, the electrode was filled with 2% solution of Pontamine Sky Blue in 0.5% sodium acetate, previously filtered in a Millex®-GS filter (Millipore®) with a 0.22 μm pore diameter. The tip of the electrode was broken to a diameter of 1-2 μm under a microscopy (Olympus Optical Co., model CH-2) with 40X magnification.

3.2.3.3. Recording and neuronal identification

The electrophysiological recordings of SNr and EP neurons were performed at least three weeks after 6-OHDA or vehicle injection or twenty-four hours after the last L-DOPA administration in the case of 6-OHDA L-DOPA group. In same animals, single-

unit extracellular recordings of the SNr or EP were obtained simultaneously to the LFP and ECoG.

For single-unit extracellular recording, the electrode was lowered in the above described coordinates of the SNr and EP by a hydraulic microdrive (David Kopf® Instruments, Tujunga, California, EEUU, model 640). The extracellular signal from the electrode was first pre-amplified (10x) and amplified (10x) later with a high-input impedance amplifier (Cibertec S.A., model amplifier AE-2), and then simultaneously monitored on an oscilloscope (HAMEG® analog digital scope HM407-2) and on an audio monitor (Cibertec S.A., model AN-10) (**Figure 3.6**). Next, the signal was bandpass filtered at 30-5000 Hz in a second amplifier (Cibertec S.A., model amplifier 63AC) and finally neuron action potentials or "spikes" were digitized using computer software (CED micro 1401 interface and Spike2 software, Cambridge Electronic Design, UK).

The LFP was recorded through the same glass electrodes used for single-unit extracellular recordings. The signal was pre-amplified (10x) then amplified (10x) and bandpass filtered (0.1–5000 Hz). In a second amplifier, the LFP signal was amplified (10x) and bandpass filtered (0.1–100 Hz). The discriminated LFP activity (sampled at 2500 Hz) was digitized, stored and later analysed using computer software.

Additionally, the ECoG was simultaneously recorded via a 1-mm-diameter steel screw, which was juxtaposed to the dura mater above the right frontal somatic sensory-motor cortex (AP: +4.5 mm and ML: -2.5 mm to bregma) (Paxinos and Watson, 1997), as described by Aristieta et al. (2016). The signal was pre-amplified (10x), amplified (200x) and bandpass filtered (0.1–1000 Hz) in an amplifier (Cibertec S.A., model amplifier 63AC). The discriminated ECoG activity (sampled at 2500 Hz) was digitized, stored and analysed using computer software.

At the end of the experiments, a 5 µA cathodal current was passed through the recording glass electrode to deposit a discrete mark of Pontamine Sky on the recording site. **Figure 3.7** illustrates the single-unit extracellular recording of the SNr and EP simultaneously performed with SNr-LFPs or EP-LFPs and ECoGs.
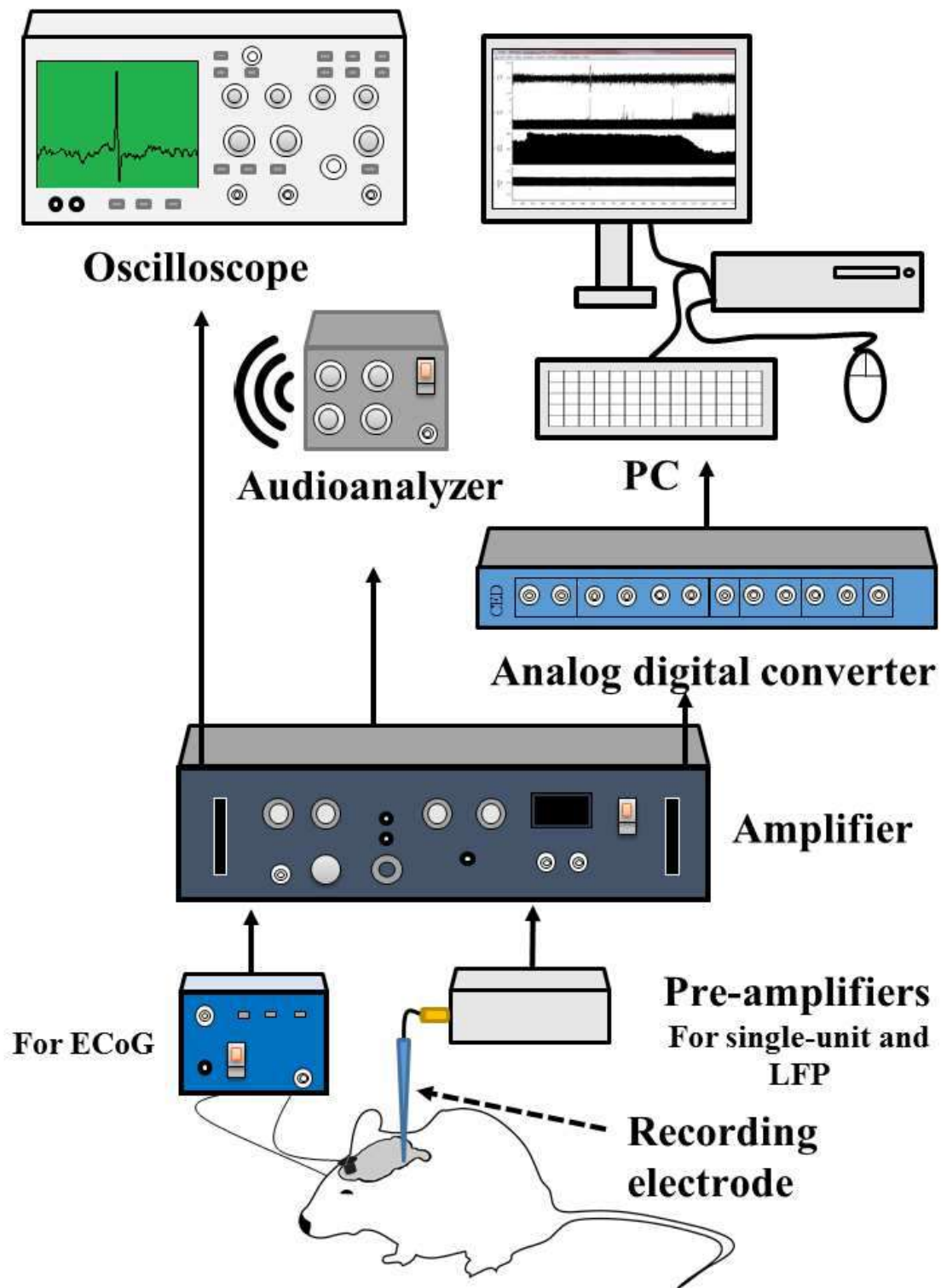
Figure 3.6. Schematic illustration of the electrophysiological procedure. Glass electrode was used for recording the LFP and single-unit extracellular signal. Neuron activity was passed through a high-input impedance amplifier, displayed in an oscilloscope and monitored with an audioanalyzer. Single-unit neuronal spikes were isolated and analysed by means of PC-based software Spike2. For recording the ECoG, a steel screw was implanted in the motor cortex. LFP and ECoG were amplified and filtered, and later analysed using Spike2.

SNr neurons were identified by established criteria. These neurons were easily distinguished based on their action potentials waveforms, firing rates, and location ventral to the SNc. SNr neurons displayed smooth, sharp, biphasic action potentials with an average duration of 0.5–1.2 ms, and firing rates between 10 and 40 Hz, described by Waszczak et al. (1980) and Aristieta et al. (2016). Finally, EP neurons were identified following criteria described by Ruskin et al. (2002). Recorded EP neurons were located ventral to the ventral thalamic nuclei and thalamic reticular nucleus, after passing 100–200 μm of silence through the dorsal aspect of the internal capsule. EP neurons showed biphasic waveforms with short wide-duration action potentials 0.8–0.9 ms and the firing rates between 10 and 20 Hz and it was increased after 6-OHDA lesion (Aristieta et al., 2019; Darbin et al., 2016).
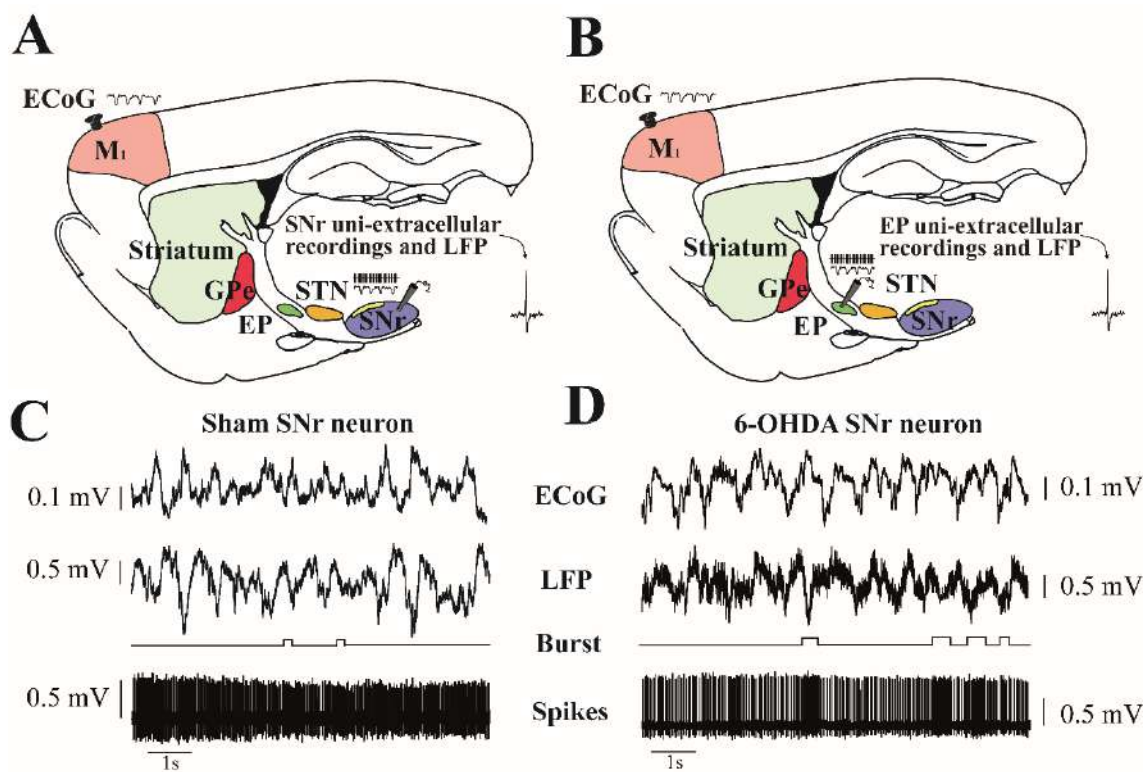
Figure 3.7. Schematic parasagittal section of a rat brain, showing the motor cortex and the basal ganglia nuclei. Glass electrodes were placed in the SNr (A) or EP (B) for recording single-unit extracellular activity and LFP. For recording the ECoG, a steel screw was implanted in the somatic motor cortex (M_1). A single spike from SNr (A) and EP (B) neurons recorded in vivo. A recording trace containing SNr spikes, SNr-LFP and ECoG from a neuron, which exhibited a regular firing pattern (C), the most common neuron firing pattern in the sham group. A recording track containing SNr spikes, SNr-LFP and ECoG from a neuron, which exhibited burst firing pattern (D), the most representative neuron firing pattern in 6-OHDA saline and 6-OHDA L-DOPA groups. ECoG: electrocorticogram; LFP: local field potential; EP: entopeduncular; SNr: substantia nigra pars reticulata.

3.2.3.4. Local administration

A calibrated micropipette glued adjacent to the recording micropipette was filled with 0.25 M of buspirone in Dulbecco's buffered saline solution as previously performed by Sagarduy et al. (2016). Local buspirone injection in the SNr and EP was applied with pressure pulses (50–150 ms) using a Picospritzer™ II. The injected volume was measured by monitoring the meniscus movement in a calibrated pipette. Every pipette was calibrated so that each pulse corresponded to the injection of 2 nl of solution. The firing rate of each dose was recorded until the neuron recovered. Doses of buspirone were calculated as the volume of solution locally administered (i.e., number of ejection pulses multiplied by 2 nl/pulse) multiplied by the drug concentration in the pipette solution.

3.2.3.5. Motor cortex stimulation and substantia nigra pars reticulata or entopeduncular neuron recordings

The motor cortex (relative to bregma and dura, AP: +3.0 to +3.5 mm, ML: -3.2 mm and DV: -1.2 to -1.6 mm) (Paxinos & Watson, 1997) ipsilateral to the recording site was stimulated at 1 Hz (pulse width 600 μs; intensity 1 mA) using a bipolar stainless-steel electrode (diameter, 250 μm; tip diameter, 100 μm; tip-to-barrel distance, 300 μm) (Cibertec S.A.).

Cortical stimulation evoked characteristic triphasic responses consisting of a combination of an early excitation, inhibition and/or late excitation in SNr neurons in according to Antonazzo et al. (2019) and in EP as previously described by Chiken et al., (2015) in mice (**Figure 3.8A** and **3.8B**, respectively).

Peristimulus time histograms (**Figure 3.8C** and **D**) were generated from 180s period using 1 ms bins and the criterion used to determine the existence of response was performed as stated in by Antonazzo et al. (2019). An excitatory response was considered when there was an increase of two-fold the standard deviation, plus the mean of the number of spikes compared with the pre-stimulus frequency, for at least three consecutive bins. The amplitude of excitatory responses was quantified by calculating the difference between the mean number of spikes evoked within the time window of the excitation and the mean number of spikes occurring spontaneously before the stimulation. The duration

of an inhibitory response corresponded to the time interval without spikes were observed, for at least three consecutive bins.
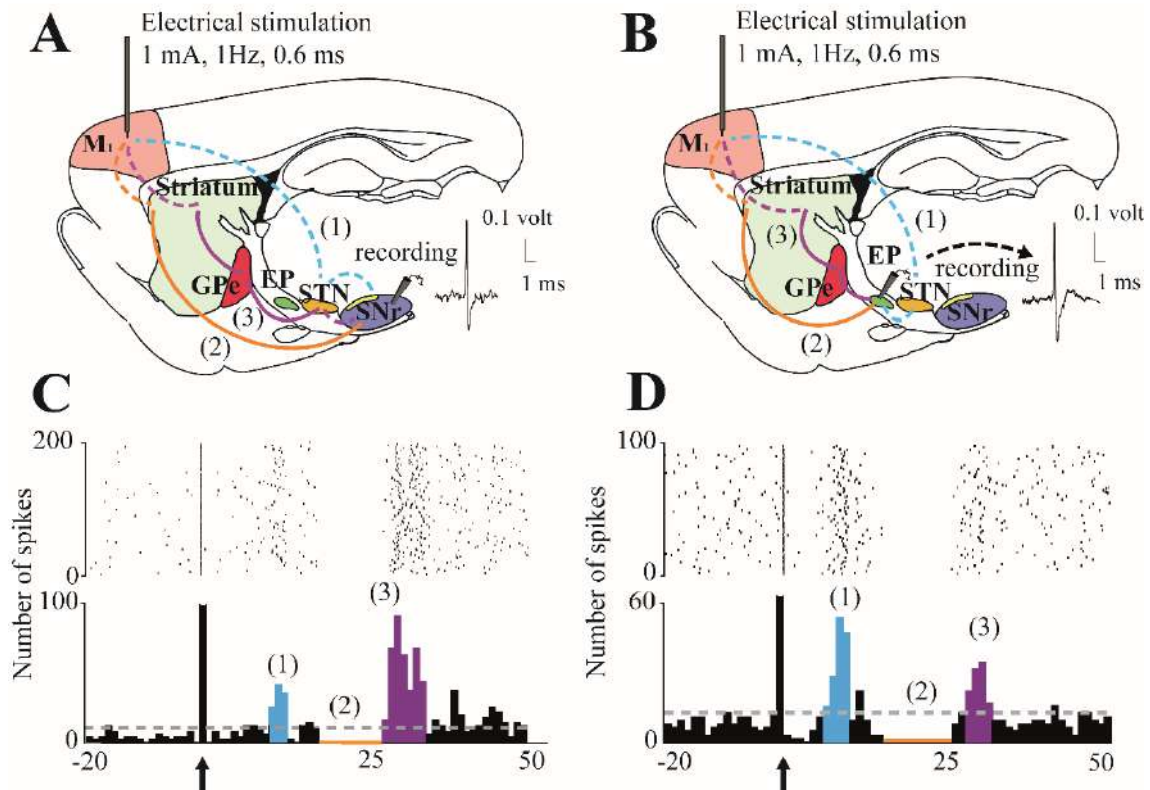
Figure 3.8. Illustration of cortical stimulation evoked triphasic response in the basal ganglia output nuclei in anaesthetised rats. Schematic parasagittal sections of a rat brain showing the M_1 and the BG nuclei: striatum, GPe, STN, SNr (A) and EP (B) and a respective example of single spike. The abscissa and ordinate axes represent duration (ms) and amplitude (volt) of the action potential. Dashed lines represent glutamatergic projections and blunt line GABAergic projections. (C) Raster plot and peristimulus time histogram showing the characteristic cortically-evoked triphasic response in SNr neurons: (1) Early excitation in blue: activation of hyperdirect pathway (cortex-STN-SNr), (2) Inhibition in orange: activation of direct pathway (cortex-striatum-SNr), and (3) Late excitation in purple: activation of indirect pathway (cortex-striatum-GPe-STN-SNr). (D) Raster plot and peristimulus time histogram showing the characteristic cortically-evoked triphasic response in EP neurons: (1) Early excitation in blue: activation of hyperdirect pathway (cortex-STN-EP), (2) Inhibition in orange: activation of direct pathway (cortex-striatum-EP), and (3) Late excitation in purple: activation of indirect pathway (cortex-striatum-GPe-STN-EP). Arrows indicate the time when the stimulus was applied. GPe: external globus pallidus; EP: entopeduncular nucleus; M_1: motor cortex; STN: subthalamic nucleus; SNr: substantia nigra pars reticulata.

3.2.3.6. Integrated in vivo optogenetic stimulation of the subthalamic nucleus coupled to subthalamic and entopeduncular electrophysiological recordings

For in vivo optogenetic stimulation, the optic bare fibers (200/230 μm core; 1.5m length, 94063, Plexon, Texas, USA) was inserted in a modified glass capillary and positioned above the transfected STN as showed in **Figure 3.9**. Photostimulation of the STN was obtained by using the PlexBright 465 nm blue LED for Optogenetic Stimulation System (94002-002, Plexon, Texas, USA). The stimulation was digitally controlled by Spike2 software (version 7). Blue light was passed through a LED fiber to reach the brain. At the beginning of the experiment, the power intensity at the tip of the optic fiber was tested by a digital photodetector kit (PM100D, Thorlabs, New Jersey, USA) and calibrated with a protocol that exponentially grows from 0.5 V to 5 V. The intensity was set between 10 and 20 mW.

Next, the LED fiber was lowered into the STN at 30º angle to the horizontal plane (relative to bregma and dura, AP: -8.23 mm, ML: -2.5 mm and DV: -8.66 mm) by a hydraulic drive micromanipulator (Narishige, Japan, MO-10). Neuron activity was recorded firstly in STN at the following coordinates (relative to bregma and dura, AP: -3.6 mm, ML: -2.5 mm and DV: -7 to -8 mm) to check functional expression of ChR. Three optical stimulation protocols were applied. The first one consisted of twenty single 2V-pulse (~5.5 mW), delivered for 1 s every 5 s. The second protocol consisted of ten single 5V-pulses (~14 mW), delivered for 0.5 s every 10 s. Finally, the third stimulation protocol consisted of train of 5V-pulses (~14mW) at 25 Hz frequency delivered for 7 ms once every 10 seconds.

Peristimulus time histograms were generated from 100 s period using 1 ms bins, 1.5 – 3 s width, and 0.5 – 1 s offset to determine the type of response of EP evoked by STN stimulation. With the peristimulus, the firing rate was analysed prior to (pre) and during (light-on). The protocols were randomized applied per neuron, and were separated by 5 min. The protocols were also applied before and after buspirone administration (4 mg/kg i.p.).
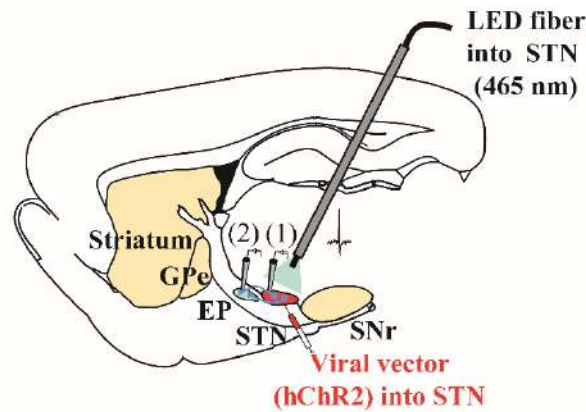
Figure 3.9. Illustration of integrated optogenetic stimulation of subthalamic nucleus coupled to in vivo electrophysiology in anaesthetised rats. Schematic parasagittal sections of a rat brain showing the viral vector AAV-hSyn-hChR2(H134R)-EYFP injection into the STN. 4 weeks after the viral injection, the LED fiber was positioned into the STN as well as a glass electrode for recording the STN single-unit extracellular activity. Later EP single-unit extracellular activity was recorded when the STN was optically stimulated (2). During the experiment, EP neuron activity was modulated by photoestimulation of STN terminals through LED fiber controlled by Spike2 software. GPe: external globus pallidus: EP: entopeduncular; STN: subthalamic nucleus; SNr: substantia nigra pars reticulata.

3.2.3.7. Electrophysiological data analysis

Electrophysiological experiments were analysed off-line using Spike2 software (version 7). The following parameters were estimated:

Firing rate: Defined as the number of neuronal discharges per second. Data were represented in a bar histogram that showed the mean firing rate each 10 seconds. Basal firing rate was recorded for 300 seconds and mean firing rate after drug administration for 60-300 seconds (depending on plateau effect for each drug).

Coefficient of variation: The coefficient of variation (CV) is a parameter related to the interval between consecutive discharges (inter-spike interval) and gives an idea of the regularity of the firing. The representation of the inter-spike interval histogram followed by the analysis ran by Spike2 (script Meaninx.s2s) lead to the numerical value. Data was expressed in percentage, as the division between standard deviation and mean value. The recording period analysed was the same used for the firing rate.

Burst firing pattern: Burst-related parameters such as the number of bursts, mean duration of burst, number of spikes per burst, recurrence of bursts, and intraburst

frequency were analysed during time epochs of 90 s applying a Spike2 script ("surprise.s2s"), based on the Poisson surprise algorithm. Two different firing patterns were described: "non-bursting firing pattern" characterized by a symmetrical density distribution histogram and "bursting firing pattern" characterized by a distribution histogram which is significantly different ($p < 0.05$) from a Poisson distribution. The bursting firing pattern presents a significantly positive skewness ($p < 0.05$) of the density discharge distribution histogram and a minimum of three spikes per burst.

Oscillatory activity and synchronization: Spike train activity, LFPs and ECoGs were also analysed off-line by Spike2 software as we previously described (Ariesta et al. 2016; 2019). LFP and ECoG signals (sampled at 2500 Hz) were smoothed to 1 ms and action potentials were converted to series of events (sampled at 2500 Hz). Then, these events were transformed to a spike continuous waveform (1 ms smoothing period) using a custom-made script "convert_event_to_waveform.s2s". The power spectrum of smoothed ECoGs, LFPs and SNr or EP spike waveforms and the coherence analyses between SNr or EP-LFPs and SNr or EP-spikes waveforms, between ECoGs and SNr or EP-spikes, and finally between SNr or EP-LFPs and ECoGs were analysed using the fast Fourier transform (8192 blocks size) in the low frequency range 0–5 Hz range from 90 seconds of data. The significance of the coherence was determined by the equation described by Rosenberg et al. (1989): $1 - (1 - \alpha) \, 1 / (L - 1)$, where α is 0.95 and L is the number of windows used. The area under the curve (AUC) of coherence and power spectrum curves were calculated in the 0 to 5 Hz low frequency range in all the neurons, before and after drug administration.

3.2.4. Intracerebral microdialysis in freely moving rats

3.2.4.1. Microdialysis probes manufacture

For this study, concentric microdialysis probes were made using AN69 (Gambro Industries, Meyzieu, France) semipermeable hollow membranes (65-kDa molecular-weight cutoff: 340 μm outer diameter with an active surface of 2.0 mm active membrane length in the case of SNr).

3.2.4.2. Stereotaxical microdialysis probe implantation

Rats were deeply anaesthetised with isoflurane (4% for induction and 1.5–2.0% for maintenance) and placed in the stereotaxic frame. Once the head was horizontally immobilized, a sagittal incision was performed to expose the skull surface. Meninges were carefully removed to allow vertical insertion of the probe.

Intracerebral microdialysis probes were stereotaxically implanted into the right SNr (relative to Bregma and dura: AP= -5.5 mm, ML= -2.2 mm and DV= -8.7 mm) according to Paxinos and Watson (1997). Together with three holes were also drilled for screw placements, which aids fixation to the skull with the dental cement and resin. Ringer buffer solution was perfused during the surgical procedure through all the process to avoid blockage and breakage of the dialysis membrane and facilitate the implantation. Probes were fixed and reinforced with dental cement. Once the implantation was finished, the microdialysis probe was checked and the end of the polyethylene tubes was clamped.

After surgery, animals were left to recover one night, housed in individual cages provided with ad libitum access to food and water. Animals needed to recover between 10 a 24 hours due to inflammation, the low local cerebral blood flow and low glucose metabolism, and damages in the neuronal morphology near probe (De Lange et al., 1997; Imperato & Di Chiara, 1984). A probe implantation that lasts more than 72 hours might result in a gliosis near to microdialysis probe increasing the risk of reducing dialysis and neurotransmitters detection.

3.2.4.3. Dialysate sample collection

Twenty-four hours after surgery, the probes were perfused with a Ringer's solution, and sample collection (45 µl) at a flow rate of 3 µl/min began after 6 hours of washout. GLU and GABA levels were monitored every 15 minutes up to 3 hours. Each animal implanted with a single microdialysis probe was randomized to Ringer/Ringer or Ringer/buspirone (50 nM, 150 nM, and 500 nM) in the first microdialysis session, and treatments were crossed in the second session to test the effectiveness of the treatment (**Figure 3.10**). At the end of the experiments, animals were anaesthetised with isofluorane and cresyl violet solution (0.15%) was perfused through the probe to facilitate its location. Five minutes later, rats were sacrificed by an overdose of isoflurane and decapitated. The brains were removed, ultrafreezing, cryopreserved with 2-methyl-butane and storage at -80 ℃. Dialysate samples were also storage at -80 ℃ until HPLC detection.

3.2.4.4. Glutamate and gamma-aminobutyric acid detection

GLU and GABA were measured by HPLC coupled with fluorometric detection as previously described (Bido et al., 2011). Thirty microliters of o-phthaldialdehyde/mercaptoethanol reagent was added to the aliquots containing 30-µl of sample, and 50 µl of the mixture was automatically injected (Triathlon autosampler; Spark Holland, Emmen, Netherlands) onto a 5-C18 Hypersil ODS analytical column (3-mm inner diameter, 10-cm length; Thermo Fisher Scientific, Waltham, MA), which was perfused at a flow rate of 0.48 ml/min (Jasco PU-2089 Plus quaternary pump; Jasco, Tokyo, Japan) with a mobile phase containing 0.1 M sodium acetate, 10% methanol and 2.2% tetrahydrofuran (pH 6.5). GLU and GABA were detected by means of a fluorescence spectrophotometer FP-2020 plus (Jasco, Tokyo, Japan) managed by ChromNAV 2.0 HPLC software (Jasco, MD, USA). The excitation and the emission wavelengths were set at 370 and 450 nm, respectively. Under these conditions, the limits of detection for GLU and GABA were ~1 nM (i.e., ~147 pg/ml) and ~0.5 nM (i.e., 51 pg/ml), and the retention times were between 2.8 and 4 minutes for GLU and between 16 and 19 minutes for GABA.
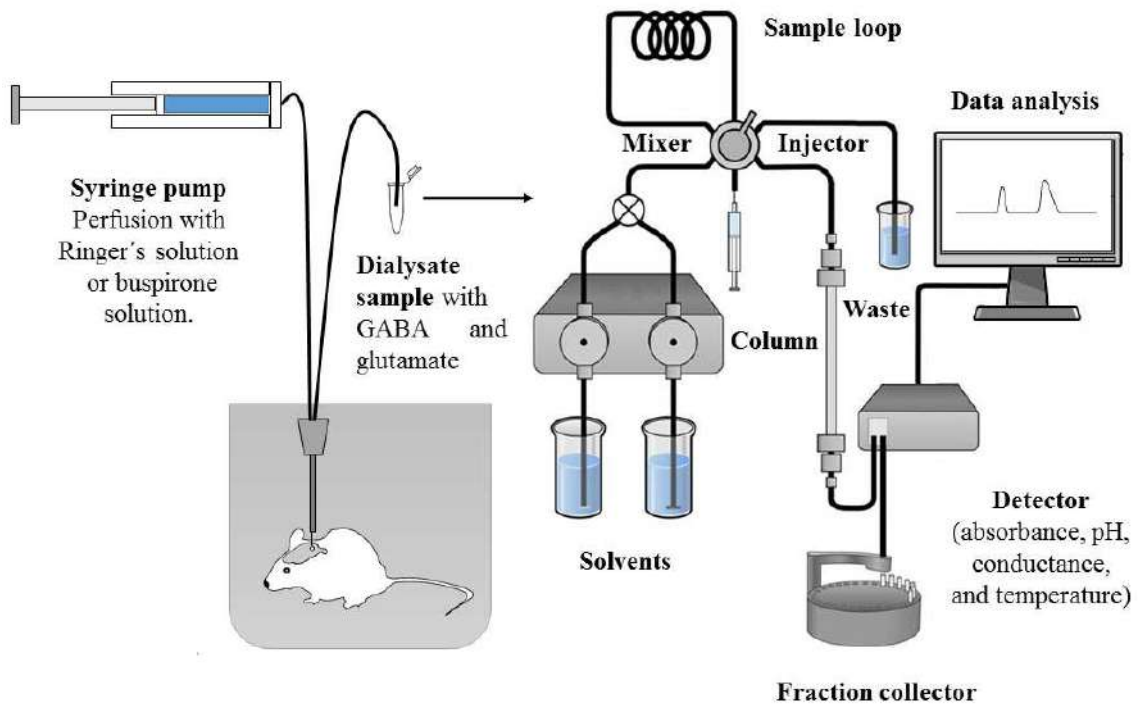
Figure 3.10. Schematic representation of the microdialysis procedure in an awake freely moving rat. First microdialysis probes were implanted in the right SNr under anaesthesia. Next day after rat recovered, the probes were perfused with a Ringer´s solution at uniform flow (3 µl/min) by a syringe pump. After 6 hours of washout each set of experiments was started with perfusion of Ringer´s solution or buspirone. During the experiment, dialysis samples (45 µl) containing GLU and GABA were collected every 15 min. Before sampling, each Eppendorf tube was storage -80ºC until transferring to HPLC (High performance liquid chromatography) equipment coupled to fluorescence spectrophotometer. GABA: gamma-aminobutyric; GLU: glutamate.

3.2.5. Histological and quantification procedures

3.2.5.1. Histological procedures

Animals were deeply anaesthetised and transcardially perfused with saline followed by 4% ice-cold paraformaldehyde and 0.2% picric acid prepared in 0.1 M phosphate saline buffer. Brains were kept in paraformaldehyde and transferred the following day to a 25% sucrose solution until they sank. The brains were serially cut in coronal 40-μm sections using a freezing microtome, and slices were conserved in a cryoprotectant solution at -20 °C until further processing.

3.2.5.2. Immunohistochemical assays

Tyrosine hydroxylase

Tyrosine (TH) immunostaining was used to examine the degree of DA denervation in the striatum and the SNc according to our established protocol (Aristieta et al., 2016). Sections were rinsed three times in potassium phosphate buffered saline (KPBS; 0.02 M and pH=7.4). Then, endogenous peroxidase were quenched using 3% H_2O_2 and 10% (v/v) methanol in KPBS for 30 minutes at room temperature. After three rising steps in KPBS, brain sections were preincubated in 1% Triton X-100 with KPBS (KPBS-T) and 5% normal goat serum (NGS) for 1 hour at room temperature. Then, they were incubated with primary antibody (rabbit anti-TH, AB152, 1:1000, Merck Millipore, Spain) overnight at room temperature. Afterwards, the sections were then incubated with secondary antibody (biotinylated goat anti-rabbit IgG, BA-1000, 1:200, Vector Laboratories, California, USA) in KPBS-T with 2.5% NGS for 2 hours at room temperature. All the sections were incubated with an avidin–biotin–peroxidase complex (ABC kit, PK-6100, Vector Laboratories, California, USA) as chromogen, and peroxidase activity was visualized with 0.05% 3,3′-diaminobenzidine (DAB) and 0.03% H_2O_2 for 1-2 min. Then reaction was stopped by rinsing the sections in KPBS for 5 min. Finally, sections were mounted onto gelatin-coated slides, dehydrated in ascending series of ethanol, cleared in xylene and coverslipped with DPX mounting medium.

Serotonin transporter and 5-HT$_{1A}$ receptor

SERT and 5-HT$_{1A}$ receptor expression in the BG nuclei and the DRN was investigate using immunohistochemical procedures. Coronal slices presented an anteroposterior distance of 200 µm. At least three slices containing the area of interest were selected for each subject. Sections of interest from the BG nuclei and raphe were firstly rinsed two times in phosphate buffer (PB; 0.1 M and pH = 7.4) and later were incubated in 30% methanol and 3% H$_2$O$_2$ in 0.1 M PB for 30 minutes. Later, the sections were rinsed in PB for 5 minutes and after in 1% sodium borohydride for 30 minutes. Afterwards, the sections were profusely washed with PB before rinsing in Trizma base saline (TS; 0.1M, pH=7.6) for 10 min. Brain sections were then incubated in 0.5% bovine serum albumin (BSA) and 0.25% Triton X-100 in TS (TS-T) for 30 minutes and later incubated 48 hours and room temperature with primary antibody (rabbit anti-SERT, 1: 2500, Immunostar, Hudson, WI, USA or rabbit anti-5-HT$_{1A}$r, 1: 200, GTX104703, Genetex, California, USA) in TS-T with 0.5% BSA. Later, the sections were rinsed in TS for 30 minutes and incubated in the secondary antibodies (biotinylated donkey anti-rabbit IgG, 1:400, Jackson Immunoresearch, Stratech Scientific, UK; or biotinylated goat anti-rabbit IgG, BA-1000, 1:200, Vector Laboratories, California, USA) for 2 hours at room temperature. Sections were rinsed with TS for 30 minutes followed by incubation for 60 minutes in ABC-kit. The peroxide reaction product was visualized by incubation in a solution containing 0.022% DAB and 0.003% H$_2$O$_2$ for 10 – 15 minutes, as described previously (Aristieta et al., 2014). The reaction was stopped by rinsing in TS for 5 minutes followed by PB for 15 min. Finally, brain sections were mounted, dehydrated and coverslipped.

3.2.5.2. Histochemical essays

Cytochrome c oxidase staining

Metabolic activation of the BG nuclei and DRN was investigated by histochemical staining for the activity of the mitochondrial enzyme COX, a marker of neuronal activation using a slightly modified method of a metal-enhanced technique as described by other authors (Armentero et al., 2006; Blandini et al., 2007; Kaya et al., 2008). Coronal slices presented an anteroposterior distance of 200 µm. At least three slices containing the area of interest were selected for each subject. Then, the sections of interest from the BG nuclei and raphe were placed in incubation medium with 0.05M PBS pH 7.4, 1% sucrose, 0.05% nickel sulphate (II), 2.5µM imidazole (Fluka), 0.025% DAB, 0.015% cytochrome c (Sigma-Aldrich-Merck), and finally 0.01% catalase (Sigma-Aldrich-Merck) was added to start the enzymatic reaction. COX staining was performed in darkness for 5 hours at 37ºC. Sections were washed twice with PBS 0.05M and mounted on gelatin-coated slices. Finally, sections were dehydrated in ascending series of alcohols and cleared in xylene and coverslipped with DPX mounting medium.

Neutral red and Nissl-thionine staining

As mentioned before, at the end of each electrophysiological experiment, a Pontamina Sky Blue mark was deposited in the recording site for posterior verification. 5 µA cathodic current was constantly applied for 7-10 minutes through the recording electrode (Digital Midgard precision current source, 515595, Stoelting, Illinois, USA). Brain sections containing the SNr and EP nuclei of recorded regions were mounted on gelatinized glass slices. Later, the slices were incubated with neutral red staining for 8-10 minutes. Next, sections were washed twice in distilled water, dehydrated in alcohols and xylene for 2 minutes. Afterwards, these slices were coverslipped with DPX medium. The location of the recording site was checked microscopically and only experiments with a clear localitation in the SNr or EP were included in the analysis.
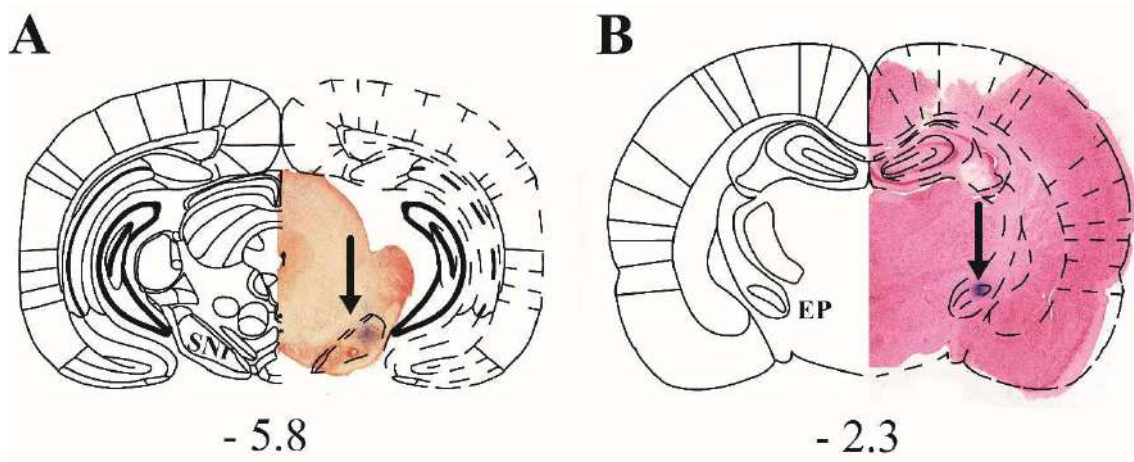
Figure 3.11. Histological verification of the recording site in the substantia nigra pars reticulata (A) and entopeduncular nucleus (B). A pontamina sky blue dot was deposited in the recording area by a cathodal current of 10 µA during 7 minutes. Animals were perfused and brains cut into 40 µm slices. After neutral red staining, brain sections were analysed and the anatomical position of the blue point was microscopically verified. Only recordings performed within the SNr and EP were included in the study (relative to bregma, AP = -5.3 and AP= -2.3, respectively).

The Nissl-thionine staining has been used to facilitate the localization of specific BG nuclei after immunostainings and verify cortical stimulation of the motor cortex (**Figure 3.12**). For that, sections were mounted on gelatin-coated slices, and processed for thionine staining [distilled water (2x5 min), 70% ethanol (10 min), 96% ethanol (2 min), 96% ethanol/10% paraformaldehyde (4/1, 5 min), 96% ethanol (2 min), chloroform/ethyl ether/96% alcohol (8/1/1, 10 min), 96% ethanol (2 min), 100% ethanol (2x2 min), xylene (5 min), 100% ethanol (2x2 min), 96% ethanol (2 min), 96% ethanol (10 min), 70% ethanol (5 min), 50% ethanol (5 min), thionine (1g/100 ml, 20–45 min), distilled water (1 min), distilled water/glacial acetic acid (1000/3, 1 min and 30 s), 70% alcohol/glacial acetic acid (1000/3, 1 min and 30 s), 96% ethanol (2 min), 100% ethanol (2 min), xylene (2x8 min)]. Immediately after the staining, the slices were coverslipped with DPX mounting medium.
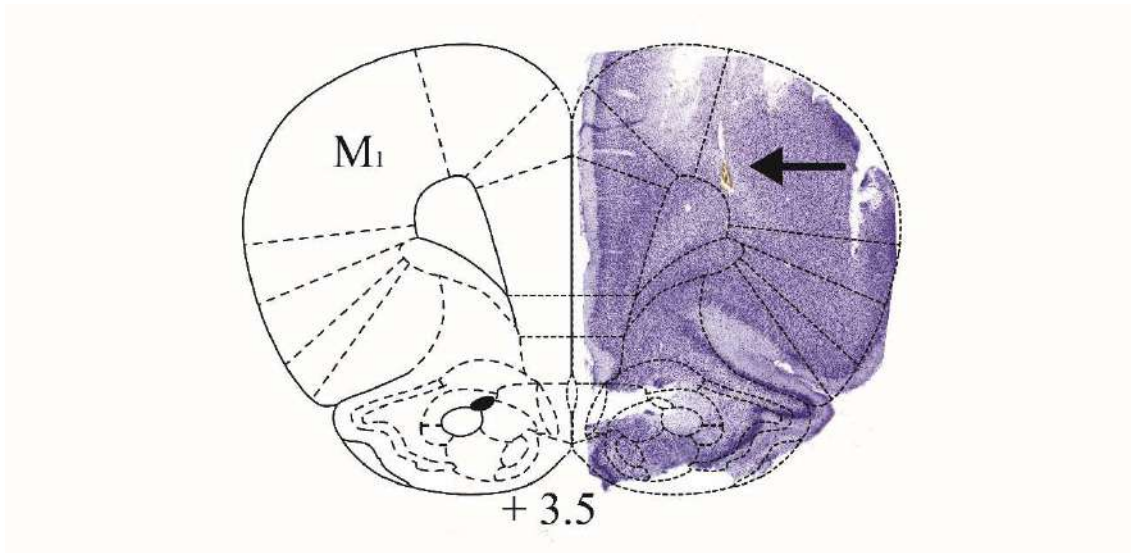
Figure 3.12. Histological verification of the electrical stimulation of the motor cortex. For verification of the stimulation electrode, a deposit of iron was made at the tip of the electrode by a 1 mA cathodal current during 10 minutes. Brains were removed after perfusion, and post-fixed in a solution containing an 80% of a 4% paraformaldehyde solution, 20% of ethanol containing 2% acetic acid, and 1% (w/v) of potassium ferricyanide Indicating the stimulation. Afterwards, 40 μm thick coronal sections were stained with Nissl to microscopically verify the anatomical position of the stimulation place in motor cortex (M_1) (Relative to Bregma: AP = +3.5).

3.2.5.3. Quantification procedures

Integrated optical densitometry of TH

The degree of DA loss produced by the 6-OHDA lesion was verified by the mean integrated optical density (IOD) of striatal dopaminergic innervation based on TH-immunoreactivity. Between 3 and 6 striatal sections were digitally captured using a scanner EPSON perfection V700 photo. Images were analysed using NIH-produced software, ImageJ win64 Fiji (https://imagej.net/Fiji). For each slide, the whole striatum was delimited and its optical TH-immunoreactivity IOD was expressed as a percentage of the contralateral or intact non-lesioned hemisphere with respect to the intact or ipsilateral lesioned hemisphere subtracting the cortex as background for each hemisphere. The values were between 100% for an intact striatum and 0% for completely DA depleted striatum.

Integrated optical densitometry of serotonin transporter and 5-HT₁ₐ receptor

The IOD of SERT terminals and 5-HT$_{1A}$ receptors in the BG nuclei and DRN were measured using ImageJ win64 Fiji for reading optical densities as grey levels. Digital images from sections were obtained with 20X objective of an automatic panoramic digital slide scanner (Pannoramic MIDI II, 3DHistech, Hungary) using CaseViewer 2.3 (64-bit version) software. The mean IOD was determined in each BG nuclei subtracting the background for each section. Measurements were performed from 2 to 6 sections throughout the nucleus of interest and the mean per animal was calculated. Results were expressed as the ratio of the contralateral or intact non-lesioned hemisphere with respect to the intact or ipsilateral lesioned hemisphere. The background of each slide was set as non-immunoreactive structures such as internal capsule or other fibers.

Integrated optical densitometry of cytochrome c oxidase

The IOD of COX activity was performed as previously described (Armentero et al., 2006; Blandini et al., 2007). Digital images were obtained with 2.5X objective of a Leica M80 Stereomicroscope equipped with IC80 HD camera and Leica Application Suite, LAS core software. The mean IOD was determined by the nuclei of interest in the BG and subtracting the background for each section. Measurements were performed on every section (2 – 6 per interested nucleus) and calculated the mean per animal. Results were expressed as the ratio of the contralateral or intact non-lesioned hemisphere with respect to the intact or ipsilateral lesioned hemisphere. The background of each slide was set as structures without colour such as internal capsule or other fibers.

3.2.6.   Statistical analysis

In the electrophysiological experiments, when more than one neuron were recorded per animal (one to five per rat), data values were averaged per animal. Electrophysiological parameters (firing rate and CV) from independent groups were analysed by unpaired Student's t test for the comparison between two experimental groups or one-way analysis of variance (ANOVA) for the comparison between three experimental groups. The AUC values from power spectrum of LFP and ECOG and coherence were also analysed with One-way ANOVA for the comparison between three

experimental groups. To assess differences in the percentage of neurons with burst firing neurons in two or three experimental groups, Fisher's exact test was used and the parameters related to bursting activity pattern (i.e., number, duration, and spikes per burst, recurrence of burst, and intraburst frequency) were analysed using the Mann–Whitney rank sum test or, when necessary, Student's two-tailed unpaired t test. The effect of the different drugs on the electrophysiological parameters (firing rate, CV and AUC of oscillatory activity and synchronization) was analysed by repeated measures (RM) two-way ANOVA. F values were expressed as F (lesioned; within-groups) or F (treatment; between groups) and only one neuron was tested per animal. To determine whether these drugs were altering the burst-related parameters of these neurons or not, RM one-way ANOVA was used. Cortically-evoked responses (i.e., duration, latency, and amplitude of the excitations) were also averaged per animal, so that one value per animal was shown. Parameters related to the cortical stimulation evoked were analysed by two-tailed unpaired Student's t test for looking at differences between sham and 6-OHDA groups. To determine whether the drugs were affecting cortically-evoked from sensorimotor circuit responses differently, a RM two-way ANOVA was performed. In optogenetic experiments, two-tailed paired Student's t test was performed to compare STN or EP neuron activity before (laser off) and during (laser on) STN optoillumination. The effect of buspirone on STN photostimulation response was also analysed by RM two-way ANOVA. For behavioural experiments, unpaired t-test (sham vs 6-OHDA) or paired t-test (ipsilateral vs contralateral paw) was used.

In the microdialysis experiments, the mean value was calcultated and GABA and GLU levels expressed as percentages of this baseline concentration. Basal values among groups were compared using one-way ANOVA, whereas the effect of buspirone was analysed using RM two-way ANOVA. In these analyses, all the experimental points including basal values were considered. Complementary, net area under the curve (AUC net) was also calculated as the summation of the percentage changes with respect to the baseline during the full period after buspirone administration and were also calculated the effect per each dose. Two-way ANOVA was used to compare AUC of the different groups.

In SERT and 5-HT$_{1A}$ immunostaining and COX staining results, one-way ANOVA was used. All statistically significant ANOVAs were followed by Bonferroni's post hoc

test and no significant variance in homogeneity. The level of statistical significance was set at $p < 0.05$. Data are presented as mean ± standard error of the mean (S.E.M.).

3.2.7. Experimental design

Study I

A total of 84 rats were used in this study. Animals were divided into three groups which are referred to as sham/naïve, 6-OHDA, and 6-OHDA L-DOPA groups. **Figure 3.13** shows the timeline and the number of animals (in brackets) used in each experiment. For SNr electrophysiology recordings (experiment 1), rats received 6-OHDA or vehicle injections into the MFB, and the severity of the 6-OHDA lesion was screened using the cylinder test at least two weeks later. L-DOPA was then administered daily for three weeks, and AIMs were evaluated at baseline and on the 21st day. Electrophysiological recordings or perfusion were performed at least three weeks after the lesion (sham or 6-OHDA group) or 24 h after the last of L-DOPA treatment (6-OHDA L-DOPA group). At the end of the electrophysiological experiments, animals were perfused and brains removed for histological verification. For microdialysis experiments (experiment 2), rats received 6-OHDA injections and were screened using the bar and drag tests three weeks later. L-DOPA was administered for three weeks and AIMs score was evaluated. At least three weeks after the lesion or 24 h after the last L-DOPA injection, rats were implanted with microdialysis probes. Each animal underwent two microdialysis sessions (24 and 48 h after surgery) and received Ringer solution or buspirone administration in a randomized fashion. Samples were collected every 20 min for a total of 4 h. At the end of the experiment the animals were sacrificed, brains were removed, and the probe location in the SNr was verified.

Figure 3.13. Schematic representation of the experimental design. At the beginning of the experiments, animals received a vehicle or 6-OHDA injection into the right MFB. Three weeks later, dopaminergic depletion was evaluated by different asymmetry tests (cylinder or bar and drag test). After that, rats received a 21-day treatment of daily L-DOPA injections (6 mg/kg plus 12 mg/kg benserazide). AIMs were scored at baseline and at the end of the treatment. Electrophysiological recordings and microdialysis assays in the SNr were performed after the L-DOPA chronic treatment. Finally, animals were perfused transcardially and processed for histological examination. * The group was divided into three subgroups with the respective sizes.

Study II

A total of 57 rats were used in this study. Animals were divided into three groups which are referred to as sham, 6-OHDA, and 6-OHDA L-DOPA groups for the experiment 1. **Figure 3.14** shows the timeline and the number of animals (in brackets) used in each experiment. For the electrophysiological recordings in the EP (experiment 1), rats received 6-OHDA or vehicle injections into the MFB, and the severity of the 6-OHDA lesion was screened using the cylinder test at least two weeks later. L-DOPA was then administered daily for three weeks, and AIMs score was evaluated at baseline and on the 21st day. Electrophysiological recordings or perfusion were performed at least three weeks after the lesion (sham or 6-OHDA group) or 24 h after the last of L-DOPA treatment (6-OHDA L-DOPA group). At the end of the electrophysiological experiments, animals were perfused and brains removed for histological verification. At the beginning of the experiment 2, control rats received an AAV5-ChR2-EYFP injection in the STN. Four weeks later, optogenetic illumination of the STN was coupled to electrophysiological recordings in the STN and in the EP. Afterwards, animals were transcardially perfused and histological verifications by confocal microscopy were performed to confirm the correct viral transfection of the STN.
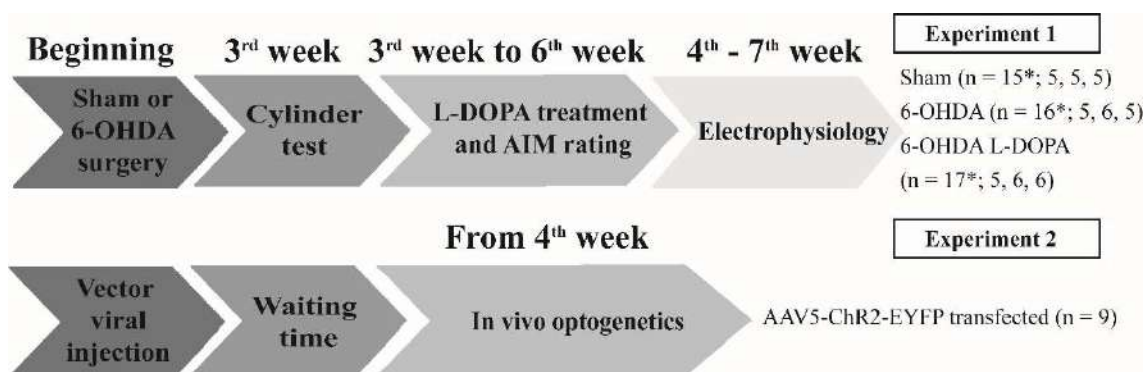
Figure 3.14. Schematic representation of the experimental design. At the beginning of the experiment 1, animals received a vehicle or 6-OHDA injection into the right MFB. Three weeks later, dopaminergic depletion was evaluated by the cylinder test. After that, rats received a 21-day treatment of daily L-DOPA injections (6 mg/kg plus 12 mg/kg benserazide). AIMs were scored at baseline and at the end of the treatment. Electrophysiological recordings in the EP nucleus were performed after the L-DOPA chronic treatment. Finally, animals were perfused transcardially and processed for histological examination. * The group was divided into three subgroups with the respective sizes. At the beginning of the experiment 2, animals received a vector viral transfection (AAV5-ChR2-EYFP). Four weeks after the viral transfection, STN optogenetic illumination and STN and EP electrophysiological recordings were performed. Afterwards, histological verifications were performed.

To use the minimum number of animals possible and to avoid effects induced by local administration. We only studied the local or systemic effect of buspirone per nucleus. For instance, after local administration of buspirone in the SNr, a new recording electrode was used and the systemic effect of the drug was studied in the EP. Thus, we never applied local and systemic buspirone in the same neuron or nucleus.

Study III

A total of 53 rats were used in this study. Animals were divided into two groups which are referred to as sham and 6-OHDA groups for the experiment 1. **Figure 3.15** shows the timeline and the number of animals (in brackets) used in each experiment. At the beginning of the experiments, rats received 6-OHDA or vehicle injections into the MFB, and the severity of the dopaminergic lesion was screened using the cylinder test at least two weeks later. The experimental design is shown in **Figure 3.15**. At the beginning of experiments, rats received 6-OHDA or vehicle injections into the MFB and the severity of the DA lesion was screened using the cylinder test at 2 weeks after the 6-OHDA lesion. The stimulation of motor cortex evoked a triphasic response in the SNr (experiment 1) or in the EP (experiment 2). The electrophysiological recordings were performed 4 weeks after the 6-OHDA lesion in both sham and 6-OHDA groups. At the end of the

electrophysiological experiments, animals were perfused and brains removed for histological verification.
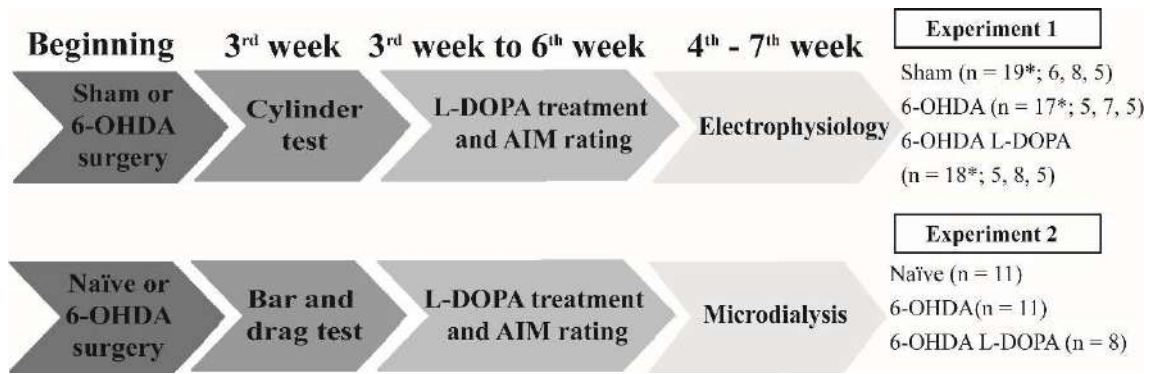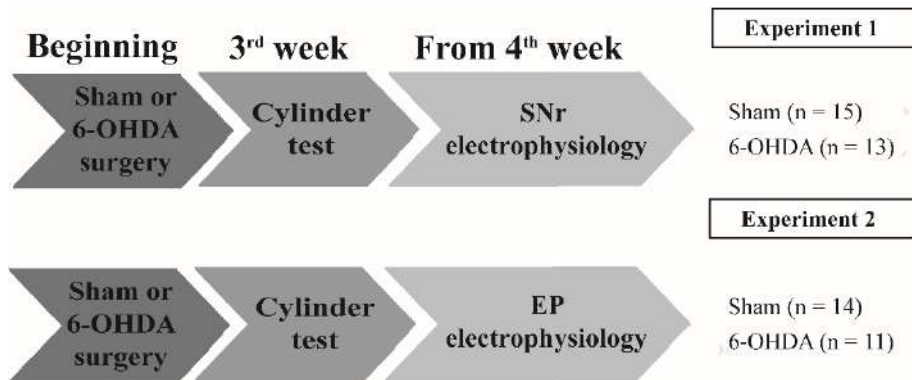

Figure 3.15. Schematic representation of the experimental design. At the beginning of the experiments 1 and 2, animals received a vehicle or 6-OHDA injection into the right MFB. Three weeks later, dopaminergic depletion was evaluated by the cylinder test. Electrophysiological recordings in the SNr (experiment 1) or EP (experiment 2) were performed from the 4th week after the 6-OHDA lesion. Finally, animals were perfused transcardially and processed for histological examination. * The group was divided into two subgroups with the respective sizes.

Study IV

A total of 33 rats were used in this study. Not all animals included in this study took part in the two experiments. Animals were divided into three groups which are referred to as sham, 6-OHDA, and 6-OHDA L-DOPA groups. **Figure 3.16** shows the timeline and the number of animals (in brackets) used in each experiment. In both experiments (1 and 2), rats received 6-OHDA or vehicle injections into the MFB, and the severity of the 6-OHDA lesion was screened using the cylinder test at least two weeks later. L-DOPA was then administered daily for three weeks, and AIMs score was evaluated at baseline and on the 21st day. The perfusion was performed 4 week after the lesion (sham or 6-OHDA group) or 24 hours after the last of L-DOPA treatment (6-OHDA L-DOPA group).
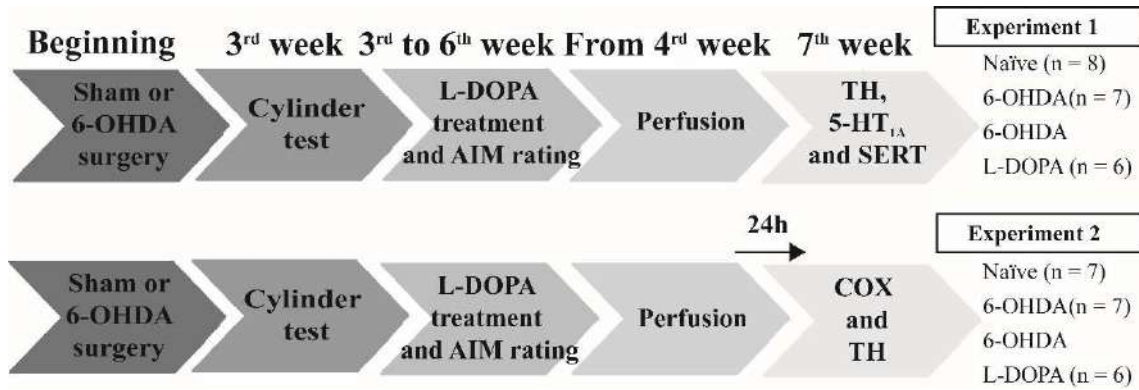
Figure 3.16. Schematic representation of the experimental design. At the beginning of the experiments 1 and 2, animals received a vehicle or 6-OHDA injection into the right MFB. Three weeks later, dopaminergic depletion was evaluated by the cylinder test. After that, rats received a 21-day treatment of daily L-DOPA injections (6 mg/kg plus 12 mg/kg benserazide). AIMs were scored at baseline and at the end of the treatment. Finally, sham and 6-OHDA groups were perfused transcardially and processed for histological examination at the 4th week and 6-OHDA L-DOPA was perfused 24 hours after the last of L-DOPA treatment. COX staining was performed right after sectioning the brain. TH, SERT and 5-HT$_{1A}$ immunostaining were performed later. COX: Cytochrome c oxidase; SERT: serotonin transporter; TH: Tyrosine hydroxylase.

4. RESULTS

4. RESULTS

Validation of the 6-hydroxydopamine lesion and levodopa-induced abnormal involuntary movements

Two to three weeks after the 6-OHDA or vehicle injection, animals were tested for forelimb asymmetry using the cylinder test (animals used for electrophysiology recordings or immunostaining assays) and the bar and drag test (animals used for microdialysis experiments). All the 6-OHDA-lesioned animals included in these studies showed severe forelimb asymmetry. The 6-OHDA-lesioned animals (n = 110) preferentially used the ipsilateral forepaw in the cylinder test ($p < 0.001$, two-tailed paired t-test; **Fig. 4.1A**) in contrast to sham (n = 46). The time spent in the bar was shorter in the bar test ($p < 0.001$, two-tailed paired t-test, n = 15; **Fig. 4.1B**) and the use of the contralateral forelimb was significantly lower than the ipsilateral one in the drag test ($p < 0.001$, two-tailed paired t-test, n = 15; **Fig. 4.1C**). All the 6-OHDA-lesioned rats treated with long-term L-DOPA (n = 43) showed axial, limb and orolingual abnormal movements and increased locomotion activity that were evident after 10-20 min, reached the peak at 40-60 min and lasted for 140-160 min after single injection of L-DOPA (**Fig. 4.1D** and **E**).

Finally, DA denervation was confirmed by TH-immunostaining. All animals included in the 6-OHDA groups showed a severe reduction (> 95%) in TH-fibre density in the striatum and TH-neurons in the SNc on the ipsilateral side to the lesion (**Fig. 4.1F**).
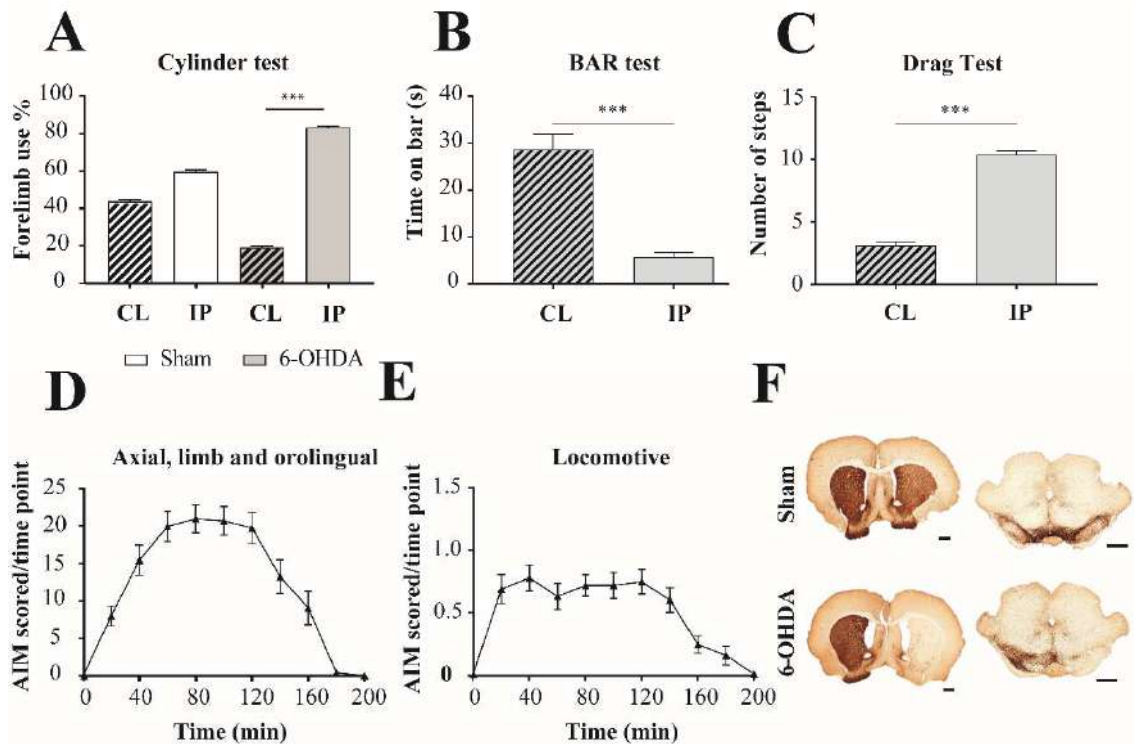
Figure 4.1. Validation of the 6-hydroxydopamine lesion and levodopa-induced abnormal involuntary movements. Motor asymmetry was evaluated comparing the use of the forelimb contralateral (CL) and ipsilateral (IL) to the lesion in three behavioural tests. In the cylinder test (A), data are expressed as the mean value of the percentage of ipsilateral or contralateral touches divided into the total number $\pm$ S.E.M. (***$p < 0.001$, two-tailed paired Student's t test). In the bar test (B), data are expressed as mean $\pm$ S.E.M. of immobility time in seconds and in the drag test (C), results are mean $\pm$ S.E.M. of number of steps. Evolution of dyskinesia scores showing (D) the time course of abnormal involuntary movements (AIMs) scores for axial, limb and orolingual ratings and (E) locomotive score, on the last session after L-DOPA chronic treatment. Results are expressed as mean $\pm$ S.E.M. Coronal sections (F) from sham and 6-OHDA group showing the lack of TH-immunoreactivity in the striatum and substantia nigra. Scale bar = 1 mm. ***$p < 0.001$ (two-tailed paired Student's t test).

4.1. STUDY I: EFFECT OF BUSPIRONE ON AMINO ACID RELEASE AND NEURON ACTIVITY OF THE SUBSTANTIA NIGRA PARS RETICULATA IN SHAM, 6-HYDROXYDOPAMINE AND LONG-TERM L-DOPA TREATED 6-HYDROXYDOPAMINE RATS

4.1.1. Effect of 5-HT$_{1A}$ agonists on substantia nigra pars reticulata neuron activity

A total of 92 GABAergic neurons from 54 animals were recorded in the SNr of anaesthetised rats; 31 from the sham group (n = 19 rats), 29 from the 6-OHDA group (n = 17 rats) and, 32 from the 6-OHDA L-DOPA group (n = 18 rats). All cells recorded were located within the SNr and displayed the characteristic firing properties described for SNr GABAergic neurons in our previous publication (Aristieta et al., 2016). Thus, the mean value of the basal firing rate was higher in the 6-OHDA L-DOPA group (F $_{(2, 51)}$ = 3.738, $p < 0.05$, one-way ANOVA), the CV was increased in the 6-OHDA group (F $_{(2, 51)}$ = 4.111, $p < 0.05$, one-way ANOVA) and the number of bursty neurons was increased in the 6-OHDA and 6-OHDA L-DOPA groups (Fisher´s exact test, $p < 0.05$). Mean values ± S.E.M. of the firing rate and firing pattern parameters are shown in **Table 4.1**. Specifically, the effect of local and systemic buspirone or 8-OH-DPAT administration was evaluated.

Local effect of buspirone was studied on 54 SNr neurons from a total of 16 animals: 18 neurons from the sham group (n = 6), 17 neurons from the 6-OHDA group (n = 5) and 19 neurons from the 6-OHDA L-DOPA group (n = 5). As it is shown in **Figure 4.2A** and **C**, local administration of buspirone (0.25–2 nM) caused a marked, dose-dependent inhibition of neuronal activity in the three experimental groups, with a maximal reduction of the firing rate of ~ 70% of the basal value (buspirone: F $_{(4, 52)}$ = 48.74, $p < 0.001$ and lesion: F $_{(2, 13)}$ = 3.38, $p > 0.05$; RM two-way ANOVA; **Fig. 4.2C**). No difference in the efficacy of local buspirone among groups was detected when compared the percentage of effect with respect to the basal firing values (**Fig. 4.2C**). The inhibitory effect of buspirone was blocked (two-tailed unpaired Student´s t test, $p < 0.05$) by previous systemic administration of the 5-HT$_{1A}$ antagonist WAY-100635 (100 µg/kg, intravenously [i.v.]) (n = 6 neurons from 2 control animals; **Fig. 4.2D**).

Table 4.1. Firing properties of substantia nigra pars reticulata neurons.

	Sham (n = 19)	6-OHDA (n = 17)	6-OHDA L-DOPA (n = 18)
Firing rate (Hz)	20.9 ± 2.0	26.4 ± 2.0	28.4 ± 2.0*
CV (%)	35.7 ± 3.9	53.1 ± 5.6*	48.5 ± 5.2
Neurons exhibiting burst firing pattern (%)	41.9	$68.9^{\#\#\#}$	$75.0^{\#\#\#}$
Number of bursts	13.7 ± 2.7	25.8 ± 8.9	23.9 ± 9.9
Duration of burst (ms)	0.8 ± 0.2	1.2 ± 0.6	1.2 ± 0.7
Nº spikes/burst	21.3 ± 7.1	31.6 ± 16.6	57.5 ± 31.8
Recurrence of burst (nº burst/min)	8.9 ± 1.7	13.2 ± 4.3	14.6 ± 5.9
Intraburst frequency (spike/s)	49.9 ± 5.7	59.0 ± 6.4	69.1 ± 9.7

Data from the firing rate, the CV and burst related parameters are expressed as mean $\pm$ S.E.M. of n rats. *$p < 0.05$ vs sham (One-way ANOVA followed by Bonferroni´s post hoc test) and $^{\#\#\#}p < 0.001$ vs sham (Fisher´s exact test).
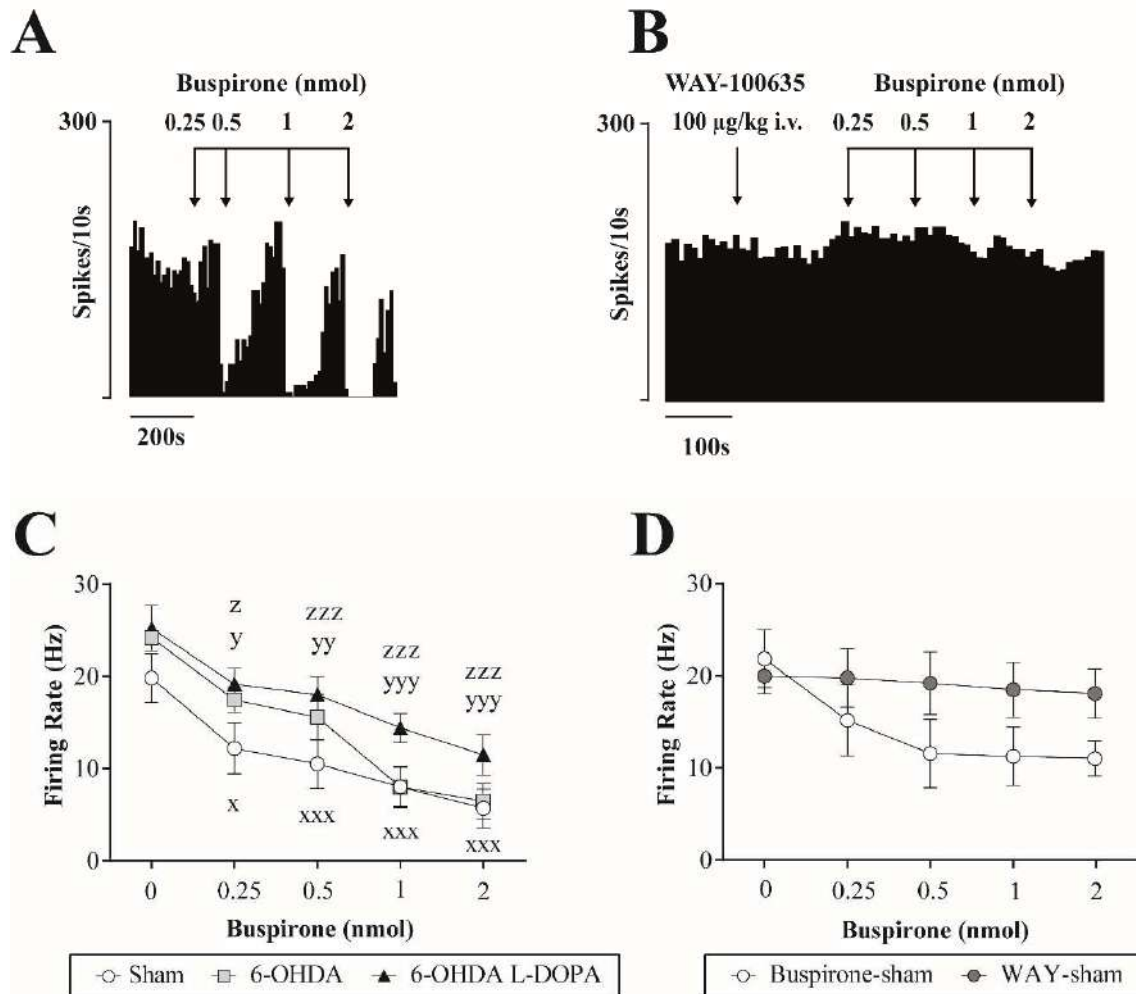
Figure 4.2. Effect of local administration of buspirone on substantia nigra pars reticulata neuron activity. Representative firing rate histogram illustrating the inhibitory local effect of buspirone on neurons in the sham group (A). Representative firing rate histogram illustrating the blockage of the inhibitory local effect of the previous buspirone by previous administration of WAY-100635 (B). Buspirone (0.25–2 nmol) locally injected into the SNr induced a dose-dependent inhibitory effect in all three experimental groups (C). The inhibitory local effect of buspirone (white circles; n = 5 neurons from 2 sham rats) was blocked by the systemic administration of WAY-100635 (0.1 mg/kg, i.v.) (two-tailed paired Student´s t test) (Grey circle; n = 6 neurons from the same 2 sham rats) (D). Data are expressed as mean ± S.E.M. xx < 0.01 and xxx < 0.001 vs. sham baseline (n = 5), y < 0.05, yy < 0.01, and yyy < 0.001 vs. 6-OHDA baseline (n = 5), and finally, z < 0.05 and zzz < 0.001 vs. 6-OHDA L-DOPA baseline (n = 5) (RM two-way ANOVA followed by Bonferroni's post hoc test).

Next, the effect of cumulative doses of buspirone (from 0.6125 mg/kg to 5 mg/kg, i.v.) on the firing rate and pattern of SNr neurons was studied. One neuron per animal was pharmacology tested from a total of 23 animals: sham group (n = 8), 6-OHDA group (n = 7) and 6-OHDA L-DOPA group (n = 8) (**Fig. 4.3A-C**). As shown in **Figure 4.3**, systemic administration of buspirone did not modify the firing rate of SNr neurons (buspirone: $F_{(4, 80)} = 2.043$, $p > 0.05$; and lesion: $F_{(2, 20)} = 1.158$, $p > 0.05$; RM two-way ANOVA; **Fig. 4.3D**) nor the CV (buspirone: $F_{(4, 80)} = 0.852$, $p > 0.05$ and lesion: $F_{(2, 20)} = 1.209$, $p > 0.05$; RM two-way ANOVA; **Fig. 4.3E**) in any of the groups. However, systemic buspirone decreased the number of bursty neurons in the 6-OHDA and 6-OHDA L-DOPA groups but not in the sham group ($p < 0.05$, Fisher´s exact test; **Fig. 4.3F**). No changes in intraburst parameters were observed. Followed systemic administration of the 5-HT$_{1A}$ antagonist WAY-100635 (0.5 and 1 mg/kg) did not modify buspirone effect. **Table 4.2** summarizes mean ± S.E.M. values of all firing activity parameters before and after buspirone administration in the three experimental groups.

Finally, we investigated the effect of systemic administration of 8-OH-DPAT (from 20 µg/kg to 160 µg/kg; i.v.). One neuron per animal was pharmacologically tested from a total of 15 animals (n = 5 in each group) (**Fig. 4.4A-C**). A dose-dependent inhibition of SNr neuron firing rate was observed in the sham group (n = 5), with a maximal reduction of 47% of the basal value (**Fig. 4.4A** and **D**). Conversely, 8-OH-DPAT did not modify the firing rate of neurons in 6-OHDA and 6-OHDA L-DOPA groups (8-OH-DPAT: $F_{(4, 48)} = 5.467$, $p < 0.001$, and lesion: $F_{(2, 12)} = 5.917$, $p < 0.05$; RM two-way ANOVA; **Fig. 4.4D**). No change was also observed in the CV (8-OH-DPAT: $F_{(4, 48)} = 1.127$, $p > 0.05$, and lesion: $F_{(2, 12)} = 1.22$, $p > 0.05$; **Fig. 4.4E**). In contrast, 8-OH-DPAT administration significantly decreased the number of bursty neurons in the three experimental groups ($p < 0.05$, Fisher´s exact test; **Fig. 4.4F**) without modifying intraburst parameters (**Table 4.3**). WAY-100635 (0.5 -1 mg/kg, i.v.) partially reversed the effect of 8-OH-DPAT (**Fig. 4.4F**). **Table 4.3** summarizes mean value ± S.E.M. of all firing activity parameters before and after 8-OH-DPAT in the three experimental groups.

Figure 4.3. Effect of systemic administration of buspirone on substantia nigra pars reticulata neuron activity. Representative firing rate histogram illustrating the lack of effect of buspirone (0.06125–2.5 mg/kg, i.v.) and WAY-100635 (0.1 mg/kg, i.v) on SNr neuronal firing rate, and schematic representation of burst firing events that shows the loss of burst firing activity after drug administration in sham (A) 6-OHDA (B) and 6-OHDA L-DOPA groups (C). Graphical representation of the mean ± S.E.M. of the firing rate (D), the CV (E), and the number of neurons with burst (F) in the three experimental groups, sham (n = 8), 6-OHDA (n = 7), and 6-OHDA L-DOPA (n = 8) before and after increasing doses of buspirone and WAY-100635. [##]p < 0.01 and [###]p < 0.001 vs. sham group and [&]p < 0.05 and [&&&]p < 0.001 vs. respective baseline (Fisher´s exact test for firing pattern).

Table 4.2. Effect of systemic administration of buspirone (0.6125–5 mg/kg, i.v.) and WAY-101635 (0.5–1 mg/kg, i.v.) on firing properties of substantia nigra pars reticulata neurons.

		Buspirone (mg/kg)					WAY-101635 (mg/kg)	
		Basal	0.6125	1.25	2.5	5	0.5	1
Sham (n = 8)	1	23.0 ± 4.2	23.5 ± 4.5	23.3 ± 4.6	22.6 ± 5.0	23.4 ± 5.2	20.7 ± 5.9	18.1 ± 5.8
	2	27.6 ± 4.7	29.1 ± 4.1	31.7 ± 4.2	34.3 ± 5.1	29.1 ± 2.5	39.0 ± 7.9	45.1 ± 18
	3	50	75[&]	50	50	62.5	50	40
	4	4.4 ± 2.6	1.7 ± 0.6	3.4 ± 1.5	7.3 ± 4.1	7.4 ± 4.6	5.0 ± 4.4	5.2 ± 3.4
	5	0.5 ± 0.3	0.4 ± 0.2	0.5 ± 0.2	0.8 ± 0.4	0.7 ± 0.4	5.0 ± 4.4	0.6 ± 0.6
	6	9.9 ± 6.5	8.3 ± 3.7	9.5 ± 4.9	11.3 ± 5.0	9.0 ± 3.6	1.0 ± 0.9	18.3 ± 16
	7	3.0 ± 1.8	1.1 ± 0.4	2.2 ± 1.0	4.6 ± 2.6	4.6 ± 2.8	3.0 ± 2.2	3.2 ± 2.1
	8	27.5 ± 12	38.0 ± 13	20.6 ± 10	23.3 ± 12	41.4 ± 16	36.1 ± 18	20.6 ± 14
6-OHDA (n = 7)	1	30.1 ± 4.2	26.3 ± 6.0	31.6 ± 4.3	28.1 ± 3.9	28.1 ± 3.9	28.9 ± 5.3	26.6 ± 4.1
	2	44.3 ± 9.5	37.8 ± 6.2	38.5 ± 6.2	38.7 ± 6.9	42.8 ± 10	48.9 ± 18	48.6 ± 13
	3	85.7[###]	71.4	57.1[&]	57.1[&]	42.9[&&]	57.1[&]	33.3[&&&]
	4	9.0 ± 4.1	7.0 ± 3.8	6.3 ± 3.3	4.4 ± 2.3	4.1 ± 2.5	7.9 ± 3.9	6.8 ± 5.0
	5	0.2 ± 0.1	0.1 ± 0.1	0.1 ± 0.0	0.3 ± 0.1	0.5 ± 0.3	0.6 ± 0.2	0.2 ± 0.1
	6	7.7 ± 2.2	7.4 ± 2.5	5.8 ± 2.4	11.2 ± 5.1	25.6 ± 19	18.4 ± 7.8	5.9 ± 3.7
	7	5.2 ± 2.8	4.4 ± 2.3	4.0 ± 2.0	2.9 ± 1.5	2.7 ± 1.7	5.2 ± 2.6	4.6 ± 3.3
	8	60.3 ± 12	53.0 ± 17	44.7 ± 17	31.2 ± 12	25.6 ± 14	21.4 ± 8.8	11.0 ± 7.3
6-OHDA L-DOPA (n = 8)	1	27.4 ± 3.4	37.5 ± 6.4	33.9 ± 6.6	31.1 ± 6.7	30.7 ± 6.3	29.5 ± 6.1	36.3 ± 8.1
	2	30.4 ± 5.2	37.0 ± 5.9	44.3 ± 8.3	47.4 ± 9.3	39.1 ± 7.2	38.6 ± 7.7	31.9 ± 6.9
	3	75[##]	37.5[&&]	50[&]	50[&]	50[&]	50[&]	12.5[&&&]
	4	19.2 ± 16	21.5 ± 16	28.5 ± 16	30.5 ± 16	31.2 ± 19	28.2 ± 21	16.3
	5	0.1 ± 0.1	0.1 ± 0.0	0.2 ± 0.1	0.2 ± 0.1	0.1 ± 0.0	0.2 ± 0.1	0.025
	6	9.5 ± 3.7	5.9 ± 3.6	11.7 ± 4.4	8.5 ± 3.5	7.0 ± 3.2	10.4 ± 5.0	3.4
	7	11.7 ± 9.7	13.2 ± 9.9	17.6 ± 11	18.8 ± 9.7	18.9 ± 12	17.3 ± 12	9.8
	8	82.5 ± 27	49.7 ± 28	52.7 ± 26	53.6 ± 27	52.9 ± 27	57.5 ± 26	23.2

Data from the firing rate, the CV and burst related parameters are expressed as mean ± S.E.M. [&]p < 0.05, [&&]p < 0.01 and [&&&]p < 0.001 vs baseline, and [##]p < 0.01 and [###]p < 0.001 vs sham (Fisher´s exact test). (**1**) Firing rate (Hz), (**2**) CV (%), (**3**) neurons exhibiting burst firing pattern (%), (**4**) number of bursts, (**5**) duration of burst (ms), (**6**) nº spikes/burst, (**7**) recurrence of burst (nº burst/min), and (**8**) intraburst frequency (spike/s).

Table 4.3. Effect of of systemic administration of 8-OH-DPAT (20–160 μg/kg, i.v.) and WAY-101635 (0.5–1 mg/kg, i.v.) on firing properties of substantia nigra pars reticulata neurons.

		8-OH-DPAT (μg/kg)					WAY-101635 (mg/kg)	
		Basal	20	40	80	160	0.5	1
Sham (n = 5)	1	20.3 ± 1.5	15.8 ± 1.7	13.0 ± 1.1	9.4 ± 1.9	10.3 ± 1.8	23.9 ± 7.6	22.1 ± 7.3
	2	31.0 ± 6.0	29.2 ± 3.7	32.9 ± 4.4	28.2 ± 4.9	40.7 ± 7.2	33.7 ± 8.5	40.8 ± 15
	3	40	20$^{\&}$	0$^{\&\&\&}$	0$^{\&\&\&}$	40	0$^{\&\&\&}$	0$^{\&\&\&}$
	4	9.3 ± 8.8	2	0	0	7.3 ± 6.3	0	0
	5	0.1 ± 0.1	6.8	0	0	0.2 ± 0.1	0	0
	6	4.3 ± 3.4	154	0	0	2.3 ± 12	0	0
	7	5.6 ± 5.3	1.25	0	0	4.3 ± 3.8	0	0
	8	31 ± 15.6	21.21	0	0	34.0 ± 29	0	0
6-OHDA (n = 5)	1	25.3 ± 3.1	27.9 ± 4.7	25.6 ± 4.1	22.4 ± 3.7	20.9 ± 3.6	17.7 ± 4.2	17.4 ± 4.4
	2	33.3 ± 11	33.3 ± 9.7	29.6 ± 9.0	31.7 ± 12	35.3 ± 9.1	29.8 ± 5.1	38.1 ± 7.0
	3	50	50	33.3$^{\&}$	33.3$^{\&}$	100$^{\&}$	50	66.6
	4	11.5 ± 5.9	2.5 ± 2.1	1.7 ± 1.5	1.8 ± 1.6	3.5 ± 1.3	1.0 ± 0.5	1.9 ± 1.0
	5	1.1 ± 1.0	0.2 ± 0.1	0.1 ± 0.0	0.4 ± 0.3	0.4 ± 0.1	0.1 ± 0.0	4.6 ± 3.7
	6	7.1 ± 3.9	4.9 ± 2.5	2.8 ± 1.9	9.6 ± 7.2	8.3 ± 2.2	3.6 ± 2.1	87.7 ± 48
	7	3.9 ± 3.4	1.5 ± 1.2	1.0 ± 0.9	1.1 ± 1.0	2.1 ± 0.8	0.7 ± 0.3	1.1 ± 0.6
	8	25.8 ± 12	25.0 ± 14	17.6 ± 13	8.2 ± 5.3	45.7 ± 8.1	26.9 ± 13	40.4 ± 19
6-OHDA L-DOPA (n = 5)	1	32.0 ± 3.1	31.5 ± 4.6	30.7 ± 5.9	29.0 ± 5.8	28.9 ± 6.6	23.9 ± 3.8	21.9 ± 4.1
	2	46.0 ± 17	38.4 ± 13	45.7 ± 18	50.5 ± 21	51.1 ± 18	36.2 ± 7.7	25.1 ± 1.8
	3	60$^{\#}$	40$^{\&}$	40$^{\&}$	40$^{\&}$	80$^{\&}$	40$^{\&}$	20$^{\&}$
	4	40.3 ± 26	32.3 ± 29	39.3 ± 38	37.3 ± 34	42.5 ± 34	2.3 ± 0.8	3
	5	2.4 ± 2.3	0.1 ± 0.1	0.1 ± 0.1	0.6 ± 0.5	0.7 ± 0.5	2.3 ± 1.9	0.32
	6	19.0 ± 9.2	4.9 ± 3.3	4.4 ± 2.6	21.0 ± 15	21.0 ± 15	60.3 ± 40	11.3
	7	17.7 ± 17	29.1 ± 17	23.3 ± 22	25.6 ± 20	25.6 ± 21	1.4 ± 0.5	1.8
	8	48.2 ± 20	37.1 ± 25	38.0 ± 25	46.7 ± 22	45.9 ± 23	27.2 ± 11	39.7

Data from the firing rate, the CV and burst related parameters are expressed as mean ± S.E.M. $^{\&}$p < 0.05, $^{\&\&}$p < 0.01 and $^{\&\&\&}$p < 0.001 vs baseline and $^{\#}$p < 0.05 vs sham (Fisher´s exact test). (**1**) Firing rate (Hz), (**2**) CV (%), (**3**) neurons exhibiting burst firing pattern (%), (**4**) number of bursts, (**5**) duration of burst (ms), (**6**) nº spikes/burst, (**7**) recurrence of burst (nº burst/min), and (**8**) intraburst frequency (spike/s).
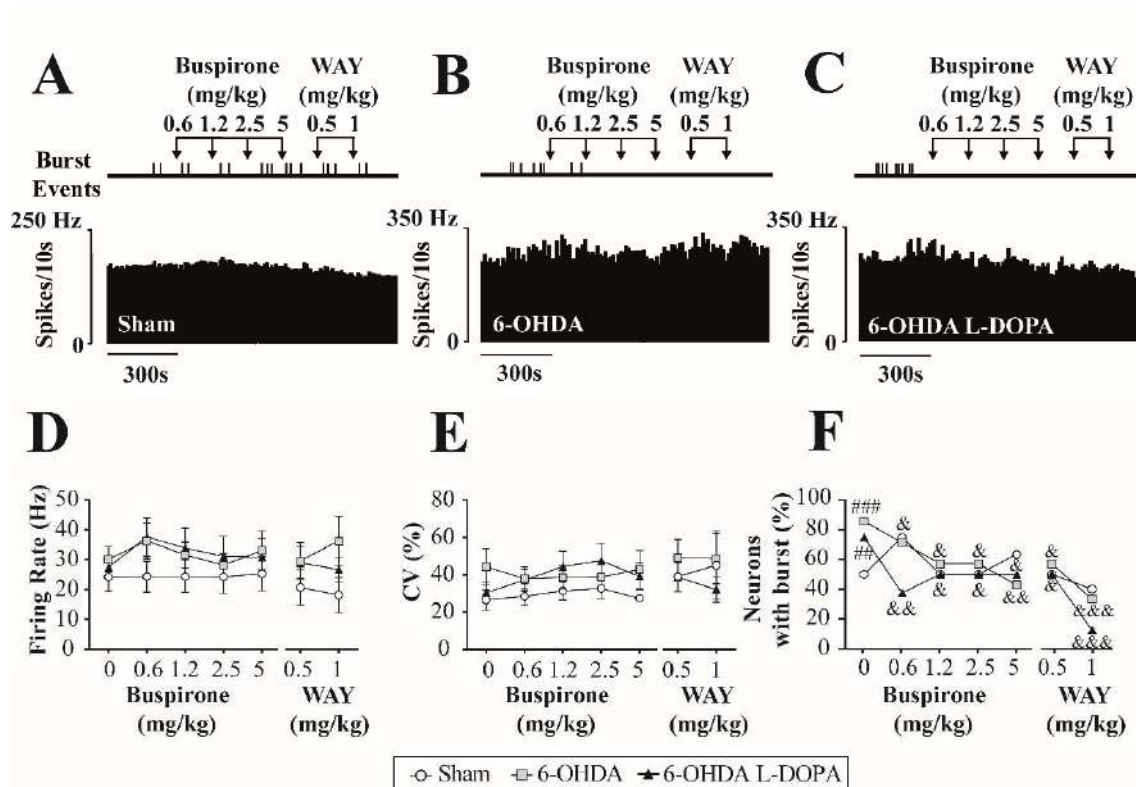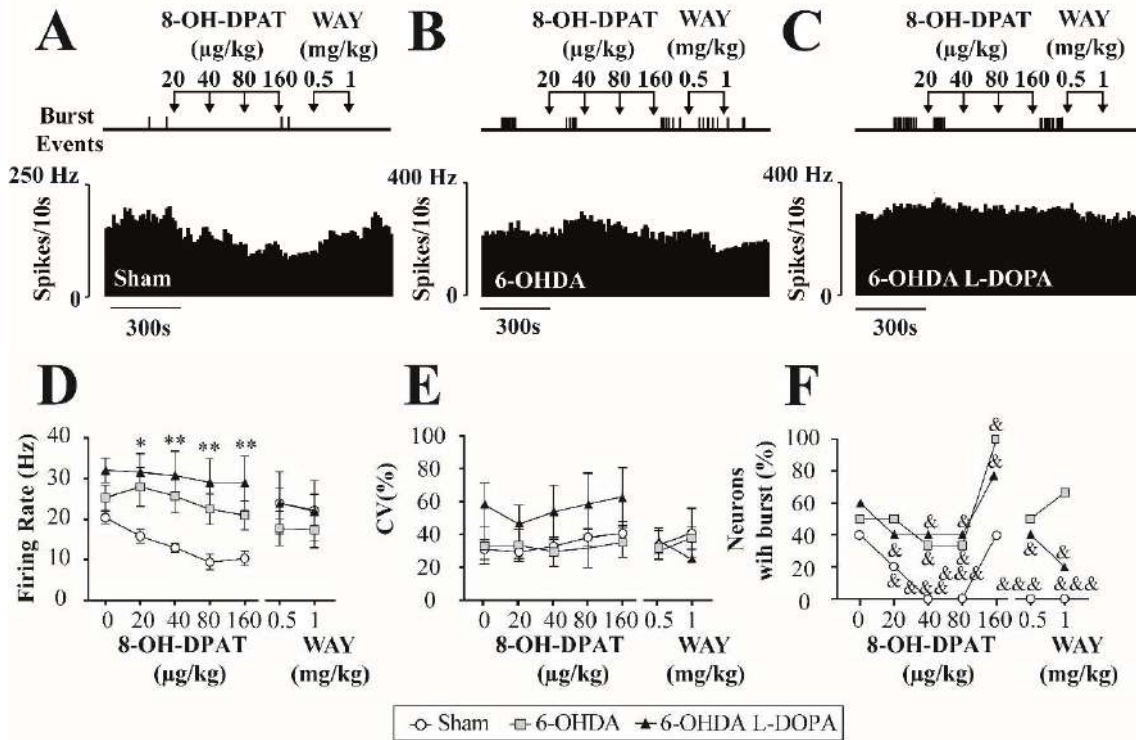
Figure 4.4. Effect of systemic administration of 8-OH-DPAT on substantia nigra pars reticulata neuron activity. Representative firing rate histogram illustrating the absence of effects of 8-OH-DPAT (20–160 µg/kg, iv) and WAY-100635 (0.1 mg/kg, i.v) on SNr neuronal firing rate, and schematic representation of burst firing events that shows the loss of burst firing activity after drug administration in sham (A), 6-OHDA (B), and 6-OHDA L-DOPA groups (C). Graphical representation of the mean ± S.E.M. of the firing rate (D), the CV (E), and the number of neurons with burst (F) in the three experimental groups, sham (n = 5), 6-OHDA (n = 5), and 6-OHDA L-DOPA (n = 5) before and after increasing doses of 8-OH-DPAT and WAY-100635. Data are expressed as mean ± S.E.M. *$p < 0.05$ and **$p < 0.01$ vs. sham group (Two-way ANOVA followed by Bonferroni's post hoc test) and &$p < 0.05$ and &&&$p < 0.001$ vs. corresponding basal value (Fisher´s exact test for firing pattern).

4.1.2. Effect of 5-HT₁ₐ agonists on the low oscillatory activity and synchronization in the substantia nigra pars reticulata and motor cortex

Simultaneously with the single-unit extracellular recordings of SNr neurons, SNr-LFP and motor cortex (ECoG) were recorded. We analysed the power spectrum and the coherence in the 0–5 Hz range to determine the parameters of low frequency activity and synchronization into the SNr and between this nucleus and the motor cortex. 31 neurons from the sham group (n = 19 rats), 29 neurons from the 6-OHDA group (n = 17 rats) and, 32 neurons from the 6-OHDA L-DOPA group (n = 18 rats) were included in the analysis.

In agreement with our previous publication (Aristieta et al., 2016), power spectra analysis showed a low oscillatory activity in the ECoG and the LFP with a peak, near to 1 Hz in all experimental groups (**Fig. 4.5A** and **B**). AUC values of the ECoG power spectrum was similar among the groups ($F_{(2, 51)} = 1.86$, $p > 0.05$, one-way ANOVA; **Fig. 4.5A**) whereas the LFP AUC value was higher in the 6-OHDA group ($F_{(2, 51)} = 4.21$, $p < 0.05$, one-way ANOVA; **Fig. 4.5B**). The coherence analysis showed that synchronization between ECoG and SNr spikes (**Fig. 4.6A**) and between SNr-LFP and SNr spikes (**Fig. 4.6B**) was higher after 6-OHDA lesion and L-DOPA treatment with the AUC value obtained from the coherence curves being significantly larger in the 6-OHDA and 6-OHDA L-DOPA group ($F_{(2, 51)} = 9.351$, $p < 0.001$ one-way ANOVA and $F_{(2, 51)} = 12.52$, $p < 0.001$; one-way ANOVA). No difference was observed in the synchronization between ECoG and SNr-LFP ($F_{(2, 51)} = 1.469$, $p > 0.05$; one-way ANOVA; **Fig. 4.6C**).

Next, to investigate the effect of 5-HT drugs on low oscillatory activity and synchronization between the SNr and ECoG, we compared the power spectrum and coherence obtained before and after the systemic administration of increasing doses of buspirone or 8-OH-DPAT. One neuron per animal was pharmacologically tested with buspirone in a total of 23 animals: sham group (n = 8), 6-OHDA group (n = 7) and 6-OHDA L-DOPA group (n = 8). Buspirone administration produced an effect on the ECoG (buspirone: $F_{(4, 80)} = 9.816$, $p < 0.001$, and lesion: $F_{(2, 20)} = 0.3387$, $p > 0.05$; RM two-way ANOVA; **Fig. 4.5C**) and LFP (buspirone: $F_{(4, 80)} = 4.034$, $p < 0.05$, and lesion: $F_{(2, 20)} = 0.0266$, $p > 0.05$; RM two-way ANOVA; **Fig. 4.5D**). This effect was only significant for the first dose in ECoG of sham and 6-OHDA groups. As it is shown in **Figure 4.6D**, buspirone administration did not modify the synchronization between ECoG and SNr

spikes (buspirone: $F_{(4, 80)} = 0.1971$, $p > 0.05$ and lesion: $F_{(2, 20)} = 2.012$, $p > 0.05$; RM two-way ANOVA). Nevertheless, buspirone produced a slight effect between LFP and SNr spikes synchronization (buspirone: $F_{(4, 80)} = 2.633$, $p < 0.05$ and lesion: $F_{(2, 20)} = 0.178$, $p > 0.05$; RM two-way ANOVA; **Fig. 4.6E**). Synchronization between ECoG and LFP was not affected much by buspirone (buspirone: $F_{(4, 80)} = 5.718$, $p < 0.05$, and lesion: $F_{(2, 20)} = 0.03768$, $p > 0.05$; RM two-way ANOVA; **Fig. 4.6F**).

Finally, we investigated the effect of systemic 8-OH-DPAT administration on the oscillatory activity and synchronization. One neuron per animal was pharmacologically tested in a total of 15 animals (n = 5 in each group). As it is shown in **Figures 4.5E** and **F**, 8-OH-DPAT did not cause any change in the AUC of the ECoG and LFP power spectra (For ECoG, 8-OH-DPAT: $F_{(4, 48)} = 1.04$, $p > 0.05$ and lesion: $F_{(2, 12)} = 1.231$, $p > 0.05$; For LFP, 8-OH-DPAT: $F_{(4, 48)} = 2.37$, $p > 0.05$ and lesion: $F_{(2, 12)} = 0.2284$, $p > 0.05$; RM two-way ANOVA). In addition, analysis of coherence revealed that 8-OH-DPAT had a slight effect on AUC of the coherence between ECoG and SNr spike but no differences between the three experimental groups were observed (8-OH-DPAT: $F_{(4, 48)} = 2.977$, $p < 0.05$, and lesion: $F_{(2, 12)} = 0.02681$, $p > 0.05$; RM two-way ANOVA; **Fig. 4.6G**). 8-OH-DPAT did not cause any effect in the AUC of the coherence between LFP and SNr spikes (8-OH-DPAT: $F_{(4, 48)} = 1.1$, $p > 0.05$, and lesion: $F_{(2, 12)} = 0.4539$, $p > 0.05$; RM two-way ANOVA; **Fig. 4.6H**). In the coherence between ECoG and LFP there was a reduction in 6-OHDA L-DOPA group with the first dose of 8-OH-DPAT, but no effect was observed for subsequent doses (8-OH-DPAT: $F_{(4, 48)} = 2.796$, $p < 0.05$, and lesion: $F_{(2, 12)} = 2.609$, $p < 0.05$; RM two-way ANOVA; **Fig. 4.6I**).
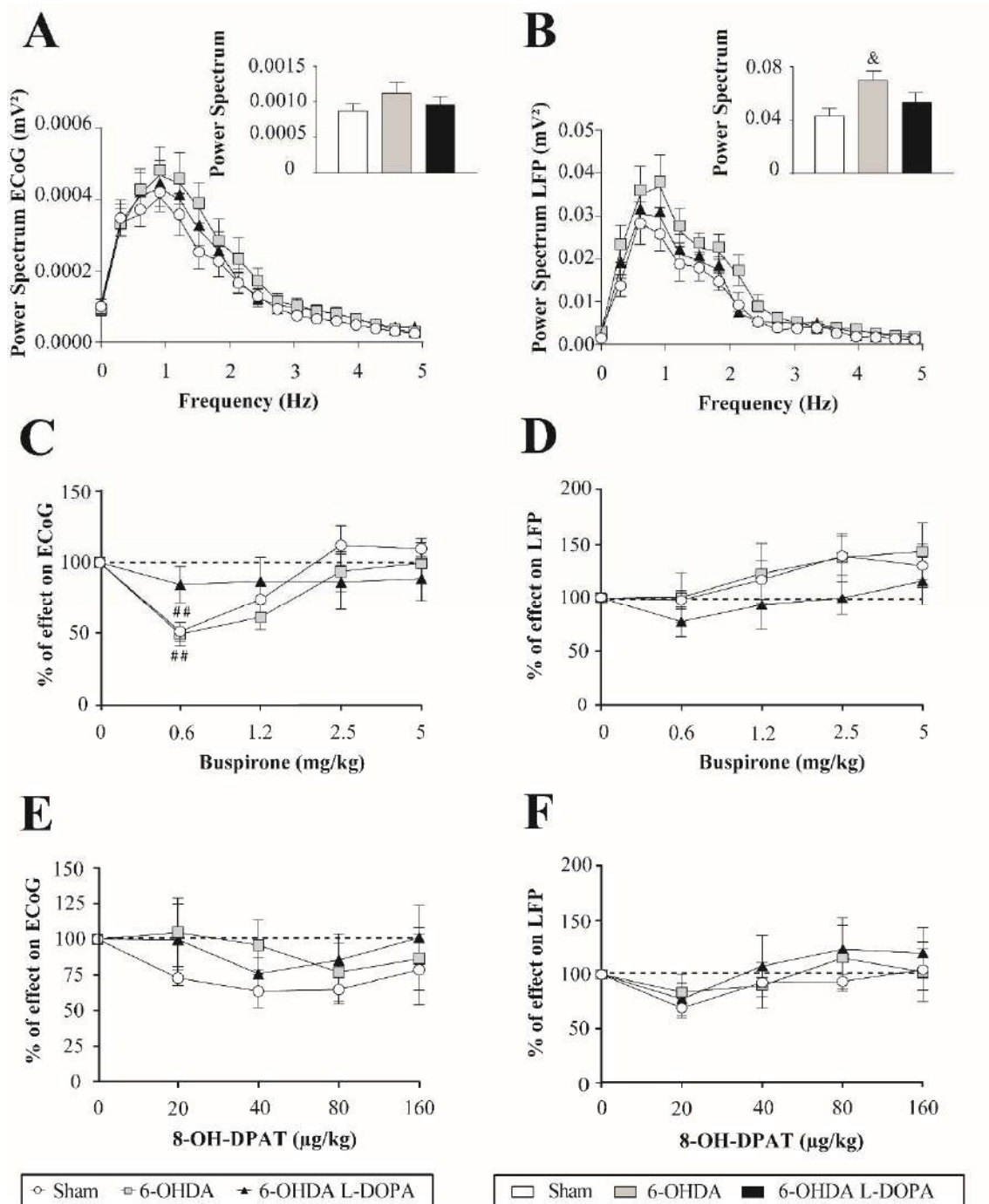
Figure 4.5. Effect of systemic administration of buspirone and 8-OH-DPAT on the power spectrum of the local field potential of substantia nigra pars reticulata and the motor cortex in low oscillatory frequency range (0–5 Hz). Power spectra and AUC values obtained from the ECoG (A) and SNr-LFP (B) in the sham (n = 19), 6-OHDA (n = 17), and 6-OHDA L-DOPA (n = 18) animals. Effect of administration of increasing doses of buspirone (0.6125–5 mg/kg, i.v.) on the AUC of the power spectrum of the ECoG (C) and SNr-LFP (D) in the sham (n = 8), 6-OHDA (n = 7), and 6-OHDA L-DOPA (n = 8) animals. Effect of administration of increasing doses of 8-OH-DPAT (20–160 µg/kg, i.v.) on the AUC of the power spectrum of the ECoG (E) and SNr-LFP (F) obtained from the three experimental groups, sham (n = 5), 6-OHDA (n = 5), and 6-OHDA L-DOPA (n = 5). Data are expressed as mean ± S.E.M. $^{\&}p < 0.05$ vs sham (one-way ANOVA followed by Bonferroni´s post-hoc test) $^{\#\#}p < 0.01$, and $^{\#\#\#}p < 0.001$ vs respective baseline (two-way ANOVA followed by Bonferroni´s post-hoc test).
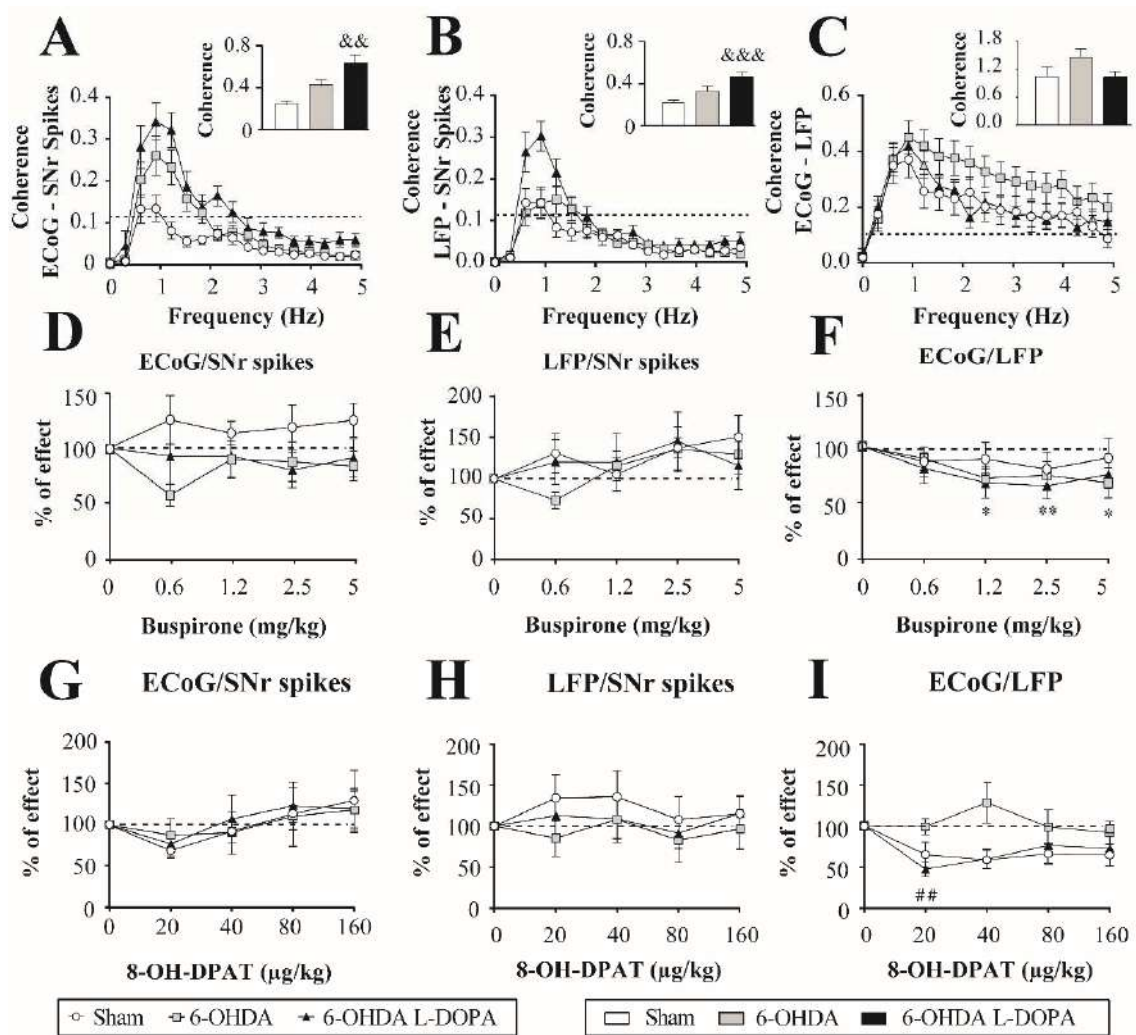
Figure 4.6. Effect of systemic administration of buspirone and 8-OH-DPAT on substantia nigra pars reticulata neuron spikes, the local field potential of substantia nigra pars reticulata neuron and the motor cortex coherence in low frequency range (0–5 Hz). Coherence power spectra between the ECoG and SNr spikes simultaneously recorded in the sham (n = 19), 6-OHDA (n = 17), and 6-OHDA L-DOPA (n = 18) groups. AUC value obtained from coherence between the ECoG and SNr spikes was augmented in 6-OHDA L-DOPA group (A). AUC values obtained from SNr-LFP/ SNr spikes coherence curves showed an increase in 6-OHDA L-DOPA group (A, medium). AUC values obtained from ECoG/SNr-LFP coherence curves showed no differences (B). Effect of administration of acute doses of buspirone (0.6125–5 mg/kg, i.v.) on the synchronization between ECoG and SNr spikes (D), between SNr-LFP and SNr spikes (E), and between ECoG and SNr-LFP spikes (F) in the sham (n = 8), 6-OHDA (n = 7), and 6-OHDA L-DOPA (n = 8) groups. Effect of administration of acute doses of 8-OH-DPAT (20–160 µg/kg, i.v.) on the synchronization between ECoG and SNr spikes (G), between SNr-LFP and SNr spikes (H), and between ECoG and SNr-LFP spikes (I) in the sham (n = 5), 6-OHDA (n = 5), and 6-OHDA L-DOPA (n = 5) groups. Data are expressed as mean ± S.E.M. $^{\&\&}p < 0.01$ and $^{\&\&\&}p < 0.001$ vs sham (one-way ANOVA followed by Bonferroni´s post-hoc test), $^{*}p < 0.05$ and $^{**}p < 0.01$ vs sham and $^{\#\#}p < 0.01$ vs respective baseline (RM two-way ANOVA followed by Bonferroni´s post-hoc test).

4.1.3. Effect of buspirone on the amino acid release of substantia nigra pars reticulata

The effect of locally perfused buspirone on the levels of GABA and GLU in the SNr was studied in naïve (n = 11), 6-OHDA (n = 11), and 6-OHDA L-DOPA rats (n = 8). Basal GABA and GLU levels in the SNr did not differ among the three experimental groups (for GABA: $F_{(2, 27)}$ = 0.1225, $p > 0.05$ and for GLU: $F_{(2, 27)}$ = 1.95, $p > 0.05$; one-way ANOVA), being 7.28 ± 2.65 nM and 94.35 ± 11.99 nM in naïve, 8.44 ± 1.89 nM and 110.27 ± 16.01 in 6-OHDA and 8.73 ± 1.58 and 71.87 ± 7.65 in 6-OHDA L-DOPA animals. Local stepwise perfusion of buspirone (50 nM, 150 nM and 500 nM) raised GABA levels in naïve and 6-OHDA groups but had no effect in 6-OHDA L-DOPA animals (**Fig. 4.7A**). However GABA enhancement was significantly lower in the 6-OHDA group when compared to the naïve group (buspirone: $F_{(15, 360)}$ = 2.611, $p < 0.001$ and lesion: $F_{(2, 24)}$ = 6.408, $p < 0.01$, RM two-way ANOVA; **Fig. 4.7B** and **C**). Likewise, buspirone also elevated GLU release in control and 6-OHDA groups but it had no effect in 6-OHDA L-DOPA animals (**Fig. 4.7D**, **E** and **F**). Again the effect of buspirone on 6-OHDA-lesioned rats was significantly less when compared to the effect on naïve rats (**Fig. 4.7E** and **F**) (buspirone: $F_{(15, 345)}$ = 3.009, $p < 0.001$ and lesion: $F_{(2, 23)}$ = 5.654, $p < 0.01$, RM two-way ANOVA; **Fig. 4.7D**).
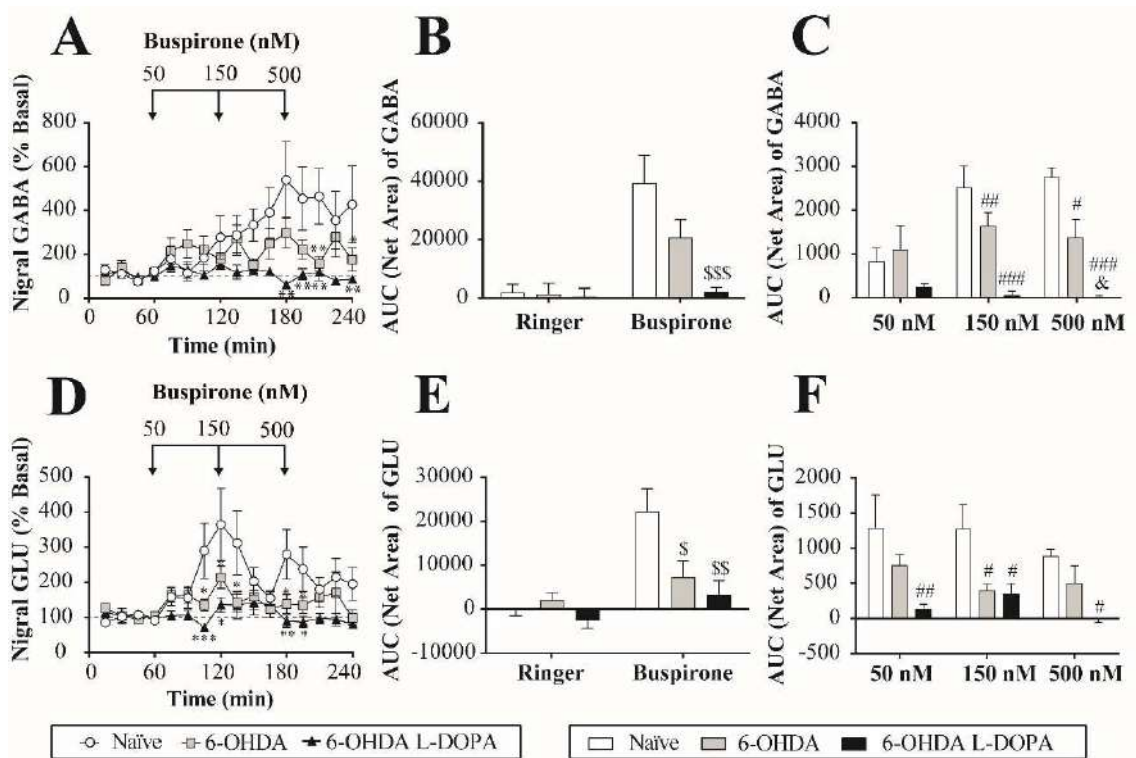
Figure 4.7. Effect of local perfusion of buspirone (50 nM–500 nM) on nigral amino acid levels of gamma-aminobutyric acid and glutamate. Local perfusion of buspirone raised nigral **gamma-aminobutyric** (GABA) levels in naïve (n = 9) and 6-OHDA (n = 11) groups, but with less intensity, and it had no effect in 6-OHDA L-DOPA (n = 7) group (A). Buspirone also raised nigral glutamate (GLU) levels in naïve (n = 10) and in 6-OHDA (n = 9) groups, with less intensity, and it had no effect in 6-OHDA L-DOPA (n = 7) group (D). Bar representation (mean ± S.E.M.) of the AUC (60–240 min) (B and E) and AUC 60 min after administration of the respective buspirone concentration dose (C and F). Data are expressed as percentage of basal levels calculated as the mean of the two samples preceding buspirone perfusion. *$p < 0.05$, **$p < 0.01$ and ***$p < 0.001$ vs. naïve group; $^{\$}p < 0.05$, $^{\$\$}p < 0.01$, and $^{\$\$\$}p < 0.001$ vs. Net Area of naïve group; $^{\#}p < 0.05$, $^{\#\#}p < 0.01$, and $^{\#\#\#}p < 0.001$ vs. respective concentration of naïve group, and $^{\&}p < 0.05$ vs respective concentration of 6-OHDA group (RM two-way ANOVA followed by Bonferroni's post-hoc test).

4.2. STUDY II: EFFECT OF BUSPIRONE ON ENTOPEDUNCULAR NEURON ACTIVITY IN SHAM, 6-HYDROXYDOPAMINE AND LONG-TERM L-DOPA TREATED 6-HYDROXYDOPAMINE RATS

4.2.1. Effect of 5-HT$_{1A}$ agonists on entopeduncular neuron activity

A total of 90 GABAergic neurons were recorded in the EP of anaesthetised rats; 26 from the sham group (n = 15 rats), 27 from the 6-OHDA group (n = 16 rats) and, 32 from the 6-OHDA L-DOPA group (n = 17 rats). Additionally, 5 neurons from a group of 6-OHDA-lesioned rats which did not show a total dopaminergic fiber loss (< 80%) was included (n = 5) (see later). All cells recorded were located within the EP and displayed the characteristic firing properties of EP-GABAergic neurons that we previously described (Aristieta et al., 2019). The mean value of the basal firing rate (F$_{(3, 49)}$ = 4.4, p < 0.01, one-way ANOVA) and the CV were higher in the 6-OHDA L-DOPA group (F$_{(3, 49)}$ = 2.9, p < 0.05, one-way ANOVA) and the number of bursty neurons was increased in the 6-OHDA and 6-OHDA L-DOPA groups (p < 0.05, Fisher´s exact test, **Table 4.4**). The mean value per animal ± S.E.M. of the firing rate, CV and firing pattern parameters for all experimental groups are shown in **Table 4.4**. After the analysis of the basal firing properties, the effect of local and systemic buspirone or systemic 8-OH-DPAT administration was evaluated.

Table 4.4. Firing properties of entopeduncular neurons.

Parameters	Sham (n =15)	Partially 6-OHDA [1] (n = 5)	6-OHDA (n = 16)	6-OHDA L-DOPA (n = 17)
Firing rate (Hz)	17.4 ± 1.7	13.2 ± 3.9	24.6 ± 2.7	26.7 ± 2.7*$^\$$
CV (%)	46.8 ± 6.0	54.2 ± 6.2	55.0 ± 9.4	80.3 ± 10.8*
Neurons exhibiting burst firing pattern (%)	61.5	80[#]	77.8[#]	87.5[###]
Number of bursts	46.8 ± 13.6	60.6 ± 34.3	29.4 ± 10.9	46.9 ± 13.9
Duration of burst (ms)	0.6 ± 0.3	0.2 ± 0.1	0.3 ± 0.1	0.3 ± 0.1
Nº spikes/burst	11.3 ± 2.5	5.4 ± 1.9	14.1 ± 6.4	14.4 ± 2.2
Recurrence of burst (nº burst/min)	33.3 ± 9.5	34.1 ± 20.1	19.6 ± 7.4	24.6 ± 6.2
Intraburst frequency (spike/s)	71.5 ± 14.3	58.5 ± 19.2	62.6 ± 8.9	66.2 ± 5.1

Values are expressed as mean $\pm$ S.E.M. *$p < 0.05$ vs sham and $^\$p < 0.05$ vs partially 6-OHDA (One-way ANOVA followed by Bonferroni´s post hoc test) and [#]$p < 0.05$ and [###]$p < 0.001$, vs sham (Fisher´s exact test). [1] It refers to a group of 6-OHDA animals which did not show a total dopaminergic fiber loss (> 80%).

Figure 4.8. Effect of local administration of buspirone on entopeduncular neuron activity. Representative firing rate histograms illustrating the inhibitory local effect of buspirone in an EP neuron from the sham (A), 6-OHDA (B) and 6-OHDA L-DOPA groups (C). When buspirone (0.25-2 nmol) was locally applied into EP induced a dose-dependent inhibitory effect in the three experimental groups (D). Data are expressed as mean $\pm$ S.E.M. xxx: $p < 0.001$ vs. sham baseline (n = 5), y < 0.05, yy < 0.01 and yyy < 0.001 vs. 6-OHDA baseline (n = 5) and zzz < 0.001 vs. 6-OHDA L-DOPA baseline (n = 5) (RM two-way ANOVA followed by Bonferroni's posthoc test).

Local effect of buspirone was studied on 50 EP neurons: 15 neurons from the sham group (n = 5), 15 neurons from the 6-OHDA group (n = 5) and 20 neurons from the 6-OHDA L-DOPA group (n = 5). As shown in **Figure 4.8**, local administration of buspirone (0.25–2 nM) caused a marked dose-dependent inhibition of the neuron activity in the three experimental groups with a maximal reduction of the firing rate of ~ 70% of the basal value (buspirone: $F_{(4, 48)} = 54.72$, $p < 0.001$, RM two-way ANOVA). No difference in the efficacy of local buspirone was detected among the groups (lesion: $F_{(2, 12)} = 1.426$, $p > 0.05$, RM two-way ANOVA).

Next, the effect of cumulative doses of buspirone (from 0.6125 mg/kg to 5 mg/kg, i.v.) on the firing rate and pattern of EP neurons (sham n = 5, partial 6-OHDA n=5, 6-OHDA, n = 6 and 6-OHDA L-DOPA, n = 6 animals) were studied in 22 rats (**Fig. 4.9A-D**). One neuron per animal was pharmacological tested. As shown in **Figure 4.9E**, systemic administration of buspirone only inhibited the firing rate of EP neurons in the sham (**Fig. 4.9A**) and partially 6-OHDA-lesioned groups (buspirone: $F_{(4, 72)} = 21.34$, $p < 0.001$; and lesion: $F_{(3, 18)} = 9.835$, $p < 0.001$, RM two-way ANOVA). Buspirone also increased the CV only in the sham group (buspirone: $F_{(4, 72)} = 7.31$, $p < 0.001$ and lesion: $F_{(3, 18)} = 1.786$, $p > 0.05$, RM two-way ANOVA; **Fig. 4.9F**). In contrast, this effect was almost totally absent in the 6-OHDA and 6-OHDA L-DOPA groups. Moreover, buspirone administration slightly decreased the number of bursty neurons in the 6-OHDA and 6-OHDA L-DOPA groups, while the number of bursty neurons was increased in sham and partial 6-OHDA groups ($p < 0.05$, Fisher´s exact test; **Table 4.5**). There were no changes in intraburst parameters (**Table 4.5**). The inhibitory effect observed in sham and partial 6-OHDA groups was partially reversed by the intravenous administration of the 5-HT$_{1A}$ antagonist WAY-100635 (0.5 and 1 mg/kg) (two-tailed paired Student´s t test, $p < 0.05$; **Fig. 4.9A** and **B**). **Table 4.5** summarizes mean value ± S.E.M. of all firing activity parameters before and after buspirone administration in the three experimental groups.
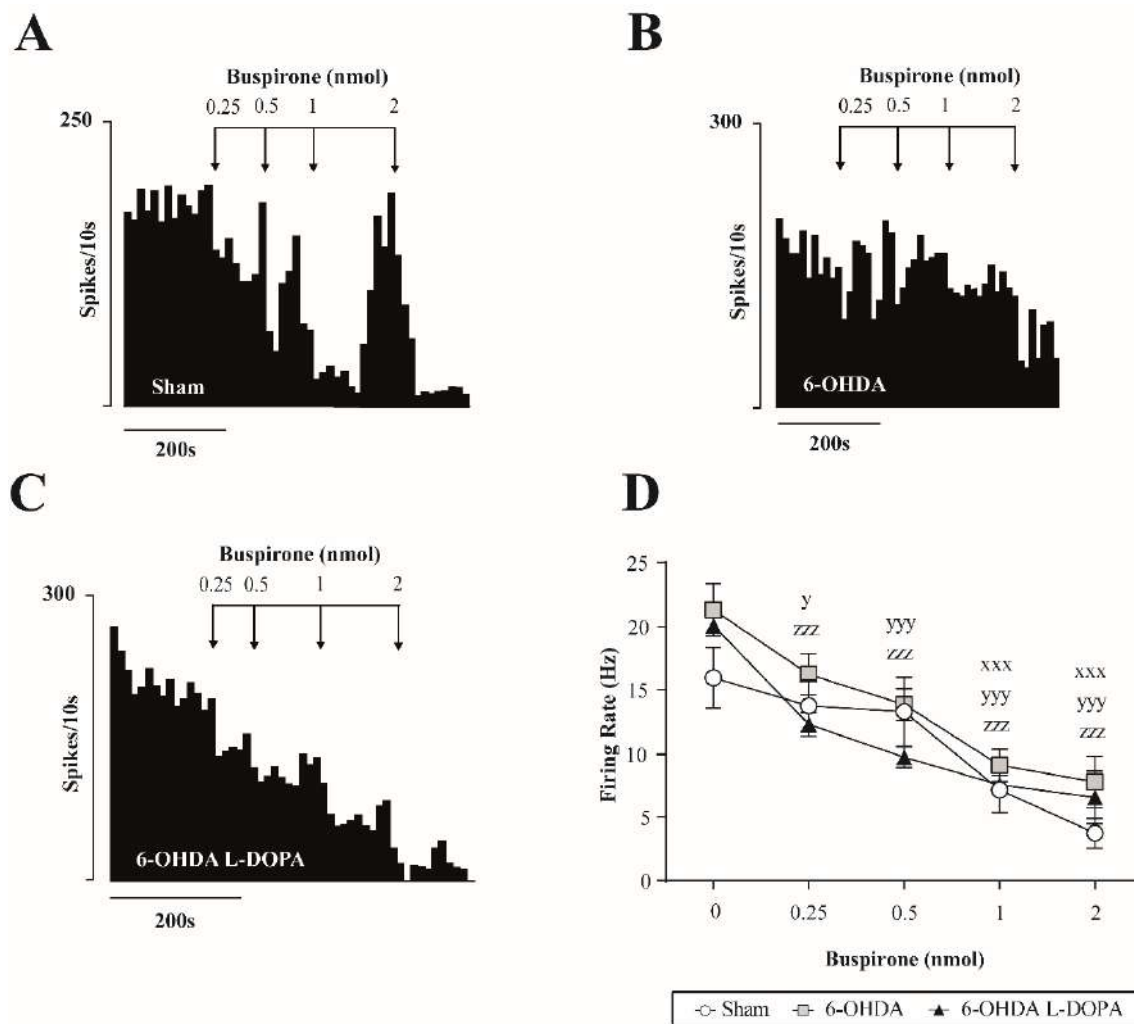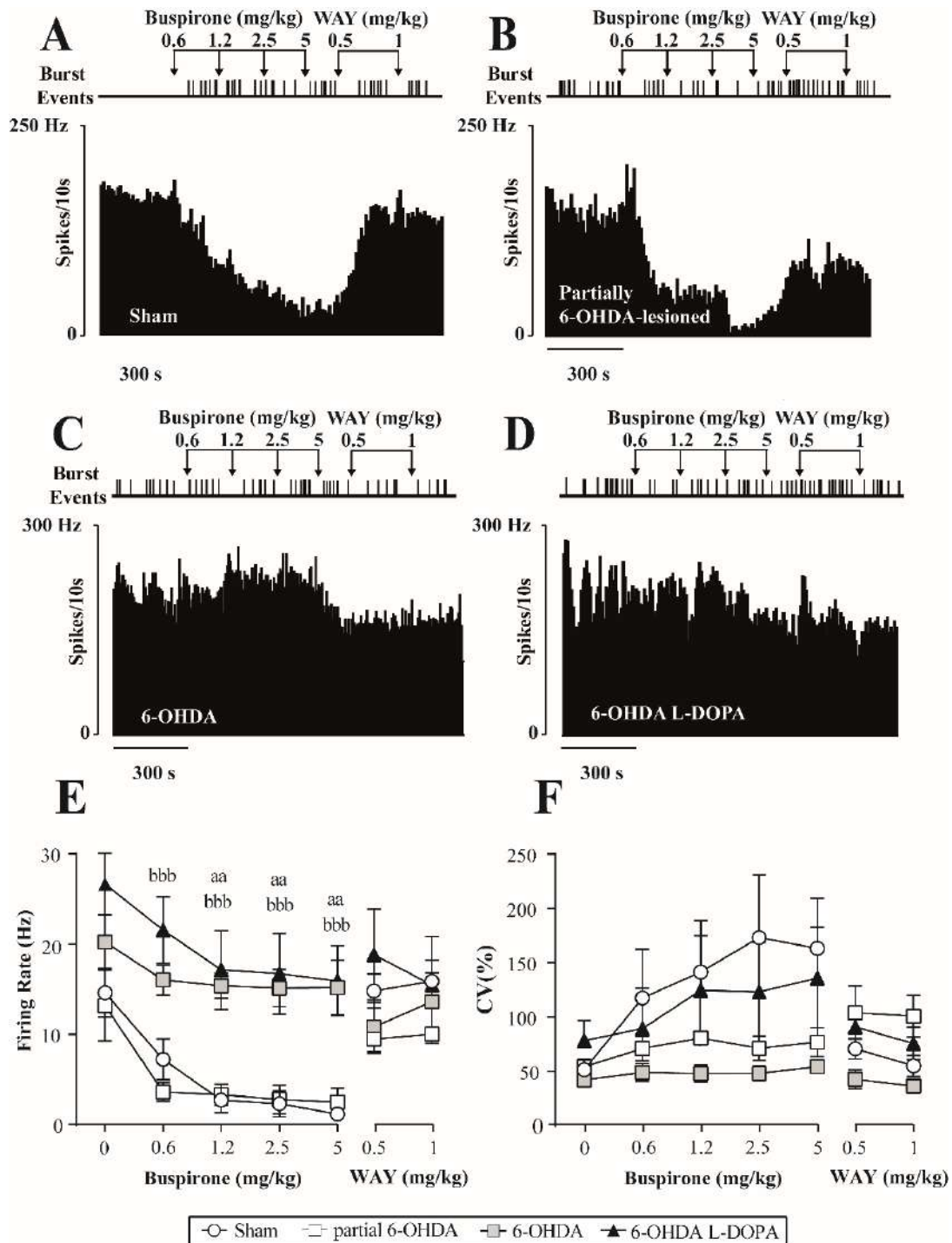
Figure 4.9. Effect of systemic administration of buspirone on entopeduncular neuron activity. Representative firing rate histogram illustrating that buspirone (0.06125-2.5 mg/kg, i.v.) inhibited the EP firing rate in sham (A) and partially 6-OHDA-lesioned (B). WAY-100635 (0.1 mg/kg, i.v) partially reverted the effect. No inhibition was seen in 6-OHDA (C) and 6-OHDA L-DOPA (D) groups. On the top, the schematic representation of burst firing events shows the loss of burst firing activity after buspirone administration in 6-OHDA group and higher burst firing activity in sham, partially lesioned and 6-OHDA L-DOPA group. Graphics representing the mean ± S.E.M. of the firing rate (E), and the CV (F), in the four experimental groups, sham (n = 5), partial 6-OHDA (n = 5) 6-OHDA (n = 6), 6-OHDA L-DOPA (n = 6) before and after increasing doses of buspirone and WAY-100635. aa < 0.01 6-OHDA group vs sham group; bbb < 0.001, 6-OHDA L-DOPA group vs. sham group (RM two-way ANOVA followed by Bonferroni's post hoc test).

Table 4.5. Effect of systemic administration of buspirone (0.6125–5 mg/kg, i.v.) and WAY-101635 (0.5–1 mg/kg, i.v.) on firing properties of entopeduncular neurons.

			Buspirone (mg/kg)				WAY-101635 (mg/kg)	
		Basal	0.6125	1.25	2.5	5	0.5	1
Sham (n = 5)	1	14.6 ± 2.7	7.2 ± 2.3*	2.7 ± 1***	2.3 ± 1***	1 ± 0.6***	14.8 ± 2##	15.9 ± 0.9
	2	51.6 ± 9.9	117.6 ± 45*	142 ± 48***	173 ± 58***	163 ± 46***	71.3 ± 9.5	55.4 ± 9.6
	3	60	100&&&	100&&&	100&&&	100&&&	75&	75&
	4	19.2 ± 15	13.2 ± 6.2	14.2 ± 7.0	18.6 ± 7.6	25.0 ± 11	36.2 ± 31	37.8 ± 37
	5	0.8 ± 0.6	2.6 ± 1.2	1.8 ± 0.8	1.8 ±0.7	1.4 ± 0.8	2.7 ± 2.6	0.7 ± 0.6
	6	10.7 ± 5.3	8.4 ± 3.5	5.4 ± 0.6	5.3 ± 0.7	6.0 ± 1.7	4.4 ± 1.6	4.7 ± 1.7
	7	12.7 ± 10	8.7 ± 4.2	9.4 ± 4.6	9.4 ± 4.6	16.8 ± 7.6	24.3 ± 22	24.3 ± 23
	8	31.7 ± 20	41.1 ± 19	37.0 ± 17	36.9 ± 17	55.8 ± 32	53.6 ± 41	49.4 ± 36
Partially 6-OHDA (n = 5) [1]	1	13.2 ± 3.9	3.6 ± 1.0**	3.3 ± 1**	3 ± 1.5***	2.5 ± 2***	9.5 ± 1.5##	10.1 ± 0.7
	2	54.2 ± 6.2	71.2 ± 11	80.6 ± 4.8	71.3 ± 11	77.0 ± 13	104.5 ± 73	101.3 ± 19
	3	80#	80	100&&&	100&&&	100&&&	80	100&
	4	60.6 ± 34	17.0 ± 9.6	10.6 ± 7.0	5.0 ± 2.1	20.0 ± 13	41.8 ± 27	46.6 ± 26
	5	0.2 ± 0.1	2.9 ± 2.5	2.9 ± 1.0	3.0 ± 1.4	0.3 ± 0.1	0.2 ± 0.1	0.3 ± 0.1
	6	5.4 ± 1.9	8.7 ± 5.9	4.9 ± 0.9	12.1 ± 3.8	4.9 ± 2.1	4.9 ± 2.1	6.9 ± 2.5
	7	34.1 ± 20	10.1 ± 5.8	6.9 ± 4.8	3.1 ± 1.2	25.3 ± 16	25.3 ± 16	29.0 ± 15
	8	58.5 ± 19	18.5 ± 12	8.3 ± 4.6	26.2 ± 17	35.2 ± 18	35.2 ± 18	44.3 ± 10
6-OHDA (n = 6)	1	20.2 ± 3.0	16.0 ± 1.6	15.4 ± 1.4	15.1 ± 2.0	15.2 ± 3.0	10.8 ± 2.7	13.6 ± 4.6
	2	42.2 ± 4.4	49.0 ± 8.1	48.1 ± 7.8	48.3 ± 6.8	54.5 ± 6.1	43.3 ± 7.0	35.2 ± 5.9
	3	66.7	50&	50&	66.7	66.7	50&	33.3&&&
	4	14.2 ± 8.7	11.6 ± 5.9	11.6 ± 7.9	10 ± 7.8	12.2 ± 9.7	12.2 ± 10.2	9.4 ± 6.8
	5	0.2 ± 0.1	0.4 ± 0.3	0.2 ± 0.1	0.2 ± 0.1	0.2 ± 0.1	0.2 ± 0.1	0.1 ± 0.1
	6	6.2 ± 3.4	9.5 ± 6.0	5.3 ± 2.3	6.4 ± 2.4	6.1 ± 2.4	5.1 ± 2.1	3.4 ± 2.2
	7	8.9 ± 5.3	7.4 ± 5.0	7.4 ± 5.0	6.5 ± 5.0	8.2 ± 6.5	7.9 ± 6.6	6.5 ± 4.7
	8	39.7 ± 10.2	19.4 ± 8.6	19.4 ± 8.6	30.7 ± 9.7	27.8 ± 10.6	22.5 ± 9.9	15.4 ± 9.4

6-OHDA (n = 6)	**1**	25.4 ± 3.1	22.1 ± 3.1	$18 \pm 4^{***}$	$17 \pm 4^{***}$	$17 \pm 3^{***}$	18.8 ± 5.0	15.5 ± 5.4
	2	71.2 ± 17.2	81.3 ± 32.4	112 ± 44.6	110 ± 40.7	$121 \pm 42^{*}$	91.4 ± 18.6	76.2 ± 14.9
	3	$83.3^{\#\#\#}$	$50^{\&\&\&}$	$66.6^{\&\&}$	83.3	$100^{\&\&\&}$	$100^{\&\&\&}$	83.3
	4	55.8 ± 33.1	15.0 ± 9.3	19.3 ± 11.0	32.2 ± 12.3	39.0 ± 12.5	44.3 ± 13.3	29.7 ± 9.7
	5	0.3 ± 0.1	0.2 ± 0.1	0.3 ± 0.1	0.3 ± 0.1	0.3 ± 0.1	0.4 ± 0.2	0.2 ± 0.1
	6	13.2 ± 5.2	9.0 ± 4.2	10.1 ± 3.8	19.2 ± 7.1	10.6 ± 2.1	13.0 ± 2.7	4.5 ± 1.6
	7	22.5 ± 11.2	7.5 ± 4.2	32.2 ± 12.3	36.4 ± 8.8	23.4 ± 7.5	27.4 ± 8.2	18.3 ± 6.0
	8	53.9 ± 13.0	26.1 ± 12.0	28.1 ± 9.7	36.4 ± 8.9	44.8 ± 5.7	45.5 ± 8.2	21.1 ± 7.1

Data from the firing rate, the CV and burst related parameters are expressed as mean $\pm$ S.E.M. $^{*}p < 0.05$, $^{**}p < 0.01$ and $^{***}p < 0.001$ vs baseline (RM two-way ANOVA followed by Bonferroni´s post hoc), $^{\&}p < 0.05$, $^{\&\&}p < 0.01$ and $^{\&\&\&}p < 0.001$ vs baseline, $^{\#}p < 0.05$, $^{\#\#}p < 0.01$ and $^{\#\#\#}p < 0.001$ vs sham (Fisher´s exact test). (**1**) Firing rate (Hz), (**2**) CV (%), (**3**) neurons exhibiting burst firing pattern (%), (**4**) number of bursts, (**5**) duration of burst (ms), (**6**) nº spikes/burst, (**7**) recurrence of burst (nº burst/min), and (**8**) intraburst frequency (spike/s). [1] It refers to a group of 6-OHDA animals which did not show a total dopaminergic fiber loss (> 80%).

Finally, we investigated the effect of the systemic administration of 8-OH-DPAT (from 20 µg/kg to 160 µg/kg; i.v.) in 16 animals (sham n = 5, 6-OHDA, n = 5 and 6-OHDA L-DOPA, n = 6 animals; **Fig. 4.10A-C**). As we had observed with buspirone administration, 8-OH-DPAT caused a significant dose-dependent inhibition of EP neuron firing rate only in the sham group (**Fig. 4.10A**) and did not modify the firing rate of neurons in the 6-OHDA and the 6-OHDA L-DOPA groups (8-OH-DPAT: $F_{(4, 52)} = 3.275$, $p < 0.05$, and lesion: $F_{(2, 13)} = 10.05$, $p < 0.01$, RM two-way ANOVA; **Fig. 4.10D**). On the other hand, 8-OH-DPAT administration had slight effect on the CV in the 6-OHDA L-DOPA group (8-OH-DPAT: $F_{(4, 52)} = 3.35$, $p < 0.05$, and lesion: $F_{(2, 13)} = 2.129$, $p > 0.05$; **Fig. 4.10E**). 8-OH-DPAT administration decreased the number of bursty neurons in the three experimental groups, however, the highest effect was observed in the sham group ($p < 0.05$, Fisher´s exact test). 8-OH-DPAT administration did not modify the intraburst parameters (**Table 4.6**). Following administration of WAY-100635(0.5 -1 mg/kg, i.v.) partially reversed the inhibitory effect of 8-OH-DPAT (**Fig. 4.10A** and **D**). **Table 4.6** summarizes mean value $\pm$ S.E.M. of all firing activity parameters before and after buspirone in the three experimental groups.
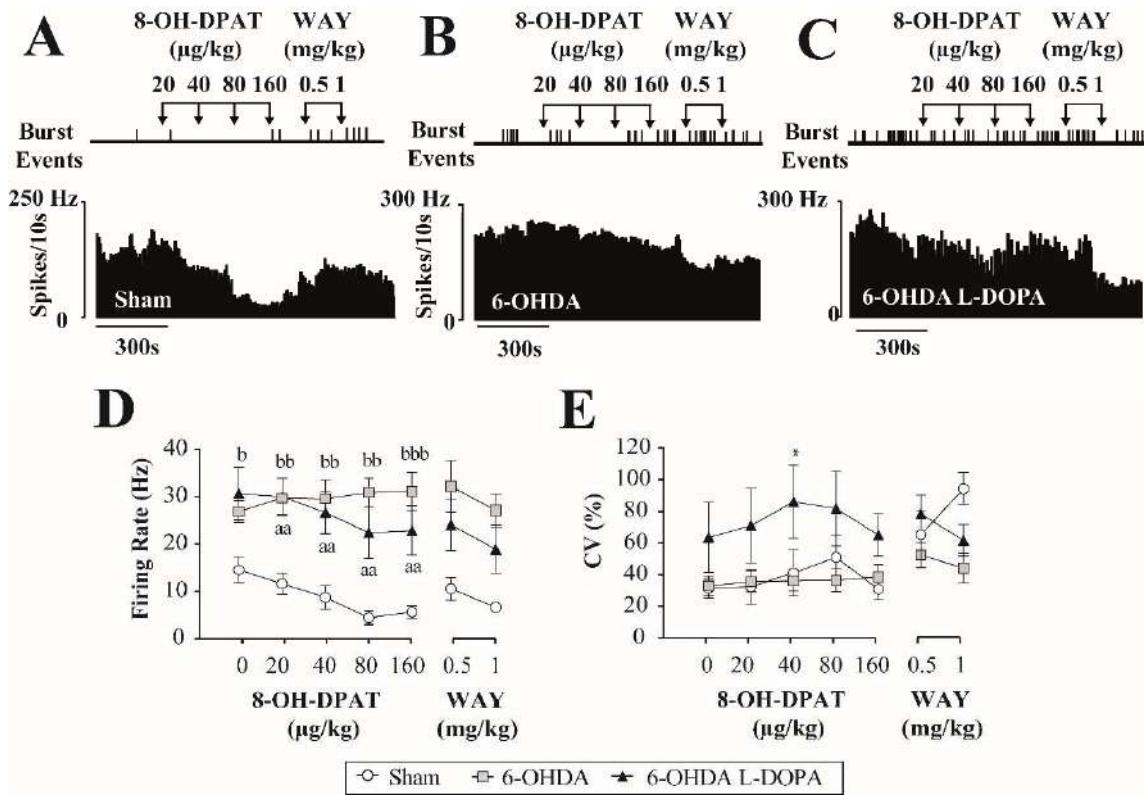
Figure 4.10. Effect of 8-OH-DPAT on entopeduncular neuron activity. Representative firing rate histogram illustrating the effect of 8-OH-DPAT (20-160 µg/kg, i.v.) and WAY-100635 (0.1 mg/kg, i.v) on EP neuronal firing rate and schematic representation of burst firing events that shows the loss of burst firing activity after drug administration in sham (A) 6-OHDA group (B) and 6-OHDA L-DOPA group (C). Graphics representing the mean ± S.E.M. of the firing rate (D), the CV in the three experimental groups, sham (n = 5), 6-OHDA (n = 5), 6-OHDA L-DOPA (n = 6) before and after increasing doses of 8-OH-DPAT and WAY-100635. *p < 0.05 vs baseline, aa < 0.01 6-OHDA group vs sham group; b < 0.05; bb < 0.01 and bbb < 0.001, 6-OHDA L-DOPA group vs sham group (RM two-way ANOVA followed by Bonferroni's post hoc test).

Table 4.6. Effect of systemic administration of 8-OH-DPAT (20–160 µg/kg, i.v.) and WAY–101635 (0.5-1 mg/kg, i.v.) on firing properties of entopeduncular neurons.

| | | 8-OH-DPAT (µg/kg) i.v. | | | | | WAY-101635 (mg/kg) | |
		Basal	20	40	80	160	0.5	1
Sham (n = 5)	1	14.3 ± 2.6	11.4 ± 2.2	8.6 ± 2.4	4.3 ± 1.4*	5.5 ± 1.2	10.2 ± 2.1	6.6 ± 0.4
	2	29.6 ± 5.9	30.6 ± 10.3	38.8 ± 14.1	48.3 ± 13.7	29.0 ± 6.5	49.7 ± 7.6	41.8 ± 9.1
	3	40	20[&&]	0[&&&]	20[&&]	60[&&]	60[&&]	40
	4	2.5 ± 1.7	1	0	20	4.0 ± 2.5	8.5 ± 7.5	16.2 ± 15.6
	5	0.2 ± 0.2	0.8	0	0.1	0.5 ± 0.3	3.3 ± 3.2	0.6 ± 0.5
	6	3.6 ± 2.8	13	0	1	3.1 ±1.4	6.7 ± 4.1	5.9 ± 4.2
	7	1.5 ± 1.0	0.6	0	0.7	2.5 ± 1.5	5.3 ± 4.6	9.8 ± 9.4
	8	43.6 ± 33.8	4.3	0	3.9	17.9 ± 11.2	22.4 ± 10.9	12.5 ± 9.6
Partially 6-OHDA (n = 5)	1	26.4 ± 2.3	29.2 ± 3.6	29.1 ± 4.0	30.4 ± 2.9	30.6 ± 3.9	29.9 ± 5.0	25.2 ± 3.3
	2	31.1 ± 10.3	33.6 ± 6.3	34.1 ± 6.4	34.3 ± 6.8	36.5 ± 7.4	49.7 ± 7.6	41.8 ± 9.1
	3	60[#]	60	20[&&&]	60	60	80[&&]	60
	4	6.3 ± 3.3	10.0 ± 9.3	11	8.0 ± 5.5	9.0 ± 4.1	19.5 ± 11.1	8.8 ± 7.1
	5	0.1 ± 0.1	0.3 ± 0.2	0.06	0.1 ± 0.0	0.2 ± 0.1	0.2 ± 0.0	0.4 ± 0.3
	6	6.1 ± 3.4	13.1 ± 7.1	3.8	6.7 ± 3.4	10.2 ± 4.6	9.9 ± 3.4	15.6 ± 11.9
	7	4.0 ± 2.2	6.2 ± 5.7	6.6	5.1 ± 3.4	6.1 ± 2.6	12.6 ± 7.4	5.8 ± 4.8
	8	53.4 ± 21.3	45.2 ± 17.5	16.3	55.9 ± 18.7	57.5 ± 19.2	76.7 ± 10.7	40.9 ± 16.4
6-OHDA (n = 6)	1	30.1 ± 5.4	29.5 ± 3.8	26.1 ± 4.3	22.0 ± 5.3*	22.5 ± 5.1	22.5 ± 4.9	17.7 ± 4.6
	2	60.3 ± 21.2	67.4 ± 22.4	81.7 ± 23*	77.8 ± 22.6	61.8 ± 12.8	50.1 ± 24.9	74.4 ± 17.9
	3	100[###]	50[&&&]	66.67[&&&]	100	100	83.33[&&&]	83.33[&&&]
	4	24.8 ± 15.2	21.2 ± 14.0	25.5 ± 15.3	25.2 ± 10.3	26.5 ± 8.1	15.2 ± 6.8	25.3 ± 12.7
	5	0.3 ± 0.1	0.1 ± 0.1	0.1 ± 0.1	0.4 ± 0.1	3.6 ± 3.3	4.4 ± 4.2	4.4 ± 4.2
	6	15.4 ± 3.9	5.8 ± 3.0	6.8 ± 2.8	12.0 ± 2.3	15.9 ± 5.0	16.3 ± 8.4	16.3 ± 8.4
	7	12.5 ± 7.7	13.4 ± 8.7	15.9 ± 9.5	15.6 ± 7.1	17.0 ± 3.8	16.3 ± 8.4	16.3 ± 8-2
	8	67.7 ± 11.5	33.9 ± 17.0	40.9 ± 15.7	55.1 ± 12.1	49.3 ± 14.4	56.7 ± 17.1	39.8 ± 20.9

Data from the firing rate, the CV and burst related parameters are expressed as mean ± S.E.M. *p < 0.05 vs baseline (RM two-way ANOVA followed by Bonferroni´s post hoc), [&]p < 0.05, [&&]p < 0.01 and [&&&]p < 0.001 vs baseline, [#]p < 0.05 and [###]p < 0.001 vs sham (Fisher´s exact test). (**1**) Firing rate (Hz), (**2**) CV (%), (**3**) neurons exhibiting burst firing pattern (%), (**4**) number of bursts, (**5**) duration of burst (ms), (**6**) nº spikes/burst, (**7**) recurrence of burst (nº burst/min), and (**8**) intraburst frequency (spike/s).

4.2.2. Effect of 5-HT$_{1A}$ agonists on the low oscillatory activity and synchronization in the entopeduncular nucleus and the motor cortex

We recorded EP-LFP and ECoG simultaneously with single-unit extracellular recordings of EP neurons. We analysed the power spectrum and the coherence in the 0–5 Hz range to determinate the parameters of low frequency activity and synchronization in the EP and between this nucleus and the motor cortex. 26 neurons from the sham group (n = 15 rats), 27 neurons from the 6-OHDA group (n = 16 rats) and, 32 neurons from the 6-OHDA L-DOPA group (n = 17 rats) were included in the analysis.

In agreement with our previous publication (Aristieta et al., 2019), power spectra analysis showed low oscillatory activity in the ECoG and the LFP with a peak, near to 1 Hz in the three experimental groups. The AUC values of the ECoG power spectrum revealed no significant differences among the three experimental groups ($F_{(2, 45)} = 0.6479$, $p > 0.05$, one-way ANOVA; **Fig. 4.11A**) whereas LFP AUC value was higher in the 6-OHDA group ($F_{(2, 45)} = 3.464$, $p < 0.05$, one-way ANOVA; **Fig. 4.11B**). The coherence analysis showed that synchronization between ECoG and EP spikes and between EP-LFP and EP spikes was higher after 6-OHDA lesion and L-DOPA treatment being the AUC value obtained from the coherence curves significantly larger in the 6-OHDA L-DOPA group ($F_{(2, 45)} = 4.109$, $p < 0.05$ one-way ANOVA and $F_{(2, 45)} = 4.727$, $p < 0.05$; one-way ANOVA; **Fig. 4.12A** and **B,** respectively). No difference was observed in the synchronization between ECoG and EP-LFP ($F_{(2, 45)} = 1.712$, $p > 0.05$; one-way ANOVA; **Fig. 4.12C**).

Next, to investigate the effect of 5-HT drugs on low oscillatory activity and synchronization between the EP and ECoG. We compared the power spectrum and coherence obtained before and after the systemic administration of increasing doses of buspirone or 8-OH-DPAT. One neuron per animal was pharmacology tested with buspirone from a total of 17 animals: sham (n = 5), 6-OHDA (n = 6) and 6-OHDA L-DOPA (n = 6) groups. The first dose of buspirone produced a significant effect on the ECoG in the sham group (buspirone: $F_{(4, 56)} = 3.357$, $p < 0.05$ and lesion: $F_{(2, 14)} = 4.767$, $p < 0.05$; RM two-way ANOVA; **Fig. 4.11C**). While, the highest doses of buspirone enhanced the oscillatory activity of LFP-EP only in 6-OHDA L-DOPA group (buspirone: $F_{(4, 56)} = 6.044$, $p < 0.001$ and lesion: $F_{(2, 14)} = 5.585$, $p < 0.05$; RM two-way ANOVA;

Fig. 4.11D). As it is shown in **Figure 4.12D**, buspirone administration did not modify the coherence between ECoG and EP spikes (buspirone: $F_{(4, 56)} = 1.433$, $p > 0.05$ and lesion: $F_{(2, 14)} = 3.108$, $p > 0.05$; RM two-way ANOVA). Buspirone administration did not affect the synchronization between LFP and EP spikes (buspirone: $F_{(4, 80)} = 1.861$, $p > 0.05$ and lesion: $F_{(2, 14)} = 0.293$, $p > 0.05$; RM two-way ANOVA; **Fig. 4.12E**). Buspirone also failed to alter the synchronization between ECoG and LFP (buspirone: $F_{(4, 56)} = 1.249$, $p > 0.05$ and lesion: $F_{(2, 14)} = 1.178$, $p > 0.05$; RM two-way ANOVA; **Fig. 4.12F**).

Finally, we investigated the effect of systemic 8-OH-DPAT on the oscillatory activity and coherence in the sham group (n = 5), 6-OHDA group (n = 5) and, 6-OHDA L-DOPA group (n = 6). As it is shown in **Figure 4.11E**, 8-OH-DPAT administration did not modify the AUC of the ECoG power spectrum (8-OH-DPAT: $F_{(4, 52)} = 2.008$ $p > 0.05$ and lesion: $F_{(2, 13)} = 1.767$, $p > 0.05$). However, 8-OH-DPAT significant reduced AUC values of LFP in the 6-OHDA L-DOPA group (8-OH-DPAT: $F_{(4, 52)} = 2.158$, $p > 0.05$ and lesion: $F_{(2, 13)} = 8.224$, $p < 0.01$; RM two-way ANOVA; **Fig. 4.11F**). On the other hand, the analysis of coherence revealed that 8-OH-DPAT did not cause any effect on synchronization between ECoG and EP spikes ($F_{(4, 52)} = 1.743$, $p > 0.05$ and lesion: $F_{(2, 13)} = 2.713$, $p > 0.05$; RM two-way ANOVA; **Fig. 4.12G**). In contrast 8-OH-DPAT significant reduced the AUC values of the coherence between LFP and EP spikes in 6-OHDA L-DOPA group (8-OH-DPAT: $F_{(4, 52)} = 4.013$, $p < 0.01$ and lesion: $F_{(2, 13)} = 7.428$, $p < 0.01$; RM two-way ANOVA; **Fig. 4.12H**). Finally, 8-OH-DPAT also failed to modify the coherence between ECoG and LFP (8-OH-DPAT: $F_{(4, 52)} = 0.7439$, $p > 0.05$ and lesion: $F_{(2, 13)} = 2.03$ $p > 0.05$; RM two-way ANOVA; **Fig. 4.12I**).
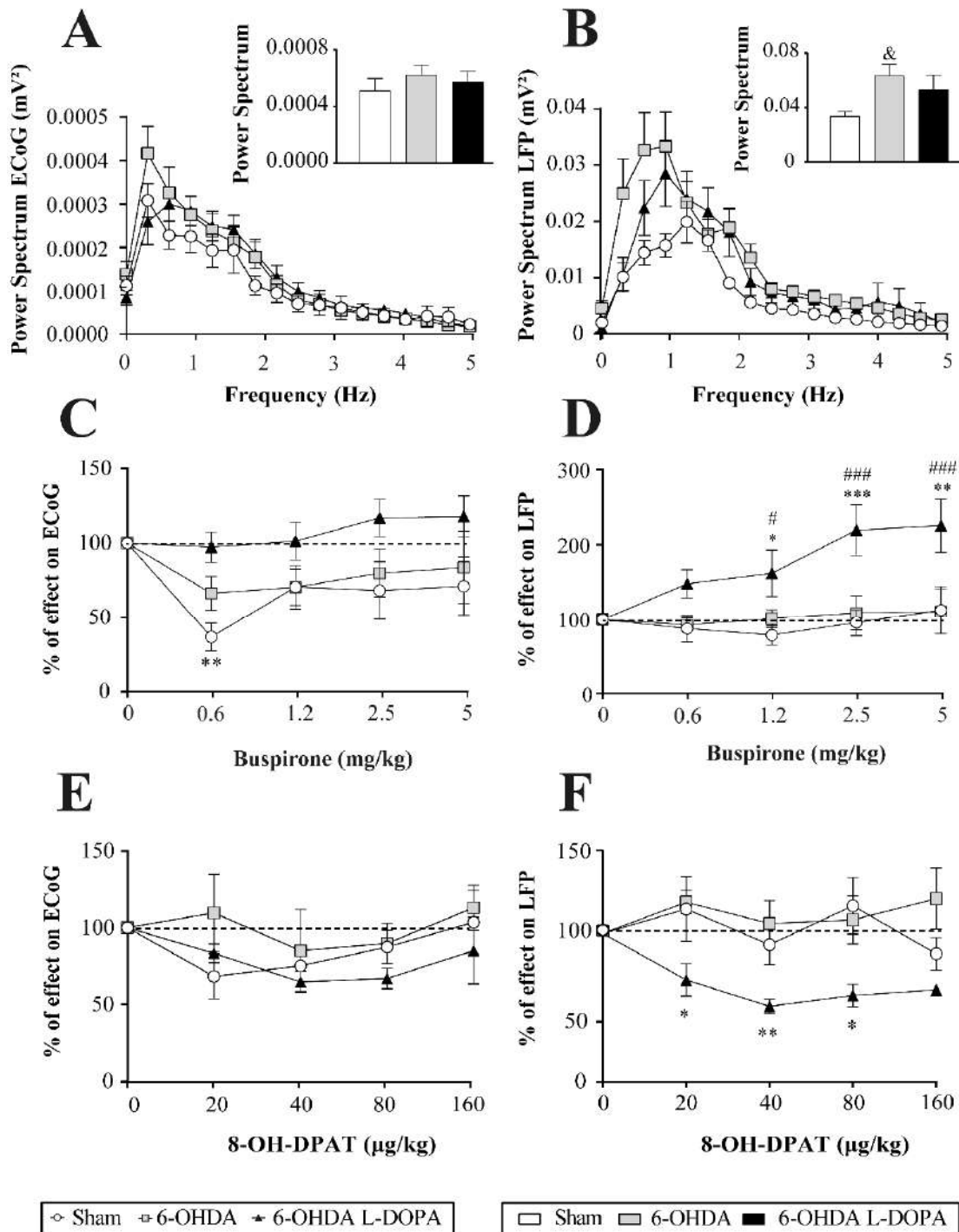
Figure 4.11. Effect of systemic administration of buspirone and 8-OH-DPAT on the power spectra of the local field potential of entopeduncular nucleus and the motor cortex in the low oscillatory frequency range (0–5 Hz). Power spectra and AUC values obtained from the ECoG (A) and EP-LFP (B) in the sham (n = 15), 6-OHDA (n = 16) and 6-OHDA L-DOPA (n = 17) animals. Effect of increasing doses of buspirone administration (0.6125 – 5 mg/kg, i.v.) on the AUC of the power spectrum of the ECoG (C) and EP-LFP (D) in the sham (n = 5), 6-OHDA (n = 6) and 6-OHDA L-DOPA (n = 6). Effect of increasing doses of 8-OH-DPAT administration (20 – 160 µg/kg, i.v.) on the AUC of the power spectrum of the ECoG (E) and the EP-LFP (F) obtained from the three experimental groups, sham (n = 5), 6-OHDA (n = 5) and 6-OHDA L-DOPA (n = 6). Data are expressed as mean ± S.E.M. $^{\&}p < 0.05$ vs sham (One-way ANOVA), $^{*}p < 0.05$, $^{**}p < 0.01$ and $^{***}p < 0.01$ vs sham and $^{\#}p < 0.05$, and $^{\#\#\#}p < 0.001$ vs baseline (RM two-way ANOVA followed by Bonferroni´s post-hoc test).
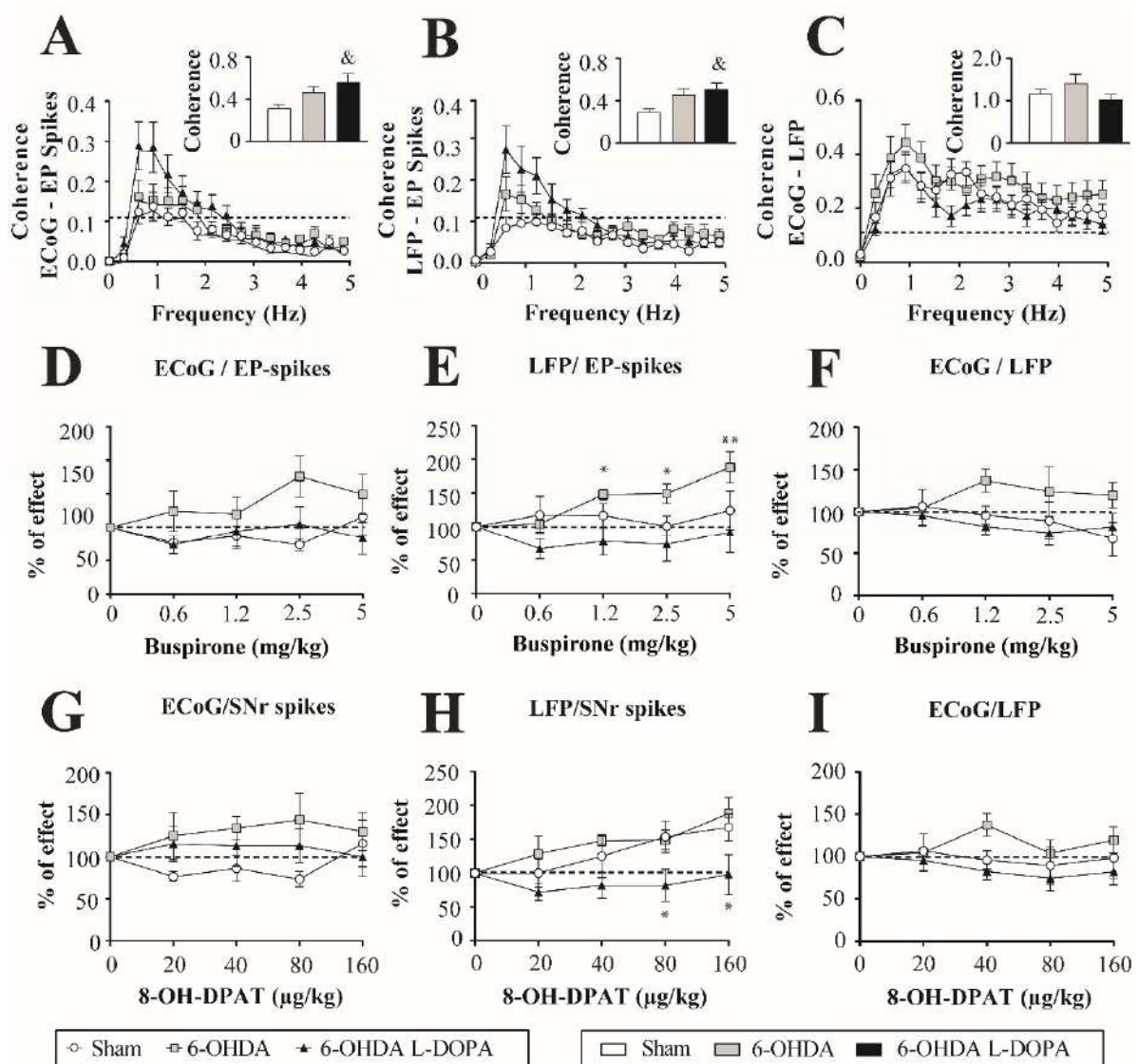
Figure 4.12. Effect of systemic administration of buspirone and 8-OH-DPAT on entopeduncular nucleus spikes, the local field potential of entopeduncular nucleus and motor cortex coherences in the low frequency range (0–5 Hz). Coherence power spectra between the ECoG and EP spikes simultaneously recorded in the sham (n = 15), 6-OHDA (n = 16), and 6-OHDA L-DOPA (n = 17) groups. Area under the curve (AUC) value obtained from coherence between the ECoG and EP spikes (A) and AUC values obtained from LFP-EP spikes coherence curves (B) were augmented in the 6-OHDA L-DOPA group. AUC values obtained from ECoG/EP-LFP coherence curves showed no differences (C). Acute doses of buspirone administration (0.6125 – 5 mg/kg, i.v.) did not modify the synchronization between ECoG and EP spikes (D). Buspirone administration increased the synchronization between EP-LFP and EP spikes (E). In contrast, no effect was observed between ECoG and EP-LFP (F) in sham (n = 5), 6-OHDA (n = 6) and 6-OHDA L-DOPA (n = 6). 8-OH-DPAT administration (20 – 160 µg/kg, i.v.) did not modify was the synchronization between ECoG and EP spikes (G). 8-OH-DPAT modified the synchronization between LFP and EP spikes (H) in 6-OHDA L-DOPA group. No effect was observed between ECoG and LFP (I) were observed in the sham (n = 5), 6-OHDA (n = 5) and 6-OHDA L-DOPA groups (n = 6). Data are expressed as mean ± S.E.M. $^{\&}p < 0.05$ vs sham (One-way ANOVA), and $*p < 0.05$ vs sham (RM two-way ANOVA followed by Bonferroni´s post-hoc test).

4.2.3. Effect of subthalamic optoillumination on subthalamic and entopeduncular neuron activity

To investigate the impact of STN stimulation on STN and EP neuron activity and its modulation by buspirone, we performed optical stimulation after AAV-hSyn-hChR2(H134R)-EYPF injection into the STN (from here ChR2-EYFP). First we carried out simultaneously 465-nm blue light stimulation and single-unit extracellular recordings of STN neurons in anaesthetised rats between 4 or 6 weeks after viral injection. Only animals that showed a stimulatory response in most recorded neurons were included in this study. After the electrophysiological experiment, histological verification was done to confirm the correct viral transfection and corresponding ChR2 overexpression in the STN (**Fig. 4.13A**). Before implantation the optic fiber a V-W calibrated curve was performed. (**Fig. 4.13B**).

A total of 40 STN neurons were recorded in 6 animals (5 – 9 neurons per animal) before and during light stimulation using three different protocols; continuous pulses (1s-duration at ~ 5.5 mW-intensity or 0.5s-duration at ~ 14 mW-intensity) and trains of light pulses (25Hz-frequency, 0.5s-duration at ~ 14 mW-intensity) (**Fig. 4.13C-G**). Regardless the protocols, light stimulation excited 35 STN neurons (87.5%) In average, during the first protocol STN neuron firing rate passed from 10.95 ± 2.29 Hz to 62.2 ± 46.3 Hz (**Fig. 4.13D**), during the second from 12.2 ± 1.57 Hz to 61.2 ± 14.5 Hz (**Fig. 4.13F**) and during the third (the train of light pulses) from 13.0 ± 1.9 Hz to 39.9 ± 10.5 Hz (**Fig. 4.13H**) (two-tailed paired Student´s t-test, $p < 0.05$).

Next, we carried out single-unit extracellullar recordings of EP neurons before and during optical stimulation through the fiber positioned in the STN, in basal conditions and after buspirone administration (4 mg/kg, i.p.). As mentioned above, light stimulation protocols were applied on the STN causing similar effect in both situations. There was an increment in the EP firing rate of 26 neurons from 36 neurons (72.2%), and in 19 neurons from 24 neurons (79.2%) in basal conditions and after buspirone administration. As it shown in **Figure 4.14A-F**, firing rate was significantly higher during the STN optoillumination with either protocol compared to the basal firing. In average, during the first protocol EP firing rate passed from 25.24 ± 4.9 Hz to 53.6 ± 43.4 Hz, during the second protocol it passed from 25.9 ± 3.7 Hz to 55.8 ± 6.3 Hz and during the last protocol,

it passed from 24.98 ± 4.1 Hz to 55.8 ± 6.3 Hz. Furthermore, RM two-way ANOVA revealed that buspirone administration did not modify the intensity of the response to STN stimulation (blue light: $F_{(1, 7)} = 25.18$, $p < 0.01$ and buspirone: $F_{(1, 7)} = 0.01$, $p > 0.05$ for the first protocol; blue light: $F_{(1, 7)} = 32$, $p < 0.001$ and buspirone: $F_{(1, 7)} = 0.65$, $p > 0.05$ for the second and blue light: $F_{(1, 5)} = 13.85$, $p < 0.01$ and buspirone: $F_{(1, 7)} = 0.757$, $p > 0.05$ for the last protocol).
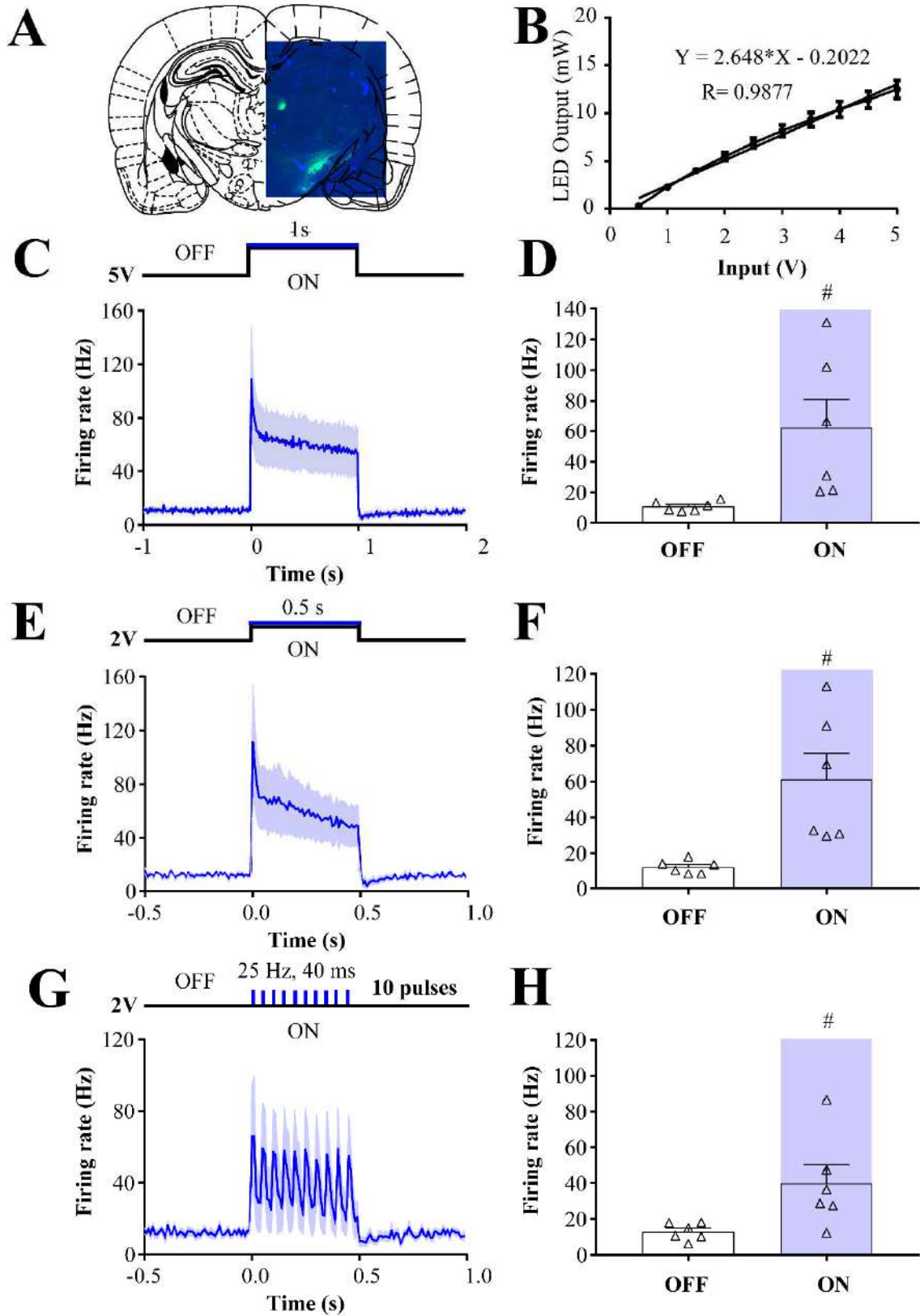
Figure 4.13. Optostimulation induced of subthalamic neurons expressing channelrhodopsin-2. Coronal section (left) showing ChR2-eYFP-H134R expression in the STN of the injected hemisphere. (A). Standard curve generated from the calibration of LED illumination at the beginning of the experiments (B). Peristimulus histograms were constructed to show the STN firing rate before and after local optical stimulation with 465-nm blue-light pulses (highlighted area). Peristimulus histogram shows the effect of light pulse (1 ms, ~5.5 mW) on the firing rate of STN neurons (C). Bars with averaged plots represents the mean firing rate value of STN (white) and the response to local illumination (highlighted area) (D). Peristimulus histogram shows the effect of light pulse (0.5 ms, ~14 mW) on the firing of STN neurons (E). Bars with averaged plots represents the mean firing rate value of STN neuron (white) and the response induced by local illumination (highlighted area) (F). Peristimulus histogram shows the effect of trains of light pulses (40 ms, at 25 Hz, ~14 mW) on the firing of STN neurons (G). Bars with averaged plots represents the mean firing rate value of STN (white) and the response induced by local illumination (highlighted area) (H). Data are represented as mean ± S.E.M. from n = 6 rats. [#]$p < 0.05$ vs light off (two-tailed paired Student´s t-test).
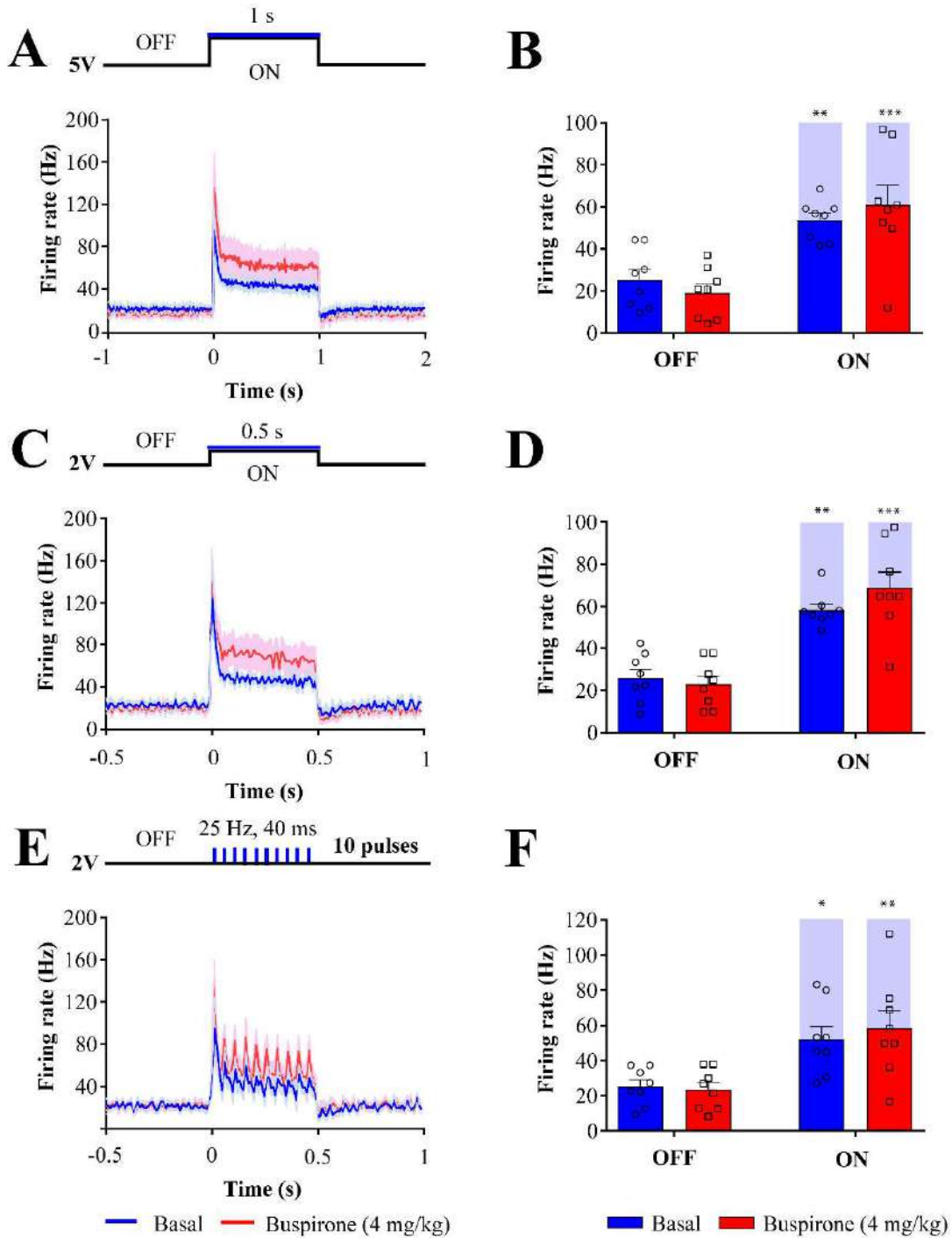
Figure 4.14. Subthalamic optostimulation increased entopendicular neuron firing frequency. Peristimulus histograms showing changes in EP firing frequency during STN stimulation with 465nm blue light pulses. Three stimulation protocols were used; continuous 1-5.5mW (A), 0.5s-14mW (C) and 25 Hz train-14mW (E) pulses. Note that buspirone administration did not modify the type of response in the EP induced by STN optoillumination. Corresponding bar histogram representing the mean firing rate value of EP neuron (B, D, F) in response to light stimulation and buspirone administration. Bars with averaged plots represents the mean firing rate value of EP neurons (blue) and when buspirone was administered (red), and the responses to STN stimulation (highlighted areas). Data are represented as mean ± S.E.M. from n = 8 rats. *p < 0.05, **p < 0.01 and ***p < 0.001 vs blue light illumination (RM two-way ANOVA followed by Bonferroni´s post hoc test).

4.3. STUDY III: EFFECT OF BUSPIRONE ON CORTICO-NIGRAL AND CORTICO-ENTOPEDUNCULAR TRANSMISSION IN SHAM AND 6-HYDROXYDOPAMINE-LESIONED RATS

4.3.1. Spontaneous discharge and cortically evoked responses of the substantia nigra pars reticulata neurons from sensorimotor circuit in sham and 6-hydroxydopamine-lesioned rats

A total of 96 SNr GABAergic neurons responding to motor cortex stimulation were recorded in 28 anaesthetised rats; 52 SNr neurons from the sham group (n = 15) and 44 SNr neurons from the 6-OHDA group (n = 13). All recorded cells displayed a narrow spike waveform and a relatively high firing rate with a regular pattern of discharge as reported in the Study I. As described in section 4.1.1, SNr neurons responding to motor cortex stimulation had similar firing frequencies in sham and 6-OHDA-lesioned rats (two-tailed unpaired Student´s t-test, $p < 0.05$), and higher CV and increased number of bursty neurons in the latter group ($p < 0.001$, two-tailed unpaired Student´s t-test, and Fisher´s exact test, $p < 0.05$ respectively). The mean values $\pm$ S.E.M. of the firing rate and firing pattern parameters are shown in **Table 4.7**.

Table 4.7. Firing properties of substantia nigra pars reticulata neurons from the sensorimotor circuit in sham and 6-hydroxydopamine-lesioned rats.

	Sham (n = 15)	6-OHDA (n = 13)
Firing rate (Hz)	22.9 ± 1.5	25.9 ± 2.3
CV (%)	35.5 ± 3.3	60.4 ± 3.9***
Neurons exhibiting burst firing pattern (%)	38	70.5[###]
Number of bursts	7.0 ± 1.1	13.3 ± 3.0[$]
Duration of burst (ms)	1.2 ± 0.4	0.78 ± 0.1
Nº spikes/burst	36.6 ± 12.2	23.6 ± 4.2
Recurrence of burst (nº burst/min)	5.4 ± 0.8	8.0 ± 1.8[$]
Intraburst frequency (spike/s)	48.7 ± 4.2	42.5 ± 5.7

Data from the firing rate, the CV and burst related parameters are expressed as mean ± S.E.M. of n rats. ***$p < 0.001$ vs sham (Two-tailed unpaired Student's t test), [###]$p < 0.001$ vs sham (Fisher´s exact test), and [&]$p < 0.05$ (Mann–Whitney rank sum test for burst parameters).

According to previous publications (Aliane et al., 2009; Antonazzo et al., 2019; Beyeler et al., 2010; Degos et al., 2005), stimulation of the motor cortex evoked three different patterns of responses in a population of SNr neurons (**Table 4.8**): (1) monophasic response (early excitation, inhibition or late excitation) (**Fig. 4.15A**), (2) a biphasic response (combination of monophasic responses) (**Fig. 4.15B**), and (3) a triphasic response that consisted of an early excitation, followed by an inhibition and a late excitation (**Fig. 4.15C**). The early excitation involves the activation of the "hyperdirect" pathway or cortico-subthalamo-nigral pathway, the inhibition involves the activation of the "direct" pathway or cortico-striato-nigral pathway and the late excitation involves the activation of the "indirect" pathway or cortico-striato-pallido-subthalamo-nigral pathway. The percentage of occurrence of these different patterns is shown in **Figure 4.15D**. While less SNr neurons exhibited monophasic response consisting of early excitation, a higher percentage of biphasic response consisting of an early excitation and late excitation pattern was observed in the 6-OHDA group ($p < 0.05$, Fisher´s exact test).

Table 4.8. Electrophysiological characteristics of the responses evoked in substantia nigra pars reticulata neurons after cortical stimulation in sham and 6-hydroxydopamine-lesioned rats.

	Sham (n = 15)	6-OHDA (n = 13)
Nº of responded neurons/ Nº tested neurons	52/80 (65%)	44/56 (79%)
Early Excitation		
Latency (ms)	6.5 ± 0.6	6.9 ± 0.9
Duration (ms)	4.3 ± 0.3	4.5 ± 0.3
Amplitude	15.8 ± 1.4	15.9 ± 1.5
Inhibition		
Latency (ms)	15.1 ± 1.3	14.2 ± 0.8
Duration (ms)	7.0 ± 1.0	7.9 ± 0.9
Late Excitation		
Latency (ms)	25.8 ± 0.9	24.0 ± 1.0
Duration (ms)	6.6 ± 0.6	5.9 ± 0.5
Amplitude	11.6 ± 1.0	11.6 ± 1.0

Data is expressed as mean ± S.E.M. of n rats.

The parameters defining each response as the latency of appearance, duration of the each component and the amplitude of the excitations were not altered by the 6-OHDA lesion ($p > 0.05$, two-tailed unpaired Student's t test; **Table 4.8**).
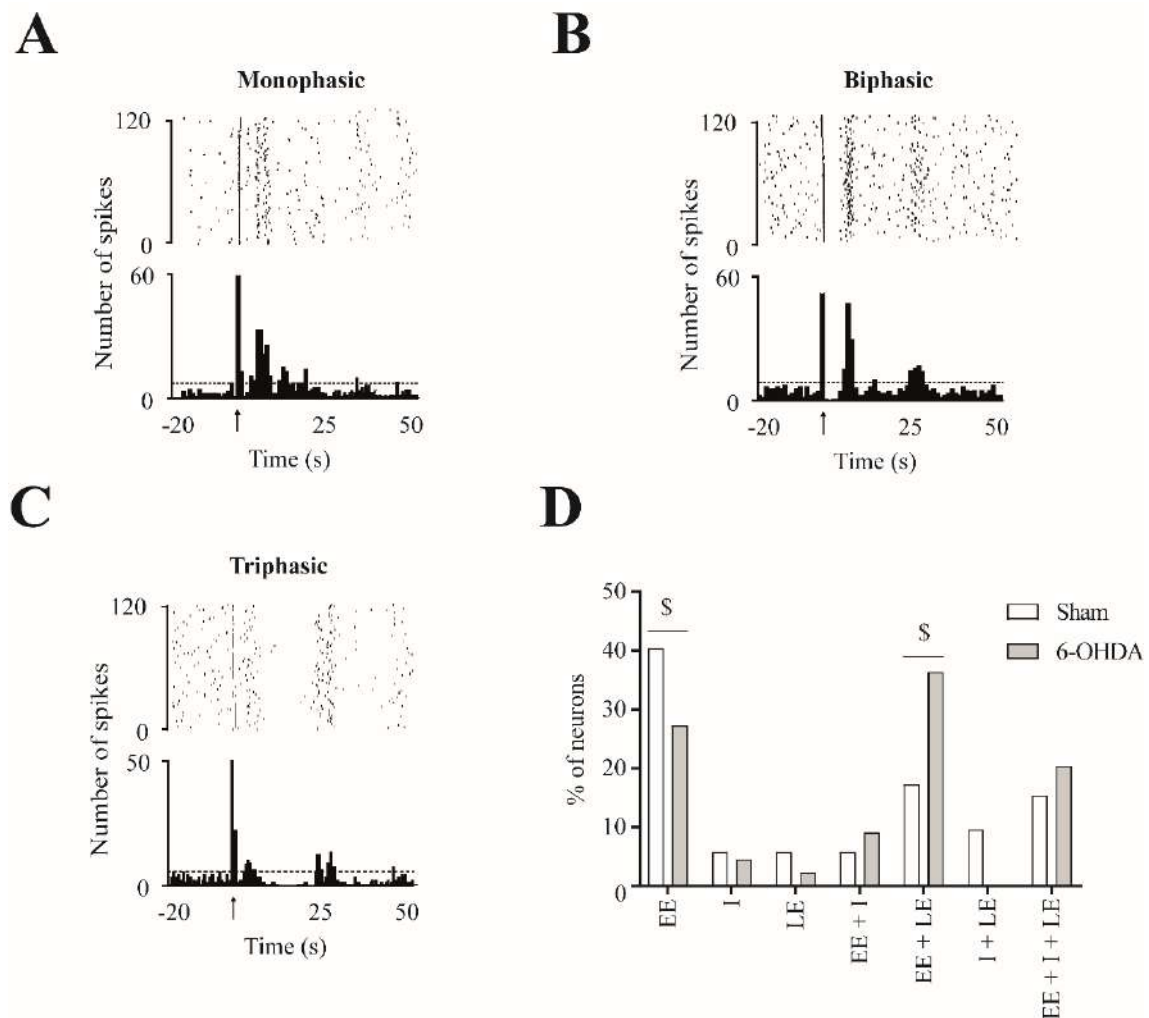
Figure 4.15. Patterns of responses evoked in substantia nigra pars reticulata neurons by motor cortex stimulation. Raster plot and peristimulus time histogram showing a representative example of a monophasic response evoked in a SNr neuron from the sham group (A). Raster plot and peristimulus time histogram showing a representative example of a biphasic response evoked in a SNr neuron of 6-OHDA group (B). Raster plot and peristimulus time histogram showing a representative example of a triphasic response in a SNr neuron from the 6-OHDA-lesioned group (C). Percentage of occurrence of the different patterns of responses evoked (D). EE: early excitation (sham: n = 42; 6-OHDA: n = 41); I: inhibition (sham: n = 18; 6-OHDA: n = 16); LE: late excitation (sham: n = 22; 6-OHDA: n = 28). Data are expressed as percentage. $^{\$}p < 0.05$ (Fisher's exact test).

4.3.2. Spontaneous discharge and cortically evoked responses of the entopeduncular neurons from sensorimotor circuit in sham and 6-hydroxydopamine-lesioned rats

In the EP we recorded a total of 90 GABAergic neurons that responded to motor cortex stimulation; 46 EP neurons from the sham group (n = 14) and 44 EP neurons from the 6-OHDA group (n = 12). All recorded EP cells displayed biphasic waveform with short wide-duration action potentials of 0.8-0.9 s as reported in the Study II. As described in section 4.2.1, EP neurons that responded to motor cortex stimulation showed higher firing frequency (two-tailed unpaired Student´s t-test, $p < 0.001$,) and higher CV (two-tailed unpaired Student´s t-test, $p < 0.05$) in the 6-OHDA-lesioned group. In addition, the 6-OHDA-lesioned group presented a larger percentage of EP neurons exhibiting bursting discharge in comparison to sham group ($p < 0.05$, Fisher´s exact test). The mean values ± S.E.M. of the firing rate and firing pattern parameters are shown in **Table 4.9**.

Table 4.9. Firing properties of entopeduncular neurons from the sensorimotor circuit in sham and 6-hydroxydopamine-lesioned rats.

	Sham (n = 14)	6-OHDA (n = 11)
Firing rate (Hz)	17.5 ± 1.8	25.6 ± 1.9**
CV (%)	52.5 ± 3.7	66.6 ± 5.5*
Neurons exhibiting burst firing pattern (%)	65.2	81.8[##]
Number of bursts	27.9 ± 6.0	15.3 ± 4.5[$]
Duration of burst (ms)	2.0 ± 1.0	1.0 ± 0.3
Nº spikes/burst	18.3 ± 5.0	28.4 ± 16.2
Recurrence of burst (nº burst/min)	18.5 ± 3.5	10.0 ± 2.7[$]
Intraburst frequency (spike/s)	50.1 ± 8.3	47.5 ± 2.1

Data from the firing rate, the CV and burst related parameters are expressed as mean ± S.E.M. of n rats. *$p < 0.05$, **$p < 0.01$ vs sham (Two-tailed unpaired Student's t test), [##]$p < 0.01$ vs sham (Fisher´s exact test for burst firing pattern) and [$]$p < 0.05$ (Mann–Whitney rank sum test for burst parameters).

In agreement with Chiken et al. (2015), motor cortex stimulation evoked three different patterns of responses in a population of EP neurons: (1) monophasic (early excitation, inhibition or late excitation) (**Fig. 4.16A**), (2) a biphasic response (combination of monophasic responses) (**Fig. 4.16B**), or (3) triphasic response (**Fig. 4.16C**) which is attributed to the activation of the different pathways along the sensorimotor cortical-BG circuit as explained above for the SNr. The early excitation involves the activation of the "hyperdirect" pathway or cortico-subthalamo-entopeduncular pathway, the inhibition involves the activation of the "direct" pathway or cortico-striato-entopeduncular pathway and the late excitation involves the activation of the "indirect" pathway or cortico-striato-pallido-subthalamo-entopeduncular pathway. The proportion of each pattern of response ($p > 0.05$, Fisher´s exact test; **Fig. 4.16D**) and parameters of each component were not altered after the 6-OHDA-lesion ($p > 0.05$, two-tailed unpaired Student's t test; **Table 4.10**).

Table 4.10. Electrophysiological characteristics of the responses evoked in entopeduncular neurons after cortical stimulation in sham and 6-hydroxydopamine- lesioned rats.

Parameters	Sham (n = 14)	6-OHDA (n = 11)
Nº of responded neurons/ Nº tested neurons	46/104 (44%)	44/65 (68%)
Early Excitation		
Latency (ms)	6.4 ± 0.7	7.2 ± 0.8
Duration (ms)	4.2 ± 0.3	4.3 ± 0.3
Amplitude	18.2 ± 1.7	14.3 ± 1.9
Inhibition		
Latency (ms)	16.5 ± 1.1	14.6 ± 1.1
Duration (ms)	6.5 ± 1.0	5.9 ± 0.5
Late Excitation		
Latency (ms)	24.9 ± 1.1	23.0 ± 0.9
Duration (ms)	6.1 ± 0.8	5.8 ± 0.6
Amplitude	11.6 ± 1.4	13.0 ± 0.9

Data is expressed as mean per animal value $\pm$ S.E.M. of n rats.
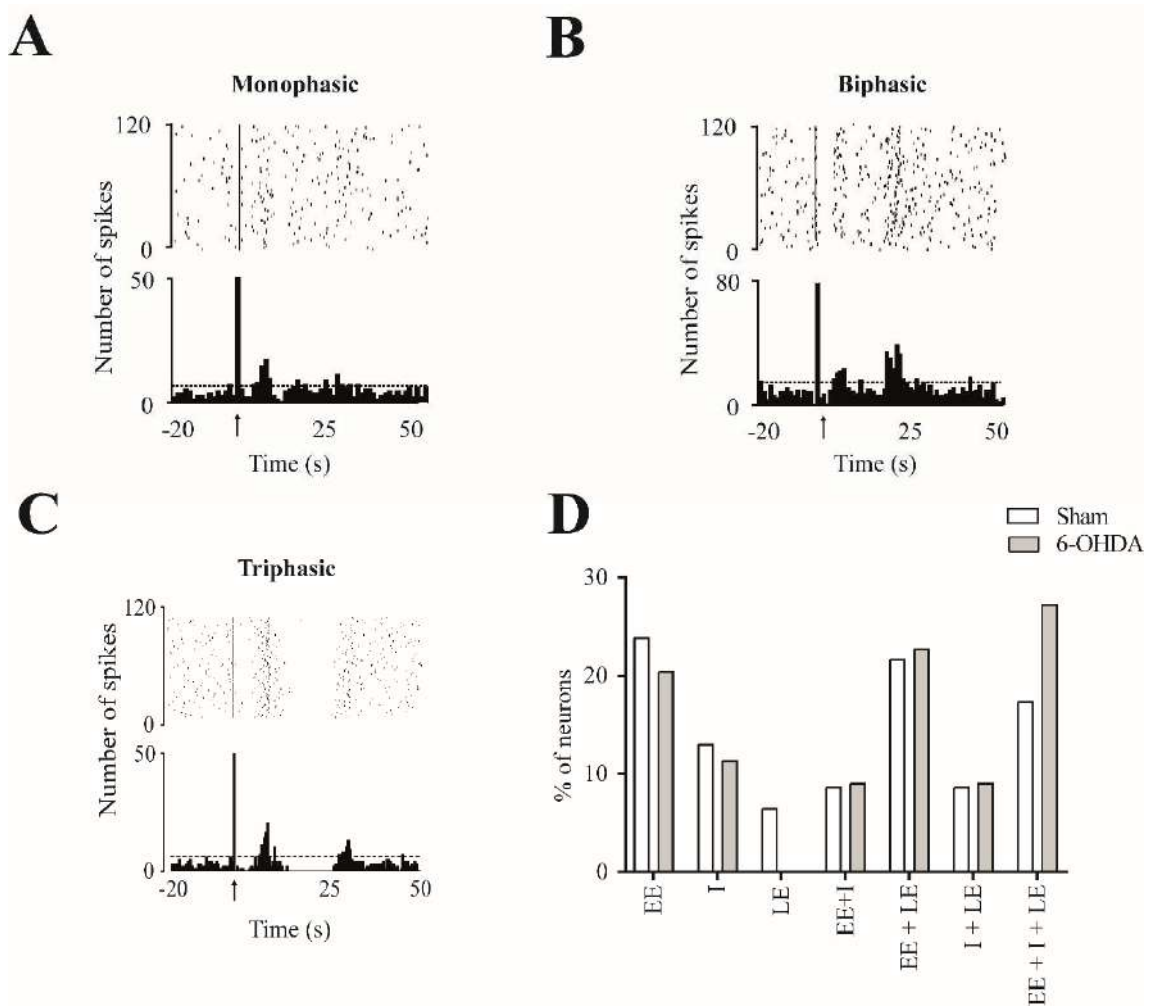
Figure 4.16. Patterns of responses evoked in entopeduncular neurons by motor cortex stimulation. Raster plot and peristimulus time histogram showing a representative example of a monophasic response evoked in an EP neuron from the sham group (A). Raster plot and peristimulus time histogram showing a representative example of a biphasic response evoked in an EP neuron of sham group (B). Raster plot and peristimulus time histogram showing a representative example of a triphasic response in an EP neuron from the 6-OHDA group (C). Percentage of occurrence of the different patterns of responses evoked (D). EE: early excitation (sham: n = 37; 6-OHDA: n = 33); I: inhibition (sham: n = 24; 6-OHDA: n = 16); LE: late excitation (sham: n = 29; 6-OHDA: n = 26). Data are expressed as percentage.

4.3.3.   Effect of buspirone on cortically evoked activity in the substantia nigra pars reticulata neurons in sham and 6-hydroxydopamine-lesioned rats

We also studied the effect of buspirone on sensorimotor cortical evoked responses in SNr cells from sham (n = 14) and 6-OHDA-lesioned (n = 12) rats. To minimize any effect on basal parameters two low doses of buspirone (0.6125 and 1.25 mg/kg, i.v.) were administered. The doses of buspirone did not modify the basal firing rate (buspirone: $F_{(2, 52)} = 0.2636$, $p > 0.05$ and lesion: $F_{(1, 26)} = 0.09252$, $p > 0.05$ RM two-way ANOVA) neither the CV (buspirone: $F_{(2, 52)} = 0.6556$, $p > 0.05$ and lesion: $F_{(1, 26)} = 10.31$, $p < 0.01$; RM two-way ANOVA) and caused little effect on burst activity ($p < 0.05$, Fisher´s exact test). Posterior WAY-100635 administration (0.5 mg/kg, i.v.) did not cause any effect on SNr neuron activity in both groups (two-tailed paired Student´s t test, $p > 0.05$; **Table 4.11**).

The analysis of the parameters of all evoked responses before and after buspirone administration shows that systemic administration of 1.25 mg/kg but not the lowest dose modified the transmission of cortical information through the hyperdirect pathway only in the 6-OHDA group (**Figure 4.17**). The mean amplitude of early excitatory component of the response was significantly higher after drug administration in the 6-OHDA group (buspirone: $F_{(2, 50)} = 3.761$, $p < 0.05$ and lesion: $F_{(1, 25)} = 0.7174$, $p > 0.05$ RM two-way ANOVA). This effect was reverted by the systemic administration of the 5-HT$_{1A}$ receptor antagonist, WAY-100635 (two-tailed paired Student´s t test, $p < 0.01$). The rest of the parameters of the early excitatory component of the response were unchanged.

The effect of buspirone (0.6125 and 1.25 mg/kg) on the transmission of sensorimotor cortical information through the direct pathway also differed between sham and 6-OHDA group. While buspirone significantly enhanced the duration of the inhibitory component of the evoked response in cells from sham rats this effect was not observed the 6-OHDA group (buspirone: $F_{(2, 30)} = 16.74$, $p < 0.001$ and lesion: $F_{(1, 15)} = 2.082$, $p > 0.05$, RM two-way ANOVA). Besides, WAY-100635 administration reverted the effect induced by buspirone (two-tailed paired Student´s t test, $p < 0.001$). The rest of parameters of the inhibitory component of the response were unchanged.

Table 4.11. Effect of buspirone on firing properties of substantia nigra pars reticulata neurons in sham and 6-hydroxydopamine-lesioned rats.

		Basal	Buspirone (mg/kg)		WAY (mg/kg)
			0.6125	1.25	0.5
Sham (n = 12)	**Firing rate (Hz)**	27.4 ± 2.3	26.7 ± 2.8	27.0 ± 2.4	25.0 ± 2.6
	CV (%)	30.8 ± 3.6	39.3 ± 5.6	39.1 ± 4.1	38.5 ± 4.7
	Neurons exhibiting burst firing pattern (%)	40	60[&&]	50	70[&&]
	Number of bursts	3.1 ± 1.8	6.5 ± 3	5.3 ± 3.2	3.9 ± 1.2
	Duration of burst (ms)	0.8 ± 0.5	1.2 ± 0.75	1.4 ± 1.1	1.5 ± 1.1
	Nº spikes/burst	23.4 ± 14.2	27.1 ± 14.7	49.3 ± 44.6	46.7 ± 28.7
	Recurrence of burst (nº burst/min)	2.1 ± 1.2	4.3 ± 1.9	3.6 ± 2.2	2.9 ± 0.8
	Intraburst frequency (spike/s)	31.6 ± 11.0	$40.1 + 10.9$	41.2 ± 18.1	49.0 ± 11.6
6-OHDA (n = 12)	**Firing (Hz)**	27.6 ± 2.8	25.6 ± 3.6	25.0 ± 3.4	22.3 ± 2.6
	CV (%)	57.9 ± 4.5**	56.40 ± 6.7	57.35 ± 7.9	49.8 ± 7.5
	Neurons exhibiting burst firing pattern (%)	76.9[###]	92.3[&&]	81.8	75
	Number of bursts	9.9 ± 4.1	11.9 ± 4.7	17.1 ± 6.3	12.7 ± 5.2
	Duration of burst (ms)	0.5 ± 0.1	0.8 ± 0.3	0.6 ± 0.1	0.4 ± 0.1
	Nº spikes/burst	14.9 ± 4.7	20.8 ± 6.1	13.9 ± 4.4	9.9 ± 2.4
	Recurrence of burst (nº burst/min)	6.4 ± 2.6	9.3 ± 4.1	13.9 ± 4.4	10.6 ± 5.0
	Intraburst frequency (spike/s)	41.5 ± 9.6	52.7 ± 9.7	41.0 ± 7.7	43.4 ± 10.3

Data is expressed as mean $\pm$ S.E.M. **$p < 0.01$ vs sham (RM two-way ANOVA followed by Bonferroni´s posthoc test), and Fisher´s exact test, [&&]$p < 0.01$ vs baseline and [###]$p < 0.001$ vs sham.
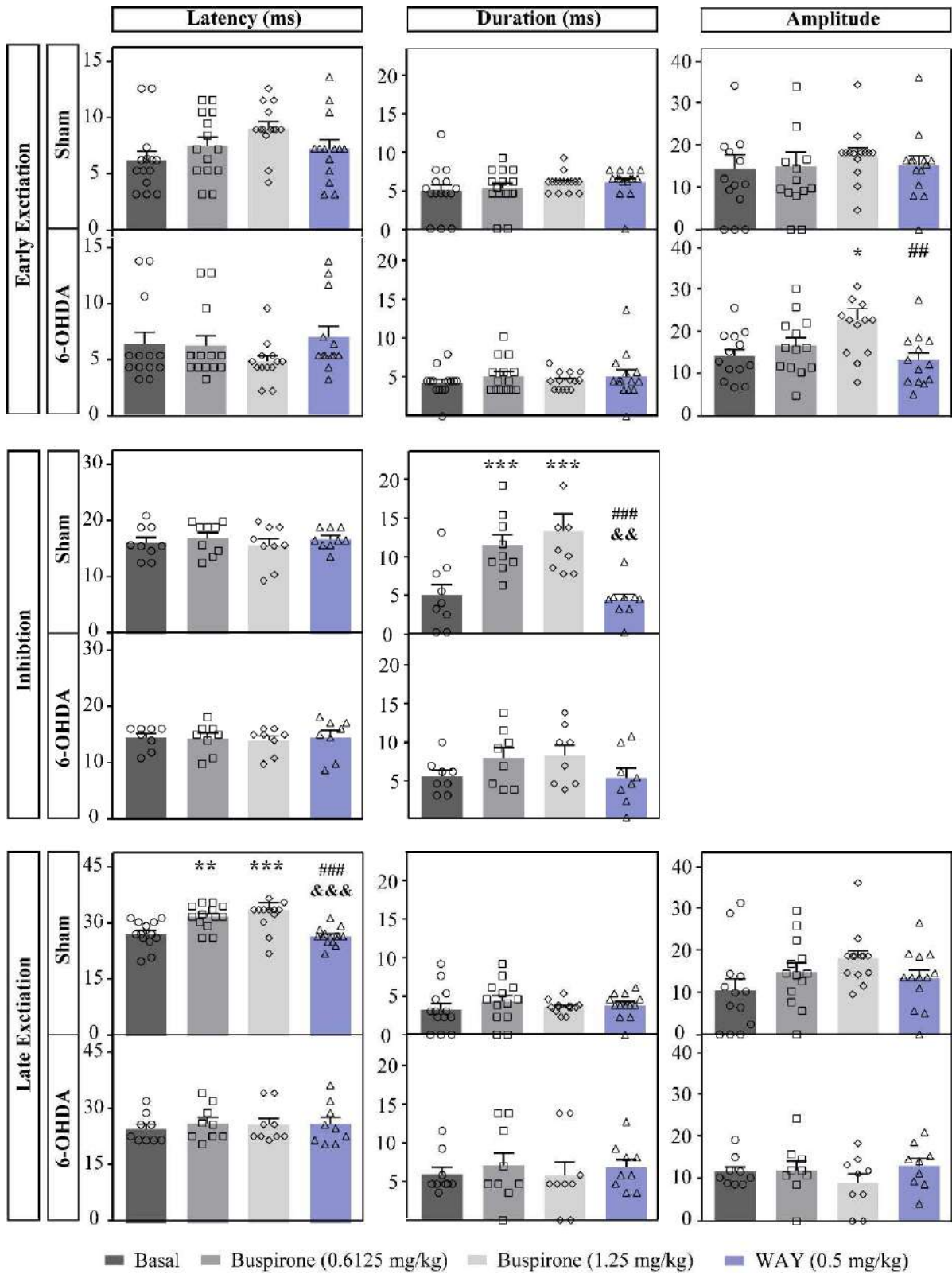
Figure 4.17. Effect of the systemic administration of buspirone on sensorimotor cortico-nigral information. Representation of characteristic parameters related to cortically-evoked responses (latency, duration, and amplitude of the responses). On the top, the latency, duration and amplitude of the early excitatory component (sham n = 11; 6-OHDA n = 13). In the middle, the latency and duration of the inhibitory component (sham n = 7; 6-OHDA n = 8). On the bottom, the latency, duration and amplitude of the late excitatory component (sham n = 10; 6-OHDA n = 9). Note that buspirone enhanced the duration of inhibition in the sham group and delayed the latency of late excitation. Each bar represents the mean ± S.E.M. Each dot represents the value from one neuron before and after buspirone (0.6125 and 1.25 mg/kg, i.v.) and WAY-100635 (0.5 mg/kg).*p < 0.05, **p < 0.01 and ***p < 0.001 vs respective sham (RM two-way ANOVA followed by Bonferroni´s post hoc test); [&&]p < 0.01 and [&&&]p < 0.001 WAY-100635 (0.5 mg/kg) administration vs buspirone (0.6125 mg/kg) administration and [##]p < 0.01 and [###]p < 0.001 WAY-100635 (0.5 mg/kg) administration vs buspirone (1.25 mg/kg) administration (two-tailed paired Student´s t test).

Finally, buspirone failed to modify the sensorimotor cortical information through the indirect pathway. Thus, as described in **Figure 4.17**, only the latency of the late excitation was significantly higher in the sham group after buspirone administration (buspirone: $F_{(2, 40)}$ = 7.40, p < 0.01 and lesion: $F_{(1, 20)}$ = 9.169, p < 0.01, RM two-way ANOVA) what was reverted by WAY-100635 (two-tailed paired Student´s t test, p < 0.001). However, this change may be due to the longer duration of inhibitory response observed after buspirone administration in sham rats.

4.3.4. Effect of buspirone on cortically evoked activity in the entopeduncular nucleus neurons in sham and 6-hydroxydopamine-lesioned rats

Finally, the effect of buspirone on sensorimotor cortico-entopeduncular transmission was studied. Although we chose a low dose of buspirone (0.6125 mg/kg), this dose caused a decrease in the firing rate (buspirone: $F_{(1, 20)} = 8.035$, $p < 0.01$ and lesion: $F_{(1, 20)} = 9.67$, $p < 0.01$, RM two-way ANOVA) and an increase the CV of EP neurons (buspirone: $F_{(1, 20)} = 0.129$, $p > 0.05$ and lesion: $F_{(1, 20)} = 1.717$, $p > 0.05$ RM two-way ANOVA) in the sham group. WAY-100635 partially reverted buspirone (two-tailed paired Student´s t test, $p < 0.05$). **Table 4.12** summaries all electrophysiological parameters before and after buspirone.

The analysis of the parameters of the evoked responses show that the transmission of sensorimotor cortical information through the hyperdirect pathway was not modulated by buspirone administration in any of experimental groups **(Figure 4.18)**. Thus, all the parameters of the early excitatory component of the response remained unaltered after buspirone administration.

Buspirone modulated the sensorimotor cortical transmission through the direct pathway in the sham group. Thus, there was an increment in the duration of the inhibitory component (buspirone: $F_{(1, 12)} = 37.92$, $p < 0.001$ and lesion: $F_{(1, 12)} = 1.943$, $p > 0.05$, RM two-way ANOVA) and anticipated latency (buspirone: $F_{(1, 12)} = 5.991$, $p < 0.05$ and lesion: $F_{(1, 12)} = 0.034$, $p > 0.05$, RM two-way ANOVA) in EP neurons recorded from the sham group. No changes were seen in the 6-OHDA-lesioned group. Posterior WAY-100635 administration reverted the effect induced by buspirone (two-tailed paired Student´s t test, $p < 0.05$,).

Finally, buspirone also modified the sensorimotor cortical information through the indirect pathway. As seen in **Figure 4.18**, only in the sham group the duration of the late excitation was significantly higher after buspirone administration (buspirone: $F_{(1, 16)} = 6.439$, $p < 0.05$ and lesion: $F_{(1, 16)} = 0.063$, $p > 0.05$; RM two-way ANOVA) while amplitude was significantly reduced (buspirone: $F_{(1, 16)} = 6.644$, $p < 0.05$ and lesion: $F_{(1, 16)} = 2.122$, $p > 0.05$; RM two-way ANOVA). Posterior WAY-100635 administration reverted the effect induced by buspirone (two-tailed paired Student´s t test, $p < 0.05$).

Table 4.12. Effect of buspirone on firing properties of entopeduncular neurons in sham and 6-hydroxydopamine-lesioned rats.

		Basal	Buspirone (mg/kg) 0.6125	WAY (mg/kg) 0.5
Sham (n = 12)	**Firing rate (Hz)**	20.39 ± 2.6	11.8 ± 2.2*	19.9 ± 3.6
	CV (%)	49.4 ± 7.7	64.9 ± 9.6*	52.4 ± 9.9
	Neurons exhibiting burst firing pattern (%)	75	66.7	63.6
	Number of bursts	29.4 ± 13.7	10.1 ± 3.1	7.7 ± 2.9
	Duration of burst (ms)	0.4 ± 0.1	0.7 ± 0.2	0.7 ± 0.3
	Nº spikes/burst	12.6 ± 3.1	12.7 ± 3.2	7.6 ± 3.2
	Recurrence of burst (nº burst/min)	19.7 ± 7.9	7.0 ± 1.9	4.9 ± 1.4
	Intraburst frequency (spike/s)	45.1 ± 11.5	36.2 ± 10.1	27.2 ± 11.7
6-OHDA (n = 9)	**Firing rate (Hz)**	27.8 ± 3.4	24.9 ± 2.8	21.3 ± 3.5
	CV (%)	54.8 ± 6.2	36.6 ± 4.4	48.8 ± 8.3
	Neurons exhibiting burst firing pattern (%)	88.9[##]	55.6[&&]	77.8[&]
	Number of bursts	9.2 ± 5.4	3.8 ± 1.9	8 ± 4.2
	Duration of burst (ms)	0.6 ± 0.3	0.2 ± 0.1	1.5 ± 1.2
	Nº spikes/burst	25.6 ± 18.3	4.8 ± 1.8	9.7 ± 2.9
	Recurrence of burst (nº burst/min)	5.1 ± 2.7	2.4 ± 1.1	5.9 ± 2.9
	Intraburst frequency (spike/s)	55.9 ± 12.6	32.0 ± 10.8	35.9 ± 7.3

Data is expressed as mean ± S.E.M. *$p < 0.05$ vs baseline (RM two-way ANOVA followed by Bonferroni´s posthoc test), and [&]$p < 0.05$ and [&&]$p < 0.01$ vs baseline and [##]$p < 0.01$ vs sham (Fisher´s exact test).
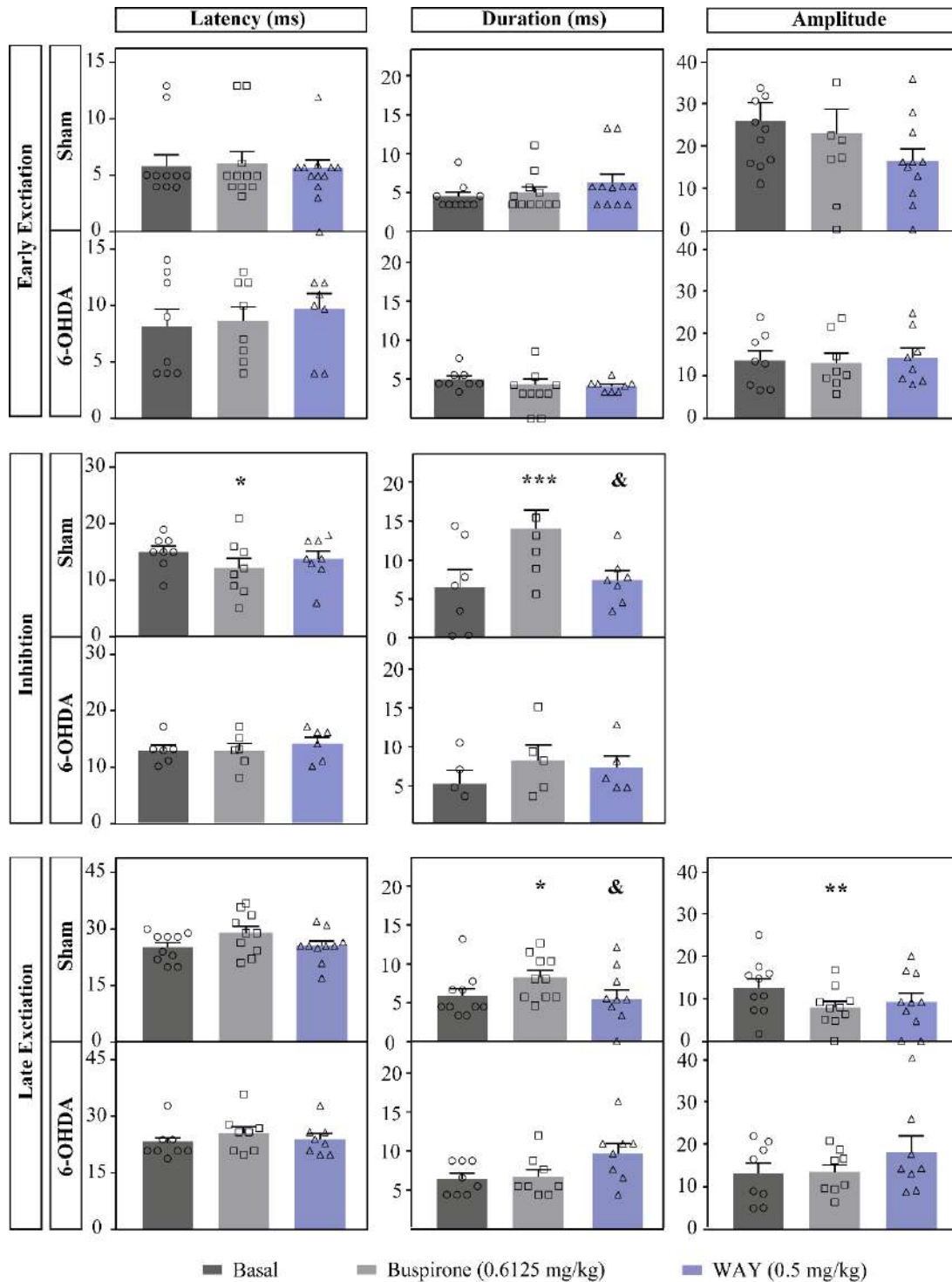
Figure 4.18. Effect of the systemic administration of buspirone on sensorimotor cortico-enteropeduncular information. Representation of characteristic parameters related to cortically-evoked responses (latency, duration, and amplitude of the responses). On the top, parameters of the early excitatory component (sham n = 11; 6-OHDA n = 8). In the middle, parameters of the inhibitory component (sham n = 7; 6-OHDA n = 6). On the bottom, parameters of the late excitatory component (sham n = 10; 6-OHDA n = 8). Note that buspirone enhanced the duration of inhibition and late excitation in the sham group. Each bar represents the mean ± S.E.M. of n rats. Each dot represents the value from one neuron before and after buspirone (0.6125 mg/kg, i.v.) and WAY-100635 (0.5 mg/kg).*p < 0.05, **p < 0.01 and ***p < 0.001 vs respective sham (RM two-way ANOVA followed by Bonferroni´s post hoc test) and [&]p < 0.05 WAY-100635 (0.5 mg/kg) administration vs buspirone administration (0.6125 mg/kg).

4.4. STUDY IV: SEROTONIN TRANSPORTER, 5-HT$_{1A}$ RECEPTOR EXPRESSION AND CYTOCHROME C OXIDASE ACTIVITY IN THE BASAL GANGLIA NUCLEI AND DORSAL RAPHE NUCLEUS IN SHAM, 6-HYDROXYDOPAMINE-LESIONED AND LONG-TERM L-DOPA TREATED 6-HYDROXYDOPAMINE-LESIONED RATS

4.4.1. Serotonin transporter and 5-HT$_{1A}$ immunoreactivity expression in the basal ganglia and the dorsal raphe nucleus

In order to investigate the mechanism involved in the observed changes produced by buspirone on the BG output nuclei after 6-OHDA lesion and long-term L-DOPA treatment, we evaluated SERT and 5-HT$_{1A}$ immunoreactivity in the BG nuclei and the DRN in the three experimental groups (sham n = 7, 6-OHDA n = 7, and 6-OHDA L-DOPA n = 6 animals). The areas of interest were delimited according to Paxinos and Watson´s Rat Brain Atlas and Nissl staining images (**Fig. 4.19A** and **B**). **Figures 4.19C** and **D** show an example of SERT, 5-HT$_{1A}$ receptor immunostaining in the coronal sections used for IOD quantification. Changes in the ratio between the immunoreactivity of the ipsilateral vs contralateral hemisphere was compared between the three experimental groups. Detailed statistical results belonging to this study are shown in ANNEX I.

The average IOD for SERT or 5-HT$_{1A}$ receptor immunoreactivity was decreased in the dorsal striatum nuclei of the lesioned hemisphere: dorsal striatum in the 6-OHDA groups (**Fig. 4.20A** and **4.21A**, respectively). No effect was observed in the ventral striatum (Acc) in both 6-OHDA and 6-OHDA L-DOPA groups (**Fig. 4.20B** and **4.21B**, respectively). In the GPe, SERT expression was unchanged in the 6-OHDA group and decreased in the 6-OHDA L-DOPA group (**Fig. 4.20C**). Decreased 5-HT$_{1A}$ receptor expression was found in both 6-OHDA and 6-OHDA L-DOPA groups (**Fig. 4.21C**). On the other hand, in the EP, SERT and 5-HT$_{1A}$ receptor immunoreactivity was unchanged in the 6-OHDA group but it was decreased in the 6-OHDA L-DOPA group (**Fig. 4.20D** and **4.21D**, respectively). In the STN, SERT immunoreactivity was unchanged in both 6-OHDA groups (**Fig. 4.20E**) and 5-HT$_{1A}$ receptor immunoreactivity was decreased in the

6-OHDA L-DOPA group (**Fig. 4.21E**). In the SN, SERT and 5-HT_{1A} receptor immunoreactivity was unchanged in the 6-OHDA group. By contrast, an increased SERT and a decreased 5-HT_{1A} receptor immunoreactivity were found in the 6-OHDA L-DOPA group (**Fig. 4.20F** and **4.21F**).

Finally, since the DRN is the main serotonergic nucleus in the brain, SERT and 5-HT_{1A} immunoreactivity was studied in the dorsal, ventral and lateral regions (DRD, DRV and DRL, respectively). Reduced SERT expression was observed in the DRD and DRL in both 6-OHDA and 6-OHDA L-DOPA groups (**Fig. 4.20G** and **I**, respectively). In the DRV, a reduced SERT expression was only observed in the 6-OHDA L-DOPA group (**Fig. 4.20H**). Conversely, 5-HT_{1A} receptor expression in the DRD, DRV and DRL was unchanged in the 6-OHDA group and moderate reduced in the 6-OHDA L-DOPA group (**Fig. 4.21G-I**). To sum up, slight reduction of SERT and 5-HT_{1A} expression was seen in some nuclei from the BG and DRN in 6-OHDA-lesioned rats. This reduction was more consistently observed in the majority of BG and DRN after the treatment with L-DOPA.
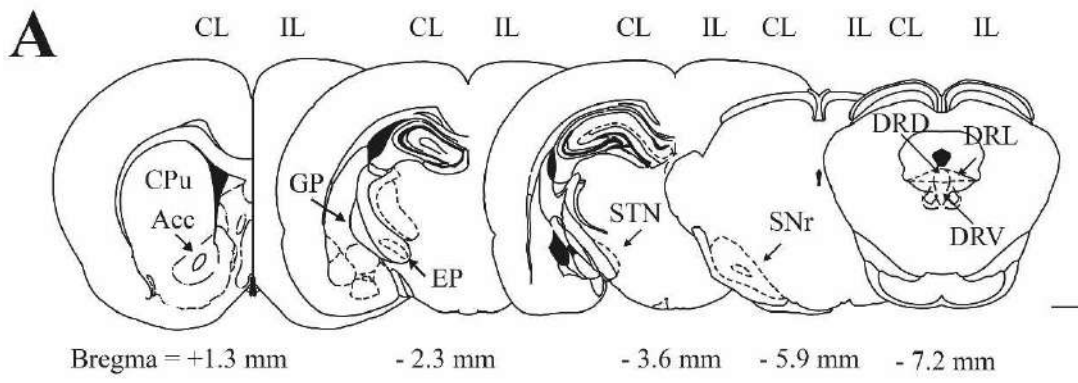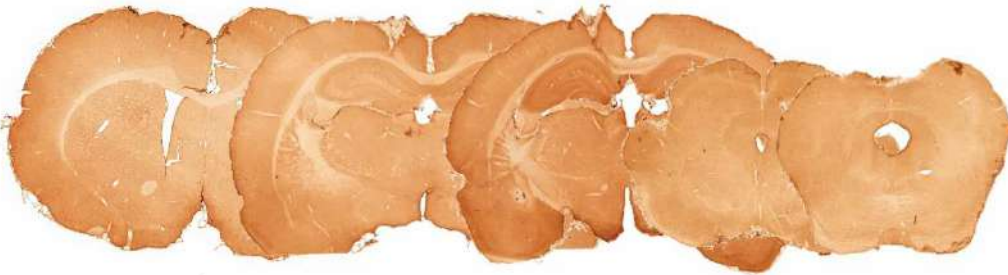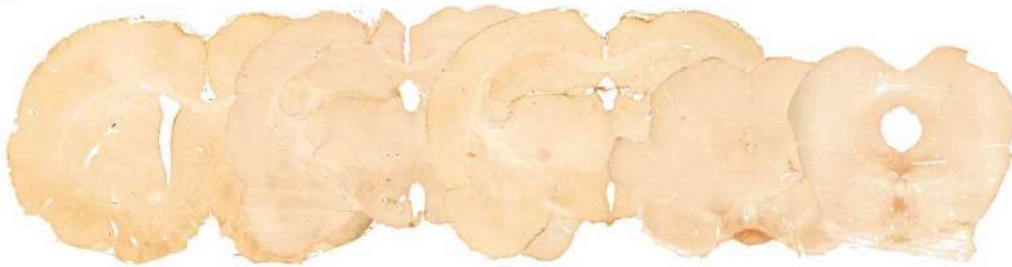
**Figure 4.19. Illustration of the coronal sections used in the histological evaluation of the basal ganglia nuclei and dorsal raphe nucleus.** Representative coronal sections of the BG nuclei and the dorsal raphe nucleus (DRN) with the delimited regions from ipsilateral (IL) and contralateral (CL) hemispheres adapted from Paxinos and Watson, 1997 (A). Representative brain coronal slices of the BG nuclei and the DRN in Nissl staining (B). Examples of coronal sections for SERT immunostaining from a sham animal (C). Examples of coronal sections for 5-HT$_{1A}$ receptor immunostaining from a sham animal (D). Examples of coronal sections for cytochrome c oxidase (COX) staining from a sham animal (E). From the left to the right we can find the following nuclei, AP = +1.3 mm: the striatum and nucleus accumbens (Acc); AP = -2.3 mm: the external globus pallidus (GPe) and in the entopeduncular nucleus (EP); AP = -3.6 mm: subthalamic nucleus (STN); AP = -5.9 mm; the substantia nigra (SN) AP = -7.2 mm, the raphe nucleus divided in the dorsal (DRD), ventral (DRV) and lateral (DRL) regions (relative to bregma). Scale bar = 1 mm.
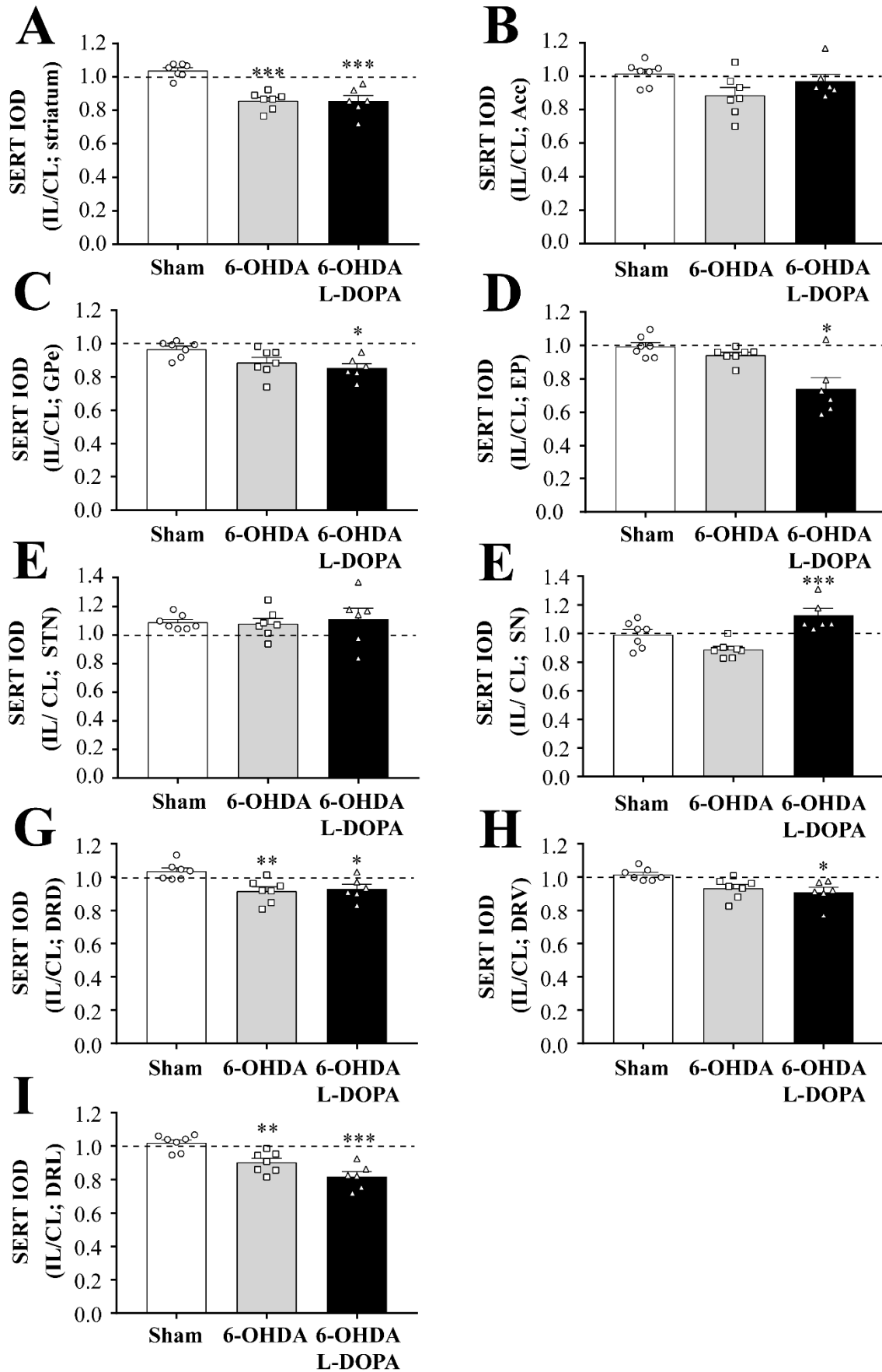
Figure 4.20. Serotonin transporter immunoreactivity in the basal ganglia and dorsal raphe nucleus. The IOD of SERT was expressed on the ratio between ipsilateral (IL) and contralateral (CL) hemispheres in the three experimental groups. Different patterns were observed in the striatum (A), nucleus accumbens (Acc) (B), external globus pallidus (GPe) (C), the entopeduncular nucleus (EP) (D), the subthalamic nucleus (STN) (E), the substantia nigra (SN) (F) and the three different regions of the dorsal raphe nucleus (DRN): the dorsal (DRD) (G), ventral (DRV) (H), and lateral (DRL) (I) regions. The three experimental groups included in the analysis are sham (n = 7), 6-OHDA-lesioned (n = 7), and 6-OHDA L-DOPA (n = 6). Each bar represents the mean ± S.E.M. $*p < 0.05$, $**p < 0.01$, and $***p < 0.001$ vs sham group (one-way ANOVA followed by Bonferroni's post-hoc test).
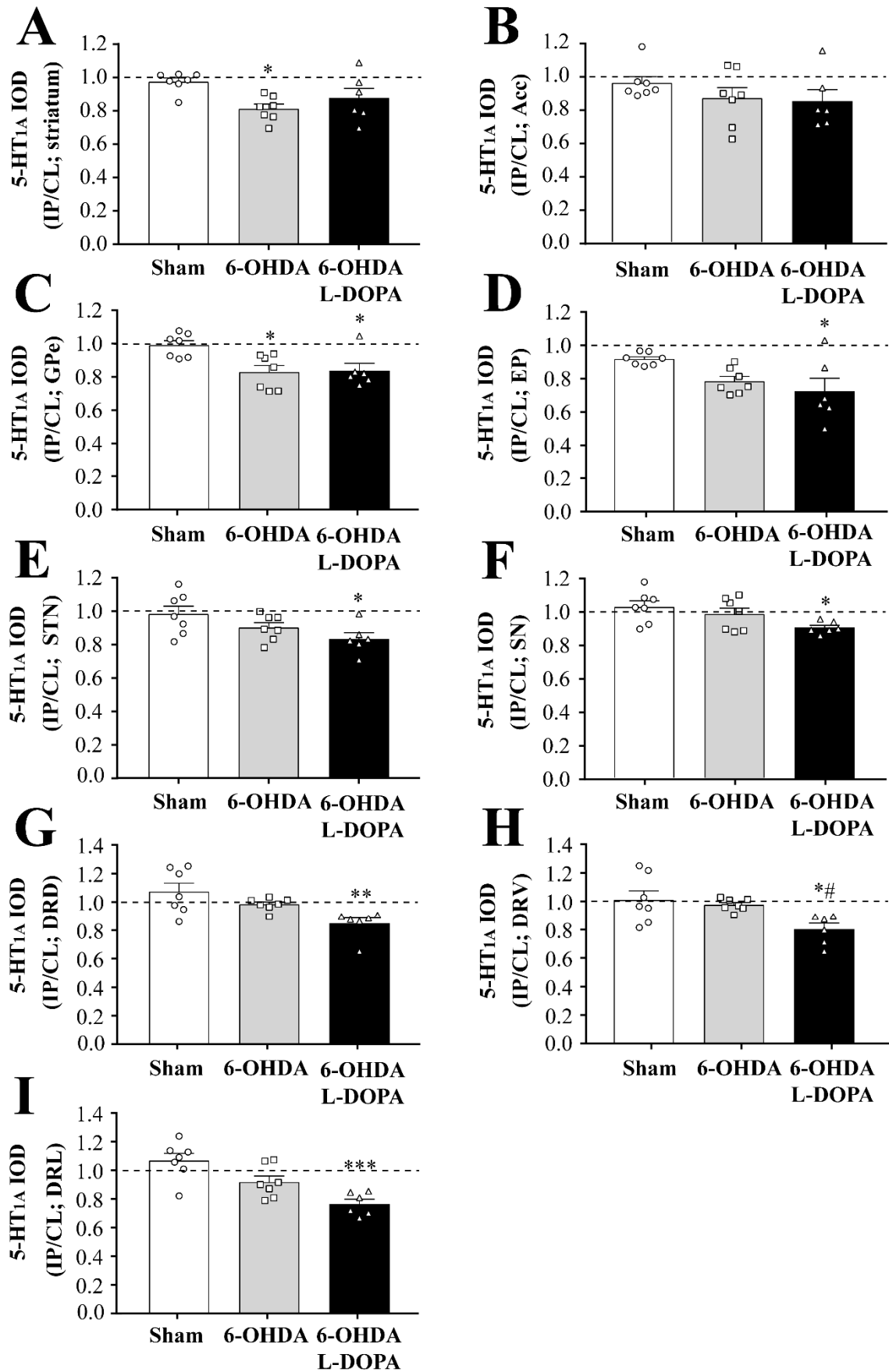
Figure 4.21. 5-HT$_{1A}$ receptor immunoreactivity expression in the basal ganglia and dorsal raphe nucleus. The IOD of 5-HT$_{1A}$ receptor was expressed on the ratio between ipsilateral (IL) and contralateral (CL) hemispheres in the three experimental groups. Different patterns were observed in the striatum (A), nucleus accumbens (Acc) (B), external globus pallidus (GPe) (C), the entopeduncular nucleus (EP) (D), the subthalamic nucleus (STN) (E), the substantia nigra (SN) (F) and the three different regions of the dorsal raphe nucleus (DRN): the dorsal (DRD) (G), ventral (DRV) (H), and lateral (DRL) (I) regions. Three experimental groups included in the analysis are sham (n = 7), 6-OHDA-lesioned (n = 7), and 6-OHDA L-DOPA (n = 6). Each bar represents the mean $\pm$ S.E.M. *p < 0.05, **p < 0.01, and ***p < 0.001 vs sham group and $^{\#}$p < 0.05 vs 6-OHDA group (one-way ANOVA followed by Bonferroni's post-hoc test).

4.4.2. Cytochrome c oxidase activity in the basal ganglia and the dorsal raphe nucleus

The measurement of COX may provide information about the metabolic status of the neuron and it is used to deduce patterns of neuron activity of the different brain regions. Therefore, we evaluated the degree of COX activity between the ipsilateral and contralateral hemispheres in the BG nuclei and the DRN in the three experimental groups (sham n = 8, 6-OHDA n = 7, and 6-OHDA L-DOPA n = 6 animals). The areas of interest were also delimited according to Paxinos and Watson´s Rat Brain Atlas and Nissl staining (**Fig. 4.19A** and **B**). **Figure 4.19E** shows an example of COX staining in the coronal sections used for IOD quantification. Changes in the ratio between the ipsilateral vs contralateral hemisphere was compared between the three experimental groups. Detailed statistical results belonging to this study are shown in ANNEX I.

The overall IOD for COX activity revealed increased COX activity in the dorsal striatum as well as the Acc in both 6-OHDA and 6-OHDA L-DOPA groups (**Fig. 4.22A** and **B**, respectively). In the GP, an increase in COX activity was found in the external region (GPe) and in the internal region (EP) in both 6-OHDA and 6-OHDA L-DOPA groups (**Fig. 4.22C** and **D**). COX activity in the STN (**Fig. 4.22E**) and SN (**Fig. 4.22F**) was significantly increased in both 6-OHDA and 6-OHDA L-DOPA groups. Conversely, a different pattern was observed in the DRN. Measured COX activity remained unaltered in the DRD and DRV in both 6-OHDA and 6-OHDA L-DOPA groups. However in the DRV, a moderate decrease in COX activity was observed in the 6-OHDA group that was restored after the long-term L-DOPA treatment in the 6-OHDA L-DOPA group (**Fig. 4.22H**). Overall, most of the measured areas revealed increased COX activity both in 6-OHDA and 6-OHDA L-DOPA conditions.
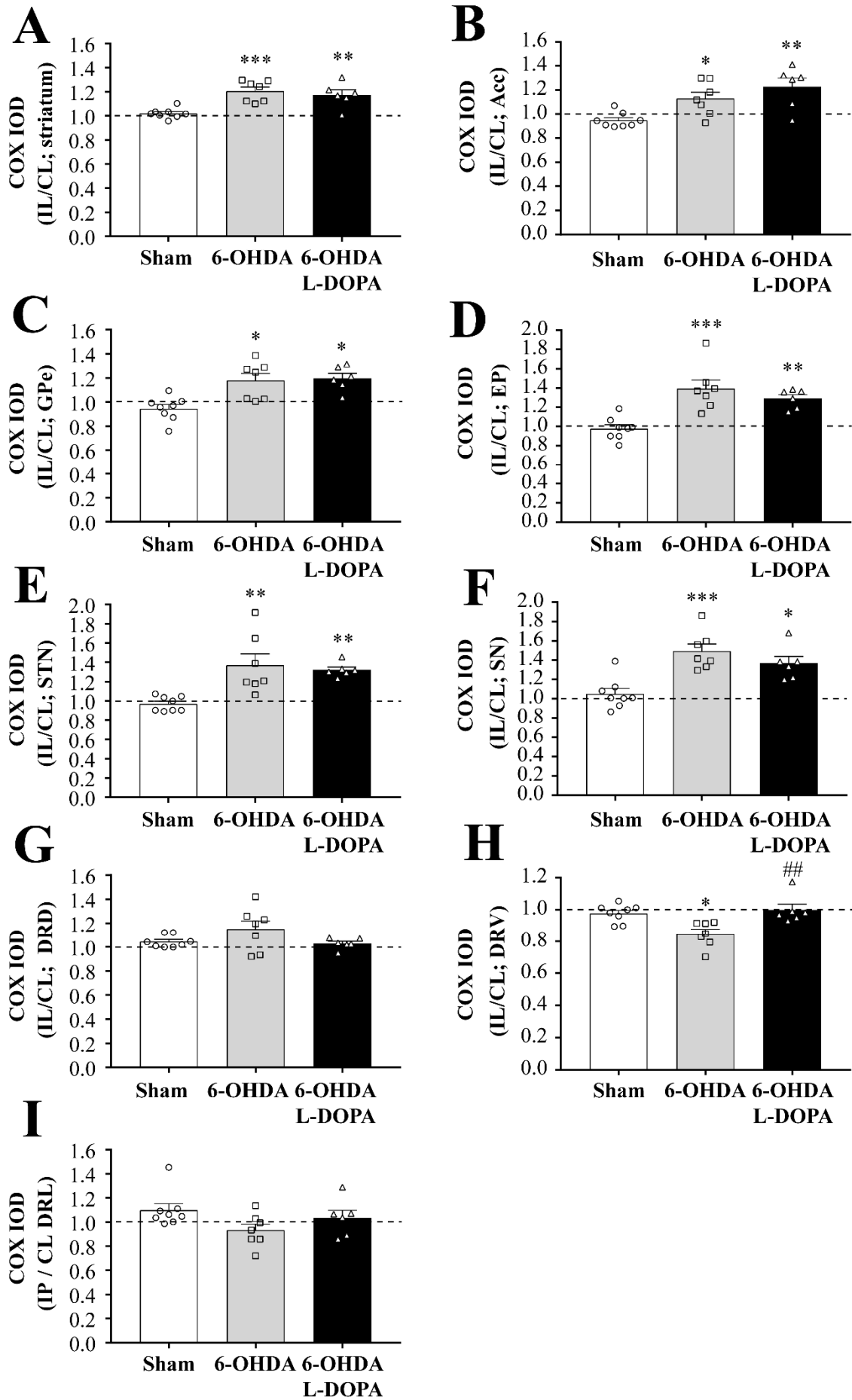
Figure 4.22. Cytochrome c oxidase reactivity in the basal ganglia nuclei and dorsal raphe nucleus. The IOD of COX was expressed on the ratio between ipsilateral (IL) and contralateral (CL) hemispheres in the three experimental groups. Different patterns were observed in the striatum (A), nucleus accumbens (Acc) (B), external globus pallidus (GPe) (C), the entopeduncular nucleus (EP) (D), the subthalamic nucleus (STN) (E), the substantia nigra (SN) (F) and the three different regions of the dorsal raphe nucleus (DRN): the dorsal (DRD) (G), ventral (DRV) (H), and lateral (DRL) (I) regions. The three experimental groups included in the analysis are sham (n = 8), 6-OHDA-lesioned (n = 7), and 6-OHDA L-DOPA (n = 6). Each bar represents the mean $\pm$ S.E.M. *$p < 0.05$, **$p < 0.01$, and ***$p < 0.001$ vs sham group and ##$p < 0.01$ vs 6-OHDA group (one-way ANOVA followed by Bonferroni's post-hoc test).

ANNEX I: A summary of one-way ANOVAs.

Assay	Basal gaglia nuclei	One-way ANOVA	P value
SERT	Striatum	$F_{(2,17)} = 20.94$	***$p < 0.001$
	Acc	$F_{(2,17)} = 2.97$	$p > 0.05$
	GP	$F_{(2,17)} = 5.044$	*$p < 0.05$
	EP	$F_{(2,17)} = 11.42$	*$p < 0.001$
	STN	$F_{(2,17)} = 0.1293$	*$p > 0.05$
	SN	$F_{(2,17)} = 11.01$	***$p < 0.001$
	DRD	$F_{(2,17)} = 7.397$	**$p < 0.01$
	DRV	$F_{(2,17)} = 6.059$	**$p < 0.01$
	DRL	$F_{(2,17)} = 17.52$	***$p < 0.001$
5-HT$_{1A}$ receptor	Striatum	$F_{(2,17)} = 5.132$	*$p < 0.05$
	Acc	$F_{(2,17)} = 1.059$	$p > 0.05$
	GP	$F_{(2,17)} = 6.331$	**$p < 0.01$
	EP	$F_{(2,17)} = 4.871$	*$p < 0.05$
	STN	$F_{(2,17)} = 3.641$	*$p < 0.05$
	SN	$F_{(2,17)} = 3.699$	*$p < 0.05$
	DRD	$F_{(2,17)} = 6.852$	*$p < 0.01$
	DRV	$F_{(2,17)} = 5.69$	*$p < 0.05$
	DRL	$F_{(2,17)} = 11.94$	***$p < 0.001$
COX	Striatum	$F_{(2,18)} = 12.36$	*$p < 0.05$
	Acc	$F_{(2,18)} = 8.733$	**$p < 0.01$
	GP	$F_{(2,18)} = 9.9$	***$p < 0.001$
	EP	$F_{(2,18)} = 13.48$	***$p < 0.001$
	STN	$F_{(2,18)} = 10.22$	***$p < 0.001$
	SN	$F_{(2,18)} = 12.63$	***$p < 0.001$
	DRD	$F_{(2,18)} = 2.414$	$p > 0.05$
	DRV	$F_{(2,18)} = 8.326$	**$p < 0.01$
	DRL	$F_{(2,18)} = 2.407$	$p > 0.05$

Statistical details for SERT and 5-HT$_{1A}$ receptor immunohistochemical assays and COX histochemical assays. *F* values and *p*-values result for the one-way ANOVA.

5. DISCUSSION

5. DISCUSSION

5.1. STUDY I: EFFECT OF BUSPIRONE ON AMINO ACID RELEASE AND NEURON ACTIVITY OF THE SUBSTANTIA NIGRA PARS RETICULATA IN SHAM, 6-HYDROXYDOPAMINE AND LONG-TERM L-DOPA TREATED 6-HYDROXYDOPAMINE RATS

We have used 6-OHDA-lesioned rats to elucidate whether the SNr could be a good target to evaluate pharmacological treatments for the motor symptoms associated with Parkinsonism. Buspirone is one of the most effective drugs in reducing motor symptoms, and it can reverse certain molecular changes induced by L-DOPA in parkinsonian rats (Azkona et al., 2014; Dekundy et al., 2007; Eskow et al., 2007). Here, we show that in anaesthetised rats, buspirone (1) reduces the firing rate of SNr neurons when administered directly into the nucleus, (2) decreases bursty activity when it is administered systemically after DA loss but not in control conditions, and (3) has no effect on LFP and synchronization between the cortex and the SNr and within the nucleus. In addition, buspirone modulates GABA and GLU levels depending on the integrity of the nigrostriatal dopaminergic pathway. Thus, amino acid levels were increased in control conditions, were little affected after DA degeneration, and were not modified after 6-OHDA lesion and L-DOPA treatment.

Effect of buspirone on substantia nigra pars reticulata neuron activity

Although numerous behavioural studies have shown the efficacy of full or partial 5-HT$_{1A}$ receptor agonists in decreasing dyskinesias (Ba et al., 2003; Iravani et al., 2006; Eskow et al., 2007; Dekundy et al., 2007; Gregoire et al., 2009; Gerlach et al., 2011; Aristieta et al., 2012; Dupre et al., 2013; Azkona et al., 2014; Ideberg et al., 2015), no study has examined how these drugs may affect the altered output BG activity in PD and LID. Here, we first showed that the firing rate of SNr neurons was reduced when buspirone was administered directly into the nucleus. However, buspirone caused no change in the firing rate of SNr neurons when was systemically administered, whereas 8-OH-DPAT dose-dependently reduced it. The effect of local as well as systemic 8-OH-DPAT can be attributed to 5-HT$_{1A}$ receptor activation since WAY-100635 antagonized

it. Altogether, these results indicate that the reduction of firing rate involves 5-HT$_{1A}$ receptors located within the SNr and 5-HT$_{1A}$ receptors located on excitatory and inhibitory neurons that project to the SNr. Thus, the systemic effect of buspirone and 8-OH-DPAT depends first on the inhibition of serotonergic neurons in the raphe nuclei and the activity modulation of the striatum, GPe, and STN and second on the direct activation of 5-HT$_{1A}$ receptors into the SNr. In fact, the DRN sends efferences to the SNr as well as to the other basal nuclei (see Di Matteo et al., 2008).

Differences between the effects of buspirone and 8-OH-DPAT likely rely on the fact that 8-OH-DPAT is a full agonist at pre and postsynaptic 5-HT$_{1A}$ receptors (which results in inhibition of the spontaneous firing rate of serotonergic neurons and 5-HT release) and reduces inhibitory responses on targeted structures (Blier et al., 1993; Martín-Ruiz & Ugedo, 2001). Conversely, buspirone acts as a full agonist at presynaptic 5-HT$_{1A}$ receptors inhibiting serotonergic neurons (VanderMaelen et al., 1986) but as a partial agonist of postsynaptic 5-HT$_{1A}$ receptors (Cowen et al., 1994) where its effect will depend on 5-HT levels at the synaptic cleft. Notably, following DA depletion and L-DOPA treatment, the effect of 8-OH-DPAT was abolished. In that sense, several studies have shown that dysfunction of 5-HT$_{1A}$ receptors in rats after DA degeneration decreases or abolishes the effect of 8-OH-DPAT on GABAergic interneurons (Hou et al., 2012) and pyramidal neurons (Wang et al., 2009). However, regarding the effect of systemic 8-OH-DPAT administration on DRN neurons, a loss in efficacy of inhibition (Wang et al., 2009) or no changes (Miguelez et al., 2016) have been reported. Interestingly, systemic administration of buspirone reduced the number of bursty SNr neurons after DA loss but not in control conditions where 8-OH-DPAT has a more pronounced effect. Precisely, an increment in bursty activity was the major change we observed in SNr neurons from the 6-OHDA and 6-OHDA L-DOPA groups. This is also in line with data from electrophysiological studies in anaesthetised rats, which have reported changes in firing patterns rather than in the firing frequency (Aristieta et al., 2016; Meissner et al., 2006; Tseng et al., 2000). SNr burst activity is also reduced by L-DOPA in 6-OHDA-lesioned rats (Aristieta et al., 2016) and by STN-DBS in patients with PD (Maltête et al., 2007). Although also no changed were obtained in 6-OHDA-lesioned rats with STN-DBS (Shi et al., 2006). Previous works have suggested that abnormally increased burst activity could drive the motor dysfunction in PD (Bergman et al., 1994; Boraud et al., 1998; Lobb & Jaeger, 2015; Thomas Wichmann et al., 1999; Thomas Wichmann & Soares, 2006).

This enhancement in burst activity may be due to changes in synaptic plasticity induced by nigrostriatal DA loss (see Lobb, 2014). It seems that bursting activity is more relevant in information-carrying signals (Chergui et al., 1996) and neurotransmitter release rather than single action potentials (Gonon, 1988). Here, we shown that buspirone regularizes burst activity in 6-OHDA and 6-OHDA L-DOPA groups. Therefore, it may be hypothesized that the decrement in burst activity induced by buspirone administration would produce less intense nigral GABA release in the same line that our microdialysis results as we will discuss below.

Effect of buspirone on neuronal oscillatory activity and synchronization of substantia nigra pars reticulata

Cortical slow-wave activity induced by urethane anaesthesia favours low-frequency oscillations in the cortex and the BG nuclei in rats, including the SNr (Aristieta et al., 2016; Brown, 2006; Clement et al., 2008; Magill et al., 2001). The cited studies have demonstrated that these electrophysiological properties are altered in 6-OHDA-lesioned groups that show increased coupling between the cortex and the SNr. In agreement with these findings, we also observed oscillatory activity in the low frequency band (0-5 Hz) in the cortex and the SNr and an increased synchronization between those areas after DA loss and L-DOPA treatment. The coherence analysis between simultaneous recorded SNr spikes and ECoGs and SNr-LFP revealed that AUC values were higher when 6-OHDA-lesioned rats were long-term treated with L-DOPA. This low frequency oscillatory activity and synchronization were not affected by buspirone or 8-OH-DPAT systemically administered at the same doses that modified bursty activity.

So far, there are no studies regarding the effect of antidyskinetic drugs on SNr-LFP in low frequency band, but our previous work found that an acute L-DOPA challenge had little effect on it (Aristieta et al., 2016). It seems therefore that low frequency oscillatory activity and synchronization does not have a relevant role in LID while they may be important in PD. In fact, recent published evidence obtained from 6-OHDA-lesioned rats indicates that oscillations in distinct spectral bands are different at every Parkinsonism stage and may be modulated by pharmacological treatments. In patients with PD, L-DOPA treatment decreased abnormal beta oscillatory activity while increased high gamma oscillatory activity in the motor cortex and BG nuclei (Litvak et al., 2012; López-

Azcárate et al., 2010). Some studies have investigated how 5-HT$_{1A}$ agonists may modulate gamma oscillations and LID. Thus, recordings performed in awake animals have shown that, apart from decreasing dyskinesia, 5-HT-antidyskinetic drugs suppressed 80 Hz oscillation activity, but not the oscillations in other bands (5–10 Hz and 110–140 Hz) in the SNr (Brys et al., 2018). Another recent publication revealed that theta oscillations (5–8 Hz) were elevated in dyskinetic rats and correlated with AIMs score and were reduced by eltoprazine, a 5HT$_{1A/B}$ receptor agonist (Wang et al., 2019). Finally, the aberrant gamma activity (> 60 Hz) found in cortical and SNr-LFP and LID were also reduced by 8-OH-DPAT administration (Dupre et al., 2016).

Effect of buspirone on substantia nigra pars reticulata amino acid release

In this study, using microdialysis approaches we found no significant changes in GABA and GLU basal levels after DA loss with or without prolonged L-DOPA treatment. This finding is consistent with those of other studies performed in freely moving 6-OHDA-lesioned rats (Bianchi et al., 2003; Mela et al., 2007). However, we found that the enhancement in GABA and GLU release induced by locally perfused buspirone in control animals was significantly reduced after 6-OHDA lesion and almost abolished after prolonged L-DOPA treatment. The sources of GABA in the SNr include striatal and GPe terminals and collaterals from GABAergic neurons in the SNr, while the STN provides the major glutamatergic input to the SNr (Kita & Kitai, 1987). In control conditions, GABA and GLU release in the SNr may be regulated by 5-HT$_{1A}$ receptors localized on serotonergic terminals coming from the raphe nuclei, striatal, GPe, and STN terminals and nigral GABAergic neurons. The fact that the inhibitory effect of buspirone on SNr neuron activity was unchanged after 6-OHDA lesion rules out the possibility that changes in 5-HT$_{1A}$ receptors on GABAergic neurons are responsible for the reduction of GABA release as it is shown previously (Lindenbach et al., 2013; Paolone et al., 2015). However, this may reflect altered responsiveness from afferent terminals as shown for nigral GABA release following striatal kainate application and for GLU release following local application of potassium in 6-OHDA-lesioned rats (Bianchi et al., 2003). Furthermore, buspirone, besides its mentioned 5-HT$_{1A}$ receptor partial agonist activity, is also endowed with dopamine D$_2$ and D$_3$/D$_4$ receptor antagonist activity (Bergman et al., 2013). These receptors, whose activity is modulated by 6-OHDA lesion (Avalos-Fuentes et al., 2013), are present in the pallidonigral and striatonigral terminals, modulate GABA release

(Acosta-García et al., 2009; Avalos-Fuentes et al., 2015), and are involved in the antidyskinetic effect of buspirone (Azkona et al., 2014; Shin et al., 2014). Therefore, changes in GABA and GLU release induced by buspirone may involve modulation of several receptors apart from 5-HT$_{1A}$ receptor. In fact, as we see in the study IV, we only found a decrease in optical density of 5-HT$_{1A}$ receptors in the SNr from 6-OHDA-lesioned rats with prolonged L-DOPA treatment where buspirone effect on amino acid release was negligible. After DA degeneration, although buspirone effect was significantly low than in control rats, no changes in 5-HT$_{1A}$ receptor expression was observed.

Conclusion

In summary, the results of this study shows that buspirone modulates amino acid release and neuronal activity, mainly burst activity, in the SNr of the rat. Abnormal burst activity seems to be a more important pathophysiological mechanism than the increased neuronal firing rate observed after nigrostriatal DA loss and long-term L-DOPA treatment. Altogether, our findings point out the importance of burst activity in the SNr from 6-OHDA-lesioned rats as a functional basis to test antiparkinsonian and antidyskinetic drugs.

5.2. STUDY II: EFFECT OF BUSPIRONE ON ENTOPEDUNCULAR NEURON ACTIVITY IN SHAM, 6-HYDROXYDOPAMINE AND LONG-TERM L-DOPA TREATED 6-HYDROXYDOPAMINE RATS

We have previously shown that nigrostriatal degeneration plus the L-DOPA treatment induces alterations in the EP activity that correlates with STN hyperactivity (Aristieta et al., 2019). Here to extend these results, we have evaluated the impact of 5-HT_{1A} receptor agonists in the EP activity of rats with nigrostriatal degeneration that received long-term L-DOPA treatment. Results show that in anaesthetised rats, buspirone (1) reduces the firing rate of EP neurons when administered directly into the nucleus, (2) when it is systemically administered it reduces the firing rate of EP neurons in control conditions and decreases bursty activity after DA loss, and (3) has no effect on the LFP and synchronization between the cortex and the EP, and within the nucleus. In addition, (4) the STN optoillumination increases the firing rate of the STN and EP, and the posterior buspirone administration failed to modify STN optoillumination this effect.

Effect of buspirone on the entopeduncular nucleus activity

It is well established that PD and LID are associated with altered neuron activity at several levels in the BG (Alonso-Frech et al., 2006). In agreement with previous studies, the present results show an increment in bursty activity in EP neurons after DA loss (Ruskin et al., 2002; Lagière et al., 2013; Darbin et al., 2016; Jin et al., 2016; Rumpel et al., 2017; Aristieta et al., 2019) resembling the altered bursting activity found in GPi neurons in patients with PD (Gale et al., 2009; Hutchison et al., 1994; Starr et al., 2005) and in MPTP-injected monkeys (Boraud et al., 1998; Miller & DeLong, 1988; Muralidharan et al., 2017).

When we evaluated the effect of buspirone directly applied into the nucleus there was a reduction of the firing rate of EP neurons that was not influenced by dopaminergic integrity. However, the systemic effect of buspirone or 8-OH-DPAT reduced EP neuron firing rate in control conditions and reduced bursty activity after the severe DA loss. Several studies have investigated whether DA agonists or DBS could normalize abnormal bursting activity providing different results. Some authors found that DA agonists reduce burst activity in the striatum, GPe, and GPi of MPTP-injected monkeys motor function

(Filion & Tremblay, 1991; Singh et al., 2015). The STN-DBS did not change burst activity of the GPi (Hashimoto et al., 2003) or even reduced bursting activity in MPTP-injected monkeys (Hahn et al., 2008; Hahn & McIntyre, 2010). In the same line, the GPi-DBS has demonstrated no effect on bursting activity in the GPe and GPi from humans with PD (Cleary et al., 2013) and MPTP-injected monkeys (McCairn & Turner, 2015). Interestingly, we appreciated that when animals had a partial loss of dopaminergic fibers, the effect of buspirone was similar to that we observed in intact rats. These results point out, as we have discussed in Study I, the importance of the nigrostriatal DA pathway in the 5-HT$_{1A}$ receptor mediated effect of buspirone (WAY-100635 reverted buspirone effects) on the output BG nuclei. In this regard, we obtained similar results to those observed in the STN using the same experimental model of PD (Sagarduy et al., 2016). In that work, we observed that buspirone inhibited STN neuron activity in control conditions and decreased bursty activity after DA depletion (Sagarduy et al., 2016). In that line, chemical ablation of STN resulted in a reduction of severity of LID as well as an attenuation of the antidyskinetic effect of buspirone (Aristieta et al., 2012). So it could be hypothesized that buspirone antidyskinetic effect involved the STN together with the GPi/EP and or SNr.

Both the GPi/EP and STN are well-established target nuclei for DBS treatment of motor complication in patients with PD (Ramirez-Zamora & Ostrem, 2018). Furthermore, while there is consensus about the efficacy of GPi-DBS and STN-DBS in reducing motor symptoms in PD, their effects on LID is still a matter of discussion (Ramirez-Zamora & Ostrem, 2018). A recent publication where the efficacy of STN-DBS or GPi-DBS in reducing LID is compared, authors conclude that GPi-DBS exerts greater direct antidyskinetic effects than STN-DBS (Fan et al., 2020). There are few pharmacological studies concerning the modulation of the EP by 5-HT drugs, that agree with our results. Thus, injection of a 5-HT$_{2C}$ agonist, Ro 60-0175, into the EP promotes abnormal oral movements in 6-OHDA-lesioned rats but not in control rats (Lagière et al., 2013). Then, systemic administration elicits different effect on the firing rate of EP neurons depending on nigrostriatal pathway integrity.

Effect of buspirone on the entopeduncular nucleus oscillatory activity

Patients with PD and animal models exhibit an increased oscillatory activity and higher synchronization between BG nuclei and with the cerebral cortex (Aristieta et al., 2019; Galati et al., 2009, 2010; Magill et al., 2001; Parr-Brownlie et al., 2007; Walters et al., 2007). In urethane-anaesthetised animals, the cortical slow-wave activity or low frequency oscillatory activity is increased after DA loss as we observed in the present study and in previous publications (Jin et al., 2016; Aristieta et al., 2019). This low frequency activity is also present in other brain areas as for example the hippocampus (Vanderwolf, 1969). Among the mechanisms that modulate hippocampal oscillations 5-HT is directly implicated (Olvera-Cortés et al., 2013) and 5-HT$_{1A}$ receptor agonists may increase or suppress oscillatory activity depending on the location of drug application and the animal species used (Horváth et al., 2015; Matulewicz et al., 2010; Olvera-Cortés et al., 2013; Vertes et al., 1994). In this study, neither buspirone nor 8-OH-DPAT altered the low frequency oscillatory activity as it happened in the SNr. However, in our previous work, we observed that an acute L-DOPA challenge reverted the low frequency oscillatory activity and synchronization in the EP from long-term L-DOPA treated 6-OHDA-lesioned rats (Aristieta et al., 2019). In the same line, L-DOPA challenge reduced high synchronization between motor cortex and the EP in 6-OHDA-lesioned rats in theta and beta frequency bands from 6-OHDA-lesioned with and without long-term L-DOPA treatment (Jin et al., 2016). Again, it seems that the important marker of the antidyskinetic efficacy of buspirone is the alteration in bursty activity more that firing frequency and oscillatory activity as our previous studies suggested (Aristieta et al., 2016, 2019).

Optogenetic stimulation of the subthalamic nucleus on the local neuron activity and the entopeduncular neuron activity

Over the last years, optogenetic technology allows researchers to study the brain functionality on multiple scales from the inhibition or excitation of specific neuronal populations to the manipulation of brain circuits. The optogenetic technologies provides a novel way to understand and characterize the BG motor circuit in PD. Nowadays, optogenetics can be an alternative way for high-frequency stimulation to study the impact of STN control on the BG nuclei. Optogenetically-DBS, unlike electrical DBS, allows the selective high-frequency stimulation of the STN neurons in 6-OHDA-lesioned rodents

(Gradinaru et al., 2009; Yoon et al., 2016). Other studies have been focused on the manipulation of the different subpopulations of neurons. Thus in the GPe, the optogenetic stimulation of the arkypallidal neurons suppressed motor activity (Glajch et al., 2016) and the stimulation of prototypical neurons showed hyperkinesia (Tian et al., 2018). The optogenetic approach has also been used for the selective activation of striatal dMSNs from the direct pathway, which increases locomotor activity, while specific activation of striatal iMSNs from the indirect pathway causes akinesia and freezing in mice (Borgkvist et al., 2015; Freeze et al., 2013; Kravitz et al., 2010). A recent study have demonstrated that optogenetic stimulation of dMSNs inhibited SNr neurons and induces LID in 6-OHDA-lesioned mice regardless L-DOPA administration (Keifman et al., 2019).

The STN plays an important role in the BG neuronal network. Especially, nigrostriatal dopaminergic degeneration, results in a hyperactivity of the SNr and the GPi/EP, originated mainly by the overactivity of the STN (DeLong, 1990; DeLong & Wichmann, 2007). In line with this, in our experiments, STN optostimulation derived to increased EP neuron activity. We found that our protocol consisting in continuous blue-light pulses of 1s-duration and 5.5 mW-intensity is enough to get the maximum excitation of STN and EP neuron activity. However, when we applied other design protocol based on trains of 25Hz-pulses of 0.5s-duration and ~14 mW-intensity, the excitation of STN and EP neurons was lower than the previous one. Other authors have reported that ChR2, including our mutation ChR2-H134R, are inactivated by saturation of the kinetic profile under high levels of light intensities (more than a few mW), and especially, more continuous (not pulsing) light frequencies (Herman et al., 2014; Lin, 2011; Lin et al., 2009). Therefore, the moderate excitation in the train-pulses-protocol may be compromised by the saturation of ChR2-H134R activation.

Next, we studied the effect of buspirone on EP neuron activity and found that buspirone did not produce any different effect during the stimulation. Altogether, these results are in agreement with our previous publications (Aristieta et al., 2012; Sagarduy et al., 2016) and show that it is difficult to consider that the antidiskinetic property of buspirone is exclusively mediated by the reduction of the STN hyperactivity.

Conclusion

In summary, the results of this study shows that buspirone reduced the firing rate in the EP from controls and 6-OHDA-lesioned animals which do not present a severe lesion, and modulated mainly the abnormal burst activity observed in 6-OHDA and 6-OHDA L-DOPA groups. On the other hand, optogenetic manipulation of STN neuron activity allows us to evaluate the impact of STN control over other BG output nuclei such as the EP. Although buspirone did not produce any different effect during the stimulation. Our findings suggest again the importance of burst activity in the EP in parkinsonian animals for testing drugs with antiparkinsonian and antidyskinetic efficacy.

5.3. STUDY III: EFFECT OF BUSPIRONE ON CORTICO-NIGRAL AND CORTICO-ENTOPEDUNCULAR TRANSMISSION IN SHAM AND 6-HYDROXYDOPAMINE-LESIONED RATS

In the present study, we analysed whether nigrostriatal DA loss affects cortico-nigral and cortico-entopeduncular information transmission through the sensorimotor circuit of the BG. We also studied the effect of buspirone on these circuits. These main results suggest that: (1) the DA loss induced by the 6-OHDA lesion does not alter the parameters of the evoked response in the SNr after motor cortex stimulation. However, monophasic responses (early excitation) are less frequent while biphasic response pattern (early excitation and late excitation) is more often observed. (2) In the EP, the parameters of motor cortex stimulation evoked response and the pattern of the response are similar in controls and the 6-OHDA-lesioned animals. (3) Buspirone differentially modulates the cortico-nigral and cortico-entopeduncular information transfer through the sensorimotor circuit after the 6-OHDA lesion.

Effect of the 6-hydroxydopamine lesion on cortico-nigral and cortico-entopeduncular information transfer through the sensorimotor circuit

The electrical stimulation of the motor cortex allows to mimic the sensorimotor processing during voluntary movements and provides important clues for understanding the transmission of information through the BG (Chiken et al., 2008, 2015). The activation of the direct striato-nigral/entopeduncular pathway facilitates movement while activation of the indirect trans-striatal pathway inhibits it. In the healthy state, the direct and indirect pathways are meant to be balanced; however, dopaminergic degeneration during PD produces an imbalance between both pathways, leading to decreased inhibition of the BG output nuclei that results in higher inhibition of the motor thalamus causing akinesia.

As we have previously shown in Study II, the nigrostriatal DA loss by 6-OHDA lesion increased the number of bursty SNr neurons without producing changes in the firing rate. In agreement with previous publications (Beyeler et al., 2010; Deniau et al., 2007; Kolomiets et al., 2003; Mailly et al., 2001), 65% of SNr neurons from the sham and

79% of the cells from the 6-OHDA group responded to the motor cortex stimulation. The reason why not all SNr neurons responded may be that not all stimulated cortical projections are involved in the cortico-nigral information transfer through the sensorimotor circuit (Beyeler et al., 2010; Deniau et al., 2007; Kolomiets et al., 2003; Mailly et al., 2001). Moreover, the SNr receives cortical inputs from other non-motor areas. The stimulation of the motor cortex elicited a triphasic response in SNr neurons in both sham and 6-OHDA-lesioned rats as described by us and others in control rats (Aliane et al., 2009; Antonazzo et al., 2019; Beyeler et al., 2010; Degos et al., 2005). However, after the 6-OHDA-lesion, monophasic early excitation was the less frequent response pattern, while biphasic response consisting of early excitation followed by late excitation was the most frequent response type. So far, only one publication has reported the effect of the 6-OHDA lesion in the pattern of response evoked by motor cortex stimulation using awake mice (Sano & Nambu, 2019). The authors found that in the 6-OHDA-lesioned mice, monophasic early excitation pattern was the most frequent response and that inhibitory pattern was more unusual. In terms of the triphasic response, they also observed that parkinsonian mice showed shorter duration of both early excitation and inhibition corresponding to direct and indirect pathways, respectively. On the other hand, Degos et al. (2005) have showed that the interruption of dopaminergic transmission caused by the systemic administration of neuroleptics evokes 1) shorter duration of the inhibition and 2) earlier latency and longer duration of the late excitation, Altogether, these results confirm that nigrostriatal degeneration leads to an imbalance of the direct pathway and indirect pathway after nigrostriatal degeneration.

As again mentioned in Study II, the nigrostriatal DA loss induced abnormal burst firing and more irregular pattern in EP neurons. So far, few studies have analysed the triphasic response, studied here, in the EP. We observed that the parameters of the triphasic response and its pattern remained unchanged after DA depletion. One publication performed in anaesthetised 6-OHDA-lesioned rats, studied the response of EP neurons to the stimulation of the cingulate cortex but did not characterize the evoked response (Lagière et al., 2013). Another study has characterized the evoked triphasic response in EP neurons from awake transgenic mice with deletion of dopaminergic D_1 receptors (Chiken et al., 2015). The authors showed that when the motor cortex was electrically stimulated, the response related to the direct pathway was absent without changing the firing rate and burst pattern of EP cells. The suppression of D_1 receptor

resulted in the loss of transmission through the direct pathway and the consequent reduction of the motor activity in those mice. Here, we showed that the stimulation of the motor cortex evoked the typical triphasic response consisting of early excitation, inhibition, and late excitation in both experimental groups, sham and 6-OHDA-lesioned rats. On the other hand, 44% of EP neurons responded to stimulation of the motor cortex in sham rats as it happens in the SNr, not all cortical axons are involved in the sensorimotor circuit of the BG. Moreover, apart from the motor cortex afferences, the EP also receives cortical inputs from limbic and associative regions, which are involved in emotions (Gerfen, 1984; Wallace et al., 2017).

The electrical stimulation of the motor cortex also elicits a triphasic response in other BG nuclei as the GPe in awake mice (Chiken et al., 2008; Sano and Nambu et al., 2019) and the STN in rats (Janssen et al., 2017). Janssen et al. (2017) showed that the parameters and patterns of the evoked response were not altered in anaesthetised 6-OHDA-lesioned rats. As it happens in rodents, stimulation of several cortical areas in awake monkeys also elicited a similar triphasic response in the GPe, GPi and STN (Nambu et al., 1990, 2000; Tachibana et al., 2008; Yoshida et al., 1993). The stimulation of the primary motor cortex resulted in a triphasic response in GPe and GPi neurons recorded during stereotaxic neurosurgery in patients with PD and showed similarities with the evoked response observed in rodents and monkeys (Nishibayashi et al., 2011).

Effect of buspirone on cortico-nigral and cortico-entopeduncular information transfer through the sensorimotor circuit

Systemic administration of buspirone did not alter SNr firing rate in both experimental groups but normalized the burst activity in 6-OHDA-lesioned rats, as we described in Study I. However, buspirone modulated differently the sensorimotor circuit depending on the nigrostriatal dopaminergic integrity. In sham animals systemic administration of buspirone enhanced the duration of the inhibitory striato-nigral component and as consequence, the late excitatory trans-striatal component was delayed. By contrast, in 6-OHDA-lesioned rats we observed increased amplitude only in the hyperdirect trans-subthalamic component for the highest tested dose of buspirone. In both experimental groups, the effect of the drug was reversed by the administration of the 5-HT_{1A} receptor antagonist, WAY-100635, confirming the implication of this serotonergic

receptor subtype. The influence of 5-HT on the cortico-nigral circuits has been previously shown by Beyeler et al. (2010). These authors found that the 5-HT$_{2C}$ agonist, Ro 60-0175, markedly increased the magnitude of the late excitatory component of the triphasic response. As commented, 6-OHDA lesion can disrupt normal motor patterns, and further alter SNr activities mainly via the direct pathway. Recently, Wang et al. (2019) showed that chronic administration of the 5-HT$_{1A/1B}$ agonist, eltoprazine, could normalize the activity in the direct pathway from dyskinetic rats.

Regarding the EP, as we observed in Study II, high doses of buspirone reduced the basal firing rate in sham rats. In parkinsonian animals, buspirone systemic administration had no effect in the firing frequency but normalized the burst activity. Here, we used the lowest dose of buspirone to evaluate its effect on cortico-entopeduncular transmission transfer. In control conditions, as it happened for the SNr, buspirone enhanced the duration of the direct striato-entopenduncular component, and enhanced the duration but reduced the amplitude of the indirect trans-subthalamic component. These effects were mediated by 5-HT$_{1A}$ receptors since WAY-100635 reverted the mentioned changes. In the 6-OHDA-lesioned group, motor cortex evoked response was not modified by the same dose of buspirone.

Altogether, the present results indicate that buspirone markedly modulates the direct trans-striatal pathway through 5-HT$_{1A}$ receptors, and that this effect is compromised by the nigrostriatal dopaminergic integrity. Previous studies have reported that the stimulation of 5-HT$_{1A}$ receptors improved the catalepsy induced by the 6-OHDA lesion or neuroleptic injection (Nayebi et al., 2010; Mahmoud et al., 2011; Sharifi et al., 2012; Ahmadi et al., 2018). The stimulation of presynaptic 5-HT$_{1A}$ receptors leads to increase striatal DA release via the inhibition of adenylate cyclase activity that activates potassium but inhibits calcium channels (Harrington et al., 1988). The activation of postsynaptic 5-HT$_{1A}$ receptors in the BG nuclei, motor cortex and thalamus is known to promote motor activity in 6-OHDA-lesioned rats (Ahmadi et al., 2019; Mignon & Wolf, 2007; Nayebi et al., 2010; Prinssen et al., 2002; Shimizu et al., 2013). In vivo microdialysis studies have shown that buspirone systemic administration can evoke different effects depending on the brain region. In the DRN reduces 5-HT release (Matos et al., 1996) while in the prefrontal cortex reduces 5-HT but increases DA release in control conditions (Gobert et al., 1999; Silverstone et al., 2012). The 5-HT$_{1A}$ agonists

could inhibit GABAergic interneurons in the prefrontal cortex and evoke striatal DA release probably via GABAergic MSNs (Díaz-Mataix et al., 2005; Ng et al., 1999; Ohno et al., 2015; Sakaue et al., 2000). Additional activation of 5-HT$_{1A}$ receptors in the prefrontal cortex could also inhibit the activity of cortical glutamatergic neurons and normalize the excessive cortico-striatal glutamatergic input in 6-OHDA-lesioned rats (Antonelli et al., 2005; Dupre et al., 2008, 2011; Mignon & Wolf, 2005, 2007).

The lack of effect on the direct trans-striatal pathway observed in 6-OHDA-lesion rats could be due to the impaired ability of buspirone to increase striatal DA release and the effect on GLU and GABA release like other authors have reported. In the Studies I and II, we showed that the effect of buspirone was lower on nigral GLU and GABA release in 6-OHDA-lesioned rats compared to naïve animals. Additionally, buspirone failed to alter the firing rate of the SNr and EP after 6-OHDA-lesion while buspirone normalized the abnormal burst activity in both output nuclei from 6-OHDA-lesioned rats. Here, we observed that in control conditions, buspirone enhances direct trans-striatal pathway while inhibits the EP activity. The net effect of buspirone could be the thalamic disinhibition and movement promotion. This effect could be conditioned by the used dose as other studies have reported that acute low doses of buspirone promotes locomotion in control rats whereas high doses impairs it (File & Andrews, 1991; Pich & Samanin, 1986). The antiparkinsonian effect of buspirone would be mediated by the normalization of the burst activity by the activation of 5-HT$_{1A}$ receptors. Moreover, it is thought that 5-HT$_{1A}$ agonists could ameliorate LID stimulating 5-HT$_{1A}$ inhibitory receptors within the raphe nuclei and normalizing the excessive DA release in the striatum (Bara-Jimenez et al., 2005; Carta et al., 2008; Eskow et al., 2007; Muñoz et al., 2008; Ostock et al., 2011). Therefore, evidence from other authors as well as our results suggest that buspirone via 5-HT$_{1A}$ receptors modulates the direct trans-striatal pathway through sensorimotor-BG circuit by a complex mechanism involving the dopaminergic system and other neurotransmitter systems which are present in the BG circuit.

Conclusion

In summary, the motor cortex stimulation evoked a triphasic response in both BG output nuclei, the SNr and EP. After the 6-OHDA lesion, the parameters of the triphasic response in the SNr remained unchanged whereas the pattern of response was modified. In the EP, the parameters of the triphasic response and the pattern of the response were similar in both experimental groups. We also found that buspirone differently modulates the cortico-nigral and cortico-entopeduncular information transmission transfer through the direct pathway after the 6-OHDA lesion. Therefore, the antiparkinsonian effect of buspirone seems to be mediated though the direct trans-striatal pathway by a complex mechanism in which the activation of 5-HT$_{1A}$ receptors and other neurotransmitter systems may be involved.

5.4. STUDY IV: SEROTONIN TRANSPORTER, 5-HT₁ₐ RECEPTOR EXPRESSION AND CYTOCHROME C OXIDASE ACTIVITY IN THE BASAL GANGLIA NUCLEI AND DORSAL RAPHE NUCLEUS IN SHAM, 6-HYDROXYDOPAMINE-LESIONED AND LONG-TERM L-DOPA TREATED 6-HYDROXYDOPAMINE-LESIONED RATS

The most widely used animal model of PD is the unilaterally 6-OHDA-lesioned rodent described by Ungerstedt (1968). The neurotoxin 6-OHDA can be injected in three different sites, the striatum, SNc or MFB. The injection of 6-OHDA into the striatum destroys DA terminals in striatum first and as a consequence of axonopathy, DA cells bodies in the SNc days laters. The 6-OHDA is taken by dopaminergic neurons via DAT and noradrenaline reuptake transporters resulting in a rapid cell death. This lesion causes a slow partial degeneration that mimics the slow progression of PD. The injection of 6-OHDA in the SNc produces a nearly complete lesion of the dopaminergic cells in this region while the injection in the MFB leads to the most severe lesion type resembling late-stage PD (Shimohama et al., 2003). The induction of parkinsonism with 6-OHDA is often accompanied by pretreatment with desipramine and pargyline to increase the selectivity and efficacy of 6-OHDA lesion. Desipramine, a noradrenaline/5-HT uptake inhibitor, decreases 6-OHDA-induced noradrenaline and 5-HT depletion (Schallert et al., 2000), whereas pargyline, a monoamine oxidase inhibitor, enhances availability of 6-OHDA (Henry et al., 1998). Even if the lesion stars just at the moment of the injection, between 3 and 4 weeks are necessary to reach the stable lesion, which will remain several months (Rentsch et al., 2019). Depending on the injection site, the extension of the lesion and duration of the progression in DA loss can vary (Schwarting & Huston, 1996; Sun et al., 2011). This can explain the discrepant results obtained when the MFB or striatum models are used.

In addition, the use of drugs for testing the accuracy of DA loss induced by unilateral 6-OHDA injection may contribute to inconsistent results found in the literature. Motor deficits observed in parkinsonian animals can give an indication of the extent of the lesion (Deumens et al., 2002). The behavioural tests can be divided into drug-induced and non drug-induced ones. The apomorphine and amphetamine-induced rotational tests

have been commonly used to assess DA denervation, whereas, repeated administration of both drugs can directly and indirectly activate dopaminergic receptors causing changes in their sensitivity (Kamata & Rebec, 1983; Rebec & Lee, 1982). This is the reason why to assess the motor deficits and to discard the pharmacological impact of DA agonists in our results, we used three non-drug induced behavioural tests including the cylinder, bar and drag tests, in the three experimental groups.

Serotonin transporter and 5-HT$_{1A}$ receptor expression

Studies regarding SERT and 5-HT$_{1A}$ receptor changes in PD have provided contradictory results showing increased, decreased, or unmodified expression of these proteins both in humans and in animal models. This discrepancy may be due to methodological issues mentioned above (the stage of the disease or the drugs used to screen the degree of the lesion) or the experimental model used. Therefore, to better explain our electrophysiological and microdialysis results in the BG output nuclei, we performed immunohistochemical detection of SERT and 5-HT$_{1A}$ receptors in the BG nuclei and the DRN in the PD animal model used in Study I, II and III. As commented in the introduction, 5-HT$_{1A}$ receptors and serotonergic terminals are unevenly expressed in the BG nuclei and their distribution also differs between species, but they are highly expressed in the raphe nuclei (Di Matteo et al., 2008). The results of this section showed that 6-OHDA lesion and L-DOPA treatment induces a slight reduction of SERT and 5-HT$_{1A}$ immunoreactivity within the BG nuclei and in different regions of the DRN with the exception of the SN, mostly belonging to the SNr, where it increases.

The evaluation of SERT expression can be used as a biomarker of the serotonergic neurotransmission since it provides information about serotonergic innervation. Overall, we found slight reduction of SERT expression in the striatum and no changes in the rest of the BG after the 6-OHDA-lesion. Additional long-term L-DOPA treatment reduced SERT expression in the striatum, GPe and EP while increased it in the SNr. In other nuclei, as the Acc and STN, SERT expression was neither modified by the 6-OHDA lesion or the long-term L-DOPA treatment. Although SERT expression in parkinsonian conditions has been reported by different authors, the results are not very consistent. A recent SERT-binding study has observed that striatal SERT levels are reduced in 6-OHDA-lesioned rats but in long-term L-DOPA treated rats the values were similar to

those in the sham group (Walker et al., 2019). Other studies have shown that striatal SERT expression was upregulated (Rylander et al., 2010; Tronci et al., 2017), not modified (Prinz et al., 2013) or even decreased (Nevalainen et al., 2014) in long-term L-DOPA treated rats. Stereological studies performed in MPTP-injected monkeys have revealed sprouting of SERT terminal axons in the striatum, GPe and GPi (Gagnon et al., 2016, 2018). Our results are in line with the studies in patients with PD where reduced SERT-binding has been found in the striatum and GPe (Chinaglia et al., 1993; Kish et al., 2007). In addition, one positron emission tomography (PET) study has revealed that striatal SERT expression in patients with PD at early stages was significantly reduced compared to subjects without PD, and that this reduction was more pronounced during the progression of the disease (Albin et al., 2008).

Surprisingly, we found unchanged SERT expression in the SNr from 6-OHDA-lesioned animals while it was increased after long-term L-DOPA treatment. The reason why SERT expression was differentially regulated in the SNr may be due to the variability on density and pattern of the serotonergic innervation along the BG nuclei. In fact, according to anatomical studies, the SNr receives the highest serotonergic innervation from the DRN within the BG nuclei in rodents, primates and humans (Hashemi et al., 2011; Huang et al., 2019; Moukhles et al., 1997; Wallman et al., 2011). Overall, in our experimental approach, SERT expression suffered a slight increase in 6-OHDA-lesioned animals after long-term L-DOPA treatment. Other studies have reported an upregulation in the striatum from patients with PD and animal models and have related such increment with the development of LID (Politis et al., 2014; Roussakis et al., 2016). It is possible that the nigral serotonergic hyperinnervation observed in our study was also relevant for the appearance of LID. Indeed, in a previous publication from our group, we observed that neuronal SNr firing activity was positively correlated with limb and orolingual AIMs in long-term L-DOPA treated 6-OHDA-lesioned rats (Aristieta et al., 2016). Other authors have also related SNr activity with the expression of abnormal orofacial movements (Deniau et al., 1996).

We also appreciated a discrete reduction of SERT immunoreactivity in the DRD and DRL both after the 6-OHDA lesion and the long-term L-DOPA treatment. However, in the DRV, the SERT expression was only reduced in the 6-OHDA L-DOPA group. This result is in line with previous studies performed in humans and animal models. In MPTP-

injected monkeys, the density and morphology of serotonergic neurons remained unchanged while the axonal projections were diminished (Gagnon et al., 2016). However, PET and post-mortem studies in patients with PD showed reduced SERT levels in raphe nuclei (Chinaglia et al., 1993; Kish et al., 2003; 2007) and severe degeneration in advanced stages of the disease (Halliday et al., 1990; Politis et al., 2010).

Together with SERT, we also evaluated 5-HT_{1A} receptor expression, which was slightly decreased in the striatum and GPe from the 6-OHDA-lesioned group. Additional treatment with L-DOPA induced more pronounced decrements in the GPe, EP, STN and SN. As commented in the introduction, 5-HT_{1A} receptors are located at the presynaptic level on neurons from the raphe nuclei and postsynaptically in other brain regions such as the BG nuclei (Di Matteo et al., 2008). Results concerning 5-HT_{1A} receptor expression in animal models are also rather contradictory. In MPTP-injected monkeys, increased and decreased 5-HT_{1A} receptor levels were observed in the striatum and motor and premotor cortical areas, respectively (Frechilla et al., 2001; Huot et al., 2012a; Huot et al., 2012b) while other study found no changed expression in the striatum, GP and SN (Riahi et al., 2012). In 6-OHDA-lesioned rats, no striatal changes in mRNA levels and protein expression were found by other authors (Numan et al., 1995; Radja et al., 1993). However, PET and *post-mortem* studies in patients with PD have demonstrated that 5-HT_{1A} receptors were decreased in the caudate nucleus and cingulate cortex (Ballanger et al., 2012) but not in the GP and SN (Huot et al., 2012b).

Regarding the different regions of the DRN, we observed that 5-HT_{1A} receptor immunoreactivity was not altered in 6-OHDA-lesioned rats. Nevertheless, decreased 5-HT_{1A} receptor immunoreactivity was found after long-term L-DOPA treatment. Other authors have found the same results in our rat model (Hou et al., 2012) and MPTP-injected monkeys (Frechilla et al., 2001). It is widely accepted that raphe nuclei, especially the DRN, suffers changes during PD (Braak et al., 2003; Halliday et al., 1990) and PET studies have demonstrated a significant reduction of 5-HT_{1A} receptor levels in lower midbrain raphe of patients with PD (Doder et al., 2003). Altogether, it seems that the serotonergic system undergoes degeneration after the 6-OHDA lesion what can result in altered 5-HT_{1A} receptor expression. L-DOPA treatment produced more severe alterations of SERT expression, probably because of the proposed neurotoxic effect of the drug on 5-HT cell population (Stansley & Yamamoto, 2014).

Although the change in SERT and 5-HT_{1A} receptor expression was significant, this difference accounted only around a 10% of the control value. It could be speculated that changes in 5-HT_{1A} receptors could take place on serotonergic terminals rather than postsynaptic 5-HT_{1A} receptors on SNr or EP neurons, which could explain why local buspirone administration had a similar effect in the three experimental groups. The activation of presynaptic 5-HT_{1A} autoreceptors in the DRN decreases serotonergic neuron firing rate and 5-HT release in the soma and terminals and subsequently modulates the activity of other neurons via postsynaptic receptors. On the other hand, although the mechanism is not fully understood, the excitability of DRN serotonergic neurons and GABAergic interneurons depends on a fine balance between glutamatergic excitatory drive and GABAergic inputs from other brain regions such as the prefrontal cortex or SNr, which can be modulated by 5-HT_{1A} receptors (Celada et al., 2001; Hernández-Vázquez et al., 2019; Pollak et al., 2014; Soiza-Reilly & Commons, 2011; A. Takahashi et al., 2015; Weissbourd et al., 2014). GABAergic interneurons in the DRN play an important role in feedback inhibition because they can also regulate the activity of serotonergic neurons via 5-HT_{1A} receptors (Liu et al., 2000). Recent molecular and anatomical studies have demonstrated that DRN serotonergic neurons co-release 5-HT and GLU within the BG nuclei (Huang et al., 2019; Wang et al., 2019). Furthermore, it is observed that 6-OHDA-lesion decreased the response of GABAergic interneurons to 5-HT_{1A} receptor stimulation (Hou et al., 2012) producing higher inhibition of 5-HT cells and subsequent reduction of 5-HT and GLU release at terminal levels. Similarly, 8-OH-DPAT administration in 6-OHDA-lesioned-rats produced minor effect in GABAergic interneurons from the medial prefrontal cortex compared to control animals (Zhang et al., 2014). This evidence could help to understand the lack of the effect of buspirone on nigral amino acid release in parkinsonian animals but also suggest that 5-HT_{1A} agonists exerts a complex mechanism in the BG modulation in which other neurotransmitters systems may be also involved.

Cytochrome c oxidase activity in the basal ganglia and the dorsal raphe nucleus

COX is the last enzymatic complex (IV) of the mitochondrial electron transport chain responsible for catalysing the transfer of electrons to oxygen, which serves to generate ATP via oxidative phosphorylation (Wong-Riley, 1989). Neurons depend mostly on oxidative metabolism as an energy source. For this reason, the enzymatic activity of COX is used as a metabolic marker for neuronal activity and its quantification by histochemical approaches allows to study changes in neural metabolism (Wong-Riley, 1989). The most metabolically active regions present higher patterns of neuronal activity showing increased COX density ratios compared with the lowest neuronal activity regions (Hevner & Wong-Riley, 1989, 1991; Melendez-Ferro et al., 2013). Histochemical and *in situ* hybridization studies of COX performed in human brain has demonstrated that mRNA levels of COX in the BG nuclei from patients with PD and L-DOPA therapy were similar compared to control subjects (Vila et al., 1996, 1997). Nevertheless, a recent meta-analysis screening more than 30 studies published between January 1980 and January 2018 have examined the COX enzymatic activity in patients with PD, apart from other major psychiatric disorders and Alzheimer´s disease. Specifically, this meta-analysis points out that COX enzymatic activity was downregulated in blood, muscle and several brain regions mainly the prefrontal cortex and SNc of patients with PD (Holper et al., 2019). In the present section, we showed increased COX activity in the GPe, EP, STN and SNr after nigrostriatal degeneration as it was described in detail in 6-OHDA-lesioned rats by other works (Blandini et al., 2000, 2007). Additionally, we observed that long-term L-DOPA treatment did not alter this increased activity.

In parkinsonian animals, increased COX activity was found in the striatum and Acc according to the described hyperactivity of iMSNs (see introduction). COX activity in the STN was also increased after the 6-OHDA lesion in agreement with our electrophysiological data that demonstrated that nigrostriatal degeneration increased STN activity and the posterior L-DOPA chronic treatment did not modify this hyperactivity (Aristieta et al., 2012, 2016, 2019). Other authors have found that the hyperactivity of the STN was related to the increased COX activity (Beurrier et al., 1999; Chetrit et al., 2013). As consequence of DA loss, the GPe should be hypoactive, nevertheless, we found increased COX density in this region while others have reported unchanged COX activity in MPTP-injected monkeys (Vila et al., 1996, 1997). The GPe of rats contains two main

types of GABAergic projection cells, the prototypic parvalbumin-containing neurons that innervate exclusively the STN and the arkypallidal preproenkephalin-containing neurons that are the main GABAergic projection to the striatum (Abdi et al., 2015; Mallet et al., 2012). Double immunohistochemical detection for COX and parvalbumin revealed that non-parvalbumin cells displayed more dense staining for COX (Karmy et al., 1991). Regarding electrophysiological data, the firing rate of the arkypallidal neurons remained unaltered while prototypic neurons were found hypoactive after 6-OHDA-lesion (Abdi et al., 2015; Mallet et al., 2012). Thus, the increased COX density that we observed in the GPe could be due to arkypallidal neuron activity and not reflect the general hypoactivity observed in prototypical neurons.

The pathological hyperactivity of the STN results in an increased neural activity of the BG output nuclei. In the same line, we found increased COX activity in the SNr and EP after 6-OHDA and after long-term L-DOPA treatment. Precisely in Study I and II, an increment in bursty activity was the major electrophysiological change observed in both SNr and EP neurons after 6-OHDA lesion and 24 h after the last injection of L-DOPA. The present results from 6-OHDA-lesioned rats are in agreement with those published by Lacombe et al. (2009). However the same author found that L-DOPA treatment reversed the changes observed after 6-OHDA lesion in the STN and EP. The discrepancy may be due to the fact that they measured COX mRNA levels and we determined COX activity by histochemistry.

It is important to point out that COX activity cannot be acutely modulated in several brain regions because its catalytic activity in response to neuronal energy demand needs long periods of time (hours or even days) to be regulated (Gonzalez-Lima & Cada, 1994; Padilla et al., 2011; Riha et al., 2011; Vélez-Hernández et al., 2014). Thus, one previous work showed that chronic treatment with NMDA or mGluR5 antagonist could reduce abnormal COX activity of the SNr or STN from 6-OHDA-lesioned rats (Armentero et al., 2006) while others found that chronic co-administration of entacapone with L-DOPA could not normalize COX expression in the STN (Marin et al., 2008). Nevertheless, acute administration of different drugs in rats did not modify COX activity (Vélez-Hernández et al., 2014). Therefore, is not expected that acute dose of buspirone could modify COX activity as it happened with neuron activity in Study I and II.

When studying COX activity in the DRN, no changes were observed in the DRD and DRL. By contrast, decreased COX activity of the DRV was found in 6-OHDA-lesioned rats. In agreement with this, one work has described that the caudal-extent of the dorsal DRN is more susceptible to oxidative stress than the other extensions (Stansley & Yamamoto, 2014). Two previous histochemical studies have found increased COX activity in the DRN (Kaya et al., 2008; Tan et al., 2011) together with increased firing activity of serotonergic neurons in 6-OHDA-lesioned rats. However this result is rather discrepant, as similar studies have also reported increased (Prinz et al., 2013; Wang et al., 2009; Zhang et al., 2007), decreased (Guiard et al., 2008) or unchanged firing rate (Miguelez et al., 2011) in the DRN from 6-OHDA animals. The variability of the results may be due to the methodological differences already mentioned. In addition, we have previously observed that chronic L-DOPA treatment did not alter firing rate of the DRN (Miguelez et al., 2011, 2016). In line with this, we found that COX activity in the DRN and DRL remained unchanged in 6-OHDA and 6-OHDA L-DOPA rats with the exception of the DRV, which could be more susceptible to the 6-OHDA lesion.

Conclusion

In summary, the present results suggest that the serotonergic systemic undergoes degeneration after nigrostriatal dopaminergic denervation and that chronic L-DOPA treatment further alters it. Slight reduction of SERT and 5-HT$_{1A}$ receptor immunoreactivity was observed within the BG nuclei and the different regions of the DRN after the 6-OHDA lesion with the exception of the SNr, where it was increased in 6-OHDA L-DOPA rats. Overall, COX activity was found enhanced within the BG nuclei as consequence of nigrostriatal DA loss and posterior chronic L-DOPA treatment. Finally, COX activity in DRV neurons denotes that this region may be more vulnerable to nigrostriatal degeneration than other regions of the DRN, nevertheless, long-term L-DOPA treatment may reverse this change.

5.5   EXPERIMENTAL LIMITATIONS

One limitation of the present work is that electrophysiological recordings from Studies I, II and III were performed in urethane-anaesthetised rats and it may be argued that this does not accurately represent clinical situations. However, we have recently characterized the electrophysiological parameters in 6-OHDA-lesioned rats and have demonstrated a relationship between these electrophysiological parameters and AIMs score (Aristieta et al., 2016; 2019). It is widely recognized that urethane induces a long-lasting steady level of anaesthesia with minimal effects on autonomic and cardiovascular systems (Hara & Harris, 2002; Neville & Haberly, 2003). Urethane is considered suitable for studying the low frequency oscillatory activity (Galati et al., 2009, 2010; Magill et al., 2001; Parr-Brownlie et al., 2007; Walters et al., 2007) since this anaesthetic induces prolonged maintenance of a stable brain state (Steriade, 2006). The low frequency also called slow-wave are the most prominent oscillation type in humans during non-rapid eyes movement sleep (Steriade, 2006). Similarly, they are also prominent in urethane-anaesthetised rodents and the examination is useful to study the activity in the BG network (Walters et al., 2017). As mentioned, low frequency oscillations are found increased after DA loss. Interestingly, the burst activity after 6-OHDA lesion is still found more enhanced under anaesthesia than in the awake state (Lobb & Jaeger, 2015; Magill et al., 2001; Tseng et al., 2001). Nevertheless, future experiments should explore these initial observations in awake animals because it is more close to physiological conditions. Using multi-electrode recording technology increases the robustness of the data since it makes possible to record LFP and several single spikes from different neurons at the same, permitting the analysis of the synchronization between those signals. In addition, different behavioural tests can be performed simultaneously to the electrophysiological recordings.

It could be argued that buspirone is not a selective drug. However, a single dose of buspirone has showed efficacy in reducing AIMs score in animal models (Aristieta et al., 2012; Azkona et al., 2014; Dekundy et al, 2007; Eskow et al., 2007; Gerlach et al., 2011; Sagarduy et al., 2016) and has demonstrated certain clinical efficacy in open-label trials performed in PD patients (Bonifati et al., 1994; Kleedorfer et al., 1991; Politis et al., 2014). Since then, the antidyskinetic properties of monotherapy of buspirone have been re-evaluated in a phase III clinical trial (NCT02617017) and the efficacy of the

combination with amantadine is being investigated in another phase I clinical trial (NCT02589340), however, the results are still unpublished. From the experimental point of view, it would be interesting to study the effect of buspirone in freely moving animals as well as to further elucidate the effect of buspirone in the triphasic response from urethane-anaesthetised 6-OHDA rats chronically treated with L-DOPA.

The neurotoxin-based models are widely used to understand the nigrostriatal dopaminergic degeneration that occurs in PD. Unfortunately, these models cannot mimic the full pathophysiology and progression observed in PD. In the last few years, new PD animal models based on transgenic overexpression or intracerebral injection of aberrant α-syn aggregations have emerged. These models seem to reproduces better the pathological hallmarks of PD (Dehay et al., 2016; Visanji et al., 2016). Thus, the use of α-syn-based models could drive to significant advances in the understanding of the pathophysiology of PD and would be useful for developing new therapeutic strategies.

The major limitation of immunohistochemistry assays observed in Study IV is that we cannot perform manual counting of 5-HT_{1A} receptor-positive cells and SERT fibers due to the elevated density, distribution and compact morphology. It is widely accepted that the proportion of immunostaining intensity is suitable to estimate or to measure the antigen expression. However, the resolution is limited due to the chromogenic substrate precipitate, as well as the thickness of the sections analysed by the light microscope. The saturation of chromogen may also interfere in the quantitative analyses. For these reasons, in this study, quantification is only performed in regions of interest (the BG nuclei and DRN) and always compared to the contralateral region using selecting non-immunoreactive structures as background. We also used a digital slide scanner with the same source of light and same experimental conditions. Few limitations of these experiments were that we did not take into account the diverse neuron subpopulations that inhabit the studied areas or managed to perform double immunostaining $SERT/5HT_{1A}$. More specific antibodies and an automatic software specifically designed for these markers could improve these technical details.

6. CONCLUSIONS

6. CONCLUSIONS

The different results obtained in the aforementioned studies lead us to the following conclusions:

1. The nigrostriatal DA loss and long-term treatment with L-DOPA did not alter the inhibitory effect induced by buspirone, locally applied into the BG output nuclei, the SNr and EP. These findings suggest that the local mechanisms involved in the effect of buspirone are not affected by DA loss.

2. Systemic administration of buspirone in control conditions did not alter the firing frequency in the SNr but reduced it in EP neurons. Buspirone, however, normalized the burst activity enhanced by DA loss. Abnormal burst activity seems to be a more important pathophysiological mechanism than the increased neuronal firing rate observed after nigrostriatal DA loss and long-term L-DOPA treatment.

3. Systemic administration of the full 5-HT$_{1A}$ agonist, 8-OH-DPAT, reduced the firing rate of SNr and EP neurons in control conditions and the burst activity that was increased in 6-OHDA-lesioned and long-term L-DOPA treated 6-OHDA-lesioned rats. Therefore, the effect of 8-OH-DPAT depends on the integrity of the nigrostriatal pathway.

4. The enhanced low frequency oscillatory activity and synchronization between the motor cortex and the SNr or EP found after 6-OHDA lesion and L-DOPA treatment were not modified by buspirone or 8-OH-DPAT when systemically applied.

5. Buspirone effect on nigral GABA and GLU levels depends on the integrity of the nigrostriatal dopaminergic pathway. Thus, nigral GABA and GLU levels were increased in the naïve group, little affected after DA degeneration, and not affected after 6-OHDA lesion and long-term L-DOPA treatment.

6. The optogenetic stimulation of the STN enhanced EP neuron activity. Nevertheless, the systemic administration of buspirone did not modify the EP neuron response induced by optogenetic stimulation of the STN.

7. After nigrostriatal degeneration the parameters of the triphasic response evoked by motor cortex stimulation in the SNr remained unchanged, however, less frequency of monophasic responses (early excitation) and more frequency biphasic responses (early excitation and late excitation) were observed. By contrast, buspirone required the nigrostriatal integrity to modulate the sensorimotor cortico-nigral information transmission through the direct trans-striatal pathway.

8. The nigrostriatal degeneration did not alter the parameters of the triphasic response and the type of evoked response in the EP. Nevertheless, buspirone required intact nigrostriatal integrity to modulate the sensorimotor cortico-entopeduncular information transmission through the direct trans-striatal pathway.

9. The serotonergic system undergoes down regulation after the 6-OHDA-lesion, which was manifested by decreased expression of SERT in the dorsal striatum and DRN, and 5-HT$_{1A}$ receptors in the striatum and the GPe. Long-term L-DOPA treatment further decreased these changes in most BG nuclei and the DRN. By contrast, SERT expression was enhanced in the SN from 6-OHDA-lesioned rats.

10. Overall, COX activity was increased within the BG nuclei as consequence of the nigrostriatal DA loss and it was not altered by the chronic L-DOPA treatment. Within the DRN, the DRV showed reduced COX activity after DA loss and long-term treatment with L-DOPA attenuated it.

In summary, the present results indicate that DA loss alters the effects induced by buspirone in the BG output nuclei, the SNr and EP, and that the main effect of this drug and other full 5-HT$_{1A}$ receptor agonist, 8-OH-DPAT, is to normalize the burst activity. Altogether, these findings suggest that the regulation of burst activity of the BG output nuclei may be a good predictor for antiparkinsonian and antidyskinetic effects. They also point out the importance of using an experimental models of PD and LID when investigating the potential therapeutic effect of new drugs.

7. REFERENCES

7. REFERENCES

Aarsland, D., Marsh, L., & Schrag, A. (2009). Neuropsychiatric symptoms in Parkinson's disease. In *Movement Disorders* (Vol. 24, Issue 15, pp. 2175–2186). https://doi.org/10.1002/mds.22589

Abdi, A., Mallet, N., Mohamed, F. Y., Sharott, A., Dodson, P. D., Nakamura, K. C., Suri, S., Avery, S. V., Larvin, J. T., Garas, F. N., Garas, S. N., Vinciati, F., Morin, S., Bezard, E., Baufreton, J., & Magill, P. J. (2015). Prototypic and arkypallidal neurons in the dopamine-intact external globus pallidus. *Journal of Neuroscience*, *35*(17), 6667–6688. https://doi.org/10.1523/JNEUROSCI.4662-14.2015

Acosta-García, J., Hernández-Chan, N., Paz-Bermúdez, F., Sierra, A., Erlij, D., Aceves, J., & Florán, B. (2009). D4 and D1 dopamine receptors modulate [3H]GABA release in the substantia nigra pars reticulata of the rat. *Neuropharmacology*, *57*(7–8), 725–730. https://doi.org/10.1016/j.neuropharm.2009.08.010

Ahlskog, J. E., & Muenter, M. D. (2001). Frequency of levodopa-related dyskinesias and motor fluctuations as estimated from the cumulative literature. *Movement Disorders : Official Journal of the Movement Disorder Society*, *16*(3), 448–458. http://www.ncbi.nlm.nih.gov/pubmed/11391738

Ahmadi, S. A., Sabahi, M., & Haddadi, R. (2019). The effect of acute and repeated administration of buspirone, 8-OHDPAT and fluoxetine on haloperidol-induced extrapyramidal symptoms. *Neuropsychopharmacologia Hungarica : A Magyar Pszichofarmakologiai Egyesulet Lapja = Official Journal of the Hungarian Association of Psychopharmacology*, *21*(2), 59–68. http://www.ncbi.nlm.nih.gov/pubmed/31378723

Albin, R L, Makowiec, R. L., Hollingsworth, Z. R., Dure, L. S., Penney, J. B., & Young, A. B. (1992). Excitatory amino acid binding sites in the basal ganglia of the rat: a quantitative autoradiographic study. *Neuroscience*, *46*(1), 35–48. https://doi.org/10.1016/0306-4522(92)90006-n

Albin, Roger L., Koeppe, R. A., Bohnen, N. I., Wernette, K., Kilbourn, M. A., & Frey, K. A. (2008). Spared caudal brainstem SERT binding in early Parkinson's disease. *Journal of Cerebral Blood Flow and Metabolism*, *28*(3), 441–444. https://doi.org/10.1038/sj.jcbfm.9600599

Alex, K. D., & Pehek, E. A. (2007). Pharmacologic mechanisms of serotonergic regulation of dopamine neurotransmission. *Pharmacology & Therapeutics*, *113*(2), 296–320. https://doi.org/10.1016/j.pharmthera.2006.08.004

Alexander, G. E., DeLong, M. R., & Strick, P. L. (1986). Parallel Organization of Functionally Segregated Circuits Linking Basal Ganglia and Cortex. *Annual Review of Neuroscience*, *9*(1), 357–381. https://doi.org/10.1146/annurev.ne.09.030186.002041

Alexander, S. P. H., Christopoulos, A., Davenport, A. P., Kelly, E., Marrion, N. V., Peters, J. A., Faccenda, E., Harding, S. D., Pawson, A. J., Sharman, J. L., Southan, C., & Davies, J. A. (2017). THE CONCISE GUIDE TO PHARMACOLOGY 2017/18: G protein-coupled receptors. *British Journal of Pharmacology*, *174*, S17–S129. https://doi.org/10.1111/bph.13878

Aliane, V., Pérez, S., Nieoullon, A., Deniau, J.-M., & Kemel, M.-L. (2009). Cocaine-

induced stereotypy is linked to an imbalance between the medial prefrontal and sensorimotor circuits of the basal ganglia. *The European Journal of Neuroscience*, *30*(7), 1269–1279. https://doi.org/10.1111/j.1460-9568.2009.06907.x

Alonso-Frech, F., Zamarbide, I., Alegre, M., Rodríguez-Oroz, M. C., Guridi, J., Manrique, M., Valencia, M., Artieda, J., & Obeso, J. A. (2006). Slow oscillatory activity and levodopa-induced dyskinesias in Parkinson's disease. *Brain*, *129*(7), 1748–1757. https://doi.org/10.1093/brain/awl103

Amadio, S., Montilli, C., Picconi, B., Calabresi, P., & Volonté, C. (2007). Mapping P2X and P2Y receptor proteins in striatum and substantia nigra: An immunohistological study. *Purinergic Signalling*, *3*(4), 389–398. https://doi.org/10.1007/s11302-007-9069-8

Andersson, M., Hilbertson, A., & Cenci, M. A. (1999). Striatal fosB expression is causally linked with L-DOPA-induced abnormal involuntary movements and the associated upregulation of striatal prodynorphin mRNA in a rat model of Parkinson's disease. *Neurobiology of Disease*, *6*(6), 461–474. https://doi.org/10.1006/nbdi.1999.0259

Antonazzo, M., Gutierrez-Ceballos, A., Bustinza, I., Ugedo, L., & Morera-Herreras, T. (2019). Cannabinoids differentially modulate cortical information transmission through the sensorimotor or medial prefrontal basal ganglia circuits. *British Journal of Pharmacology*, *176*(8), 1156–1169. https://doi.org/10.1111/bph.14613

Antonini, A., & Nitu, B. (2018). Apomorphine and levodopa infusion for motor fluctuations and dyskinesia in advanced Parkinson disease. *Journal of Neural Transmission (Vienna, Austria : 1996)*, *125*(8), 1131–1135. https://doi.org/10.1007/s00702-018-1906-0

Arcuri, L., Novello, S., Frassineti, M., Mercatelli, D., Pisanò, C. A., Morella, I., Fasano, S., Journigan, B. V, Meyer, M. E., Polgar, W. E., Brambilla, R., Zaveri, N. T., & Morari, M. (2018). Anti-Parkinsonian and anti-dyskinetic profiles of two novel potent and selective nociceptin/orphanin FQ receptor agonists. *British Journal of Pharmacology*, *175*(5), 782–796. https://doi.org/10.1111/bph.14123

Aristieta, A., Ruiz-Ortega, J. A., Miguelez, C., Morera-Herreras, T., & Ugedo, L. (2016). Chronic L-DOPA administration increases the firing rate but does not reverse enhanced slow frequency oscillatory activity and synchronization in substantia nigra pars reticulata neurons from 6-hydroxydopamine-lesioned rats. *Neurobiology of Disease*, *89*, 88–100. https://doi.org/10.1016/j.nbd.2016.02.003

Aristieta, A., Ruiz-Ortega, J. A., Morera-Herreras, T., Miguelez, C., & Ugedo, L. (2019). Acute L-DOPA administration reverses changes in firing pattern and low frequency oscillatory activity in the entopeduncular nucleus from long term L-DOPA treated 6-OHDA-lesioned rats. *Experimental Neurology*, *322*, 113036. https://doi.org/10.1016/j.expneurol.2019.113036

Aristieta, A., Azkona, G., Sagarduy, A., Miguelez, C., Ruiz-Ortega, J. Á., Sanchez-Pernaute, R., & Ugedo, L. (2012). The role of the subthalamic nucleus in L-DOPA induced dyskinesia in 6-hydroxydopamine lesioned rats. *PLoS ONE*, *7*(8). https://doi.org/10.1371/journal.pone.0042652

Armentero, M. T., Fancellu, R., Nappi, G., Bramanti, P., & Blandini, F. (2006). Prolonged blockade of NMDA or mGluR5 glutamate receptors reduces nigrostriatal degeneration while inducing selective metabolic changes in the basal ganglia circuitry in a rodent model of Parkinson's disease. *Neurobiology of Disease*, *22*(1),

1–9. https://doi.org/10.1016/j.nbd.2005.09.010

Aubert, I., Guigoni, C., Håkansson, K., Li, Q., Dovero, S., Barthe, N., Bioulac, B. H., Gross, C. E., Fisone, G., Bloch, B., & Bezard, E. (2005). Increased D1 dopamine receptor signaling in levodopa-induced dyskinesia. *Annals of Neurology*, *57*(1), 17–26. https://doi.org/10.1002/ana.20296

Avalos-Fuentes, A., Albarrán-Bravo, S., Loya-Lopéz, S., Cortés, H., Recillas-Morales, S., Magaña, J. J., Paz-Bermúdez, F., Rangel-Barajas, C., Aceves, J., Erlij, D., & Florán, B. (2015). Dopaminergic denervation switches dopamine D3 receptor signaling and disrupts its Ca2+ dependent modulation by CaMKII and calmodulin in striatonigral projections of the rat. *Neurobiology of Disease*, *74*, 336–346. https://doi.org/10.1016/j.nbd.2014.12.008

Avalos-Fuentes, A., Loya-López, S., Flores-Pérez, A., Recillas-Morales, S., Cortés, H., Paz-Bermúdez, F., Aceves, J., Erlij, D., & Florán, B. (2013). Presynaptic CaMKIIα modulates dopamine D3 receptor activation in striatonigral terminals of the rat brain in a Ca2+ dependent manner. *Neuropharmacology*, *71*, 273–281. https://doi.org/10.1016/j.neuropharm.2013.04.010

Azkona, G., Sagarduy, A., Aristieta, A., Vazquez, N., Zubillaga, V., Ruíz-Ortega, J. A., Pérez-Navarro, E., Ugedo, L., & Sánchez-Pernaute, R. (2014). Buspirone anti-dyskinetic effect is correlated with temporal normalization of dysregulated striatal DRD1 signalling in l-DOPA-treated rats. *Neuropharmacology*, *79*, 726–737. https://doi.org/10.1016/j.neuropharm.2013.11.024

Azmitia, E. C., & Nixon, R. (2008). Dystrophic serotonergic axons in neurodegenerative diseases. *Brain Research*, *1217*, 185–194. https://doi.org/10.1016/j.brainres.2008.03.060

Baldo, B. A., Daniel, R. A., Berridge, C. W., & Kelley, A. E. (2003). Overlapping distributions of orexin/hypocretin- and dopamine-beta-hydroxylase immunoreactive fibers in rat brain regions mediating arousal, motivation, and stress. *The Journal of Comparative Neurology*, *464*(2), 220–237. https://doi.org/10.1002/cne.10783

Ballanger, B., Klinger, H., Eche, J., Lerond, J., Vallet, A. E., Le Bars, D., Tremblay, L., Sgambato-Faure, V., Broussolle, E., & Thobois, S. (2012). Role of serotonergic 1A receptor dysfunction in depression associated with Parkinson's disease. *Movement Disorders*, *27*(1), 84–89. https://doi.org/10.1002/mds.23895

Bandyopadhyay, U., Bandhyopadhyay, U., & Cuervo, A. M. (2007). Chaperone-mediated autophagy in aging and neurodegeneration: lessons from alpha-synuclein. *Experimental Gerontology*, *42*(1–2), 120–128. https://doi.org/10.1016/j.exger.2006.05.019

Bara-Jimenez, W., Bibbiani, F., Morris, M. J., Dimitrova, T., Sherzai, A., Mouradian, M. M., & Chase, T. N. (2005). Effects of serotonin 5-HT1A agonist in advanced Parkinson's disease. *Movement Disorders : Official Journal of the Movement Disorder Society*, *20*(8), 932–936. https://doi.org/10.1002/mds.20370

Barcia, C., De Pablos, V., Bautista-Hernández, V., Sánchez-Bahillo, Á., Bernal, I., Fernández-Villalba, E., Martín, J., Bañón, R., Fernández-Barreiro, A., & Herrero, M. T. (2005). Increased plasma levels of TNF-α but not of IL1-β in MPTP-treated monkeys one year after the MPTP administration. *Parkinsonism and Related Disorders*, *11*(7), 435–439. https://doi.org/10.1016/j.parkreldis.2005.05.006

7. References

Barcia, C., Hunot, S., Guillemin, G. J., & Pitossi, F. (2011). Inflammation and parkinson's disease. In *Parkinson's Disease* (Vol. 2011, p. 729054). https://doi.org/10.4061/2011/729054

Barker, R. A., Drouin-Ouellet, J., & Parmar, M. (2015). Cell-based therapies for Parkinson disease-past insights and future potential. In *Nature Reviews Neurology* (Vol. 11, Issue 9, pp. 492–503). Nature Publishing Group. https://doi.org/10.1038/nrneurol.2015.123

Bartus, R. T., & Johnson, E. M. (2017a). Clinical tests of neurotrophic factors for human neurodegenerative diseases, part 1: Where have we been and what have we learned? In *Neurobiology of Disease* (Vol. 97, Issue Pt B, pp. 156–168). Academic Press Inc. https://doi.org/10.1016/j.nbd.2016.03.027

Bartus, R. T., & Johnson, E. M. (2017b). Clinical tests of neurotrophic factors for human neurodegenerative diseases, part 2: Where do we stand and where must we go next? In *Neurobiology of Disease* (Vol. 97, Issue Pt B, pp. 169–178). Academic Press Inc. https://doi.org/10.1016/j.nbd.2016.03.026

Belluscio, M. A., Riquelme, L. A., & Murer, M. G. (2007). Striatal dysfunction increases basal ganglia output during motor cortex activation in parkinsonian rats. *European Journal of Neuroscience*, *25*(9), 2791–2804. https://doi.org/10.1111/j.1460-9568.2007.05527.x

Benabid, A. L. (2003). Deep brain stimulation for Parkinson's disease. In *Current Opinion in Neurobiology* (Vol. 13, Issue 6, pp. 696–706). Elsevier Ltd. https://doi.org/10.1016/j.conb.2003.11.001

Benarroch, E. E. (2009). Serotonergic modulation of basal ganglia circuits: complexity and therapeutic opportunities. *Neurology*, *73*(11), 880–886. https://doi.org/10.1212/WNL.0b013e3181b784e7

Benito-Leon, J. (2018). [Epidemiology of Parkinson's disease in Spain and its contextualisation in the world]. *Revista de Neurologia*, *66*(4), 125–134. https://doi.org/10.33588/rn.6604.2017440

Bergman, H., Wichmann, T., Karmon, B., & DeLong, M. R. (1994). The primate subthalamic nucleus. II. Neuronal activity in the MPTP model of parkinsonism. *Journal of Neurophysiology*, *72*(2), 507–520. https://doi.org/10.1152/jn.1994.72.2.507

Bergström, A. L., Kallunki, P., & Fog, K. (2016). Development of Passive Immunotherapies for Synucleinopathies. In *Movement Disorders* (Vol. 31, Issue 2, pp. 203–213). John Wiley and Sons Inc. https://doi.org/10.1002/mds.26481

Betarbet, R., Sherer, T. B., MacKenzie, G., Garcia-Osuna, M., Panov, A. V., & Greenamyre, J. T. (2000). Chronic systemic pesticide exposure reproduces features of Parkinson's disease. *Nature Neuroscience*, *3*(12), 1301–1306. https://doi.org/10.1038/81834

Beurrier, C., Congar, P., Bioulac, B., & Hammond, C. (1999). Subthalamic nucleus neurons switch from single-spike activity to burst- firing mode. *Journal of Neuroscience*, *19*(2), 599–609. https://doi.org/10.1523/jneurosci.19-02-00599.1999

Beyeler, A., Kadiri, N., Navailles, S., Boujema, M. Ben, Gonon, F., Moine, C. Le, Gross, C., & De Deurwaerdère, P. (2010). Stimulation of serotonin2C receptors elicits abnormal oral movements by acting on pathways other than the sensorimotor one in

the rat basal ganglia. *Neuroscience*, *169*(1), 158–170. https://doi.org/10.1016/j.neuroscience.2010.04.061

Bézard, E., Ferry, S., Mach, U., Stark, H., Leriche, L., Boraud, T., Gross, C., & Sokoloff, P. (2003). Attenuation of levodopa-induced dyskinesia by normalizing dopamine D3 receptor function. *Nature Medicine*, *9*(6), 762–767. https://doi.org/10.1038/nm875

Bezard, E., Tronci, E., Pioli, E. Y., Li, Q., Porras, G., Björklund, A., & Carta, M. (2013). Study of the antidyskinetic effect of eltoprazine in animal models of levodopa-induced dyskinesia. *Movement Disorders : Official Journal of the Movement Disorder Society*, *28*(8), 1088–1096. https://doi.org/10.1002/mds.25366

Bianchi, L., Ballini, C., Colivicchi, M. A., Della Corte, L., Giovannini, M. G., & Pepeu, G. (2003). Investigation on acetylcholine, aspartate, glutamate and GABA extracellular levels from ventral hippocampus during repeated exploratory activity in the rat. *Neurochemical Research*, *28*(3–4), 565–573. https://doi.org/10.1023/a:1022881625378

Bido, S., Marti, M., & Morari, M. (2011). Amantadine attenuates levodopa-induced dyskinesia in mice and rats preventing the accompanying rise in nigral GABA levels. *Journal of Neurochemistry*, *118*(6), 1043–1055. https://doi.org/10.1111/j.1471-4159.2011.07376.x

Bishop, C., George, J. A., Buchta, W., Goldenberg, A. A., Mohamed, M., Dickinson, S. O., Eissa, S., & Eskow Jaunarajs, K. L. (2012). Serotonin transporter inhibition attenuates l-DOPA-induced dyskinesia without compromising l-DOPA efficacy in hemi-parkinsonian rats. *The European Journal of Neuroscience*, *36*(6), 2839–2848. https://doi.org/10.1111/j.1460-9568.2012.08202.x

Bishop, C., Krolewski, D. M., Eskow, K. L., Barnum, C. J., Dupre, K. B., Deak, T., & Walker, P. D. (2009). Contribution of the striatum to the effects of 5-HT1A receptor stimulation in L-DOPA-treated hemiparkinsonian rats. *Journal of Neuroscience Research*, *87*(7), 1645–1658. https://doi.org/10.1002/jnr.21978

Björklund, A., Björklund, T., & Kirik, D. (2009). Gene therapy for dopamine replacement in Parkinson's disease. In *Science Translational Medicine* (Vol. 1, Issue 2, p. 2ps2). American Association for the Advancement of Science. https://doi.org/10.1126/scitranslmed.3000350

Blandini, F., Levandis, G., Bazzini, E., Nappi, G., & Armentero, M. T. (2007). Time-course of nigrostriatal damage, basal ganglia metabolic changes and behavioural alterations following intrastriatal injection of 6-hydroxydopamine in the rat: New clues from an old model. *European Journal of Neuroscience*, *25*(2), 397–405. https://doi.org/10.1111/j.1460-9568.2006.05285.x

Blandini, F., Nappi, G., Tassorelli, C., & Martignoni, E. (2000). Functional changes of the basal ganglia circuitry in Parkinson's disease. In *Progress in Neurobiology* (Vol. 62, Issue 1, pp. 63–88). https://doi.org/10.1016/S0301-0082(99)00067-2

Blier, P., Lista, A., & De Montigny, C. (1993). Differential properties of pre- and postsynaptic 5-hydroxytryptamine1A receptors in the dorsal raphe and hippocampus: I. Effect of spiperone. *The Journal of Pharmacology and Experimental Therapeutics*, *265*(1), 7–15. http://www.ncbi.nlm.nih.gov/pubmed/8474032

Bloem, B. R., Hausdorff, J. M., Visser, J. E., & Giladi, N. (2004). Falls and freezing of

Gait in Parkinson's disease: A review of two interconnected, episodic phenomena. In *Movement Disorders* (Vol. 19, Issue 8, pp. 871–884). https://doi.org/10.1002/mds.20115

Bonifati, V., Fabrizio, E., Cipriani, R., Vanacore, N., & Meco, G. (1994). Buspirone in levodopa-induced dyskinesias. *Clinical Neuropharmacology*, *17*(1), 73–82. http://www.ncbi.nlm.nih.gov/pubmed/8149361

Boraud, T., Bezard, E., Guehl, D., Bioulac, B., & Gross, C. (1998). Effects of L-DOPA on neuronal activity of the globus pallidus externalis (GPe) and globus pallidus internalis (GPi) in the MPTP-treated monkey. *Brain Research*, *787*(1), 157–160. https://doi.org/10.1016/s0006-8993(97)01563-1

Borgkvist, A., Avegno, E. M., Wong, M. Y., Kheirbek, M. A., Sonders, M. S., Hen, R., & Sulzer, D. (2015). Loss of Striatonigral GABAergic Presynaptic Inhibition Enables Motor Sensitization in Parkinsonian Mice. *Neuron*, *87*(5), 976–988. https://doi.org/10.1016/j.neuron.2015.08.022

Boyes, J., & Bolam, J. P. (2007). Localization of GABA receptors in the basal ganglia. In *Progress in Brain Research* (Vol. 160, pp. 229–243). https://doi.org/10.1016/S0079-6123(06)60013-7

Braak, H, Rüb, U., Gai, W. P., & Del Tredici, K. (2003). Idiopathic Parkinson's disease: possible routes by which vulnerable neuronal types may be subject to neuroinvasion by an unknown pathogen. *Journal of Neural Transmission (Vienna, Austria : 1996)*, *110*(5), 517–536. https://doi.org/10.1007/s00702-002-0808-2

Braak, Heiko, & Del Tredici, K. (2017). Neuropathological Staging of Brain Pathology in Sporadic Parkinson's disease: Separating the Wheat from the Chaff. In *Journal of Parkinson's Disease* (Vol. 7, Issue s1, pp. S73–S87). IOS Press. https://doi.org/10.3233/JPD-179001

Brahic, M., Bousset, L., Bieri, G., Melki, R., & Gitler, A. D. (2016). Axonal transport and secretion of fibrillar forms of α-synuclein, Aβ42 peptide and HTTExon 1. *Acta Neuropathologica*, *131*(4), 539–548. https://doi.org/10.1007/s00401-016-1538-0

Brooks, D. J. (1998). The early diagnosis of parkinson's disease. *Annals of Neurology*, *44*(S1), S10–S18. https://doi.org/10.1002/ana.410440704

Brown, J., Pan, W. X., & Dudman, J. T. (2014). The inhibitory microcircuit of the substantia nigra provides feedback gain control of the basal ganglia output. *ELife*, *2014*(3). https://doi.org/10.7554/eLife.02397

Brown, P. (2006a). Bad oscillations in Parkinson's disease. In *Parkinson's Disease and Related Disorders* (pp. 27–30). Springer Vienna. https://doi.org/10.1007/978-3-211-45295-0_6

Brown, P. (2006b). Bad oscillations in Parkinson's disease. *Journal of Neural Transmission, Supplement*, *70*, 27–30. https://doi.org/10.1007/978-3-211-45295-0_6

Brundin, P., & Melki, R. (2017). Prying into the prion hypothesis for parkinson's disease. *Journal of Neuroscience*, *37*(41), 9808–9818. https://doi.org/10.1523/JNEUROSCI.1788-16.2017

Brys, I., Halje, P., Scheffer-Teixeira, R., Varney, M., Newman-Tancredi, A., & Petersson, P. (2018). Neurophysiological effects in cortico-basal ganglia-thalamic circuits of antidyskinetic treatment with 5-HT 1A receptor biased agonists. *Experimental*

Neurology, *302*, 155–168. https://doi.org/10.1016/j.expneurol.2018.01.010

Burke, R. E., & Kholodilov, N. G. (1998). Programmed cell death: does it play a role in Parkinson's disease? *Annals of Neurology*, *44*(3 Suppl 1), S126-33. https://doi.org/10.1002/ana.410440719

Buzsáki, G., & Chrobak, J. J. (1995). Temporal structure in spatially organized neuronal ensembles: a role for interneuronal networks. *Current Opinion in Neurobiology*, *5*(4), 504–510. https://doi.org/10.1016/0959-4388(95)80012-3

Carlsson, A., Lindqvist, M., Magnusson, T., & Waldeck, B. (1958). On the presence of 3-hydroxytyramine in brain. *Science*, *127*(3296), 471. https://doi.org/10.1126/science.127.3296.471

Carlsson, T., Winkler, C., Burger, C., Muzyczka, N., Mandel, R. J., Cenci, A., Björklund, A., & Kirik, D. (2005). Reversal of dyskinesias in an animal model of Parkinson's disease by continuous L-DOPA delivery using rAAV vectors. *Brain*, *128*(3), 559–569. https://doi.org/10.1093/brain/awh374

Carta, M., Carlsson, T., Kirik, D., & Bjorklund, A. (2007). Dopamine released from 5-HT terminals is the cause of L-DOPA-induced dyskinesia in parkinsonian rats. *Brain*, *130*(7), 1819–1833. https://doi.org/10.1093/brain/awm082

Carta, M., Carlsson, T., Muñoz, A., Kirik, D., & Björklund, A. (2008). Serotonin-dopamine interaction in the induction and maintenance of L-DOPA-induced dyskinesias. In *Progress in Brain Research* (Vol. 172, pp. 465–478). https://doi.org/10.1016/S0079-6123(08)00922-9

Carter, D. A., & Fibiger, H. C. (1978). The projections of the entopeduncular nucleus and globus pallidus in rat as demonstrated by autoradiography and horseradish peroxidase histochemistry. *The Journal of Comparative Neurology*, *177*(1), 113–123. https://doi.org/10.1002/cne.901770108

Cebrián, C., Parent, A., & Prensa, L. (2005). Patterns of axonal branching of neurons of the substantia nigra pars reticulata and pars lateralis in the rat. *Journal of Comparative Neurology*, *492*(3), 349–369. https://doi.org/10.1002/cne.20741

Celada, P., Victoria Puig, M., Casanovas, J. M., Guillazo, G., & Artigas, F. (2001). Control of dorsal raphe serotonergic neurons by the medial prefrontal cortex: Involvement of serotonin-1A, GABAA, and glutamate receptors. *Journal of Neuroscience*, *21*(24), 9917–9929. https://doi.org/10.1523/jneurosci.21-24-09917.2001

Cenci, M. A., Lee, C. S., & Björklund, A. (1998). L-DOPA-induced dyskinesia in the rat is associated with striatal overexpression of prodynorphin- and glutamic acid decarboxylase mRNA. *European Journal of Neuroscience*, *10*(8), 2694–2706. https://doi.org/10.1046/j.1460-9568.1998.00285.x

Cenci, M. A., & Lundblad, M. (2007). Ratings of L -DOPA-Induced Dyskinesia in the Unilateral 6-OHDA Lesion Model of Parkinson's Disease in Rats and Mice . In *Current Protocols in Neuroscience*. John Wiley & Sons, Inc. https://doi.org/10.1002/0471142301.ns0925s41

Charcot, J.-M. (1825-1893). A. du texte. (1875). *Leçons sur les maladies du système nerveux : faites à la Salpêtrière. Tome 2 / par J.-M. Charcot,... ; recueillies et publ. par Bourneville,...*

Chatha, B. T., Bernard, V., Streit, P., & Bolam, J. P. (2000). Synaptic localization of

ionotropic glutamate receptors in the rat substantia nigra. *Neuroscience*, *101*(4), 1037–1051. https://doi.org/10.1016/S0306-4522(00)00432-2

Chergui, K., Nomikos, G. G., Mathé, J. M., Gonon, F., & Svensson, T. H. (1996). Burst stimulation of the medial forebrain bundle selectively increases Fos-like immunoreactivity in the limbic forebrain of the rat. *Neuroscience*, *72*(1), 141–156. https://doi.org/10.1016/0306-4522(95)00513-7

Chetrit, J., Taupignon, A., Froux, L., Morin, S., Bouali-Benazzouz, R., Naudet, F., Kadiri, N., Gross, C. E., Bioulac, B., & Benazzouz, A. (2013). Inhibiting subthalamic d5 receptor constitutive activity alleviates abnormal electrical activity and reverses motor impairment in a rat model of parkinson's disease. *Journal of Neuroscience*, *33*(37), 14840–14849. https://doi.org/10.1523/JNEUROSCI.0453-13.2013

Chiken, S., Sato, A., Ohta, C., Kurokawa, M., Arai, S., Maeshima, J., Sunayama-Morita, T., Sasaoka, T., & Nambu, A. (2015). Dopamine D1 Receptor-Mediated Transmission Maintains Information Flow Through the Cortico-Striato-Entopeduncular Direct Pathway to Release Movements. *Cerebral Cortex (New York, N.Y. : 1991)*, *25*(12), 4885–4897. https://doi.org/10.1093/cercor/bhv209

Chiken, S., Shashidharan, P., & Nambu, A. (2008). Cortically evoked long-lasting inhibition of pallidal neurons in a transgenic mouse model of dystonia. *The Journal of Neuroscience : The Official Journal of the Society for Neuroscience*, *28*(51), 13967–13977. https://doi.org/10.1523/JNEUROSCI.3834-08.2008

Chinaglia, G., Landwehrmeyer, B., Probst, A., & Palacios, J. M. (1993). Serotoninergic terminal transporters are differentially affected in Parkinson's disease and progressive supranuclear palsy: An autoradiographic study with [3H]citalopram. *Neuroscience*, *54*(3), 691–699. https://doi.org/10.1016/0306-4522(93)90240-G

Clarke, N. P., & Bolam, J. P. (1998). Distribution of glutamate receptor subunits at neurochemically characterized synapses in the entopeduncular nucleus and subthalamic nucleus of the rat. *Journal of Comparative Neurology*, *397*(3), 403–420. https://doi.org/10.1002/(SICI)1096-9861(19980803)397:3<403::AID-CNE7>3.0.CO;2-6

Cleary, D. R., Raslan, A. M., Rubin, J. E., Bahgat, D., Viswanathan, A., Heinricher, M. M., & Burchiel, K. J. (2013). Deep brain stimulation entrains local neuronal firing in human globus pallidus internus. *Journal of Neurophysiology*, *109*(4), 978–987. https://doi.org/10.1152/jn.00420.2012

Clement, E. A., Richard, A., Thwaites, M., Ailon, J., Peters, S., & Dickson, C. T. (2008). Cyclic and sleep-like spontaneous alternations of brain state under urethane anaesthesia. *PloS One*, *3*(4), e2004. https://doi.org/10.1371/journal.pone.0002004

Coffey, R. J. (2009). Deep brain stimulation devices: A brief technical history and review. In *Artificial Organs* (Vol. 33, Issue 3, pp. 208–220). Artif Organs. https://doi.org/10.1111/j.1525-1594.2008.00620.x

Conti, M. M., Ostock, C. Y., Lindenbach, D., Goldenberg, A. A., Kampton, E., Dell'Isola, R., Katzman, A. C., & Bishop, C. (2014). Effects of prolonged selective serotonin reuptake inhibition on the development and expression of l-DOPA-induced dyskinesia in hemi-parkinsonian rats. *Neuropharmacology*, *77*, 1–8. https://doi.org/10.1016/j.neuropharm.2013.09.017

Cooper, J. R., & Melcer, I. (1961). The enzymic oxidation of tryptophan to 5-

hydroxytryptophan in the biosynthesis of serotonin. *The Journal of Pharmacology and Experimental Therapeutics*, *132*, 265–268. http://www.ncbi.nlm.nih.gov/pubmed/13695323

Corvaja, N., Doucet, G., & Bolam, J. P. (1993). Ultrastructure and synaptic targets of the raphe-nigral projection in the rat. *Neuroscience*, *55*(2), 417–427. https://doi.org/10.1016/0306-4522(93)90510-m

Cotzias, G. C. (1968). L-Dopa for Parkinsonism. *The New England Journal of Medicine*, *278*(11), 630. https://doi.org/10.1056/NEJM196803142781127

Cotzias, G. C., Papavasiliou, P. S., & Gellene, R. (1969). Modification of Parkinsonism--chronic treatment with L-dopa. *The New England Journal of Medicine*, *280*(7), 337–345. https://doi.org/10.1056/NEJM196902132800701

Coupland, K. G., Mellick, G. D., Silburn, P. A., Mather, K., Armstrong, N. J., Sachdev, P. S., Brodaty, H., Huang, Y., Halliday, G. M., Hallupp, M., Kim, W. S., Dobson-Stone, C., & Kwok, J. B. J. (2014). DNA methylation of the MAPT gene in Parkinson's disease cohorts and modulation by vitamin E in vitro. *Movement Disorders : Official Journal of the Movement Disorder Society*, *29*(13), 1606–1614. https://doi.org/10.1002/mds.25784

Cowen, P. J., Power, A. C., Ware, C. J., & Anderson, I. M. (1994). 5-HT1A receptor sensitivity in major depression. A neuroendocrine study with buspirone. *The British Journal of Psychiatry : The Journal of Mental Science*, *164*(3), 372–379. https://doi.org/10.1192/bjp.164.3.372

Crane, J. W., Shimizu, K., Carrasco, G. A., Garcia, F., Jia, C., Sullivan, N. R., D'Souza, D. N., Zhang, Y., Van de Kar, L. D., Muma, N. A., & Battaglia, G. (2007). 5-HT1A receptors mediate (+)8-OH-DPAT-stimulation of extracellular signal-regulated kinase (MAP kinase) in vivo in rat hypothalamus: Time dependence and regional differences. *Brain Research*, *1183*(1), 51–59. https://doi.org/10.1016/j.brainres.2007.07.101

Crittenden, J. R., & Graybiel, A. M. (2011). Basal ganglia disorders associated with imbalances in the striatal striosome and matrix compartments. In *Frontiers in Neuroanatomy* (Vol. 5, Issue SEP, p. 59). https://doi.org/10.3389/fnana.2011.00059

Cuervo, A. M., & Wong, E. (2014). Chaperone-mediated autophagy: roles in disease and aging. *Cell Research*, *24*(1), 92–104. https://doi.org/10.1038/cr.2013.153

Darbin, O., Jin, X., Von Wrangel, C., Schwabe, K., Nambu, A., Naritoku, D. K., Krauss, J. K., & Alam, M. (2016). Neuronal Entropy-Rate Feature of Entopeduncular Nucleus in Rat Model of Parkinson's Disease. *International Journal of Neural Systems*, *26*(2), 1550038. https://doi.org/10.1142/S0129065715500380

De Deurwaerdère, P., Di Giovanni, G., & Millan, M. J. (2017). Expanding the repertoire of L-DOPA's actions: A comprehensive review of its functional neurochemistry. In *Progress in Neurobiology* (Vol. 151, pp. 57–100). Elsevier Ltd. https://doi.org/10.1016/j.pneurobio.2016.07.002

De Lange, E. C. M., Danhof, M., De Boer, A. G., & Breimer, D. D. (1997). Methodological considerations of intracerebral microdialysis in pharmacokinetic studies on drug transport across the blood-brain barrier. In *Brain Research Reviews* (Vol. 25, Issue 1, pp. 27–49). Brain Res Brain Res Rev. https://doi.org/10.1016/S0165-0173(97)00014-3

7. References

Deczkowska, A., Keren-Shaul, H., Weiner, A., Colonna, M., Schwartz, M., & Amit, I. (2018). Disease-Associated Microglia: A Universal Immune Sensor of Neurodegeneration. In *Cell* (Vol. 173, Issue 5, pp. 1073–1081). Cell Press. https://doi.org/10.1016/j.cell.2018.05.003

Degos, B., Deniau, J.-M., Thierry, A.-M., Glowinski, J., Pezard, L., & Maurice, N. (2005). Neuroleptic-induced catalepsy: electrophysiological mechanisms of functional recovery induced by high-frequency stimulation of the subthalamic nucleus. *The Journal of Neuroscience : The Official Journal of the Society for Neuroscience*, *25*(33), 7687–7696. https://doi.org/10.1523/JNEUROSCI.1056-05.2005

Dehay, B., Bové, J., Rodríguez-Muela, N., Perier, C., Recasens, A., Boya, P., & Vila, M. (2010). Pathogenic lysosomal depletion in Parkinson's disease. *Journal of Neuroscience*, *30*(37), 12535–12544. https://doi.org/10.1523/JNEUROSCI.1920-10.2010

Dekundy, A., Lundblad, M., Danysz, W., & Cenci, M. A. (2007). Modulation of l-DOPA-induced abnormal involuntary movements by clinically tested compounds: Further validation of the rat dyskinesia model. *Behavioural Brain Research*, *179*(1), 76–89. https://doi.org/10.1016/j.bbr.2007.01.013

Del Rey, N. L. G., Quiroga-Varela, A., Garbayo, E., Carballo-Carbajal, I., Fernández-Santiago, R., Monje, M. H. G., Trigo-Damas, I., Blanco-Prieto, M. J., & Blesa, J. (2018). Advances in parkinson's disease: 200 years later. In *Frontiers in Neuroanatomy* (Vol. 12, p. 113). Frontiers Media S.A. https://doi.org/10.3389/fnana.2018.00113

DeLong, M. R. (1990). Primate models of movement disorders of basal ganglia origin. In *Trends in Neurosciences* (Vol. 13, Issue 7, pp. 281–285). https://doi.org/10.1016/0166-2236(90)90110-V

DeLong, M. R., & Wichmann, T. (2007). Circuits and circuit disorders of the basal ganglia. In *Archives of Neurology* (Vol. 64, Issue 1, pp. 20–24). https://doi.org/10.1001/archneur.64.1.20

Deniau, J. M., Mailly, P., Maurice, N., & Charpier, S. (2007). The pars reticulata of the substantia nigra: a window to basal ganglia output. In *Progress in Brain Research* (Vol. 160, pp. 151–172). https://doi.org/10.1016/S0079-6123(06)60009-5

Deniau, J. M., Menetrey, A., & Charpier, S. (1996). The lamellar organization of the rat substantia nigra pars reticulata: Segregated patterns of striatal afferents and relationship to the topography of corticostriatal projections. *Neuroscience*, *73*(3), 761–781. https://doi.org/10.1016/0306-4522(96)00088-7

Deniau, J. M., Menetrey, A., & Thierry, A. M. (1994). Indirect nucleus accumbens input to the prefrontal cortex via the substantia nigra pars reticulata: A combined anatomical and electrophysiological study in the rat. *Neuroscience*, *61*(3), 533–545. https://doi.org/10.1016/0306-4522(94)90432-4

Deumens, R., Blokland, A., & Prickaerts, J. (2002). Modeling Parkinson's disease in rats: an evaluation of 6-OHDA lesions of the nigrostriatal pathway. *Experimental Neurology*, *175*(2), 303–317. https://doi.org/10.1006/exnr.2002.7891

Di Matteo, V., Pierucci, M., Esposito, E., Crescimanno, G., Benigno, A., & Di Giovanni, G. (2008). Serotonin modulation of the basal ganglia circuitry: therapeutic

implication for Parkinson's disease and other motor disorders. In *Progress in Brain Research* (Vol. 172, pp. 423–463). https://doi.org/10.1016/S0079-6123(08)00921-7

Díaz-Mataix, L., Scorza, M. C., Bortolozzi, A., Toth, M., Celada, P., & Artigas, F. (2005). Involvement of 5-HT1A receptors in prefrontal cortex in the modulation of dopaminergic activity: Role in atypical antipsychotic action. *Journal of Neuroscience*, *25*(47), 10831–10843. https://doi.org/10.1523/JNEUROSCI.2999-05.2005

Doder, M., Rabiner, E. A., Turjanski, N., Lees, A. J., & Brooks, D. J. (2003). Tremor in Parkinson's disease and serotonergic dysfunction: An 11C-WAY 100635 PET study. *Neurology*, *60*(4), 601–605. https://doi.org/10.1212/01.WNL.0000031424.51127.2B

Dorszewska, J., Prendecki, M., Oczkowska, A., Rozycka, A., Lianeri, M., & Kozubski, W. (2014). Polymorphism of the COMT, MAO, DAT, NET and 5-HTT Genes, and Biogenic Amines in Parkinson's Disease. *Current Genomics*, *14*(8), 518–533. https://doi.org/10.2174/1389202914666131210210241

Doshi, P. K. (2011). Long-term surgical and hardware-related complications of deep brain stimulation. *Stereotactic and Functional Neurosurgery*, *89*(2), 89–95. https://doi.org/10.1159/000323372

Dostrovsky, J., & Bergman, H. (2004). Oscillatory activity in the basal ganglia-relationship to normal physiology and pathophysiology. In *Brain* (Vol. 127, Issue 4, pp. 721–722). Oxford University Press. https://doi.org/10.1093/brain/awh164

Doucet, J. P., Nakabeppu, Y., Bedard, P. J., Hope, B. T., Nestler, E. J., Jasmin, B. J., Chen, J. S., Ladarola, M. J., St-Jean, M., Wigle, N., Blanchet, P., Grondin, R., & Robertson, G. S. (1996). Chronic alterations in dopaminergic neurotransmission produce a persistent elevation of AFosB-like protein(s) in both the rodent and primate striatum. *European Journal of Neuroscience*, *8*(2), 365–381. https://doi.org/10.1111/j.1460-9568.1996.tb01220.x

Dudman, J. T., & Gerfen, C. R. (2015). The Basal Ganglia. In *The Rat Nervous System: Fourth Edition* (pp. 391–440). Elsevier Inc. https://doi.org/10.1016/B978-0-12-374245-2.00017-6

Dupre, K. B., Cruz, A. V, McCoy, A. J., Delaville, C., Gerber, C. M., Eyring, K. W., & Walters, J. R. (2016). Effects of L-dopa priming on cortical high beta and high gamma oscillatory activity in a rodent model of Parkinson's disease. *Neurobiology of Disease*, *86*, 1–15. https://doi.org/10.1016/j.nbd.2015.11.009

Dupre, K. B., Eskow, K. L., Barnum, C. J., & Bishop, C. (2008). Striatal 5-HT1A receptor stimulation reduces D1 receptor-induced dyskinesia and improves movement in the hemiparkinsonian rat. *Neuropharmacology*, *55*(8), 1321–1328. https://doi.org/10.1016/j.neuropharm.2008.08.031

Dupre, K. B., Eskow, K. L., Negron, G., & Bishop, C. (2007). The differential effects of 5-HT1A receptor stimulation on dopamine receptor-mediated abnormal involuntary movements and rotations in the primed hemiparkinsonian rat. *Brain Research*, *1158*, 135–143. https://doi.org/10.1016/j.brainres.2007.05.005

Dupre, K. B., Ostock, C. Y., Eskow Jaunarajs, K. L., Button, T., Savage, L. M., Wolf, W., & Bishop, C. (2011). Local modulation of striatal glutamate efflux by serotonin 1A receptor stimulation in dyskinetic, hemiparkinsonian rats. *Experimental*

Neurology, 229(2), 288–299. https://doi.org/10.1016/j.expneurol.2011.02.012

Durif, F., Debilly, B., Galitzky, M., Morand, D., Viallet, F., Borg, M., Thobois, S., Broussolle, E., & Rascol, O. (2004). Clozapine improves dyskinesias in Parkinson disease A double-blind, placebo-controlled study. *Neurology*, 62(3), 381–388. https://doi.org/10.1212/01.WNL.0000110317.52453.6C

Durif, F., Vidailhet, M., Bonnet, A. M., Blin, J., & Agid, Y. (1995). Levodopa-induced dyskinesias are improved by fluoxetine. *Neurology*, 45(10), 1855–1858. https://doi.org/10.1212/WNL.45.10.1855

Dzamko, N., Geczy, C. L., & Halliday, G. M. (2015). Inflammation is genetically implicated in Parkinson's disease. In *Neuroscience* (Vol. 302, pp. 89–102). Elsevier Ltd. https://doi.org/10.1016/j.neuroscience.2014.10.028

Ehringer, H., & Hornykiewicz, O. (1960). [Distribution of noradrenaline and dopamine (3-hydroxytyramine) in the human brain and their behavior in diseases of the extrapyramidal system]. *Klinische Wochenschrift*, 38, 1236–1239. https://doi.org/10.1007/bf01485901

Eskow, K. L., Gupta, V., Alam, S., Park, J. Y., & Bishop, C. (2007). The partial 5-HT1A agonist buspirone reduces the expression and development of l-DOPA-induced dyskinesia in rats and improves l-DOPA efficacy. *Pharmacology Biochemistry and Behavior*, 87(3), 306–314. https://doi.org/10.1016/J.PBB.2007.05.002

Espay, A. J., Morgante, F., Merola, A., Fasano, A., Marsili, L., Fox, S. H., Bezard, E., Picconi, B., Calabresi, P., & Lang, A. E. (2018). Levodopa-induced dyskinesia in Parkinson disease: Current and evolving concepts. In *Annals of Neurology* (Vol. 84, Issue 6, pp. 797–811). John Wiley and Sons Inc. https://doi.org/10.1002/ana.25364

Fan, S. Y., Wang, K. L., Hu, W., Eisinger, R. S., Han, A., Han, C. L., Wang, Q., Michitomo, S., Zhang, J. G., Wang, F., Ramirez-Zamora, A., & Meng, F. G. (2020). Pallidal versus subthalamic nucleus deep brain stimulation for levodopa-induced dyskinesia. *Annals of Clinical and Translational Neurology*, 7(1), 59–68. https://doi.org/10.1002/acn3.50961

Fearnley, J. M., & Lees, A. J. (1991). Ageing and parkinson's disease: Substantia nigra regional selectivity. *Brain*, 114(5), 2283–2301. https://doi.org/10.1093/brain/114.5.2283

Fénelon, G., & Alves, G. (2010). Epidemiology of psychosis in Parkinson's disease. *Journal of the Neurological Sciences*, 289(1–2), 12–17. https://doi.org/10.1016/j.jns.2009.08.014

Fernández-Santiago, R., Carballo-Carbajal, I., Castellano, G., Torrent, R., Richaud, Y., Sánchez-Danés, A., Vilarrasa-Blasi, R., Sánchez-Pla, A., Mosquera, J. L., Soriano, J., López-Barneo, J., Canals, J. M., Alberch, J., Raya, Á., Vila, M., Consiglio, A., Martín-Subero, J. I., Ezquerra, M., & Tolosa, E. (2015). Aberrant epigenome in iPSC-derived dopaminergic neurons from Parkinson's disease patients . *EMBO Molecular Medicine*, 7(12), 1529–1546. https://doi.org/10.15252/emmm.201505439

Ferrer, I., Perez, E., Dalfó, E., & Barrachina, M. (2007). Abnormal levels of prohibitin and ATP synthase in the substantia nigra and frontal cortex in Parkinson's disease. *Neuroscience Letters*, 415(3), 205–209. https://doi.org/10.1016/j.neulet.2007.01.026

Fidalgo, C., Ko, W. K. D., Tronci, E., Li, Q., Stancampiano, R., Chuan, Q., Bezard, E., & Carta, M. (2015). Effect of serotonin transporter blockade on L-DOPA-induced dyskinesia in animal models of Parkinson's disease. *Neuroscience*, *298*, 389–396. https://doi.org/10.1016/j.neuroscience.2015.04.027

Fields, C. R., Bengoa-Vergniory, N., & Wade-Martins, R. (2019). Targeting Alpha-Synuclein as a Therapy for Parkinson's Disease. In *Frontiers in Molecular Neuroscience* (Vol. 12). Frontiers Media S.A. https://doi.org/10.3389/fnmol.2019.00299

File, S. E., & Andrews, N. (1991). Low but not high doses of buspirone reduce the anxiogenic effects of diazepam withdrawal. *Psychopharmacology*, *105*(4), 578–582. https://doi.org/10.1007/BF02244384

Filion, M., & Tremblay, L. (1991). Abnormal spontaneous activity of globus pallidus neurons in monkeys with MPTP-induced parkinsonism. *Brain Research*, *547*(1), 140–144. https://doi.org/10.1016/0006-8993(91)90585-J

Fisher, R., Hikima, A., Morris, R., Jackson, M. J., Rose, S., Varney, M. A., Depoortere, R., & Newman-Tancredi, A. (2020). The selective 5-HT1A receptor agonist, NLX-112, exerts anti-dyskinetic and anti-parkinsonian-like effects in MPTP-treated marmosets. *Neuropharmacology*, *167*, 107997. https://doi.org/10.1016/j.neuropharm.2020.107997

Fitoussi, A., Dellu-Hagedorn, F., & De Deurwaerdère, P. (2013). Monoamines tissue content analysis reveals restricted and site-specific correlations in brain regions involved in cognition. *Neuroscience*, *255*, 233–245. https://doi.org/10.1016/j.neuroscience.2013.09.059

Forsaa, E. B., Larsen, J. P., Wentzel-Larsen, T., Goetz, C. G., Stebbins, G. T., Aarsland, D., & Alves, G. (2010). A 12-year population-based study of psychosis in Parkinson disease. *Archives of Neurology*, *67*(8), 996–1001. https://doi.org/10.1001/archneurol.2010.166

Fox, S. H. (2013). Non-dopaminergic Treatments for Motor Control in Parkinson's Disease. *Drugs*, *73*(13), 1405–1415. https://doi.org/10.1007/s40265-013-0105-4

Frechilla, D., Cobreros, A., Saldise, L., Moratalla, R., Insausti, R., Luquin, M. R., & Del Ro, J. (2001). Serotonin 5-HT1A receptor expression is selectively enhanced in the striosomal compartment of chronic Parkinsonian monkeys. *Synapse*, *39*(4), 288–296. https://doi.org/10.1002/1098-2396(20010315)39:4<288::AID-SYN1011>3.0.CO;2-V

Freed, C. R., Greene, P. E., Breeze, R. E., Tsai, W. Y., DuMouchel, W., Kao, R., Dillon, S., Winfield, H., Culver, S., Trojanowski, J. Q., Eidelberg, D., & Fahn, S. (2001). Transplantation of embryonic dopamine neurons for severe Parkinson's disease. *New England Journal of Medicine*, *344*(10), 710–719. https://doi.org/10.1056/NEJM200103083441002

Freed, J., & Chakrabarti, L. (2016). Defining a role for hemoglobin in Parkinson's disease. *Npj Parkinson's Disease*, *2*(1), 16021. https://doi.org/10.1038/npjparkd.2016.21

Freeze, B. S., Kravitz, A. V., Hammack, N., Berke, J. D., & Kreitzer, A. C. (2013). Control of basal ganglia output by direct and indirect pathway projection neurons. *Journal of Neuroscience*, *33*(47), 18531–18539.

https://doi.org/10.1523/JNEUROSCI.1278-13.2013

Frouni, I., Kwan, C., Bédard, D., Belliveau, S., Bourgeois-Cayer, É., Gaudette, F., Beaudry, F., Hamadjida, A., & Huot, P. (2018). Effect of the selective 5-HT2A receptor antagonist EMD-281,014 on l-DOPA-induced abnormal involuntary movements in the 6-OHDA-lesioned rat. *Experimental Brain Research*. https://doi.org/10.1007/s00221-018-5390-4

Gagnon, D, Gregoire, L., Di Paolo, T., & Parent, M. (2016). Serotonin hyperinnervation of the striatum with high synaptic incidence in parkinsonian monkeys. *Brain Structure & Function*, *221*(7), 3675–3691. https://doi.org/10.1007/s00429-015-1125-5

Gagnon, D., Eid, L., Coudé, D., Whissel, C., Paolo, T. Di, Parent, A., & Parent, M. (2018). Evidence for sprouting of dopamine and serotonin axons in the pallidum of parkinsonian monkeys. *Frontiers in Neuroanatomy*, *12*, 38. https://doi.org/10.3389/fnana.2018.00038

Galati, S., D'Angelo, V., Olivola, E., Marzetti, F., Di Giovanni, G., Stanzione, P., & Stefani, A. (2010). Acute inactivation of the medial forebrain bundle imposes oscillations in the SNr: A challenge for the 6-OHDA model? *Experimental Neurology*, *225*(2), 294–301. https://doi.org/10.1016/j.expneurol.2010.06.020

Galati, S., Stanzione, P., D'Angelo, V., Fedele, E., Marzetti, F., Sancesario, G., Procopio, T., & Stefani, A. (2009). The pharmacological blockade of medial forebrain bundle induces an acute pathological synchronization of the cortico-subthalamic nucleus-globus pallidus pathway. *The Journal of Physiology*, *587*(18), 4405–4423. https://doi.org/10.1113/jphysiol.2009.172759

Galbiati, A., Verga, L., Giora, E., Zucconi, M., & Ferini-Strambi, L. (2019). The risk of neurodegeneration in REM sleep behavior disorder: A systematic review and meta-analysis of longitudinal studies. In *Sleep Medicine Reviews* (Vol. 43, pp. 37–46). W.B. Saunders Ltd. https://doi.org/10.1016/j.smrv.2018.09.008

Gale, J. T., Shields, D. C., Jain, F. A., Amirnovin, R., & Eskandar, E. N. (2009). Subthalamic nucleus discharge patterns during movement in the normal monkey and Parkinsonian patient. *Brain Research*, *1260*, 15–23. https://doi.org/10.1016/j.brainres.2008.12.062

García-Ramos, R., López Valdés, E., Ballesteros, L., Jesús, S., & Mir, P. (2016). The social impact of Parkinson's disease in Spain: Report by the Spanish Foundation for the Brain. In *Neurologia* (Vol. 31, Issue 6, pp. 401–413). Spanish Society of Neurology. https://doi.org/10.1016/j.nrl.2013.04.008

Gasser, T. (2003). Overview of the genetics of parkinsonism. *Advances in Neurology*, *91*, 143–152. http://www.ncbi.nlm.nih.gov/pubmed/12442673

Gerfen, C. R. (1984). The neostriatal mosaic: Compartmentalization of corticostriatal input and striatonigral output systems. *Nature*, *311*(5985), 461–464. https://doi.org/10.1038/311461a0

Gerfen, C. R., Engber, T. M., Mahan, L. C., Susel, Z., Chase, T. N., Monsma, F. J., & Sibley, D. R. (1990). D1 and D2 dopamine receptor-regulated gene expression of striatonigral and striatopallidal neurons. *Science*, *250*(4986), 1429–1432. https://doi.org/10.1126/science.2147780

Gerfen, C. R., & Surmeier, D. J. (2011). Modulation of Striatal Projection Systems by

Dopamine. *Annual Review of Neuroscience*, *34*(1), 441–466. https://doi.org/10.1146/annurev-neuro-061010-113641

Gerlach, M., Beck, J., Riederer, P., & van den Buuse, M. (2011). Flibanserin attenuates l-DOPA-sensitized contraversive circling in the unilaterally 6-hydroxydopamine-lesioned rat model of Parkinson's disease. *Journal of Neural Transmission*, *118*(12), 1727–1732. https://doi.org/10.1007/s00702-010-0570-9

Giguère, N., Nanni, S. B., & Trudeau, L. E. (2018). On cell loss and selective vulnerability of neuronal populations in Parkinson's disease. In *Frontiers in Neurology* (Vol. 9, Issue JUN, p. 455). Frontiers Media S.A. https://doi.org/10.3389/fneur.2018.00455

Gil-Martínez, A. L., Cuenca, L., Sánchez, C., Estrada, C., Fernández-Villalba, E., & Herrero, M. T. (2018). Effect of NAC treatment and physical activity on neuroinflammation in subchronic Parkinsonism; is physical activity essential? *Journal of Neuroinflammation*, *15*(1), 328. https://doi.org/10.1186/s12974-018-1357-4

Giménez-Amaya, J. M., & Graybiel, A. M. (1990). Compartmental origins of the striatopallidal projection in the primate. *Neuroscience*, *34*(1), 111–126. https://doi.org/10.1016/0306-4522(90)90306-O

Giovanni, A., Capone, F., di Biase, L., Ferreri, F., Florio, L., Guerra, A., Marano, M., Paolucci, M., Ranieri, F., Salomone, G., Tombini, M., Thut, G., & Di Lazzaro, V. (2017). Oscillatory activities in neurological disorders of elderly: Biomarkers to target for neuromodulation. In *Frontiers in Aging Neuroscience* (Vol. 9, Issue JUN). Frontiers Media S.A. https://doi.org/10.3389/fnagi.2017.00189

Glajch, K. E., Kelver, D. A., Hegeman, D. J., Cui, Q., Xenias, H. S., Augustine, E. C., Hernández, V. M., Verma, N., Huang, T. Y., Luo, M., Justice, N. J., & Chan, C. S. (2016). Npas1+ Pallidal Neurons Target Striatal Projection Neurons. *The Journal of Neuroscience : The Official Journal of the Society for Neuroscience*, *36*(20), 5472–5488. https://doi.org/10.1523/JNEUROSCI.1720-15.2016

Gobert, A., Rivet, J. M., Cistarelli, L., Melon, C., & Millan, M. J. (1999). Buspirone modulates basal and fluoxetine-stimulated dialysate levels of dopamine, noradrenaline and serotonin in the frontal cortex of freely moving rats: Activation of serotonin(1A) receptors and blockade of α2-adrenergic receptors underlie its actions. *Neuroscience*, *93*(4), 1251–1262. https://doi.org/10.1016/S0306-4522(99)00211-0

Goetz, C. G., Damier, P., Hicking, C., Laska, E., Müller, T., Olanow, C. W., Rascol, O., & Russ, H. (2007). Sarizotan as a treatment for dyskinesias in Parkinson's disease: A double-blind placebo-controlled trial. *Movement Disorders*, *22*(2), 179–186. https://doi.org/10.1002/mds.21226

Goetz, C. G., Liu, Y., Stebbins, G. T., Wang, L., Tilley, B. C., Teresi, J. A., Merkitch, D., & Luo, S. (2016). Gender-, age-, and race/ethnicity-based differential item functioning analysis of the movement disorder society–sponsored revision of the Unified Parkinson's disease rating scale. *Movement Disorders*, *31*(12), 1865–1873. https://doi.org/10.1002/mds.26847

Gonon, F. G. (1988). Nonlinear relationship between impulse flow and dopamine released by rat midbrain dopaminergic neurons as studied by in vivo electrochemistry. *Neuroscience*, *24*(1), 19–28. https://doi.org/10.1016/0306-

4522(88)90307-7

González-Hernández, T., & Rodríguez, M. (2000). Compartmental organization and chemical profile of dopaminergic and GABAergic neurons in the substantia nigra of the rat. *The Journal of Comparative Neurology*, *421*(1), 107–135. https://doi.org/10.1002/(sici)1096-9861(20000522)421:1<107::aid-cne7>3.3.co;2-6

Gonzalez-Lima, F., & Cada, A. (1994). Cytochrome oxidase activity in the auditory system of the mouse: A qualitative and quantitative histochemical study. *Neuroscience*, *63*(2), 559–578. https://doi.org/10.1016/0306-4522(94)90550-9

Gradinaru, V., Mogri, M., Thompson, K. R., Henderson, J. M., & Deisseroth, K. (2009). Optical deconstruction of parkinsonian neural circuitry. *Science (New York, N.Y.)*, *324*(5925), 354–359. https://doi.org/10.1126/science.1167093

Grégoire, L., Samadi, P., Graham, J., Bédard, P. J., Bartoszyk, G. D., & Di Paolo, T. (2009). Low doses of sarizotan reduce dyskinesias and maintain antiparkinsonian efficacy of l-Dopa in parkinsonian monkeys. *Parkinsonism & Related Disorders*, *15*(6), 445–452. https://doi.org/10.1016/J.PARKRELDIS.2008.11.001

Grillner, S., & Robertson, B. (2016). The Basal Ganglia Over 500 Million Years. In *Current Biology* (Vol. 26, Issue 20, pp. R1088–R1100). Cell Press. https://doi.org/10.1016/j.cub.2016.06.041

Guiard, B. P., El Mansari, M., Merali, Z., & Blier, P. (2008). Functional interactions between dopamine, serotonin and norepinephrine neurons: An in-vivo electrophysiological study in rats with monoaminergic lesions. *International Journal of Neuropsychopharmacology*, *11*(5), 625–639. https://doi.org/10.1017/S1461145707008383

Guridi, J., González-Redondo, R., & Obeso, J. A. (2012). Clinical features, pathophysiology, and treatment of levodopa-induced dyskinesias in Parkinson's disease. In *Parkinson's Disease* (Vol. 2012, p. 943159). https://doi.org/10.1155/2012/943159

Hadaczek, P., Eberling, J. L., Pivirotto, P., Bringas, J., Forsayeth, J., & Bankiewicz, K. S. (2010). Eight years of clinical improvement in MPTP-lesioned primates after gene therapy with AAV2-hAADC. *Molecular Therapy*, *18*(8), 1458–1461. https://doi.org/10.1038/mt.2010.106

Hahn, P. J., & McIntyre, C. C. (2010). Modeling shifts in the rate and pattern of subthalamopallidal network activity during deep brain stimulation. *Journal of Computational Neuroscience*, *28*(3), 425–441. https://doi.org/10.1007/s10827-010-0225-8

Hahn, P. J., Russo, G. S., Hashimoto, T., Miocinovic, S., Xu, W., McIntyre, C. C., & Vitek, J. L. (2008). Pallidal burst activity during therapeutic deep brain stimulation. *Experimental Neurology*, *211*(1), 243–251. https://doi.org/10.1016/j.expneurol.2008.01.032

Halliday, G. M, Blumbergs, P. C., Cotton, R. G., Blessing, W. W., & Geffen, L. B. (1990). Loss of brainstem serotonin- and substance P-containing neurons in Parkinson's disease. *Brain Research*, *510*(1), 104–107. https://doi.org/10.1016/0006-8993(90)90733-r

Halliday, G. M, & Stevens, C. H. (2011). Glia: initiators and progressors of pathology in

Parkinson's disease. *Movement Disorders : Official Journal of the Movement Disorder Society*, *26*(1), 6–17. https://doi.org/10.1002/mds.23455

Hamadjida, A., Nuara, S. G., Bédard, D., Gaudette, F., Beaudry, F., Gourdon, J. C., & Huot, P. (2018). The highly selective 5-HT2A antagonist EMD-281,014 reduces dyskinesia and psychosis in the l-DOPA-treated parkinsonian marmoset. *Neuropharmacology*, *139*, 61–67. https://doi.org/10.1016/j.neuropharm.2018.06.038

Hamani, C., Saint-Cyr, J. A., Fraser, J., Kaplitt, M., & Lozano, A. M. (2004). The subthalamic nucleus in the context of movement disorders. In *Brain* (Vol. 127, Issue 1, pp. 4–20). https://doi.org/10.1093/brain/awh029

Hara, K., & Harris, R. A. (2002). The Anesthetic Mechanism of Urethane: The Effects on Neurotransmitter-Gated Ion Channels. *Anesthesia & Analgesia*, *94*(2), 313–318. https://doi.org/10.1097/00000539-200202000-00015

Harding, S. D., Sharman, J. L., Faccenda, E., Southan, C., Pawson, A. J., Ireland, S., Gray, A. J. G., Bruce, L., Alexander, S. P. H., Anderton, S., Bryant, C., Davenport, A. P., Doerig, C., Fabbro, D., Levi-Schaffer, F., Spedding, M., & Davies, J. A. (2018). The IUPHAR/BPS Guide to PHARMACOLOGY in 2018: Updates and expansion to encompass the new guide to IMMUNOPHARMACOLOGY. *Nucleic Acids Research*, *46*(D1), D1091–D1106. https://doi.org/10.1093/nar/gkx1121

Harms, A. S., Delic, V., Thome, A. D., Bryant, N., Liu, Z., Chandra, S., Jurkuvenaite, A., & West, A. B. (2017). α-Synuclein fibrils recruit peripheral immune cells in the rat brain prior to neurodegeneration. *Acta Neuropathologica Communications*, *5*(1), 85. https://doi.org/10.1186/s40478-017-0494-9

Harrington, M. A., Oksenberg, D., & Peroutka, S. J. (1988). 5-Hydroxytryptamine1A receptors are linked to a Gi-adenylate cyclase complex in rat hippocampus. *European Journal of Pharmacology*, *154*(1), 95–98. https://doi.org/10.1016/0014-2999(88)90369-X

Hashemi, P., Dankoski, E. C., Wood, K. M., Ambrose, R. E., & Wightman, R. M. (2011). In vivo electrochemical evidence for simultaneous 5-HT and histamine release in the rat substantia nigra pars reticulata following medial forebrain bundle stimulation. *Journal of Neurochemistry*, *118*(5), 749–759. https://doi.org/10.1111/j.1471-4159.2011.07352.x

Hashimoto, T., Elder, C. M., Okun, M. S., Patrick, S. K., & Vitek, J. L. (2003). Stimulation of the subthalamic nucleus changes the firing pattern of pallidal neurons. *Journal of Neuroscience*, *23*(5), 1916–1923. https://doi.org/10.1523/jneurosci.23-05-01916.2003

Hauser, R. A., Li, R., Pérez, A., Ren, X., Weintraub, D., Elm, J., Goudreau, J. L., Morgan, J. C., Fang, J. Y., Aminoff, M. J., Christine, C. W., Dhall, R., Umeh, C. C., Boyd, J. T., Stover, N., Leehey, M., Zweig, R. M., Nicholas, A. P., Bodis-Wollner, I., … Tilley, B. C. (2017). Longer Duration of MAO-B Inhibitor Exposure is Associated with Less Clinical Decline in Parkinson's Disease: An Analysis of NET-PD LS1. *Journal of Parkinson's Disease*, *7*(1), 117–127. https://doi.org/10.3233/JPD-160965

Hazrati, L. N., Parent, A., Mitchell, S., & Haber, S. N. (1990). Evidence for interconnections between the two segments of the globus pallidus in primates: a PHA-L anterograde tracing study. *Brain Research*, *533*(1), 171–175. https://doi.org/10.1016/0006-8993(90)91813-V

7. References

Hely, M. A., Reid, W. G. J., Adena, M. A., Halliday, G. M., & Morris, J. G. L. (2008). The Sydney Multicenter Study of Parkinson's disease: The inevitability of dementia at 20 years. *Movement Disorders*, *23*(6), 837–844. https://doi.org/10.1002/mds.21956

Henry, B., Crossman, A. R., & Brotchie, J. M. (1998). Characterization of enhanced behavioral responses to L-DOPA following repeated administration in the 6-hydroxydopamine-lesioned rat model of Parkinson's disease. *Experimental Neurology*, *151*(2), 334–342. https://doi.org/10.1006/exnr.1998.6819

Henry, B., Crossman, A. R., & Brotchie, J. M. (1999). Effect of repeated L-DOPA, bromocriptine, or lisuride administration on preproenkephalin-A and preproenkephalin-B mRNA levels in the striatum of the 6-hydroxydopamine-lesioned rat. *Experimental Neurology*, *155*(2), 204–220. https://doi.org/10.1006/exnr.1998.6996

Herman, A. M., Huang, L., Murphey, D. K., Garcia, I., & Arenkiel, B. R. (2014). Cell type-specific and time-dependent light exposure contribute to silencing in neurons expressing Channelrhodopsin-2. *ELife*, *3*. https://doi.org/10.7554/elife.01481

Hernández-Vázquez, F., Garduño, J., & Hernández-López, S. (2019). GABAergic modulation of serotonergic neurons in the dorsal raphe nucleus. *Reviews in the Neurosciences*, *30*(3), 289–303. https://doi.org/10.1515/revneuro-2018-0014

Herrán, E., Requejo, C., Ruiz-Ortega, J. A., Aristieta, A., Igartua, M., Bengoetxea, H., Ugedo, L., Pedraz, J. L., Lafuente, J. V., & Hernández, R. M. (2014). Increased antiparkinson efficacy of the combined administration of VEGF- and GDNF-loaded nanospheres in a partial lesion model of Parkinson's disease. *International Journal of Nanomedicine*, *9*(1), 2677–2687. https://doi.org/10.2147/IJN.S61940

Herrán, E., Ruiz-Ortega, J. Á., Aristieta, A., Igartua, M., Requejo, C., Lafuente, J. V., Ugedo, L., Pedraz, J. L., & Hernández, R. M. (2013). In vivo administration of VEGF- and GDNF-releasing biodegradable polymeric microspheres in a severe lesion model of Parkinson's disease. *European Journal of Pharmaceutics and Biopharmaceutics*, *85*(3 PART B), 1183–1190. https://doi.org/10.1016/j.ejpb.2013.03.034

Hevner, R. F., & Wong-Riley, M. T. T. (1989). Brain cytochrome oxidase: Purification, antibody production, and immunohistochemical/histochemical correlations in the CNS. *Journal of Neuroscience*, *9*(11), 3884–3898. https://doi.org/10.1523/jneurosci.09-11-03884.1989

Hevner, R. F., & Wong-Riley, M. T. T. (1991). Neuronal expression of nuclear and mitochondrial genes for cytochrome oxidase (CO) subunits analyzed by in situ hybridization: Comparison with CO activity and protein. *Journal of Neuroscience*, *11*(7), 1942–1958. https://doi.org/10.1523/jneurosci.11-07-01942.1991

Higgs, M. H., & Wilson, C. J. (2016). Unitary synaptic connections among substantia nigra pars reticulata neurons. *Journal of Neurophysiology*, *115*(6), 2814–2829. https://doi.org/10.1152/jn.00094.2016

Holper, L., Ben-Shachar, D., & Mann, J. (2019). Multivariate meta-analyses of mitochondrial complex I and IV in major depressive disorder, bipolar disorder, schizophrenia, Alzheimer disease, and Parkinson disease. In *Neuropsychopharmacology* (Vol. 44, Issue 5, pp. 837–849). Nature Publishing Group. https://doi.org/10.1038/s41386-018-0090-0

Horváth, J., Barkóczi, B., Müller, G., & Szegedi, V. (2015). Anxious and nonanxious mice show similar hippocampal sensory evoked oscillations under urethane anesthesia: Difference in the effect of buspirone. *Neural Plasticity*, *2015*, 186323. https://doi.org/10.1155/2015/186323

Hou, C., Xue, L., Feng, J., Zhang, L., Wang, Y., Chen, L., Wang, T., Zhang, Q. J., & Liu, J. (2012). Unilateral lesion of the nigrostriatal pathway decreases the response of GABA interneurons in the dorsal raphe nucleus to 5-HT(1A) receptor stimulation in the rat. *Neurochemistry International*, *61*(8), 1344–1356. https://doi.org/10.1016/j.neuint.2012.09.012

Hoyer, D., Hannon, J. P., & Martin, G. R. (2002). Molecular, pharmacological and functional diversity of 5-HT receptors. In *Pharmacology Biochemistry and Behavior* (Vol. 71, Issue 4, pp. 533–554). Elsevier Inc. https://doi.org/10.1016/S0091-3057(01)00746-8

Huang, K. W., Ochandarena, N. E., Philson, A. C., Hyun, M., Birnbaum, J. E., Cicconet, M., & Sabatini, B. L. (2019). Molecular and anatomical organization of the dorsal raphe nucleus. *ELife*, *8*. https://doi.org/10.7554/eLife.46464

Hudson, J., Granholm, A. C., Gerhardt, G. A., Henry, M. A., Hoffman, A., Biddle, P., Leela, N. S., Mackerlova, L., Lile, J. D., Collins, F., & Hoffer, B. J. (1995). Glial cell line-derived neurotrophic factor augments midbrain dopaminergic circuits in vivo. *Brain Research Bulletin*, *36*(5), 425–432. https://doi.org/10.1016/0361-9230(94)00224-O

Huot, P., Johnston, T. H., Koprich, J. B., Winkelmolen, L., Fox, S. H., & Brotchie, J. M. (2012). Regulation of cortical and striatal 5-HT1A receptors in the MPTP-lesioned macaque. *Neurobiology of Aging*, *33*(1), 207.e9-19. https://doi.org/10.1016/j.neurobiolaging.2010.09.011

Huot, P., Johnston, T. H., Visanji, N. P., Darr, T., Pires, D., Hazrati, L.-N., Brotchie, J. M., & Fox, S. H. (2012). Increased levels of 5-HT1A receptor binding in ventral visual pathways in Parkinson's disease. *Movement Disorders : Official Journal of the Movement Disorder Society*, *27*(6), 735–742. https://doi.org/10.1002/mds.24964

Huse, D. M., Schulman, K., Orsini, L., Castelli-Haley, J., Kennedy, S., & Lenhart, G. (2005). Burden of illness in Parkinson's disease. *Movement Disorders : Official Journal of the Movement Disorder Society*, *20*(11), 1449–1454. https://doi.org/10.1002/mds.20609

Hutchison, W. D., Lozano, A. M., Davis, K. D., Saint-Cyr, J. A., Lang, A. E., & Dostrovsky, J. O. (1994). Differential neuronal activity in segments of globus pallidus in Parkinson's disease patients. *Neuroreport*, *5*(12), 1533–1537. https://doi.org/10.1097/00001756-199407000-00031

Iderberg, H., McCreary, A. C., Varney, M. A., Cenci, M. A., & Newman-Tancredi, A. (2015). Activity of serotonin 5-HT1A receptor 'biased agonists' in rat models of Parkinson's disease and l-DOPA-induced dyskinesia. *Neuropharmacology*, *93*, 52–67. https://doi.org/10.1016/j.neuropharm.2015.01.012

Imperato, A., & Di Chiara, G. (1984). Trans-striatal dialysis coupled to reverse phase high performance liquid chromatography with electrochemical detection: A new method for the study of the in vivo release of endogenous dopamine and metabolites. *Journal of Neuroscience*, *4*(4), 966–977. https://doi.org/10.1523/jneurosci.04-04-00966.1984

7. References

Iravani, M. M., Tayarani-Binazir, K., Chu, W. B., Jackson, M. J., & Jenner, P. (2006). In 1-methyl-4-phenyl-1,2,3,6-tetrahydropyridine-treated primates, the selective 5-hydroxytryptamine 1a agonist (R)-(+)-8-OHDPAT inhibits levodopa-induced dyskinesia but only with\ increased motor disability. *Journal of Pharmacology and Experimental Therapeutics*, *319*(3), 1225–1234. https://doi.org/10.1124/jpet.106.110429

Itoh, K., Weis, S., Mehraein, P., & Müller-Höcker, J. (1996). Cytochrome c oxidase defects of the human substantia nigra in normal aging. *Neurobiology of Aging*, *17*(6), 843–848. https://doi.org/10.1016/S0197-4580(96)00168-6

Janssen, M. L. F., Temel, Y., Delaville, C., Zwartjes, D. G. M., Heida, T., De Deurwaerdère, P., Visser-Vandewalle, V., & Benazzouz, A. (2017). Cortico-subthalamic inputs from the motor, limbic, and associative areas in normal and dopamine-depleted rats are not fully segregated. *Brain Structure and Function*, *222*(6), 2473–2485. https://doi.org/10.1007/s00429-016-1351-5

Jellinger, K. A. (2001). Cell death mechanisms in neurodegeneration. *Journal of Cellular and Molecular Medicine*, *5*(1), 1–17. https://doi.org/10.1111/j.1582-4934.2001.tb00134.x

Jenner, P., Hunot, Olanow, Beal, Kordower, Tatton, & Schapira. (2003). Oxidative stress in Parkinson's disease. In *Annals of Neurology* (Vol. 53, Issue SUPPL. 3). https://doi.org/10.1002/ana.10483

Jin, X., Schwabe, K., Krauss, J. K., & Alam, M. (2016). Coherence of neuronal firing of the entopeduncular nucleus with motor cortex oscillatory activity in the 6-OHDA rat model of Parkinson's disease with levodopa-induced dyskinesias. *Experimental Brain Research*, *234*(4), 1105–1118. https://doi.org/10.1007/s00221-015-4532-1

Kalia, L. V, & Lang, A. E. (2015). Parkinson's disease. *Lancet (London, England)*, *386*(9996), 896–912. https://doi.org/10.1016/S0140-6736(14)61393-3

Kamata, K., & Rebec, G. V. (1983). Dopaminergic and neostriatal neurons: dose-dependent changes in sensitivity to amphetamine following long-term treatment. *Neuropharmacology*, *22*(12A), 1377–1382. https://doi.org/10.1016/0028-3908(83)90227-7

Kannari, K., Kurahashi, K., Tomiyama, M., Maeda, T., Arai, A., Baba, M., Suda, T., & Matsunaga, M. (2002). [Tandospirone citrate, a selective 5-HT1A agonist, alleviates L-DOPA-induced dyskinesia in patients with Parkinson's disease]. *No to Shinkei = Brain and Nerve*, *54*(2), 133–137. http://www.ncbi.nlm.nih.gov/pubmed/11889759

Karmy, G., Carr, P. A., Yamamoto, T., Chan, S. H., & Nagy, J. I. (1991). Cytochrome oxidase immunohistochemistry in rat brain and dorsal root ganglia: visualization of enzyme in neuronal perikarya and in parvalbumin-positive neurons. *Neuroscience*, *40*(3), 825–839. https://doi.org/10.1016/0306-4522(91)90015-g

Kaya, A. H., Vlamings, R., Tan, S., Lim, L. W., Magill, P. J., Steinbusch, H. W. M., Visser-Vandewalle, V., Sharp, T., & Temel, Y. (2008). Increased electrical and metabolic activity in the dorsal raphe nucleus of Parkinsonian rats. *Brain Research*, *1221*, 93–97. https://doi.org/10.1016/j.brainres.2008.05.019

Keifman, E., Ruiz-DeDiego, I., Pafundo, D. E., Paz, R. M., Solís, O., Murer, M. G., & Moratalla, R. (2019). Optostimulation of striatonigral terminals in substantia nigra induces dyskinesia that increases after L-DOPA in a mouse model of Parkinson's

disease. *British Journal of Pharmacology*, *176*(13), 2146–2161. https://doi.org/10.1111/bph.14663

Kha, H. T., Finkelstein, D. I., Tomas, D., Drago, J., Pow, D. V., & Horne, M. K. (2001). Projections from the substantia nigra pars reticulata to the motor thalamus of the rat: Single axon reconstructions and immunohistochemical study. *The Journal of Comparative Neurology*, *440*(1), 20–30. https://doi.org/10.1002/cne.1367

Khlebtovsky, A., Rigbi, A., Melamed, E., Ziv, I., Steiner, I., Gad, A., & Djaldetti, R. (2012). Patient and caregiver perceptions of the social impact of advanced Parkinson's disease and dyskinesias. *Journal of Neural Transmission (Vienna, Austria : 1996)*, *119*(11), 1367–1371. https://doi.org/10.1007/s00702-012-0796-9

Kim, J., Inoue, K., Ishii, J., Vanti, W. B., Voronov, S. V., Murchison, E., Hannon, G., & Abeliovich, A. (2007). A microRNA feedback circuit in midbrain dopamine neurons. *Science*, *317*(5842), 1220–1224. https://doi.org/10.1126/science.1140481

Kish, S. J., Tong, J., Hornykiewicz, O., Rajput, A., Chang, L.-J., Guttman, M., & Furukawa, Y. (2007). Preferential loss of serotonin markers in caudate versus putamen in Parkinson's disease. *Brain*, *131*(Pt 1), 120–131. https://doi.org/10.1093/brain/awm239

Kish, S. J., Shannak, K., & Hornykiewicz, O. (1988). Uneven Pattern of Dopamine Loss in the Striatum of Patients with Idiopathic Parkinson's Disease. *New England Journal of Medicine*, *318*(14), 876–880. https://doi.org/10.1056/NEJM198804073181402

Kita, H., & Kitai, S. T. (1987). Efferent projections of the subthalamic nucleus in the rat: light and electron microscopic analysis with the PHA-L method. *The Journal of Comparative Neurology*, *260*(3), 435–452. https://doi.org/10.1002/cne.902600309

Kleedorfer, B., Lees, A. J., & Stern, G. M. (1991). Buspirone in the treatment of levodopa induced dyskinesias. *Journal of Neurology, Neurosurgery & Psychiatry*, *54*(4), 376–377. https://doi.org/10.1136/jnnp.54.4.376-a

Koga, H., & Cuervo, A. M. (2011). Chaperone-mediated autophagy dysfunction in the pathogenesis of neurodegeneration. In *Neurobiology of Disease* (Vol. 43, Issue 1, pp. 29–37). https://doi.org/10.1016/j.nbd.2010.07.006

Kolomiets, B. P., Deniau, J. M., Glowinski, J., & Thierry, A. M. (2003). Basal ganglia and processing of cortical information: functional interactions between trans-striatal and trans-subthalamic circuits in the substantia nigra pars reticulata. *Neuroscience*, *117*(4), 931–938. https://doi.org/10.1016/s0306-4522(02)00824-2

Kong, P., Zhang, B., Lei, P., Kong, X., Zhang, S., Li, D., & Zhang, Y. (2015). Neuroprotection of MAO-B inhibitor and dopamine agonist in Parkinson disease. *International Journal of Clinical and Experimental Medicine*, *8*(1), 431–439. http://www.ncbi.nlm.nih.gov/pubmed/25785014

Kravitz, A. V., Freeze, B. S., Parker, P. R. L., Kay, K., Thwin, M. T., Deisseroth, K., & Kreitzer, A. C. (2010). Regulation of parkinsonian motor behaviours by optogenetic control of basal ganglia circuitry. *Nature*, *466*(7306), 622–626. https://doi.org/10.1038/nature09159

Lagière, M., Navailles, S., Mignon, L., Roumegous, A., Chesselet, M. F., & De Deurwaerdère, P. (2013). The enhanced oral response to the 5-HT2 agonist Ro 60-0175 in parkinsonian rats involves the entopeduncular nucleus: Electrophysiological

correlates. *Experimental Brain Research*, *230*(4), 513–524. https://doi.org/10.1007/s00221-013-3478-4

Lang, A. E., & Espay, A. J. (2018). Disease Modification in Parkinson's Disease: Current Approaches, Challenges, and Future Considerations. In *Movement Disorders* (Vol. 33, Issue 5, pp. 660–677). John Wiley and Sons Inc. https://doi.org/10.1002/mds.27360

Langston, J., Ballard, P., Tetrud, J., & Irwin, I. (1983). Chronic Parkinsonism in humans due to a product of meperidine-analog synthesis. *Science*, *219*(4587), 979–980. https://doi.org/10.1126/science.6823561

Lanza, K., & Bishop, C. (2018). Serotonergic targets for the treatment of l-DOPA-induced dyskinesia. In *Journal of Neural Transmission* (Vol. 125, Issue 8, pp. 1203–1216). Springer-Verlag Wien. https://doi.org/10.1007/s00702-017-1837-1

Lavian, H., Loewenstern, Y., Madar, R., Almog, M., Bar-Gad, I., Okun, E., & Korngreen, A. (2018). Dopamine receptors in the rat entopeduncular nucleus. *Brain Structure and Function*, *223*(6), 2673–2684. https://doi.org/10.1007/s00429-018-1657-6

Lee, A., & Gilbert, R. M. (2016). Epidemiology of Parkinson Disease. In *Neurologic Clinics* (Vol. 34, Issue 4, pp. 955–965). W.B. Saunders. https://doi.org/10.1016/j.ncl.2016.06.012

Lee, C. R., & Tepper, J. M. (2009). Basal ganglia control of substantia nigra dopaminergic neurons. In *Journal of Neural Transmission, Supplementa* (Issue 73, pp. 71–90). https://doi.org/10.1007/978-3-211-92660-4-6

Lévesque, J. C., & André, P. (2005). GABAergic interneurons in human subthalamic nucleus. *Movement Disorders*, *20*(5), 574–584. https://doi.org/10.1002/mds.20374

LeWitt, P. A., Rezai, A. R., Leehey, M. A., Ojemann, S. G., Flaherty, A. W., Eskandar, E. N., Kostyk, S. K., Thomas, K., Sarkar, A., Siddiqui, M. S., Tatter, S. B., Schwalb, J. M., Poston, K. L., Henderson, J. M., Kurlan, R. M., Richard, I. H., Van Meter, L., Sapan, C. V., During, M. J., … Feigin, A. (2011). AAV2-GAD gene therapy for advanced Parkinson's disease: A double-blind, sham-surgery controlled, randomised trial. *The Lancet Neurology*, *10*(4), 309–319. https://doi.org/10.1016/S1474-4422(11)70039-4

Liang, C. L., Sinton, C. M., & German, D. C. (1996). Midbrain dopaminergic neurons in the mouse: Co-localization with calbindin-D(28K) and calretinin. *Neuroscience*, *75*(2), 523–533. https://doi.org/10.1016/0306-4522(96)00228-X

Lim, J., Bang, Y., Choi, J. H., Han, A., Kwon, M. S., Liu, K. H., & Choi, H. J. (2018). LRRK2 G2019S induces anxiety/depression-like behavior before the onset of motor dysfunction with 5-HT 1A receptor upregulation in mice. *Journal of Neuroscience*, *38*(7), 1611–1621. https://doi.org/10.1523/JNEUROSCI.4051-15.2017

Lim, S., Kim, H. J., Kim, D. K., & Lee, S. J. (2018). Non-cell-autonomous actions of α-synuclein: Implications in glial synucleinopathies. In *Progress in Neurobiology* (Vol. 169, pp. 158–171). Elsevier Ltd. https://doi.org/10.1016/j.pneurobio.2018.06.010

Lin, J. Y. (2011). A user's guide to channelrhodopsin variants: Features, limitations and future developments. In *Experimental Physiology* (Vol. 96, Issue 1, pp. 19–25). Blackwell Publishing Ltd. https://doi.org/10.1113/expphysiol.2009.051961

Lin, J. Y., Lin, M. Z., Steinbach, P., & Tsien, R. Y. (2009). Characterization of engineered

channelrhodopsin variants with improved properties and kinetics. *Biophysical Journal*, *96*(5), 1803–1814. https://doi.org/10.1016/j.bpj.2008.11.034

Linazasoro, G. (2000). Worsening of Parkinson's disease by citalopram. *Parkinsonism and Related Disorders*, *6*(2), 111–113. https://doi.org/10.1016/S1353-8020(99)00050-4

Lindenbach, D., Palumbo, N., Ostock, C. Y., Vilceus, N., Conti, M. M., & Bishop, C. (2015). Side effect profile of 5-HT treatments for Parkinson's disease and L-DOPA-induced dyskinesia in rats. *British Journal of Pharmacology*, *172*(1), 119–130. https://doi.org/10.1111/bph.12894

Lindenbach, David, Dupre, K. B., Eskow Jaunarajs, K. L., Ostock, C. Y., Goldenberg, A. A., & Bishop, C. (2013). Effects of 5-HT1A receptor stimulation on striatal and cortical M1 pERK induction by l-DOPA and a D1 receptor agonist in a rat model of Parkinson's disease. *Brain Research*, *1537*, 327–339. https://doi.org/10.1016/j.brainres.2013.09.020

Lindgren, H. S., Andersson, D. R., Lagerkvist, S., Nissbrandt, H., & Cenci, M. A. (2010). l-DOPA-induced dopamine efflux in the striatum and the substantia nigra in a rat model of Parkinson's disease: temporal and quantitative relationship to the expression of dyskinesia. *Journal of Neurochemistry*, *112*(6), 1465–1476. https://doi.org/10.1111/j.1471-4159.2009.06556.x

Lindvall, O., & Björklund, A. (1979). Dopaminergic innervation of the globus pallidus by collaterals from the nigrostriatal pathway. *Brain Research*, *172*(1), 169–173. https://doi.org/10.1016/0006-8993(79)90907-7

Litvak, V., Eusebio, A., Jha, A., Oostenveld, R., Barnes, G., Foltynie, T., Limousin, P., Zrinzo, L., Hariz, M. I., Friston, K., & Brown, P. (2012). Movement-related changes in local and long-range synchronization in Parkinson's disease revealed by simultaneous magnetoencephalography and intracranial recordings. *The Journal of Neuroscience : The Official Journal of the Society for Neuroscience*, *32*(31), 10541–10553. https://doi.org/10.1523/JNEUROSCI.0767-12.2012

Liu, R., Jolas, T., & Aghajanian, G. (2000). Serotonin 5-HT(2) receptors activate local GABA inhibitory inputs to serotonergic neurons of the dorsal raphe nucleus. *Brain Research*, *873*(1), 34–45. https://doi.org/10.1016/s0006-8993(00)02468-9

Lobb, C. J. (2014). Abnormal bursting as a pathophysiological mechanism in Parkinson's disease. In *Basal Ganglia* (Vol. 3, Issue 4, pp. 187–195). https://doi.org/10.1016/j.baga.2013.11.002

Lobb, C. J., & Jaeger, D. (2015). Bursting activity of substantia nigra pars reticulata neurons in mouse parkinsonism in awake and anesthetized states. *Neurobiology of Disease*, *75*, 177–185. https://doi.org/10.1016/j.nbd.2014.12.026

López-Azcárate, J., Tainta, M., Rodríguez-Oroz, M. C., Valencia, M., González, R., Guridi, J., Iriarte, J., Obeso, J. A., Artieda, J., & Alegre, M. (2010). Coupling between beta and high-frequency activity in the human subthalamic nucleus may be a pathophysiological mechanism in Parkinson's disease. *Journal of Neuroscience*, *30*(19), 6667–6677. https://doi.org/10.1523/JNEUROSCI.5459-09.2010

Louis, E. D. (2016). Diagnosis and Management of Tremor. In *CONTINUUM Lifelong Learning in Neurology* (Vol. 22, Issue 4, MovementDisorders, pp. 1143–1158). Lippincott Williams and Wilkins. https://doi.org/10.1212/CON.0000000000000346

7. References

Lucas, G., De Deurwaerdère, P., Caccia, S., & Umberto Spampinato. (2000). The effect of serotonergic agents on haloperidol-induced striatal dopamine release in vivo: opposite role of 5-HT(2A) and 5-HT(2C) receptor subtypes and significance of the haloperidol dose used. *Neuropharmacology*, *39*(6), 1053–1063. https://doi.org/10.1016/s0028-3908(99)00193-8

Lundblad, M., Andersson, M., Winkler, C., Kirik, D., Wierup, N., & Cenci Nilsson, M. A. (2002). Pharmacological validation of behavioural measures of akinesia and dyskinesia in a rat model of Parkinson's disease. *European Journal of Neuroscience*, *15*(1), 120–132. https://doi.org/10.1046/j.0953-816x.2001.01843.x

Luo, F., & Kiss, Z. H. T. (2016). Cholinergic mechanisms of high-frequency stimulation in entopeduncular nucleus. *Journal of Neurophysiology*, *115*(1), 60–67. https://doi.org/10.1152/jn.00269.2015

Mabrouk, O. S., Volta, M., Marti, M., & Morari, M. (2008). Stimulation of delta opioid receptors located in substantia nigra reticulata but not globus pallidus or striatum restores motor activity in 6-hydroxydopamine lesioned rats: new insights into the role of delta receptors in parkinsonism. *Journal of Neurochemistry*, *107*(6), 1647–1659. https://doi.org/10.1111/j.1471-4159.2008.05727.x

Magill, P. J., Bolam, J. P., & Bevan, M. D. (2001). Dopamine regulates the impact of the cerebral cortex on the subthalamic nucleus-globus pallidus network. *Neuroscience*, *106*(2), 313–330. https://doi.org/10.1016/S0306-4522(01)00281-0

Mailly, P., Charpier, S., Mahon, S., Menetrey, A., Thierry, A. M., Glowinski, J., & Deniau, J. M. (2001). Dendritic arborizations of the rat substantia nigra pars reticulata neurons: Spatial organization and relation to the lamellar compartmentation of striato-nigral projections. *Journal of Neuroscience*, *21*(17), 6874–6888. https://doi.org/10.1523/jneurosci.21-17-06874.2001

Mallet N., Delgado L., Chazalon A., Miguelez C., & Baufreton J.. (2019). Cellular and Synaptic Dysfunctions in Parkinson's Disease: Stepping out of the Striatum. *Cells*, *8*(9), 1005. https://doi.org/10.3390/cells8091005

Mallet, N., Micklem, B. R., Henny, P., Brown, M. T., Williams, C., Bolam, J. P., Nakamura, K. C., & Magill, P. J. (2012). Dichotomous Organization of the External Globus Pallidus. *Neuron*, *74*(6), 1075–1086. https://doi.org/10.1016/j.neuron.2012.04.027

Maltête, D., Jodoin, N., Karachi, C., Houeto, J. L., Navarro, S., Cornu, P., Agid, Y., & Welter, M. L. (2007). Subthalamic stimulation and neuronal activity in the substantia nigra in Parkinson's disease. *Journal of Neurophysiology*, *97*(6), 4017–4022. https://doi.org/10.1152/jn.01104.2006

Mansour, A., Thompson, R. C., Akil, H., & Watson, S. J. (1993). Delta opioid receptor mRNA distribution in the brain: Comparison to delta receptor binding and proenkephalin mRNA. *Journal of Chemical Neuroanatomy*, *6*(6), 351–362. https://doi.org/10.1016/0891-0618(93)90010-2

Marin, C., Aguilar, E., Mengod, G., Cortés, R., Rodríguez-Oroz, M. C., & Obeso, J. A. (2008). Entacapone potentiates the long-duration response but does not normalize levodopa-induced molecular changes. *Neurobiology of Disease*, *32*(3), 340–348. https://doi.org/10.1016/j.nbd.2008.07.019

Martín-Ruiz, R., & Ugedo, L. (2001). Electrophysiological evidence for postsynaptic 5-

HT(1A) receptor control of dorsal raphe 5-HT neurones. *Neuropharmacology*, *41*(1), 72–78. https://doi.org/10.1016/s0028-3908(01)00050-8

Martínez-Fernández, R., Rodríguez-Rojas, R., del Álamo, M., Hernández-Fernández, F., Pineda-Pardo, J. A., Dileone, M., Alonso-Frech, F., Foffani, G., Obeso, I., Gasca-Salas, C., de Luis-Pastor, E., Vela, L., & Obeso, J. A. (2018). Focused ultrasound subthalamotomy in patients with asymmetric Parkinson's disease: a pilot study. *The Lancet Neurology*, *17*(1), 54–63. https://doi.org/10.1016/S1474-4422(17)30403-9

Masliah, E., Dumaop, W., Galasko, D., & Desplats, P. (2013). Distinctive patterns of DNA methylation associated with Parkinson disease: Identification of concordant epigenetic changes in brain and peripheral blood leukocytes. *Epigenetics*, *8*(10), 1030–1038. https://doi.org/10.4161/epi.25865

Mason, S. T., & Fibiger, H. C. (1979). Regional topography within noradrenergic locus coeruleus as revealed by retrograde transport of horseradish peroxidase. *Journal of Comparative Neurology*, *187*(4), 703–724. https://doi.org/10.1002/cne.901870405

Matos, F. F., Urban, C., & Yocca, F. D. (1996). Serotonin (5-HT) release in the dorsal raphé and ventral hippocampus: raphé control of somatodendritic and terminal 5-HT release. *Journal of Neural Transmission (Vienna, Austria : 1996)*, *103*(1–2), 173–190. https://doi.org/10.1007/BF01292626

Matulewicz, P., Orzeł-Gryglewska, J., Hunt, M. J., Trojniar, W., & Jurkowlaniec, E. (2010). Hippocampal theta rhythm after serotonergic activation of the pedunculopontine tegmental nucleus in anesthetized rats. *Brain Research Bulletin*, *83*(5), 257–261. https://doi.org/10.1016/j.brainresbull.2010.08.003

Maurice, N., Deniau, J. M., Glowinski, J., & Thierry, A. M. (1999). Relationships between the prefrontal cortex and the basal ganglia in the rat: physiology of the cortico-nigral circuits. *The Journal of Neuroscience : The Official Journal of the Society for Neuroscience*, *19*(11), 4674–4681. http://www.ncbi.nlm.nih.gov/pubmed/10341265

Mazzucchi, S., Frosini, D., Ripoli, A., Nicoletti, V., Linsalata, G., Bonuccelli, U., & Ceravolo, R. (2015). Serotonergic antidepressant drugs and L-dopa-induced dyskinesias in Parkinson's disease. *Acta Neurologica Scandinavica*, *131*(3), 191–195. https://doi.org/10.1111/ane.12314

McCairn, K. W., & Turner, R. S. (2015). Pallidal stimulation suppresses pathological dysrhythmia in the parkinsonian motor cortex. *Journal of Neurophysiology*, *113*(7), 2537–2548. https://doi.org/10.1152/jn.00701.2014

McCreary, A. C., Varney, M. A., & Newman-Tancredi, A. (2016). The novel 5-HT1A receptor agonist, NLX-112 reduces l-DOPA-induced abnormal involuntary movements in rat: A chronic administration study with microdialysis measurements. *Neuropharmacology*, *105*, 651–660. https://doi.org/10.1016/j.neuropharm.2016.01.013

McGregor, M. M., & Nelson, A. B. (2019). Circuit Mechanisms of Parkinson's Disease. In *Neuron* (Vol. 101, Issue 6, pp. 1042–1056). Cell Press. https://doi.org/10.1016/j.neuron.2019.03.004

Meadows, S. M., Chambers, N. E., Conti, M. M., Bossert, S. C., Tasber, C., Sheena, E., Varney, M., Newman-Tancredi, A., & Bishop, C. (2017). Characterizing the differential roles of striatal 5-HT1A auto- and hetero-receptors in the reduction of

L-DOPA-induced dyskinesia. *Experimental Neurology*, *292*, 168–178. https://doi.org/10.1016/j.expneurol.2017.03.013

Meissner, W., Ravenscroft, P., Reese, R., Harnack, D., Morgenstern, R., Kupsch, A., Klitgaard, H., Bioulac, B., Gross, C. E., Bezard, E., & Boraud, T. (2006). Increased slow oscillatory activity in substantia nigra pars reticulata triggers abnormal involuntary movements in the 6-OHDA-lesioned rat in the presence of excessive extracelullar striatal dopamine. *Neurobiology of Disease*, *22*(3), 586–598. https://doi.org/10.1016/j.nbd.2006.01.009

Mejías-Aponte, C. A., Drouin, C., & Aston-Jones, G. (2009). Adrenergic and noradrenergic innervation of the midbrain ventral tegmental area and retrorubral field: prominent inputs from medullary homeostatic centers. *The Journal of Neuroscience : The Official Journal of the Society for Neuroscience*, *29*(11), 3613–3626. https://doi.org/10.1523/JNEUROSCI.4632-08.2009

Mela, F., Marti, M., Dekundy, A., Danysz, W., Morari, M., & Cenci, M. A. (2007). Antagonism of metabotropic glutamate receptor type 5 attenuates L-DOPA-induced dyskinesia and its molecular and neurochemical correlates in a rat model of Parkinson's disease. *Journal of Neurochemistry*, *101*(2), 483–497. https://doi.org/10.1111/j.1471-4159.2007.04456.x

Melendez-Ferro, M., Rice, M. W., Roberts, R. C., & Perez-Costas, E. (2013). An accurate method for the quantification of cytochrome C oxidase in tissue sections. *Journal of Neuroscience Methods*, *214*(2), 156–162. https://doi.org/10.1016/j.jneumeth.2013.01.010

Mena, M. A., & García De Yébenes, J. (2008). Glial cells as players in parkinsonism: The 'good,' the 'bad,' and the 'mysterious' glia. In *Neuroscientist* (Vol. 14, Issue 6, pp. 544–560). https://doi.org/10.1177/1073858408322839

Mignon, L., & Wolf, W. A. (2007). Postsynaptic 5-HT1A receptor stimulation increases motor activity in the 6-hydroxydopamine-lesioned rat: implications for treating Parkinson's disease. *Psychopharmacology*, *192*(1), 49–59. https://doi.org/10.1007/s00213-006-0680-0

Miguelez, C., Navailles, S., De Deurwaerdère, P., & Ugedo, L. (2016). The acute and long-term L-DOPA effects are independent from changes in the activity of dorsal raphe serotonergic neurons in 6-OHDA lesioned rats. *British Journal of Pharmacology*, 2135–2146. https://doi.org/10.1111/bph.13447

Miguelez, C., Grandoso, L., & Ugedo, L. (2011). Locus coeruleus and dorsal raphe neuron activity and response to acute antidepressant administration in a rat model of Parkinson's disease. *International Journal of Neuropsychopharmacology*, *14*(2), 187–200. https://doi.org/10.1017/S146114571000043X

Miguelez, C., Morera-Herreras, T., Torrecilla, M., Ruiz-Ortega, J. A., & Ugedo, L. (2014). Interaction between the 5-HT system and the basal ganglia: functional implication and therapeutic perspective in Parkinson's disease. *Frontiers in Neural Circuits*, *8*, 21. https://doi.org/10.3389/fncir.2014.00021

Miki, Y., Shimoyama, S., Kon, T., Ueno, T., Hayakari, R., Tanji, K., Matsumiya, T., Tsushima, E., Mori, F., Wakabayashi, K., & Tomiyama, M. (2018). Alteration of autophagy-related proteins in peripheral blood mononuclear cells of patients with Parkinson's disease. *Neurobiology of Aging*, *63*, 33–43. https://doi.org/10.1016/j.neurobiolaging.2017.11.006

Miller, D. W., & Abercrombie, E. D. (1999). Role of high-affinity dopamine uptake and impulse activity in the appearance of extracellular dopamine in striatum after administration of exogenous L-DOPA: Studies in intact and 6-hydroxydopamine-treated rats. *Journal of Neurochemistry*, *72*(4), 1516–1522. https://doi.org/10.1046/j.1471-4159.1999.721516.x

Miller, W. C., & DeLong, M. R. (1988). Parkinsonian symptomatology. An anatomical and physiological analysis. *Annals of the New York Academy of Sciences*, *515*(1), 287–302. https://doi.org/10.1111/j.1749-6632.1988.tb32998.x

Miocinovic, S., de Hemptinne, C., Chen, W., Isbaine, F., Willie, J. T., Ostrem, J. L., & Starr, P. A. (2018). Cortical potentials evoked by subthalamic stimulation demonstrate a short latency hyperdirect pathway in humans. *Journal of Neuroscience*, *38*(43), 9129–9141. https://doi.org/10.1523/JNEUROSCI.1327-18.2018

Monakow, K. H. von, Akert, K., & Künzle, H. (1978). Projections of the precentral motor cortex and other cortical areas of the frontal lobe to the subthalamic nucleus in the monkey. *Experimental Brain Research*, *33*(3–4), 395–403. https://doi.org/10.1007/BF00235561

Montagu, K. A. (1957). Catechol compounds in rat tissues and in brains of different animals [11]. In *Nature* (Vol. 180, Issue 4579, pp. 244–245). Nature Publishing Group. https://doi.org/10.1038/180244a0

Moore, R. Y., Halaris, A. E., & Jones, B. E. (1978). Serotonin neurons of the midbrain raphe: Ascending projections. *Journal of Comparative Neurology*, *180*(3), 417–438. https://doi.org/10.1002/cne.901800302

Morgante, L., Epifanio, A., Spina, E., Zappia, M., Di Rosa, A. E., Marconi, R., Basile, G., Di Raimondo, G., La Spina, P., & Quattrone, A. (2004). Quetiapine and clozapine in parkinsonian patients with dopaminergic psychosis. *Clinical Neuropharmacology*, *27*(4), 153–156. https://doi.org/10.1097/01.wnf.0000136891.17006.ec

Moukhles, H., Bosler, O., Bolam, J. P., Vallée, A., Umbriaco, D., Geffard, M., & Doucet, G. (1997). Quantitative and morphometric data indicate precise cellular interactions between serotonin terminals and postsynaptic targets in rat substantia nigra. *Neuroscience*, *76*(4), 1159–1171. https://doi.org/10.1016/S0306-4522(96)00452-6

Muñoz, A., Li, Q., Gardoni, F., Marcello, E., Qin, C., Carlsson, T., Kirik, D., Di Luca, M., Björklund, A., Bezard, E., & Carta, M. (2008). Combined 5-HT1A and 5-HT1B receptor agonists for the treatment of L-DOPA-induced dyskinesia. *Brain : A Journal of Neurology*, *131*(Pt 12), 3380–3394. https://doi.org/10.1093/brain/awn235

Muralidharan, A., Zhang, J., Ghosh, D., Johnson, M. D., Baker, K. B., & Vitek, J. L. (2017). Modulation of Neuronal Activity in the Motor Thalamus during GPi-DBS in the MPTP Nonhuman Primate Model of Parkinson's Disease. *Brain Stimulation*, *10*(1), 126–138. https://doi.org/10.1016/j.brs.2016.10.005

Muzerelle, A., Scotto-Lomassese, S., Bernard, J. F., Soiza-Reilly, M., & Gaspar, P. (2016). Conditional anterograde tracing reveals distinct targeting of individual serotonin cell groups (B5–B9) to the forebrain and brainstem. *Brain Structure and Function*, *221*(1), 535–561. https://doi.org/10.1007/s00429-014-0924-4

Nagatomo, K., Suga, S., Saitoh, M., Kogawa, M., Kobayashi, K., Yamamoto, Y., &

Yamada, K. (2017). Dopamine D1 Receptor Immunoreactivity on Fine Processes of GFAP-Positive Astrocytes in the Substantia Nigra Pars Reticulata of Adult Mouse. *Frontiers in Neuroanatomy*, *11*, 3. https://doi.org/10.3389/fnana.2017.00003

Naito, A., & Kita, H. (1994). The cortico-pallidal projection in the rat: an anterograde tracing study with biotinylated dextran amine. *Brain Research*, *653*(1–2), 251–257. https://doi.org/10.1016/0006-8993(94)90397-2

Nambu, A., Tokuno, H., Hamada, I., Kita, H., Imanishi, M., Akazawa, T., Ikeuchi, Y., & Hasegawa, N. (2000). Excitatory conical inputs to pallidal neurons via the subthalamic nucleus in the monkey. *Journal of Neurophysiology*, *84*(1), 289–300. https://doi.org/10.1152/jn.2000.84.1.289

Nambu, A., Tokuno, H., & Takada, M. (2002). Functional significance of the cortico-subthalamo-pallidal 'hyperdirect' pathway. *Neuroscience Research*, *43*(2), 111–117. https://doi.org/10.1016/S0168-0102(02)00027-5

Nambu, A., Yoshida, S. ichi, & Jinnai, K. (1990). Discharge patterns of pallidal neurons with input from various cortical areas during movement in the monkey. *Brain Research*, *519*(1–2), 183–191. https://doi.org/10.1016/0006-8993(90)90076-N

Navailles, S., Bioulac, B., Gross, C., & De Deurwaerdère, P. (2011). Chronic L-DOPA therapy alters central serotonergic function and L-DOPA-induced dopamine release in a region-dependent manner in a rat model of Parkinson's disease. *Neurobiology of Disease*, *41*(2), 585–590. https://doi.org/10.1016/j.nbd.2010.11.007

Nayebi, A. M., Rad, S. R., Saberian, M., Azimzadeh, S., & Samini, M. (2010). Buspirone improves 6-hydroxydopamine-induced catalepsy through stimulation of nigral 5-HT1a receptors in rats. *Pharmacological Reports*, *62*(2), 258–264. https://doi.org/10.1016/S1734-1140(10)70264-4

Nevalainen, N., Af Bjerkén, S., Gerhardt, G. A., & Strömberg, I. (2014). Serotonergic nerve fibers in l-DOPA-derived dopamine release and dyskinesia. *Neuroscience*, *260*, 73–86. https://doi.org/10.1016/j.neuroscience.2013.12.029

Nevalainen, N, af Bjerkén, S., Lundblad, M., Gerhardt, G. A., & Strömberg, I. (2011). Dopamine release from serotonergic nerve fibers is reduced in L-DOPA-induced dyskinesia. *Journal of Neurochemistry*, *118*(1), 12–23. https://doi.org/10.1111/j.1471-4159.2011.07292.x

Neville, K. R., & Haberly, L. B. (2003). Beta and Gamma Oscillations in the Olfactory System of the Urethane-Anesthetized Rat. *Journal of Neurophysiology*, *90*(6), 3921–3930. https://doi.org/10.1152/jn.00475.2003

Ng, C. H., Wang, X. S., & Ong, W. Y. (2000). A light and electron microscopic study of the GABA transporter GAT-3 in the monkey basal ganglia and brainstem. *Journal of Neurocytology*, *29*(8), 595–603. https://doi.org/10.1023/a:1011076219493

Ng, N. K., Lee, H. S., & Wong, P. T. (1999). Regulation of striatal dopamine release through 5-HT1 and 5-HT2 receptors. *Journal of Neuroscience Research*, *55*(5), 600–607. https://doi.org/10.1002/(SICI)1097-4547(19990301)55:5<600::AID-JNR7>3.0.CO;2-#

Ng, T. K., & Yung, K. K. (2001). Subpopulations of neurons in rat substantia nigra display GABA(B)R2 receptor immunoreactivity. *Brain Research*, *920*(1–2), 210–216. https://doi.org/10.1016/s0006-8993(01)03071-2

Nishibayashi, H., Ogura, M., Kakishita, K., Tanaka, S., Tachibana, Y., Nambu, A., Kita,

H., & Itakura, T. (2011). Cortically evoked responses of human pallidal neurons recorded during stereotactic neurosurgery. *Movement Disorders*, *26*(3), 469–476. https://doi.org/10.1002/mds.23502

Numan, S., Lundgren, K. H., Wright, D. E., Herman, J. P., & Seroogy, K. B. (1995). Increased expression of 5HT2 receptor mRNA in rat striatum following 6-OHDA lesions of the adult nigrostriatal pathway. *Molecular Brain Research*, *29*(2), 391–396. https://doi.org/10.1016/0169-328X(95)00004-C

Oh, M. Y., Abosch, A., Kim, S. H., Lang, A. E., Lozano, A. M., Benabid, A. L., Sharan, A. D., Rezai, A. R., Starr, P., & Bakay, R. A. E. (2002). Long-term hardware-related complications of deep brain stimulation. *Neurosurgery*, *50*(6), 1268–1276. https://doi.org/10.1097/00006123-200206000-00017

Oh, S. W., Harris, J. A., Ng, L., Winslow, B., Cain, N., Mihalas, S., Wang, Q., Lau, C., Kuan, L., Henry, A. M., Mortrud, M. T., Ouellette, B., Nguyen, T. N., Sorensen, S. A., Slaughterbeck, C. R., Wakeman, W., Li, Y., Feng, D., Ho, A., … Zeng, H. (2014). A mesoscale connectome of the mouse brain. *Nature*, *508*(7495), 207–214. https://doi.org/10.1038/nature13186

Ohno, Y., Shimizu, S., Tokudome, K., Kunisawa, N., & Sasa, M. (2015). New insight into the therapeutic role of the serotonergic system in Parkinson's disease. In *Progress in Neurobiology* (Vol. 134, pp. 104–121). Elsevier Ltd. https://doi.org/10.1016/j.pneurobio.2015.09.005

Olanow, C. W. (1990). Oxidation reactions in Parkinson's disease. *Neurology*, *40*(10), 32–37.

Olanow, C. Warren. (2008). Levodopa/dopamine replacement strategies in Parkinson's disease-Future directions. *Movement Disorders*, *23*(S3), S613–S622. https://doi.org/10.1002/mds.22061

Olanow, C. Warren, Goetz, C. G., Kordower, J. H., Stoessl, A. J., Sossi, V., Brin, M. F., Shannon, K. M., Nauert, G. M., Perl, D. P., Godbold, J., & Freeman, T. B. (2003). A double-blind controlled trial of bilateral fetal nigral transplantation in Parkinson's disease. *Annals of Neurology*, *54*(3), 403–414. https://doi.org/10.1002/ana.10720

Olvera-Cortés, M. E., Gutiérrez-Guzmán, B. E., López-Loeza, E., Hernández-Pérez, J. J., & López-Vázquez, M. Á. (2013). Serotonergic modulation of hippocampal theta activity in relation to hippocampal information processing. In *Experimental Brain Research* (Vol. 230, Issue 4, pp. 407–426). https://doi.org/10.1007/s00221-013-3679-x

Oorschot, D. E. (1996). Total number of neurons in the neostriatal, pallidal, subthalamic, and substantia nigral nuclei of the rat basal ganglia: A stereological study using the cavalieri and optical disector methods. *Journal of Comparative Neurology*, *366*(4), 580–599. https://doi.org/10.1002/(SICI)1096-9861(19960318)366:4<580::AID-CNE3>3.0.CO;2-0

Ostock, C. Y., Dupre, K. B., Eskow Jaunarajs, K. L., Walters, H., George, J., Krolewski, D., Walker, P. D., & Bishop, C. (2011). Role of the primary motor cortex in l-DOPA-induced dyskinesia and its modulation by 5-HT1A receptor stimulation. *Neuropharmacology*, *61*(4), 753–760. https://doi.org/10.1016/j.neuropharm.2011.05.021

Padilla, E., Shumake, J., Barrett, D. W., Sheridan, E. C., & Gonzalez-Lima, F. (2011).

Mesolimbic effects of the antidepressant fluoxetine in Holtzman rats, a genetic strain with increased vulnerability to stress. *Brain Research*, *1387*, 71–84. https://doi.org/10.1016/j.brainres.2011.02.080

Pagano, G., Rengo, G., Pasqualetti, G., Femminella, G. D., Monzani, F., Ferrara, N., & Tagliati, M. (2015). Cholinesterase inhibitors for Parkinson's disease: A systematic review and meta-analysis. *Journal of Neurology, Neurosurgery and Psychiatry*, *86*(7), 767–773. https://doi.org/10.1136/jnnp-2014-308764

Paolone, G., Brugnoli, A., Arcuri, L., Mercatelli, D., & Morari, M. (2015). Eltoprazine prevents levodopa-induced dyskinesias by reducing striatal glutamate and direct pathway activity. *Movement Disorders*, *30*(13), 1728–1738. https://doi.org/10.1002/mds.26326

Papathanou, M., Rose, S., Mccreary, A., & Jenner, P. (2011). Induction and expression of abnormal involuntary movements is related to the duration of dopaminergic stimulation in 6-OHDA-lesioned rats. *European Journal of Neuroscience*, *33*(12), 2247–2254. https://doi.org/10.1111/j.1460-9568.2011.07704.x

Parent, A., & Hazrati, L. N. (1995). Functional anatomy of the basal ganglia. I. The cortico-basal ganglia-thalamo-cortical loop. In *Brain Research Reviews* (Vol. 20, Issue 1, pp. 91–127). https://doi.org/10.1016/0165-0173(94)00007-C

Park, G., Tan, J., Garcia, G., Kang, Y., Salvesen, G., & Zhang, Z. (2016). Regulation of histone acetylation by autophagy in Parkinson disease. *Journal of Biological Chemistry*, *291*(7), 3531–3540. https://doi.org/10.1074/jbc.M115.675488

Parkinson, J. (2002). An essay on the shaking palsy. 1817. *The Journal of Neuropsychiatry and Clinical Neurosciences*, *14*(2). https://doi.org/10.1176/jnp.14.2.223

Parr-Brownlie, L. C., Poloskey, S. L., Flanagan, K. K., Eisenhofer, G., Bergstrom, D. A., & Walters, J. R. (2007). Dopamine lesion-induced changes in subthalamic nucleus activity are not associated with alterations in firing rate or pattern in layer V neurons of the anterior cingulate cortex in anesthetized rats. *European Journal of Neuroscience*, *26*(7), 1925–1939. https://doi.org/10.1111/j.1460-9568.2007.05814.x

Paxinos, G., & Watson, C. (1997). *The rat brain, in stereotaxic coordinates*. Academic Press.

Penney, J. B., & Young, A. B. (1981). GABA as the pallidothalamic neurotransmitter: implications for basal ganglia function. *Brain Research*, *207*(1), 195–199. https://doi.org/10.1016/0006-8993(81)90693-4

Perez-Lloret, S., & Rascol, O. (2018). Efficacy and safety of amantadine for the treatment of l-DOPA-induced dyskinesia. In *Journal of Neural Transmission* (Vol. 125, Issue 8, pp. 1237–1250). Springer-Verlag Wien. https://doi.org/10.1007/s00702-018-1869-1

Perkins, M. N., & Stone, T. W. (1983). Neuronal responses to 5-hydroxytryptamine and dorsal raphe stimulation within the globus pallidus of the rat. *Experimental Neurology*, *79*(1), 118–129. https://doi.org/10.1016/0014-4886(83)90383-7

Peyron, C., Petit, J. M., Rampon, C., Jouvet, M., & Luppi, P. H. (1998). Forebrain afferents to the rat dorsal raphe nucleus demonstrated by retrograde and anterograde tracing methods. *Neuroscience*, *82*(2), 443–468. https://doi.org/10.1016/s0306-

4522(97)00268-6

Picconi, B., Centonze, D., Håkansson, K., Bernardi, G., Greengard, P., Fisone, G., Cenci, M. A., & Calabresi, P. (2003). Loss of bidirectional striatal synaptic plasticity in L-DOPA-induced dyskinesia. *Nature Neuroscience*, *6*(5), 501–506. https://doi.org/10.1038/nn1040

Pich, E. M., & Samanin, R. (1986). Disinhibitory effects of buspirone and low doses of sulpiride and haloperidol in two experimental anxiety models in rats: Possible role of dopamine. *Psychopharmacology*, *89*(1), 125–130. https://doi.org/10.1007/BF00175204

Plaza-Zabala, A., Sierra-Torre, V., & Sierra, A. (2017). Autophagy and microglia: Novel partners in neurodegeneration and aging. In *International Journal of Molecular Sciences* (Vol. 18, Issue 3). MDPI AG. https://doi.org/10.3390/ijms18030598

Poewe, W., Seppi, K., Tanner, C. M., Halliday, G. M., Brundin, P., Volkmann, J., Schrag, A. E., & Lang, A. E. (2017). Parkinson disease. *Nature Reviews Disease Primers*, *3*, 1–21. https://doi.org/10.1038/nrdp.2017.13

Poisik, O. V., Shen, J. X., Jones, S., & Yakel, J. L. (2008). Functional α7-containing nicotinic acetylcholine receptors localize to cell bodies and proximal dendrites in the rat substantia nigra pars reticulata. *Journal of Physiology*, *586*(5), 1365–1378. https://doi.org/10.1113/jphysiol.2008.149963

Politis, M., Wu, K., Loane, C., Brooks, D. J., Kiferle, L., Turkheimer, F. E., Bain, P., Molloy, S., & Piccini, P. (2014a). Serotonergic mechanisms responsible for levodopa-induced dyskinesias in Parkinson's disease patients. *Journal of Clinical Investigation*, *124*(3), 1341–1349. https://doi.org/10.1172/JCI71640

Politis, M., Wu, K., Loane, C., Brooks, D. J., Kiferle, L., Turkheimer, F. E., Bain, P., Molloy, S., & Piccini, P. (2014b). Serotonergic mechanisms responsible for levodopa-induced dyskinesias in Parkinson's disease patients. *The Journal of Clinical Investigation*, *124*(3), 1340–1349. https://doi.org/10.1172/JCI71640

Politis, M., Wu, K., Loane, C., Kiferle, L., Molloy, S., Brooks, D. J., & Piccini, P. (2010). Staging of serotonergic dysfunction in Parkinson's Disease: An in vivo 11C-DASB PET study. *Neurobiology of Disease*, *40*(1), 216–221. https://doi.org/10.1016/j.nbd.2010.05.028

Pollak Dorocic, I., Fürth, D., Xuan, Y., Johansson, Y., Pozzi, L., Silberberg, G., Carlén, M., & Meletis, K. (2014). A whole-brain atlas of inputs to serotonergic neurons of the dorsal and median raphe nuclei. *Neuron*, *83*(3), 663–678. https://doi.org/10.1016/j.neuron.2014.07.002

Polymeropoulos, M. H., Lavedan, C., Leroy, E., Ide, S. E., Dehejia, A., Dutra, A., Pike, B., Root, H., Rubenstein, J., Boyer, R., Stenroos, E. S., Chandrasekharappa, S., Athanassiadou, A., Papapetropoulos, T., Johnson, W. G., Lazzarini, A. M., Duvoisin, R. C., Di Iorio, G., Golbe, L. I., & Nussbaum, R. L. (1997). Mutation in the α-synuclein gene identified in families with Parkinson's disease. *Science*, *276*(5321), 2045–2047. https://doi.org/10.1126/science.276.5321.2045

Pontone, G. M., Williams, J. R., Anderson, K. E., Chase, G., Goldstein, S. A., Grill, S., Hirsch, E. S., Lehmann, S., Little, J. T., Margolis, R. L., Rabins, P. V, Weiss, H. D., & Marsh, L. (2009). Prevalence of anxiety disorders and anxiety subtypes in patients with Parkinson's disease. *Movement Disorders : Official Journal of the Movement*

Disorder Society, *24*(9), 1333–1338. https://doi.org/10.1002/mds.22611

Postuma, R. B., Gagnon, J. F., Vendette, M., & Montplaisir, J. Y. (2009). Markers of neurodegeneration in idiopathic rapid eye movement sleep behaviour disorder and Parkinson's disease. *Brain*, *132*(12), 3298–3307. https://doi.org/10.1093/brain/awp244

Prinssen, E. P. M., Colpaert, F. C., & Koek, W. (2002). 5-HT1A receptor activation and anti-cataleptic effects: high-efficacy agonists maximally inhibit haloperidol-induced catalepsy. *European Journal of Pharmacology*, *453*(2–3), 217–221. https://doi.org/10.1016/s0014-2999(02)02430-5

Prinz, A., Selesnew, L.-M., Liss, B., Roeper, J., & Carlsson, T. (2013). Increased excitability in serotonin neurons in the dorsal raphe nucleus in the 6-OHDA mouse model of Parkinson's disease. *Experimental Neurology*, *248*, 236–245. https://doi.org/10.1016/j.expneurol.2013.06.015

Puspita, L., Chung, S. Y., & Shim, J.-W. (2017). Oxidative stress and cellular pathologies in Parkinson's disease. *Molecular Brain*, *10*(1), 53. https://doi.org/10.1186/s13041-017-0340-9

Radja, F., Descarries, L., Dewar, K. M., & Reader, T. A. (1993). Serotonin 5-HT1 and 5-HT2 receptors in adult rat brain after neonatal destruction of nigrostriatal dopamine neurons: a quantitative autoradiographic study. *Brain Research*, *606*(2), 273–285. https://doi.org/10.1016/0006-8993(93)90995-Y

Rajakumar, N., Elisevich, K., & Flumerfelt, B. A. (1994). Parvalbumin-containing GABAergic neurons in the basal ganglia output system of the rat. *Journal of Comparative Neurology*, *350*(2), 324–336. https://doi.org/10.1002/cne.903500214

Ramirez-Zamora, A., & Ostrem, J. L. (2018). Globus Pallidus Interna or Subthalamic Nucleus Deep Brain Stimulation for Parkinson Disease: A Review. *JAMA Neurology*, *75*(3), 367–372. https://doi.org/10.1001/jamaneurol.2017.4321

Rampello, L., Chiechio, S., Raffaele, R., Vecchio, I., & Nicoletti, F. (2002). The SSRI, citalopram, improves bradykinesia in patients with Parkinson's disease treated with L-dopa. *Clinical Neuropharmacology*, *25*(1), 21–24. https://doi.org/10.1097/00002826-200201000-00004

Ravina, B., Marder, K., Fernandez, H. H., Friedman, J. H., McDonald, W., Murphy, D., Aarsland, D., Babcock, D., Cummings, J., Endicott, J., Factor, S., Galpern, W., Lees, A., Marsh, L., Stacy, M., Gwinn-Hardy, K., Voon, V., & Goetz, C. (2007). Diagnostic criteria for psychosis in Parkinson's disease: Report of an NINDS, NIMH Work Group. In *Movement Disorders* (Vol. 22, Issue 8, pp. 1061–1068). https://doi.org/10.1002/mds.21382

Rebec, G. V, & Lee, E. H. (1982). Differential subsensitivity of dopaminergic and neostriatal neurons to apomorphine with long-term treatment. *Brain Research*, *250*(1), 188–192. https://doi.org/10.1016/0006-8993(82)90968-4

Reijnders, J. S. A. M., Ehrt, U., Weber, W. E. J., Aarsland, D., & Leentjens, A. F. G. (2008). A systematic review of prevalence studies of depression in Parkinson's disease. In *Movement Disorders* (Vol. 23, Issue 2, pp. 183–189). https://doi.org/10.1002/mds.21803

Reiner, A, & Anderson, K. D. (1993). Co-occurrence of gamma-aminobutyric acid, parvalbumin and the neurotensin-related neuropeptide LANT6 in pallidal, nigral and

striatal neurons in pigeons and monkeys. *Brain Research*, *624*(1–2), 317–325. https://doi.org/10.1016/0006-8993(93)90096-6

Reiner, Anton, & Anderson, K. D. (1990). The patterns of neurotransmitter and neuropeptide co-occurrence among striatal projection neurons: conclusions based on recent findings. In *Brain Research Reviews* (Vol. 15, Issue 3, pp. 251–265). Brain Res Brain Res Rev. https://doi.org/10.1016/0165-0173(90)90003-7

Rentsch, P., Stayte, S., Morris, G. P., & Vissel, B. (2019). Time dependent degeneration of the nigrostriatal tract in mice with 6-OHDA lesioned medial forebrain bundle and the effect of activin A on l-Dopa induced dyskinesia. *BMC Neuroscience*, *20*(1). https://doi.org/10.1186/s12868-019-0487-7

Reyes, J. F., Olsson, T. T., Lamberts, J. T., Devine, M. J., Kunath, T., & Brundin, P. (2015). A cell culture model for monitoring α-synuclein cell-to-cell transfer. *Neurobiology of Disease*, *77*, 266–275. https://doi.org/10.1016/j.nbd.2014.07.003

Riahi, G., Morissette, M., Lévesque, D., Rouillard, C., Samadi, P., Parent, M., & Paolo, T. Di. (2012). Effect of chronic l-DOPA treatment on 5-HT1A receptors in parkinsonian monkey brain. *Neurochemistry International*, *61*(7), 1160–1171. https://doi.org/10.1016/j.neuint.2012.08.009

Rice, P. (1984). The early diagnosis of Parkinson's disease. *Australian Family Physician*, *13*(5 Suppl), 4–5. https://doi.org/10.1212/wnl.49.1_suppl_1.s10

Riha, P. D., Rojas, J. C., & Gonzalez-Lima, F. (2011). Beneficial network effects of methylene blue in an amnestic model. *NeuroImage*, *54*(4), 2623–2634. https://doi.org/10.1016/j.neuroimage.2010.11.023

Rivera, A., Trías, S., Peñafiel, A., Narváez, J. Á., Díaz-Cabiale, Z., Moratalla, R., & De La Calle, A. (2003). Expression of D4 dopamine receptors in striatonigral and striatopallidal neurons in the rat striatum. *Brain Research*, *989*(1), 35–41. https://doi.org/10.1016/S0006-8993(03)03328-6

Rizzi, G., & Tan, K. R. (2019). Synergistic Nigral Output Pathways Shape Movement. *Cell Reports*, *27*(7), 2184-2198.e4. https://doi.org/10.1016/j.celrep.2019.04.068

Robbins, T. W., & Cools, R. (2014). Cognitive deficits in Parkinson's disease: a cognitive neuroscience perspective. *Movement Disorders : Official Journal of the Movement Disorder Society*, *29*(5), 597–607. https://doi.org/10.1002/mds.25853

Rommelfanger, K. S., & Wichmann, T. (2010). Extrastriatal dopaminergic circuits of the Basal Ganglia. *Frontiers in Neuroanatomy*, *4*(OCT), 139. https://doi.org/10.3389/fnana.2010.00139

Root, D. H., Zhang, S., Barker, D. J., Miranda-Barrientos, J., Liu, B., Wang, H. L., & Morales, M. (2018). Selective Brain Distribution and Distinctive Synaptic Architecture of Dual Glutamatergic-GABAergic Neurons. *Cell Reports*, *23*(12), 3465–3479. https://doi.org/10.1016/j.celrep.2018.05.063

Rosenberg, J. R., Amjad, A. M., Breeze, P., Brillinger, D. R., & Halliday, D. M. (1989). The Fourier approach to the identification of functional coupling between neuronal spike trains. *Progress in Biophysics and Molecular Biology*, *53*(1), 1–31. https://doi.org/10.1016/0079-6107(89)90004-7

Roussakis, A. A., Politis, M., Towey, D., & Piccini, P. (2016). Serotonin-to-dopamine transporter ratios in Parkinson disease. *Neurology*, *86*(12), 1152–1158. https://doi.org/10.1212/WNL.0000000000002494

7. References

Ruskin, D. N., Bergstrom, D. A., & Walters, J. R. (2002). Nigrostriatal lesion and dopamine agonists affect firing patterns of rodent entopeduncular nucleus neurons. *Journal of Neurophysiology*, *88*(1), 487–496. https://doi.org/10.1152/jn.00844.2001

Rylander, D., Parent, M., O'Sullivan, S. S., Dovero, S., Lees, A. J., Bezard, E., Descarries, L., & Cenci, M. A. (2010). Maladaptive plasticity of serotonin axon terminals in levodopa-induced dyskinesia. *Annals of Neurology*, *68*(5), 619–628. https://doi.org/10.1002/ana.22097

Sagarduy, A., Llorente, J., Miguelez, C., Morera-Herreras, T., Ruiz-Ortega, J. A., & Ugedo, L. (2016). Buspirone requires the intact nigrostriatal pathway to reduce the activity of the subthalamic nucleus via 5-HT1A receptors. *Experimental Neurology*, *277*, 35–45. https://doi.org/10.1016/j.expneurol.2015.12.005

Sakaue, M., Somboonthum, P., Nishihara, B., Koyama, Y., Hashimoto, H., Baba, A., & Matsuda, T. (2000). Postsynaptic 5-hydroxytryptamine(1A) receptor activation increases in vivo dopamine release in rat prefrontal cortex. *British Journal of Pharmacology*, *129*(5), 1028–1034. https://doi.org/10.1038/sj.bjp.0703139

Salvadè, A., D'Angelo, V., Di Giovanni, G., Tinkhauser, G., Sancesario, G., Städler, C., Möller, J. C., Stefani, A., Kaelin-Lang, A., & Galati, S. (2016). Distinct roles of cortical and pallidal β and γ frequencies in hemiparkinsonian and dyskinetic rats. *Experimental Neurology*, *275 Pt 1*, 199–208. https://doi.org/10.1016/j.expneurol.2015.11.005

Samii, A., Nutt, J. G., & Ransom, B. R. (2004). Parkinson's disease. *Lancet*, *363*(9423), 1783–1793. https://doi.org/10.1016/S0140-6736(04)16305-8

San Sebastian, W., Samaranch, L., Kells, A. P., Forsayeth, J., & Bankiewicz, K. S. (2013). Gene Therapy for Misfolding Protein Diseases of the Central Nervous System. In *Neurotherapeutics* (Vol. 10, Issue 3, pp. 498–510). Springer. https://doi.org/10.1007/s13311-013-0191-8

Sano, H., & Nambu, A. (2019). The effects of zonisamide on L-DOPA-induced dyskinesia in Parkinson's disease model mice. *Neurochemistry International*, *124*, 171–180. https://doi.org/10.1016/j.neuint.2019.01.011

Santini, E., Alcacer, C., Cacciatore, S., Heiman, M., Hervé, D., Greengard, P., Girault, J. A., Valjent, E., & Fisone, G. (2009). L-DOPA activates ERK signaling and phosphorylates histone H3 in the striatonigral medium spiny neurons of hemiparkinsonian mice. *Journal of Neurochemistry*, *108*(3), 621–633. https://doi.org/10.1111/j.1471-4159.2008.05831.x

Santini, E., Valjent, E., Usiello, A., Carta, M., Borgkvist, A., Girault, J. A., Hervé, D., Greengard, P., & Fisone, G. (2007). Critical involvement of cAMP/DARPP-32 and extracellular signal-regulated protein kinase signaling in L-DOPA-induced dyskinesia. *Journal of Neuroscience*, *27*(26), 6995–7005. https://doi.org/10.1523/JNEUROSCI.0852-07.2007

Saunders, A., Huang, K. W., & Sabatini, B. L. (2016). Globus Pallidus Externus Neurons Expressing parvalbumin Interconnect the Subthalamic Nucleus and Striatal Interneurons. *PLoS ONE*, *11*(2). https://doi.org/10.1371/journal.pone.0149798

Schallert, T., Fleming, S. M., Leasure, J. L., Tillerson, J. L., & Bland, S. T. (2000). CNS plasticity and assessment of forelimb sensorimotor outcome in unilateral rat models of stroke, cortical ablation, parkinsonism and spinal cord injury.

Neuropharmacology, *39*(5), 777–787. https://doi.org/10.1016/S0028-3908(00)00005-8

Schapira, A. H. V., Mann, V. M., Cooper, J. M., Dexter, D., Daniel, S. E., Jenner, P., Clark, J. B., & Marsden, C. D. (1990). Anatomic and Disease Specificity of NADH CoQ1 Reductase (Complex I) Deficiency in Parkinson's Disease. *Journal of Neurochemistry*, *55*(6), 2142–2145. https://doi.org/10.1111/j.1471-4159.1990.tb05809.x

Schenk, D. B., Koller, M., Ness, D. K., Griffith, S. G., Grundman, M., Zago, W., Soto, J., Atiee, G., Ostrowitzki, S., & Kinney, G. G. (2017). First-in-human assessment of PRX002, an anti–α-synuclein monoclonal antibody, in healthy volunteers. *Movement Disorders*, *32*(2), 211–218. https://doi.org/10.1002/mds.26878

Schroeder, J. A., & Schneider, J. S. (2002). GABAA and μ-opioid receptor binding in the globus pallidus and entopeduncular nucleus of animals symptomatic for and recovered from experimental parkinsonism. *Brain Research*, *947*(2), 284–289. https://doi.org/10.1016/S0006-8993(02)03010-X

Schwarting, R. K. W., & Huston, J. P. (1996). Unilateral 6-hydroxydopamine lesions of meso-striatal dopamine neurons and their physiological sequelae. *Progress in Neurobiology*, *49*(3), 215–266. https://doi.org/10.1016/S0301-0082(96)00015-9

Seirafi, M., Kozlov, G., & Gehring, K. (2015). Parkin structure and function. In *FEBS Journal* (Vol. 282, Issue 11, pp. 2076–2088). Blackwell Publishing Ltd. https://doi.org/10.1111/febs.13249

Sethi, K. (2008). Levodopa unresponsive symptoms in Parkinson disease. In *Movement Disorders* (Vol. 23, Issue SUPPL. 3, pp. S521-33). https://doi.org/10.1002/mds.22049

Shannak, K., Rajput, A., Rozdilsky, B., Kish, S., Gilbert, J., & Hornykiewicz, O. (1994). Noradrenaline, dopamine and serotonin levels and metabolism in the human hypothalamus: observations in Parkinson's disease and normal subjects. *Brain Research*, *639*(1), 33–41. http://www.ncbi.nlm.nih.gov/pubmed/8180836

Sharif, N. A., & Hughes, J. (1989). Discrete mapping of brain mu and delta opioid receptors using selective peptides: Quantitative autoradiography, species differences and comparison with kappa receptors. *Peptides*, *10*(3), 499–522. https://doi.org/10.1016/0196-9781(89)90135-6

Sharott, A., Gulberti, A., Zittel, S., Tudor Jones, A. A., Fickel, U., Münchau, A., Köppen, J. A., Gerloff, C., Westphal, M., Buhmann, C., Hamel, W., Engel, A. K., & Moll, C. K. E. (2014). Activity parameters of subthalamic nucleus neurons selectively predict motor symptom severity in Parkinson's disease. *Journal of Neuroscience*, *34*(18), 6273–6285. https://doi.org/10.1523/JNEUROSCI.1803-13.2014

Shi, L.-H., Luo, F., Woodward, D. J., & Chang, J.-Y. (2006). Basal ganglia neural responses during behaviorally effective deep brain stimulation of the subthalamic nucleus in rats performing a treadmill locomotion test. *Synapse (New York, N.Y.)*, *59*(7), 445–457. https://doi.org/10.1002/syn.20261

Shimizu, S., Mizuguchi, Y., Tatara, A., Kizu, T., Andatsu, S., Sobue, A., Fujiwara, M., Morimoto, T., & Ohno, Y. (2013). 5-HT1A agonist alleviates serotonergic potentiation of extrapyramidal disorders via postsynaptic mechanisms. *Progress in Neuro-Psychopharmacology and Biological Psychiatry*, *46*, 86–91.

https://doi.org/10.1016/j.pnpbp.2013.06.016

Shimohama, S., Sawada, H., Kitamura, Y., & Taniguchi, T. (2003). Disease model: Parkinson's disease. In *Trends in Molecular Medicine* (Vol. 9, Issue 8, pp. 360–365). Elsevier Ltd. https://doi.org/10.1016/S1471-4914(03)00117-5

Shin, E., Lisci, C., Tronci, E., Fidalgo, C., Stancampiano, R., Björklund, A., & Carta, M. (2014). The anti-dyskinetic effect of dopamine receptor blockade is enhanced in parkinsonian rats following dopamine neuron transplantation. *Neurobiology of Disease*, *62*, 233–240. https://doi.org/10.1016/j.nbd.2013.09.021

Silverstone, P. H., Lalies, M. D., & Hudson, A. L. (2012). Quetiapine and Buspirone Both Elevate Cortical Levels of Noradrenaline and Dopamine In vivo, but Do Not have Synergistic Effects. *Frontiers in Psychiatry*, *3*(SEP), 82. https://doi.org/10.3389/fpsyt.2012.00082

Singh, A., Liang, L., Kaneoke, Y., Cao, X., & Papa, S. M. (2015). Dopamine regulates distinctively the activity patterns of striatal output neurons in advanced parkinsonian primates. *Journal of Neurophysiology*, *113*(5), 1533–1544. https://doi.org/10.1152/jn.00910.2014

Soiza-Reilly, M., & Commons, K. G. (2011). Glutamatergic drive of the dorsal raphe nucleus. In *Journal of Chemical Neuroanatomy* (Vol. 41, Issue 4, pp. 247–255). NIH Public Access. https://doi.org/10.1016/j.jchemneu.2011.04.004

Spillantini, M. G., Crowther, R. A., Jakes, R., Hasegawa, M., & Goedert, M. (1998). α-Synuclein in filamentous inclusions of Lewy bodies from Parkinson's disease and dementia with Lewy bodies. *Proceedings of the National Academy of Sciences of the United States of America*, *95*(11), 6469–6473. https://doi.org/10.1073/pnas.95.11.6469

Stansley, B. J., & Yamamoto, B. K. (2014). Chronic L-Dopa Decreases Serotonin Neurons in a Subregion of the Dorsal Raphe Nucleus. *Journal of Pharmacology and Experimental Therapeutics*, *351*(2), 440–447. https://doi.org/10.1124/jpet.114.218966

Stansley, B. J., & Yamamoto, B. K. (2015). L-Dopa and Brain Serotonin System Dysfunction. *Toxics*, *3*(1), 75–88. https://doi.org/10.3390/toxics3010075

Stansley, B. J., & Yamamoto, B. K. (2014). Chronic L-Dopa decreases serotonin neurons in a subregion of the dorsal raphe nucleus. *Journal of Pharmacology and Experimental Therapeutics*, *351*(2), 440–447. https://doi.org/10.1124/jpet.114.218966

Stansley, B. J., & Yamamoto, B. K. (2015). Behavioral impairments and serotonin reductions in rats after chronic L-dopa. *Psychopharmacology*, *232*(17), 3203–3213. https://doi.org/10.1007/s00213-015-3980-4

Starr, P. A., Rau, G. M., Davis, V., Marks, W. J., Ostrem, J. L., Simmons, D., Lindsey, N., & Turner, R. S. (2005). Spontaneous pallidal neuronal activity in human dystonia: Comparison with Parkinson's disease and normal macaque. *Journal of Neurophysiology*, *93*(6), 3165–3176. https://doi.org/10.1152/jn.00971.2004

Starr, P. A., Vitek, J. L., & Bakay, R. A. E. (1998). Ablative surgery and deep brain stimulation for Parkinson's disease. In *Neurosurgery* (Vol. 43, Issue 5, pp. 989–1013). https://doi.org/10.1097/00006123-199811000-00001

Steinbusch, H. W. M., Niewenhuys, R., Verhofstad, A. A. J., & Van Der Kooy, D. (1981).

The nucleus raphe dorsalis of the rat and its projection upon the caudatoputamen. A combined cytoarchitectonic, immunohistochemical and retrograde transport study. *Journal de Physiologie*, *77*(2–3), 157–174.

Stephenson-Jones, M., Yu, K., Ahrens, S., Tucciarone, J. M., Van Huijstee, A. N., Mejia, L. A., Penzo, M. A., Tai, L. H., Wilbrecht, L., & Li, B. (2016). A basal ganglia circuit for evaluating action outcomes. *Nature*, *539*(7628), 289–293. https://doi.org/10.1038/nature19845

Steriade, M. (2006). Grouping of brain rhythms in corticothalamic systems. In *Neuroscience* (Vol. 137, Issue 4, pp. 1087–1106). Elsevier Ltd. https://doi.org/10.1016/j.neuroscience.2005.10.029

Sun, W., Sugiyama, K., Asakawa, T., Yamaguchi, H., Akamine, S., Ouchi, Y., Magata, Y., & Namba, H. (2011). Dynamic changes of striatal dopamine D 2 receptor binding at later stages after unilateral lesions of the medial forebrain bundle in Parkinsonian rat models. *Neuroscience Letters*, *496*(3), 157–162. https://doi.org/10.1016/j.neulet.2011.04.006

Surmeier, D. J., Halliday, G. M., & Simuni, T. (2017). Calcium, mitochondrial dysfunction and slowing the progression of Parkinson's disease. In *Experimental Neurology* (Vol. 298, Issue Pt B, pp. 202–209). Academic Press Inc. https://doi.org/10.1016/j.expneurol.2017.08.001

Surmeier, D. J., Schumacker, P. T., Guzman, J. D., Ilijic, E., Yang, B., & Zampese, E. (2017). Calcium and Parkinson's disease. In *Biochemical and Biophysical Research Communications* (Vol. 483, Issue 4, pp. 1013–1019). Elsevier B.V. https://doi.org/10.1016/j.bbrc.2016.08.168

Surmeier, D. J. (2018). Determinants of dopaminergic neuron loss in Parkinson's disease. In *FEBS Journal* (Vol. 285, Issue 19, pp. 3657–3668). Blackwell Publishing Ltd. https://doi.org/10.1111/febs.14607

Svenningsson, P., Rosenblad, C., af Edholm Arvidsson, K., Wictorin, K., Keywood, C., Shankar, B., Lowe, D. A., Björklund, A., & Widner, H. (2015). Eltoprazine counteracts l-DOPA-induced dyskinesias in Parkinson's disease: a dose-finding study. *Brain*, *138*(4), 963–973. https://doi.org/10.1093/brain/awu409

Svíženská, I., Dubový, P., & Šulcová, A. (2008). Cannabinoid receptors 1 and 2 (CB1 and CB2), their distribution, ligands and functional involvement in nervous system structures - A short review. In *Pharmacology Biochemistry and Behavior* (Vol. 90, Issue 4, pp. 501–511). https://doi.org/10.1016/j.pbb.2008.05.010

Tachibana, Y., Kita, H., Chiken, S., Takada, M., & Nambu, A. (2008). Motor cortical control of internal pallidal activity through glutamatergic and GABAergic inputs in awake monkeys. *European Journal of Neuroscience*, *27*(1), 238–253. https://doi.org/10.1111/j.1460-9568.2007.05990.x

Takada, M., Tokuno, H., Ikai, Y., & Mizuno, N. (1994). Direct projections from the entopeduncular nucleus to the lower brainstem in the rat. *The Journal of Comparative Neurology*, *342*(3), 409–429. https://doi.org/10.1002/cne.903420308

Takahashi, A., Lee, R. X., Iwasato, T., Itohara, S., Arima, H., Bettler, B., Miczek, K. A., & Koide, T. (2015). Glutamate input in the dorsal raphe nucleus as a determinant of escalated aggression in male mice. *Journal of Neuroscience*, *35*(16), 6452–6463. https://doi.org/10.1523/JNEUROSCI.2450-14.2015

7. References

Takahashi, M., Tabu, H., Ozaki, A., Hamano, T., Takeshima, T., & REBORN study group. (2018). Antidepressants for Depression, Apathy, and Gait Instability in Parkinson's Disease: A Multicenter Randomized Study. *Internal Medicine (Tokyo, Japan)*. https://doi.org/10.2169/internalmedicine.1359-18

Tan, S. K. H., Janssen, M. L. F., Jahanshahi, A., Chouliaras, L., Visser-Vandewalle, V., Lim, L. W., Steinbusch, H. W. M., Sharp, T., & Temel, Y. (2011). High frequency stimulation of the subthalamic nucleus increases c-fos immunoreactivity in the dorsal raphe nucleus and afferent brain regions. *Journal of Psychiatric Research*, *45*(10), 1307–1315. https://doi.org/10.1016/j.jpsychires.2011.04.011

Tanner, C. M. (1989). The role of environmental toxins in the etiology of Parkinson's disease. *Trends in Neurosciences*, *12*(2), 49–54. https://doi.org/10.1016/0166-2236(89)90135-5

Tanner, C. M. (2010). Advances in environmental epidemiology. *Movement Disorders*, *25*(SUPPL. 1), S58-62. https://doi.org/10.1002/mds.22721

Tatton, W. G., & Olanow, C. W. (1999). Apoptosis in neurodegenerative diseases: the role of mitochondria. *Biochimica et Biophysica Acta*, *1410*(2), 195–213. https://doi.org/10.1016/s0005-2728(98)00167-4

Tatton, William G., Chalmers-Redman, R., Brown, D., Tatton, N., Schapira, Hunot, Olanow, Isacson, & Stocchi. (2003). Apoptosis in Parkinson's disease: Signals for neuronal degradation. In *Annals of Neurology* (Vol. 53, Issue SUPPL. 3, pp. S61-70; discussion S70-2). https://doi.org/10.1002/ana.10489

Temel, Y., Visser-Vandewalle, V., Aendekerk, B., Rutten, B., Tan, S., Scholtissen, B., Schmitz, C., Blokland, A., & Steinbusch, H. W. M. (2005). Acute and separate modulation of motor and cognitive performance in parkinsonian rats by bilateral stimulation of the subthalamic nucleus. *Experimental Neurology*, *193*(1), 43–52. https://doi.org/10.1016/j.expneurol.2004.12.025

Tempel, A., & Zukin, R. S. (1987). Neuroanatomical patterns of the mu, delta, and kappa opioid receptors of rat brain as determined by quantitative in vitro autoradiography. *Proceedings of the National Academy of Sciences of the United States of America*, *84*(12), 4308–4312. https://doi.org/10.1073/pnas.84.12.4308

Tepper, J. M., & Bolam, J. P. (2004). Functional diversity and specificity of neostriatal interneurons. In *Current Opinion in Neurobiology* (Vol. 14, Issue 6, pp. 685–692). https://doi.org/10.1016/j.conb.2004.10.003

Tepper, J. M., Koós, T., Ibanez-Sandoval, O., Tecuapetla, F., Faust, T. W., & Assous, M. (2018). Heterogeneity and diversity of striatal GABAergic interneurons: Update 2018. In *Frontiers in Neuroanatomy* (Vol. 12). Frontiers Media S.A. https://doi.org/10.3389/fnana.2018.00091

Thiruchelvam, M., Brockel, B. J., Richfield, E. K., Baggs, R. B., & Cory-Slechta, D. A. (2000). Potentiated and preferential effects of combined paraquat and maneb on nigrostriatal dopamine systems: Environmental risk factors for Parkinson's disease? *Brain Research*, *873*(2), 225–234. https://doi.org/10.1016/S0006-8993(00)02496-3

Tian, J., Yan, Y., Xi, W., Zhou, R., Lou, H., Duan, S., Chen, J. F., & Zhang, B. (2018). Optogenetic stimulation of GABAergic neurons in the globus pallidus produces hyperkinesia. *Frontiers in Behavioral Neuroscience*, *12*. https://doi.org/10.3389/fnbeh.2018.00185

Toulorge, D., Schapira, A. H. V, & Hajj, R. (2016). Molecular changes in the postmortem parkinsonian brain. *Journal of Neurochemistry*, *139 Suppl 1*, 27–58. https://doi.org/10.1111/jnc.13696

Tronci, E., Napolitano, F., Muñoz, A., Fidalgo, C., Rossi, F., Björklund, A., Usiello, A., & Carta, M. (2017). BDNF over-expression induces striatal serotonin fiber sprouting and increases the susceptibility to L-DOPA-induced dyskinesia in 6-OHDA-lesioned rats. *Experimental Neurology*, *297*, 73–81. https://doi.org/10.1016/j.expneurol.2017.07.017

Tseng, K. Y., Kasanetz, F., Kargieman, L., Riquelme, L. A., & Murer, M. G. (2001). Cortical slow oscillatory activity is reflected in the membrane potential and spike trains of striatal neurons in rats with chronic nigrostriatal lesions. *Journal of Neuroscience*, *21*(16), 6430–6439. https://doi.org/10.1523/jneurosci.21-16-06430.2001

Tseng, K. Y., Riquelme, L. A., Belforte, J. E., Pazo, J. H., & Murer, M. G. (2000). Substantia nigra pars reticulata units in 6-hydroxydopamine-lesioned rats: responses to striatal D2 dopamine receptor stimulation and subthalamic lesions. *The European Journal of Neuroscience*, *12*(1), 247–256. https://doi.org/10.1046/j.1460-9568.2000.00910.x

Turski, L., Havemann, U., & Kuschinsky, K. (1984). Role of muscarinic cholinergic mechanisms in the substantia nigra pars reticulata in mediating muscular rigidity in rats. *Naunyn-Schmiedeberg's Archives of Pharmacology*, *327*(1), 14–17. https://doi.org/10.1007/bf00504985

Tysnes, O.-B., & Storstein, A. (2017). Epidemiology of Parkinson's disease. *Journal of Neural Transmission (Vienna, Austria : 1996)*, *124*(8), 901–905. https://doi.org/10.1007/s00702-017-1686-y

Uhlhaas, P. J., & Singer, W. (2006). Neural Synchrony in Brain Disorders: Relevance for Cognitive Dysfunctions and Pathophysiology. In *Neuron* (Vol. 52, Issue 1, pp. 155–168). https://doi.org/10.1016/j.neuron.2006.09.020

Ungerstedt, U. (1968). 6-hydroxy-dopamine induced degeneration of central monoamine neurons. *European Journal of Pharmacology*, *5*(1), 107–110. https://doi.org/10.1016/0014-2999(68)90164-7

Van De Vijver, D. A. M. C., Roos, R. A. C., Jansen, P. A. F., Porsius, A. J., & De Boer, A. (2002). Start of a selective serotonin reuptake inhibitor (SSRI) and increase of antiparkinsonian drug treatment in patients on levodopa. *British Journal of Clinical Pharmacology*, *54*(2), 168–170. https://doi.org/10.1046/j.1365-2125.2001.01491.x

Vande Walle, L., Lamkanfi, M., & Vandenabeele, P. (2008). The mitochondrial serine protease HtrA2/Omi: An overview. In *Cell Death and Differentiation* (Vol. 15, Issue 3, pp. 453–460). https://doi.org/10.1038/sj.cdd.4402291

VanderMaelen, C. P., Matheson, G. K., Wilderman, R. C., & Patterson, L. A. (1986). Inhibition of serotonergic dorsal raphe neurons by systemic and iontophoretic administration of buspirone, a non-benzodiazepine anxiolytic drug. *European Journal of Pharmacology*, *129*(1–2), 123–130. https://doi.org/10.1016/0014-2999(86)90343-2

Vanderwolf, C. H. (1969). Hippocampal electrical activity and voluntary movement in the rat. *Electroencephalography and Clinical Neurophysiology*, *26*(4), 407–418.

https://doi.org/10.1016/0013-4694(69)90092-3

Vegas-Suarez, S., Paredes-Rodriguez, E., Aristieta, A., Lafuente, J. V, Miguelez, C., & Ugedo, L. (2019). Dysfunction of serotonergic neurons in Parkinson's disease and dyskinesia. *International Review of Neurobiology*, *146*, 259–279. https://doi.org/10.1016/bs.irn.2019.06.013

Vélez-Hernández, M. E., Padilla, E., Gonzalez-Lima, F., & Jiménez-Rivera, C. A. (2014). Cocaine reduces cytochrome oxidase activity in the prefrontal cortex and modifies its functional connectivity with brainstem nuclei. *Brain Research*, *1542*, 56–69. https://doi.org/10.1016/j.brainres.2013.10.017

Verma, M., Wills, Z., & Chu, C. T. (2018). Excitatory dendritic mitochondrial calcium toxicity: Implications for Parkinson's and other neurodegenerative diseases. In *Frontiers in Neuroscience* (Vol. 12, Issue AUG, p. 523). Frontiers Media S.A. https://doi.org/10.3389/fnins.2018.00523

Vertes, R. P., Kinney, G. G., Kocsis, B., & Fortin, W. J. (1994). Pharmacological suppression of the median raphe nucleus with serotonin1a agonists, 8-OH-DPAT and buspirone, produces hippocampal theta rhythm in the rat. *Neuroscience*, *60*(2), 441–451. https://doi.org/10.1016/0306-4522(94)90255-0

Vijayakumar, D., & Jankovic, J. (2016a). Drug-Induced Dyskinesia, Part 1: Treatment of Levodopa-Induced Dyskinesia. In *Drugs* (Vol. 76, Issue 7, pp. 759–777). Springer International Publishing. https://doi.org/10.1007/s40265-016-0566-3

Vijayakumar, D., & Jankovic, J. (2016b). Drug-Induced Dyskinesia, Part 2: Treatment of Tardive Dyskinesia. In *Drugs* (Vol. 76, Issue 7, pp. 779–787). Springer International Publishing. https://doi.org/10.1007/s40265-016-0568-1

Vila, M., Levy, R., Herrero, M. T., Faucheux, B., Obeso, J. A., Agid, Y., & Hirsch, E. C. (1996). Metabolic activity of the basal ganglia in parkinsonian syndromes in human and non-human primates: a cytochrome oxidase histochemistry study. *Neuroscience*, *71*(4), 903–912. https://doi.org/10.1016/0306-4522(95)00549-8

Vila, M., Levy, R., Herrero, M. T., Ruberg, M., Faucheux, B., Obeso, J. A., Agid, Y., & Hirsch, E. C. (1997). Consequences of nigrostriatal denervation on the functioning of the basal ganglia in human and nonhuman primates: an in situ hybridization study of cytochrome oxidase subunit I mRNA. *The Journal of Neuroscience : The Official Journal of the Society for Neuroscience*, *17*(2), 765–773. http://www.ncbi.nlm.nih.gov/pubmed/8987798

Visanji, N. P., Gomez-Ramirez, J., Johnston, T. H., Pires, D., Voon, V., Brotchie, J. M., & Fox, S. H. (2006). Pharmacological characterization of psychosis-like behavior in the MPTP-lesioned nonhuman primate model of Parkinson's disease. *Movement Disorders*, *21*(11), 1879–1891. https://doi.org/10.1002/mds.21073

Vizuete, M. L., Traiffort, E., Bouthenet, M. L., Ruat, M., Souil, E., Tardivel-Lacombe, J., & Schwartz, J. C. (1997). Detailed mapping of the histamine H2 receptor and its gene transcripts in guinea-pig brain. *Neuroscience*, *80*(2), 321–343. https://doi.org/10.1016/s0306-4522(97)00010-9

Walker, M., Kuebler, L., Goehring, C. M., Pichler, B. J., & Herfert, K. (2019). Imaging SERT Availability in a Rat Model of L-DOPA-Induced Dyskinesia. *Molecular Imaging and Biology*. https://doi.org/10.1007/s11307-019-01418-2

Wallace, M. L., Saunders, A., Huang, K. W., Philson, A. C., Goldman, M., Macosko, E.

Z., McCarroll, S. A., & Sabatini, B. L. (2017). Genetically Distinct Parallel Pathways in the Entopeduncular Nucleus for Limbic and Sensorimotor Output of the Basal Ganglia. *Neuron*, *94*(1), 138-152.e5. https://doi.org/10.1016/j.neuron.2017.03.017

Wallman, M.-J., Gagnon, D., & Parent, M. (2011). Serotonin innervation of human basal ganglia. *The European Journal of Neuroscience*, *33*(8), 1519–1532. https://doi.org/10.1111/j.1460-9568.2011.07621.x

Walters, J. R. (2016). Abnormal Activities in Cortico-Basal Ganglia Circuits in Movement Disorders. In *Handbook of Behavioral Neuroscience* (Vol. 24, pp. 741–754). Elsevier B.V. https://doi.org/10.1016/B978-0-12-802206-1.00036-2

Walters, J. R., Hu, D., Itoga, C. A., Parr-Brownlie, L. C., & Bergstrom, D. A. (2007). Phase relationships support a role for coordinated activity in the indirect pathway in organizing slow oscillations in basal ganglia output after loss of dopamine. *Neuroscience*, *144*(2), 762–776. https://doi.org/10.1016/j.neuroscience.2006.10.006

Wang, H. L., Zhang, S., Qi, J., Wang, H., Cachope, R., Mejias-Aponte, C. A., Gomez, J. A., Mateo-Semidey, G. E., Beaudoin, G. M. J., Paladini, C. A., Cheer, J. F., & Morales, M. (2019). Dorsal Raphe Dual Serotonin-Glutamate Neurons Drive Reward by Establishing Excitatory Synapses on VTA Mesoaccumbens Dopamine Neurons. *Cell Reports*, *26*(5), 1128-1142.e7. https://doi.org/10.1016/j.celrep.2019.01.014

Wang, Q., Chen, J., Li, M., Lv, S., Xie, Z., Li, N., Wang, N., Wang, J., Luo, F., & Zhang, W. (2019). Eltoprazine prevents levodopa-induced dyskinesias by reducing causal interactions for theta oscillations in the dorsolateral striatum and substantia nigra pars reticulate. *Neuropharmacology*, *148*, 1–10. https://doi.org/10.1016/j.neuropharm.2018.12.027

Wang, S., Zhang, Q. J., Liu, J., Wu, Z. H., Wang, T., Gui, Z. H., Chen, L., & Wang, Y. (2009). Unilateral lesion of the nigrostriatal pathway induces an increase of neuronal firing of the midbrain raphe nuclei 5-HT neurons and a decrease of their response to 5-HT1A receptor stimulation in the rat. *Neuroscience*, *159*(2), 850–861. https://doi.org/10.1016/j.neuroscience.2008.12.051

Waszczak, B. L., Eng, N., & Walters, J. R. (1980). Effects of muscimol and picrotoxin on single unit activity of substantia nigra neurons. *Brain Research*, *188*(1), 185–197. https://doi.org/10.1016/0006-8993(80)90567-3

Weissbourd, B., Ren, J., DeLoach, K. E., Guenthner, C. J., Miyamichi, K., & Luo, L. (2014). Presynaptic partners of dorsal raphe serotonergic and GABAergic neurons. *Neuron*, *83*(3), 645–662. https://doi.org/10.1016/j.neuron.2014.06.024

Whitton, P. S. (2007). Inflammation as a causative factor in the aetiology of Parkinson's disease. *British Journal of Pharmacology*, *150*(8), 963–976. https://doi.org/10.1038/sj.bjp.0707167

Wichmann, T., & Dostrovsky, J. O. (2011). Pathological basal ganglia activity in movement disorders. In *Neuroscience* (Vol. 198, pp. 232–244). https://doi.org/10.1016/j.neuroscience.2011.06.048

Wichmann, Thomas, Bergman, H., Starr, P. A., Subramanian, T., Watts, R. L., & DeLong, M. R. (1999). Comparison of MPTP-induced changes in spontaneous neuronal discharge in the internal pallidal segment and in the substantia nigra pars

reticulata in primates. *Experimental Brain Research*, *125*(4), 397–409. https://doi.org/10.1007/s002210050696

Wichmann, Thomas, & Soares, J. (2006). Neuronal firing before and after burst discharges in the monkey basal ganglia is predictably patterned in the normal state and altered in parkinsonism. *Journal of Neurophysiology*, *95*(4), 2120–2133. https://doi.org/10.1152/jn.01013.2005

Williams-Gray, C. H., Foltynie, T., Brayne, C. E. G., Robbins, T. W., & Barker, R. A. (2007). Evolution of cognitive dysfunction in an incident Parkinson's disease cohort. *Brain*, *130*(7), 1787–1798. https://doi.org/10.1093/brain/awm111

Wong-Riley, M. T. T. (1989). Cytochrome oxidase: an endogenous metabolic marker for neuronal activity. In *Trends in Neurosciences* (Vol. 12, Issue 3, pp. 94–101). https://doi.org/10.1016/0166-2236(89)90165-3

Xiang, Z., Thompson, A. D., Jones, C. K., Lindsley, C. W., & Conn, P. J. (2012). Roles of the M1 muscarinic acetylcholine receptor subtype in the regulation of basal ganglia function and implications for the treatment of Parkinson's disease. *Journal of Pharmacology and Experimental Therapeutics*, *340*(3), 595–603. https://doi.org/10.1124/jpet.111.187856

Xu, J., Zhong, N., Wang, H., Elias, J. E., Kim, C. Y., Woldman, I., Pifl, C., Gygi, S. P., Geula, C., & Yankner, B. A. (2005). The Parkinson's disease-associated DJ-1 protein is a transcriptional co-activator that protects against neuronal apoptosis. *Human Molecular Genetics*, *14*(9), 1231–1241. https://doi.org/10.1093/hmg/ddi134

Ye, Z., Altena, E., Nombela, C., Housden, C. R., Maxwell, H., Rittman, T., Huddleston, C., Rae, C. L., Regenthal, R., Sahakian, B. J., Barker, R. A., Robbins, T. W., & Rowe, J. B. (2014). Selective serotonin reuptake inhibition modulates response inhibition in Parkinson's disease. *Brain*, *137*(4), 1145–1155. https://doi.org/10.1093/brain/awu032

Yoon, H. H., Min, J., Hwang, E., Lee, C. J., Suh, J. K. F., Hwang, O., & Jeon, S. R. (2016). Optogenetic Inhibition of the Subthalamic Nucleus Reduces Levodopa-Induced Dyskinesias in a Rat Model of Parkinson's Disease. *Stereotactic and Functional Neurosurgery*, *94*(1), 41–53. https://doi.org/10.1159/000442891

Yoshida, K., Sugita, T., Higuchi, H., & Hishikawa, Y. (1998). Effect of tandospirone on tardive dyskinesia and parkinsonian symptoms. *European Psychiatry*, *13*(8), 421–422. https://doi.org/10.1016/S0924-9338(99)80690-7

Yoshida, S. ichi, Nambu, A., & Jinnai, K. (1993). The distribution of the globus pallidus neurons with input from various cortical areas in the monkeys. *Brain Research*, *611*(1), 170–174. https://doi.org/10.1016/0006-8993(93)91791-P

Zappia, M., Annesi, G., Nicoletti, G., Arabia, G., Annesi, F., Messina, D., Pugliese, P., Spadafora, P., Tarantino, P., Carrideo, S., Civitelli, D., De Marco, E. V., Cirò-Candiano, I. C., Gambardella, A., & Quattrone, A. (2005). Sex differences in clinical and genetic determinants of levodopa peak-dose dyskinesias in Parkinson disease: An exploratory study. *Archives of Neurology*, *62*(4), 601–605. https://doi.org/10.1001/archneur.62.4.601

Zhang, J., Culp, M. L., Craver, J. G., & Darley-Usmar, V. (2018). Mitochondrial function and autophagy: integrating proteotoxic, redox, and metabolic stress in Parkinson's disease. *Journal of Neurochemistry*, *144*(6), 691–709.

https://doi.org/10.1111/jnc.14308

Zhang, Q.-J., Gao, R., Liu, J., Liu, Y.-P., & Wang, S. (2007). Changes in the firing activity of serotonergic neurons in the dorsal raphe nucleus in a rat model of Parkinson's disease. *Sheng Li Xue Bao : [Acta Physiologica Sinica]*, *59*(2), 183–189. http://www.ncbi.nlm.nih.gov/pubmed/17437041

Zhou, C., Huang, Y., & Przedborski, S. (2008). Oxidative stress in Parkinson's disease: A mechanism of pathogenic and therapeutic significance. *Annals of the New York Academy of Sciences*, *1147*, 93–104. https://doi.org/10.1196/annals.1427.023

Zhou, F. W., Xu, J. J., Zhao, Y., LeDoux, M. S., & Zhou, F. M. (2006). Opposite functions of histamine H1 and H2 receptors and H3 receptor in substantia nigra pars reticulata. *Journal of Neurophysiology*, *96*(3), 1581–1591. https://doi.org/10.1152/jn.00148.2006

Zold, C. L., Escande, M. V., Pomata, P. E., Riquelme, L. A., & Murer, M. G. (2012). Striatal NMDA receptors gate cortico-pallidal synchronization in a rat model of Parkinson's disease. *Neurobiology of Disease*, *47*(1), 38–48. https://doi.org/10.1016/j.nbd.2012.03.022